UNIVERSITY OF CALIFORNIA
SANTA CRUZ

ALTERED POSITIONAL SPECIFICITY OF 15-LIPOXYGENASE-1 CREATES NEW PATHWAYS FOR THE RESOLUTION OF INFLAMMATION

A dissertation submitted in partial satisfaction
of the requirements for the degree of

DOCTOR OF PHILOSOPHY

in

CHEMISTRY

by

Steven Charles Perry

December 2019

The dissertation of Steven Charles Perry is approved:

Professor Michael Stone, Chair

Professor Theodore R. Holman

Professor Carrie Partch

Quentin Williams
Acting Vice Provost and Dean of Graduate Studies

Table of Contents

List of Figures

Chapter 1

Chapter 2

Chapter 3

Chapter 4

Chapter 5

List of Tables

List of Schemes

Abstract

Altered positional specificity of 15-Lipoxygenase-1 creates new pathways for the resolution of inflammation

Steven C. Perry

The oxylipins 7S,14S-diHDHA and 7S,17S-diHDHA (RvD5) have been found in macrophages exudates and are believed to function as specialized pro-resolving mediators of inflammation. Their biosynthesis has been proposed to proceed through sequential oxidations of docosahexaenoic acid (DHA) by lipoxygenase enzymes, specifically by h5-LOX performing the first oxidation to 7S-HDHA followed by h12-LOX oxidation to form 7S,14S-diHDHA or h15-LOX-1 oxidation to form RvD5. In this work, we determine that the oxidation of 7S-HpDHA to 7S,14S-diHDHA can be carried out by either h12-LOX or h15-LOX-1, with similar kinetics. The oxidation at C14 of DHA by h12-LOX was expected, but the non-canonical reaction of h15-LOX-1 to make 7S,14S-diHDHA was unexpected. This result raised questions regarding biosynthesis of RvD5. Strikingly, we find that h15-LOX-2 oxygenates 7S-HDHA almost exclusively at C17 to form RvD5, with faster kinetics than that of h15-LOX-1. We also determine that the reactions of h5-LOX with 14S-HpDHA and 17S-HpDHA are kinetically slow, suggesting these may be minor biosynthetic routes *in vivo*.

We determine that altered positional specificity of h15-LOX-1 extends to 5S-HETE and show that 15-LOX-2 plays a greater role in generating 5S,15S-diHETE,

while h15-LOX-1 primarily generates the non-canonical product, 5S,12S-diHETE.

Previous work has indicated numerous active-site amino acids that influence regiospecificity of h15-LOX-1 with AA. We extend this work to 7S-HDHA and 5S-HETE and show that the depth of the active site as determined by I417 and F352 strongly affects the regiospecificity with these oxylipins, with F352W almost entirely reversing the altered positional specificity seen in wildtype 15-LOX-1.

Our results may extend beyond the resolution of inflammation. Specifically, we show that both 7S,14S-diHDHA and RvD5 have anti-aggregation properties with platelets at low micro-molar concentrations, which could directly regulate clot resolution. 15-(S)hydroxyeicosatrienoic acid (15-HETrE), generated by reaction of the omega-6 polyunsaturated fatty acid dihomo-γ-linolenic acid (DGLA) with h15-LOX-1, is known to inhibit platelet activation through an unknown mechanism. To investigate the basis of this inhibition, human platelets were treated with 15-HETrE and platelet aggregation was assayed by various methods. 15-HETrE was shown to inhibit platelet activation through activation of PPARβ and inhibition of 12-lipoxygenase (12-LOX).

Acknowledgements

I would like to thank my advisor, Theodore R. Holman, for his mentorship and support throughout my graduate work in the Holman lab. I would not be here without his leadership. I would also like to thank my committee members Carrie Partch and Michael Stone for their advice and guidance over many conversations.

Thank you to all the members of the Holman Lab who provided thoughtful scientific discussions, advice, troubleshooting and support; Eric Hoobler, Aby Green, Ansari Aleem, Josh Deschamps, Michelle Armstrong, Cody Freedman, Chris van Hoorbeke, Michelle Tran and Wan-Chen Tsai

I would like to acknowledge and thank Scott Conrad, James Sorrentino, Oluwayomi Akinkugbe and Leslie Bautista for their hard work in the lab and help with many experiments.

Thank you to my Fiancé Annie Hansen for her support and patience through graduate school. Lastly, thank you to my Parents for their love and support over the years.

Chapter 1

INTRODUCTION

1.1 Inflammation

Injury and sickness are a part of life. Every bruise, cut or infection elicits a complex series of responses designed to repair and rebuild tissues and return the body to homeostasis. Inflammation is the sum of these cellular responses. Early medical investigations identified 5 cardinal signs of inflammation; *dolor* (pain), *rubor* (redness), *calor* (heat), *tumor* (swelling) and *functio laesa* (loss of function).

The process of inflammation begins when a tissue experiences an infection or injury. Within these tissues reside a number of cells termed resident immune cells, whose job is to monitor tissues for signs of damage (*1*). The primary immune cells filling this role are macrophages, dendritic cells and mast cells. Macrophages, in particular, are often found as differentiated, tissue-specific versions such as histiocytes and Kupffer cells (*2*). These cells rely on innate immune mechanisms to detect two categories of inflammation-related chemicals known as damage-associated molecular patterns (DAMP's) and pathogen-associated molecular patterns (PAMP's). Recognition occurs through the action of surface-receptors called pattern-recognition receptors (PRR's) (*3*). DAMP's include proteins and small molecules, such as DNA, RNA, intracellular proteins like heat-shock proteins and certain chromatin-associated proteins and fragments of extracellular matrix (*4*). PAMP's include bacterial lipopolysaccharides, flagellin, peptidoglycan and various bacteria-associated endotoxins (*5, 6*).

Infection or tissue damage exposes resident immune cells to PAMP's and DAMP's, inducing them to secrete inflammatory signaling molecules. The immune

response can be broadly grouped into two phases, the vascular phase and the cellular phase (*7*). The vascular phase is the initial phase and occurs when activated macrophages release histamine, serotonin and nitric oxide, along with eicosanoids, like leukotriene B4. These compounds induce vasodilation and remodeling of blood vessel endothelial cells, increasing their permeability. Together, these effects allow blood plasma to leak from blood vessels and accumulate in tissue, bringing antimicrobial factors such as lysozyme, antibodies and complement proteins along with it (*8*). These molecules function to inhibit microbial growth and prevent the spread of infection to adjacent healthy areas. In the case of tissue damage, such as a laceration, this leaked plasma, or exudate, also carries fibrin and clotting factors that can prevent bleeding. Fibrin also helps form a scaffold that fibroblasts use when repairing damaged extracellular matrix (*9*). The excess blood flow and fluid accumulation of the vascular phase leads to the recognizable symptoms of redness, swelling and heat. Some of the excess fluid flushes bacteria into lymphatic vessels, where they encounter B-cells and T-cells and begin activation of the adaptive immune system.

The cellular phase of inflammation occurs once the vascular phase is underway. Circulating blood contains leukocytes that must translocate from the circulation into tissues in order to fight infection. Leukocyte recruitment begins when TNF alpha and Interleunin-1, produced by resident macrophages at the site of infection, diffuse to nearby endothelial cells and induce expression of the cell adhesion molecules p-selectin (*10*) and e-selectin (*11*) on their surface. At the same

time, vasodilation and the resulting decrease in blood flow velocity causes a decrease in shear forces in capillaries. This allows leukocytes to interact with the endothelium wall. Leukocytes express carbohydrate ligands that have a weak affinity for selectins on the surface of endothelium (*12*). This weak affinity resists the force of blood flow and allows leukocytes to slowly roll along the blood vessel wall in a process called rolling adhesion. Leukocytes follow gradients of chemo-attractive molecules secreted by resident macrophages in damaged tissue. This causes them to congregate on the blood vessel wall near site of inflammation. Additional molecules secreted by the resident macrophages cause these rolling leukocytes to express integrins, such as ICAM and VCAM on their surface (*13*), which bind more tightly to endothelial cells than selectins. This causes the leukocytes to halt their rolling movement and extend pseudopodia into the gaps between endothelial cells in a process called diapedesis (*14*). The increased permeability of the endothelium allows the cells to migrate into the intercellular space and follow the chemotactic gradient towards a site of injury. This entire process of leukocyte movement from blood into tissue is called extravasation.

Once they've moved into tissue, leukocytes take on a 3 main functions: fighting invaders, phagocytizing debris and signaling (*14*). The first cells to arrive in an area are neutrophils, which are the most abundant white blood cell in mammals. Along with eosinophils and basophils, they are considered a type of polymorphonuclear leukocyte (*15*). They are also referred to as granulocytes, due to the many cellular vesicles they contain. Neutrophils express various pattern-

recognition receptors, such as toll-like receptors that are activated by PAMP's. After encountering a PAMP, neutrophils de-granulate, releasing the contents of their vesicles into the extracellular environment. The granules contain various anti-microbial peptides of the innate immune system, such as proteases, defensins and lactoferrin (*16*).

Neutrophils express receptors that bind to the FC fragment of antibodies, which allows them to bind to pathogens that have been coated, or opsonized by antibodies (*14*). This antibody coating allows neutrophils to easily ingest bacteria, viruses and fungi without needing a specific cell surface receptor for each individual pathogen. This process of ingesting foreign particles is called phagocytosis. Once inside of neutrophils, the pathogen is localized in a large compartment called the phagosome (*17*). This compartment fuses with lysosomes to become the larger phagolysosome. The neutrophil then releases proteases and reactive oxygen species into this compartment in a process called the respiratory burst (*18*). During this process, the enzyme NADPH oxidase is activated to produce large amounts of superoxide, a reactive oxygen species. Two enzymes known as superoxide dismutase and myeloperoxidase then convert the superoxide into hydrogen peroxide and hypochlorus acid, which a primarily responsible for killing phagocytized pathogens (*19*). After the respiratory burst has occurred, neutrophils initiate apoptosis and are ingested by macrophages (*20*).

After the initial wave of neutrophils, the second type of cell recruited to sites of inflammation are macrophages. They are large, phagocytic white-blood cells that

are ubiquitous in the body (*21*). Tissues with high risk of infection contain strategically stationed macrophages known as resident macrophages (*1*). Depending on the tissue they are found in, resident macrophages take on different forms such as histiocytes, Kupffer cells, microglia and alveolar macrophages. When found in the blood, Macrophages exist as undifferentiated precursor cells known as blood monocytes (*1*).

As blood monocytes circulate throughout the body, they may encounter areas of inflammation, where chemotactic cytokines are produced at high concentration and diffuse into blood vessels. When encountering these signaling molecules, monocytes undergo a process of extravasation similar to that occurring in neutrophils. Using amoeboid movement, they cross the blood vessel endothelium and migrate towards a source of inflammation. Once inside tissue, monocytes differentiate into two types of macrophage; M1 and M2 (*22*). This process of differentiation is called polarization. The type of macrophage that a monocyte becomes depends on the mixture of cytokines it encounters.

During the early stage of inflammation, monocytes encounter DAMP's, PAMP's, interferon-γ (IFN-γ) and tumor necrosis factor (TNF) that induce them to become M1 macrophages. These macrophages take on diverse pro-inflammatory functions (*23-25*). They help fight infection by releasing complement proteins and phagocytizing bacteria and foreign particles. They attract monocytes, neutrophils and other lymphocytes to an area of inflammation by secreting pro-inflammatory cytokines (*26*). Additionally, as antigen presenting cells, they display digested

antigens on their surface that activate T-cells and B-cells to initiate the adaptive immune response.

During the late stages of inflammation, monocytes encounter a different suite of cytokines that lead to their polarization into M2 macrophages (*26*). These M2 cells begin the process of tissue repair and cleanup once the primary injury or infection has subsided. An area of tissue that has experienced acute inflammation will suffer collateral damage from neutrophil and bacterial proteases and digestive enzymes. M2 macrophages initiate the process of wound healing and release anti-inflammatory signaling molecules such as IL-10, lipoxins and resolvins (*22*). These signals oppose the action of pro-inflammatory chemotactic molecules, reducing neutrophil chemotaxis and polarization of monocytes into M1 macrophages. Neutrophils that digest sufficient bacteria will undergo apoptosis and be phagocytized by M2 Macrophages (*9*).

Although inflammation is often thought of as destructive, a strong inflammatory response is required for proper pathogen response and wound healing. Acute inflammation is the first line of defense against tissue injury. Too little inflammation may allow an infection to rapidly grow out of control, leading to death of the organism. However, this response must be properly regulated so that acute inflammation does not continue after a pathogen is removed (*9*). Most pro-inflammatory mediators have short half-lives and must be continually produced to maintain inflammation. If acute inflammation continues for too long, then it transitions into chronic inflammation. This may happen in situations where prolonged

activation of immune cells occurs without transition to resolution. Neutrophils are primarily responsible for generating acute inflammation, while M1 macrophages are responsible for chronic inflammation. For instance, macrophages in atherosclerotic plaques may become foam cells after digesting cholesterol (*27*).

1.2 Resolution of Inflammation

Historically, the resolution of inflammation was viewed as a simple, passive process, which occurred secondary to decreases in the production of pro-inflammatory mediators (*28*). However, in 1984, Serhan, Hamberg and Samuelsson reported the discovery of the lipoxins (*29*), lipid-derived mediators subsequently shown to dampen the immune response. Since then, the process of resolution has come to be understood as a complex, active process which down-regulates the immune response to prevent unnecessary collateral damage to tissues (*9*). The process promotes apoptosis of pro-inflammatory neutrophils and granulocytes, and attracts resolution-promoting cells such as M2 macrophages.

One of the most important resolution-promoting changes that distinguishes M1 and M2 macrophages is lipid mediator class-switching, which involves a switch in the types of bioactive lipid mediators produced by these cells.

1.3 Lipids

Lipids represent a broad category of aliphatic hydrocarbon molecules usually found in biological systems functionalized with a polar moiety. They are structurally

diverse, from esterified triglycerides to complex branching plasmalogens. They perform three main functions in biological systems: energy-storage, formation of lipid-bilayer membranes and as precursors for bioactive lipids. Historically, lipids were viewed as important sources of energy and components of cell membranes but were not thought to play any other cellular roles. Their importance in cell signaling was not elucidated until much later, with the discovery of the eicosanoids. Since then, research has identified many roles for fatty acid-derived molecules in inflammation and cell signaling.

Lipids are composed of simpler subunits known as fatty acids. Each fatty acid is composed of a long hydrocarbon chain with a carboxylic acid group at one end (*30*). While most fats are insoluble in aqueous systems, fatty acids containing a carboxylic acid take on a negative charge at physiological pH, which greatly increases their solubility in water and allows them to participate effectively in the cellular environment.

Fatty acids can be classified as either saturated or unsaturated. Saturated fatty acids are named because their carbon chains are saturated with hydrogen and contain no carbon-carbon double bonds. Unsaturated fats, on the other hand, contain one or more carbon-carbon double bonds, or sites of unsaturation, along their carbon chain. Fats with a single site of unsaturation are termed mono-unsaturated fats, while those with two or more are considered poly-unsaturated fatty acids (PUFA's) (*30*). Lipids obtained from animal sources tend to be high in saturated fats, while those from vegetables are high in unsaturated fats.

Fatty acids are further categorized by number of carbons and degree of unsaturation. Their constituent carbons are numbered starting at the carboxylic acid group. The Δ symbol is used to designate this site of unsaturation, along with the number of the first carbon of the double bond. Palmitoleic acid, for example, is a 16-carbon fatty acid containing one degree of unsaturation located between carbons 9 and 10. It is designated as $16{:}1^{\Delta 9}$ using standard nomenclature.

The carbon atoms in a double bond have sp2 hybridization and are unable to rotate. When the functional groups vary at each end, two possible configurations can be present. A double bond with both acyl groups located on the same side is termed cis, while a double bond with both acyl groups located on opposite sides, is termed trans (*30*). Most naturally occurring fatty acids contain double bonds in the cis conformation.

Polyunsaturated fatty acids (PUFA's) follow the previously discussed naming, with the addition that sites of unsaturation are indicated relative to the terminal methyl group of the molecule, instead of the carboxylic acid as is done for carbon numbering. The methyl end is termed the omega end and positions are named using the ω symbol instead of the Δ symbol (*30*). PUFA's are categorized by counting the number of carbons backwards from the terminal methyl group to the first double bond encountered. For instance, in an omega-3 fatty acid, the first double bond is between the 3rd and 4th carbons from the methyl end, while in an omega-6, it is between the 6th and 7th carbons from the end (**Figure 1.1**).

1.4 Essential Fatty Acids

Mammalian cells are capable of synthesizing the majority of structural and functional lipids de-novo using fatty acid synthase and various fatty acid-modifying enzymes. However, there are two important exceptions, linoleic acid (LA) and α-linolenic acid (ALA) that cannot be synthesized from precursors. These are termed the essential fatty acids. They were initially discovered in 1923 during research on Rats fed a fat-free diet. This connection to fat-free diets, led to their initially being named vitamin F. Deficiency of these compounds was shown to cause to skin problems and was curable by lipid infusion (*31*). Later research demonstrated that this vitamin was in fact the fatty acids ALA and LA (*32*).

Although vertebrates can synthesize many medium-chain fatty acids, they lack the enzymes required to introduce double bonds at the ω6 and ω3 position of fatty acids. This limitation prevents conversion of oleic acid ($18:1^{\Delta 9}$) into LA ($18:2^{\Delta 9,12}$) and ALA ($18:3^{\Delta 9,12,15}$) (*33*). Although LA and ALA are themselves important, their main role is to serve as precursors in the synthesis of a number of important omega-6 and omega-3 fatty acids. LA and ALA are similar in structure, both being 18-carbons in length (**Figure 1.1**). LA is an omega-6 PUFA containing two sites of unsaturation, which serves as precursor for synthesis of the omega-6, arachidonic acid (AA). ALA is an omega-3 with three sites of unsaturation that can be converted into the major omega-3 products eicosapentaenoic acid (EPA), docosapentaenoic acid (DPAω3), and docosahexaenoic acid (DHA). EPA and DHA are used to form a number of important signaling molecules. DHA in particular is found at higher concentrations in

the brain than any other omega-3 fatty acid (*34*). These PUFA's can be obtained by eating plants that can synthesize these compounds or by eating animals that have consumed these plants. Once ingested, both LA and ALA can be converted into longer chain fatty acids with more degrees of unsaturation through a series of alternating elongation and desaturation steps.

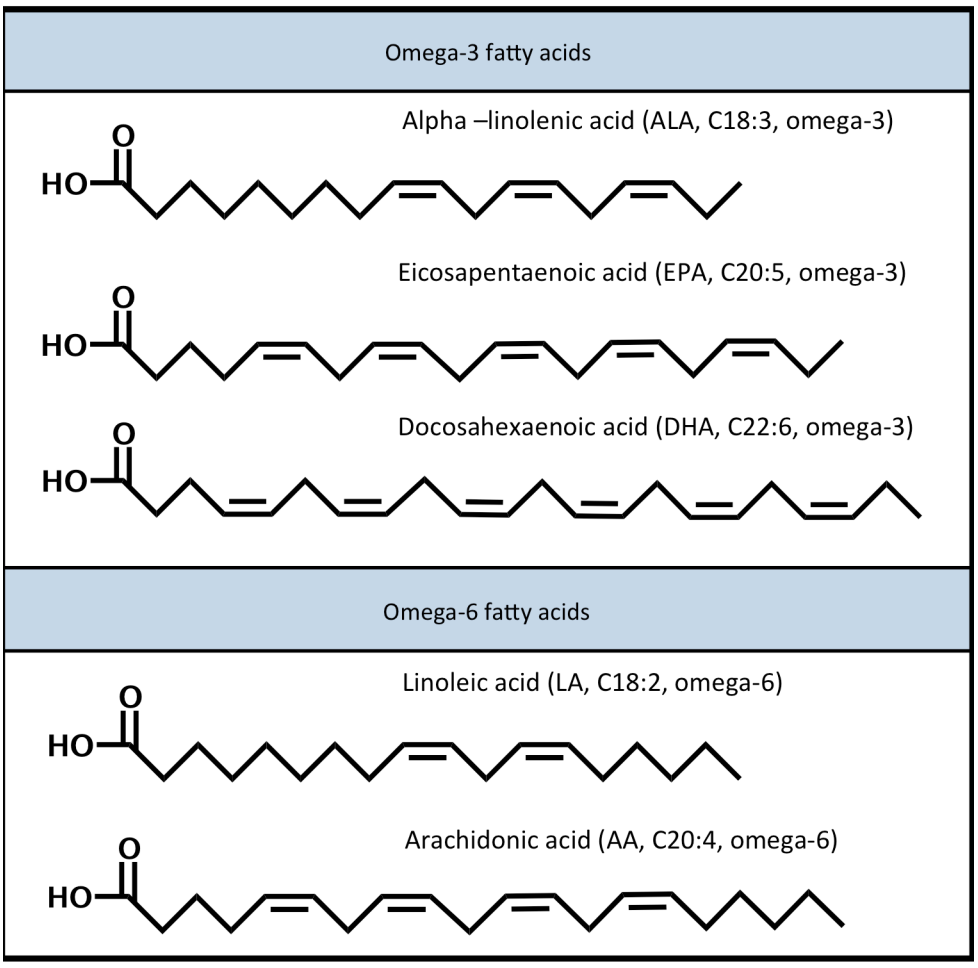

Figure 1.1 Structures of various polyunsaturated fatty acids (PUFA's). Omega-3 PUFA's, ALA, EPA and DHA, at top. Omega-6 PUFA's, LA and AA, at bottom.

1.5 Biosynthesis of Eicosapentaenoic Acid and Docosahexaenoic Acid

Fatty acid desaturases act by catalyzing the removal of two hydrogens from two adjacent carbons followed by the creation of a carbon-carbon double bond. Each desaturase introduces a double bond into the substrate at fixed position relative to the carboxy end of the fatty acid. This location is designated using the Δ symbol along with the number of the carbon in which the desaturase adds a double bond. Humans contain four different desaturases: Δ9 desaturase (D9D), Δ6-oleoyl(linolenoyl)-CoA desaturase (D6D), Δ5-eicosatrienoyl-CoA desaturase (D5D) and Δ4 desaturase (D4D) (*35*).

The conversion of ALA to DHA involves D5D and D6D and contains 7 steps; three elongation steps, three desaturation steps, and a final β-oxidation reaction. In the first step, the D6D inserts a double bond at the 6^{th} carbon of ALA, converting it to stearidonic acid. D6D is somewhat inefficient in catalyzing this reaction, making this the rate-limiting step of the pathway. The next steps are a 2-carbon elongation catalyzed by the elongases, ELOVL2 and ELOVL5, followed by desaturation by D5D to form EPA (*36*). Four more steps are required to convert EPA to DHA. ELOVL2 and ELOVL5 perform two sequential elongations, first converting EPA to docosapentaenoic acid (DPAω3) and then to tetracosapentaenoic acid. The D6D next converts tetracosapentaenoic acid to tetracosahexaenoic acid and a final Beta-oxidation step forms DHA (*37*).

Due to the complex series of steps required to transform ALA into EPA and DHA, the body is inefficient at converting ALA to EPA and DHA. Therefore, the

dietary origin of LA and ALA has important physiological consequences (*34*). Both the D5D and D6D have relatively low enzymatic activity and low expression. Healthy human females are only able to convert about 20% of dietary ALA to EPA and less than 10% to DHA. In males, the process is even less efficient, with only around 8% of ALA being converted to EPA and no conversion to DHA (*38*). The activity of D5D and D6D is decreased significantly by hyperglycemia, hypercholesterolemia and ingestion of alcohol. Conversion of ALA to EPA and DHA is further reduced by consumption of typical western diets. This occurs because western-style diets high in red meat, chicken and vegetable oils such as corn oil, safflower oil and soybean oil contain high levels of LA. Since the D5D and D6D react with both LA and ALA, high levels of LA will decrease the formation of ALA-derived products. Therefore the dietary mix of fatty acids consumed has a significant effect on EPA and DHA synthesis (*39*). Most of the omega-3 fatty acids found in plant oils, such as flax seed oil contain high levels of ALA, while the best sources of DHA and EPA are cold-water fish, krill oil and cyanobacteria.

1.6 Arachidonic Acid Biosynthesis

The symptoms of fatty acid deficiency that manifest with inadequate dietary levels of LA are in large part due to the inability of the body to synthesize arachidonic acid.

Synthesis of AA from LA is similar to that for DHA from ALA, using similar enzymes. A major difference is that the pathway requires only three steps. The first

step involves conversion of LA to γ-linolenic acid (GLA) by D6D (*40*). GLA is then elongated to dihomo-γ-linolenic acid (DGLA) by ELOVL5 and finally undergoes desaturation to AA by D5D (*34*). Similar to the omega-3 pathway, D5D and D6D are relatively inefficient at converting LA to GLA and DGLA to AA. The middle step, elongation of GLA to DGLA, occurs rapidly and therefore most GLA is converted to DGLA. The slow rate of the D6D leads DGLA to be incorporated into membrane phospholipids in place of AA. This has important consequences as the series-1 eicosanoids derived from DGLA show anti-inflammatory effects; while the series-2 eicosanoids derived from AA tend to have pro-inflammatory effects (*41*). In conditions of high LA levels, AA can also be further converted into the omega-6 docosapentaenoic acid ($22{:}5_{\omega6}$; $DPA_{\omega6}$).

GLA is found at high levels in several plant-derived oils, such as borage oil, evening primrose seed oil, hemp seed oil and black currant seed oil . Diets that contain high levels of GLA demonstrate similar cardiovascular benefits to those seen with diets high in EPA and DHA. This is likely due to the increased accumulation of DGLA. Aside from the sources listed above, DGLA is uncommon in plants and found only in trace amounts in animal products (*42*). Along with the relative ratio of omega-3 to omega-6 fatty acids, the exact composition of dietary oils influences the balance of downstream products and their associated health benefits.

Free fatty acids are shown to activate can participate in cell signaling by acting as ligands for numerous G-protein coupled receptors (GPCR's). Short-chain fatty acids are generally pro-inflammatory, while omega-3 fatty acids have anti-

inflammatory effects mediated by interaction with the free fatty acid receptor 4 (FFAR4), expressed in macrophages and adipocytes (*43*). However, the majority of signaling roles that lipids take on are due to the actions of their oxygenated derivatives. Lipids are susceptible to oxidation due to the reduced state of their carbon-hydrogen backbones. Reactivity increases with the number of double bonds, with PUFA's being particularly susceptible to oxidation at their bisallylic sites, due to the low activation energy for hydrogen abstraction. Compared to an 18-carbon saturated fat, radical mediated oxidation occurs significantly faster with increasing degrees of unsaturation (*44, 45*).

Free fatty acids are rare, as they are eventually incorporated into cell membrane phospholipids. Because of this and the relative ability of the body to synthesize EPA, DHA, DGLA and AA from LA and ALA, diet will have a large effect on membrane composition and therefore the lipids available for cells to use for signaling.

1.7 Release of Free Fatty Acids

Cell membranes are composed of phospholipids, such as phosphatidylethanolamine and phosphatidylcholine, containing two fatty acid groups esterified through their carboxy terminus to a modified phospho-glycerol head group. The most abundant fatty acids in these phospholipids are 18-carbon oleic acid and 16-carbon palmitoleic acid (*46*). Both are monounsaturated fatty acids which play little role in cell signaling. The most important PUFA found in cell membranes is arachidonic acid (AA), found primarily at the C-2 position of phospholipids. The

majority of cellular PUFA's, like AA, are bound in membrane phospholipids and unavailable for signaling. When needed, AA is cleaved from phospholipids through the action of phospholipase A2 (PLA_2), which is a lipid hydrolase that cleaves the ester bond at the C-2 position of the phospholipid glycerol linkage (*47*). Various signaling events can increase PLA_2 activity and release of free fatty acids from cell membranes.

1.8 Eicosanoids

The discovery of the eicosanoids is closely linked to the discovery of the essential fatty acids. Early research had identified a disorder caused by fatty acid deficiency, and determined that LA and ALA were the cause (*31*). In separate research, a compound was isolated from prostate-derived seminal fluid and named prostaglandin. Somewhat later, a connection was made between prostaglandin and fatty acid deficiency when it was realized that prostaglandin was derived from AA (*48*). This helped establish that the symptoms of essential fatty acid deficiency were related to the inability of the body to synthesize prostaglandin. It was not clear what the role of prostaglandin was until 1971, when research established that aspirin and related-drugs produce their effects by inhibiting the synthesis of prostaglandin (*49*). This discovery linked prostaglandins to the process of inflammation. Since then, the number of fatty acid-derived signaling molecules has expanded rapidly and research has identified many roles for these molecules in inflammation and cell signaling.

The term eicosanoid comes from the Greek word for twenty, as the first fatty acid-derived signaling molecules all originated from AA, which is 20-carbons long. These initial molecules were named after the tissues in which they were found: prostaglandins in prostate (*50*), thromboxanes in thrombocytes (platelets) and leukotrienes from leukocytes. Investigation into the enzymatic target of aspirin led researchers to the discovery of prostaglandin-endoperoxide synthetase, an iron-containing enzyme that catalyzes two sequential reactions with fatty acids, cyclooxygenation and peroxidation (*51*). There are two variants of this enzyme, colloquially referred to as COX1 and COX2 due to their cyclooxygenase activity (*52*). Reaction of COX with AA leads to formation of a distinctive oxygen-containing ring in both the prostaglandins and thromboxanes. These two compounds have since been placed into a more expansive category of eicosanoids termed prostanoids, containing many related prostaglandin and thromboxane analogues as well as prostacyclin.

Eicosanoids produced by cyclization of precursor fatty acids are considered part of the cyclic pathway of eicosanoid production. In addition to this pathway, a second exists that does not involve cyclization and is termed the linear pathway.

1.9 Leukotrienes

Similar to the cyclic pathway, products of the linear pathway are formed from AA. However, the linear pathway occurs primarily through the action of lipoxygenases. The Leukotrienes were the first lipoxygenase products discovered.

They are produced by a number of immune cells, including granulocytes, macrophages and mast cells (*53*). Their biosynthesis begins when myriad extracellular stimuli activate GPCR's that stimulate Protein kinase C and release of Ca^{2+} into the cytoplasm. This signaling cascade next activates PLA_2, which cleaves AA from Phosphoinositol diphosphate (PIP2) in phospholipid membranes (*47*). Once released, free AA becomes available to react with 5-Lipoxygenase (5-LOX), which inserts a hydroperoxy group into the 5^{th} carbon of AA. Since AA is more technically known as eicosatetraenoic acid, the product formed by reaction with h5-LOX is named 5S-hydroperoxy-eicosatetraenoic acid (5S-HpETE) (*54*). Due to the reducing character of the cytoplasm, 5S-HpETE is reduced to 5S-hydroxy-eicosatetraenoic acid (5S-HETE) by glutathione and cellular peroxidases. h5-LOX can further react with 5S-HETE to create Leukotriene A4 (LTA_4), which contains a reactive 5,6-epoxide (*55*). LTA_4 can be easily hydrolyzed by water and has a half-life of less than 30 seconds. In cells, it's rapidly converted to LTB_4 (also known as 5S,12R-diHETE) through the action of LTA_4 hydrolase, found in neutrophils and macrophages (*56*). LTB_4 exerts many important inflammatory effects by binding to two cell-surface receptors called BLT_1 and BLT_2 (*57*). Signaling through these receptors causes neutrophil chemotaxis, induces leukocyte adhesion to blood vessel endothelium and promotes activation of the neutrophil respiratory burst (*58*).

Mast cells and eosinophils contain LTC_4 synthase, which allow them to form additional members in the leukotriene pathway. LTC_4 synthase converts LTA_4 to LTC_4 by attaching glutathione to C6 of the carbon chain (*59*). The presence of the 3-

amino acid glutathione, leads LTC_4 and its derivatives to be referred to as cysteinyl leukotrienes or peptido-leukotrienes. Other cells, such as Basophils and neutrophils, contain enzymes that take LTC_4 and successively convert it to additional peptido-leukotrienes, LTD_4 and LTE_4 (*60*). These three peptido-leukotrienes were originally identified as the slow-reacting substance of anaphylaxis (SRSA). The SRSA was named due to its delayed onset and longer duration of action in the course of anaphylaxis (*61*). While histamine produces the initial rapid onset of effects and can be blocked by antihistamines, the SRSA was found to be orders of magnitude more potent could be reversed with treatment of leukotriene-receptor antagonists such as Zafirlukast and Montelukast. They signal through two cell-surface receptors CysLT1 and CysLT2 that cause smooth muscle constriction, increased blood vessel permeability and increased mucous secretion, all of which contribute to the symptoms of asthma and anaphylaxis (*62, 63*).

1.10 Lipoxins

The lipoxins are eicosanoids derived from AA that promote the resolution of inflammation. They were initially isolated from leukocyte's incubated with 15-HpETE (*29*). Their importance was realized during investigations into the mechanism of action of aspirin. Acetylsalicylic acid (aspirin) is a derivative of salicylic acid, which is found in the bark of the willow tree and has been used in traditional medicine for thousands of years. Despite this long history of use, it was not until 1971

that Vane and colleagues deduced that these compounds worked in part through modulation of cyclooxygenase and prostaglandin (*49*).

Although aspirin was initially thought solely to reduce prostaglandin formation, it was found to have a second, independent effect that occurred only at low doses. This effect led to identification of the aspirin-triggered Lipoxins (*29*). Cyclooxygenase normally carries out two reaction steps in the formation of prostaglandins; hydroperoxidation followed by cyclooxygenation. Aspirin irreversibly acetylates the active site of COX, preventing it from carrying out the second, cyclooxygenation step. The acetylated enzyme instead converts AA into 15R-hydroxyeicosatetraenoic acid (15R-HETE). This compound is metabolized by 5-LOX into 15-epi-lipoxin A_4 (15-epi-LXA_4) and 15-epi-lipoxin B_4 (15-epi-LXB_4) (*29*).

It was soon discovered that lipoxins can be formed when leukocytes adhere to blood vessels and exchange oxylipins with endothelial cells through a process called transcellular biosynthesis. These lipoxins are formed by two sequential lipoxygenase reactions and are called LXA_4 and LXB_4. They are distinguished from the aspirin-triggered lipoxins as they contain hydroxyl groups at C15 with S-stereochemistry instead of R-stereochemistry (*64*). Formation of lipoxins is thought to occur through two lipoxygenase-mediated routes. The first proposed pathway involves reaction of AA with h5-LOX in leukocytes followed h12-LOX in platelets. The second route is hypothesized to occur through reaction of AA with h15-LOX-1 in endothelial cells followed by h5-LOX in leukocytes. However, the exact biosynthetic sequence remains undetermined. 5S,15S-diHpETE and the two isomers with either the 5S or

15S position reduced to an alcohol can serve as an intermediate in their synthesis (**Figure 1.2**).

The lipoxins are ligands for the formyl peptide receptor-like 1 (FPRL1) protein, a GPCR primarily expressed on phagocytic cells involved in the immune response to infection (*65*). They have many pro-resolution effects especially in dampening neutrophil-mediated pro-inflammatory processes. Both LXA_4 and LXB_4 inhibit neutrophil chemotaxis, endothelial adhesion and extravasation. They stimulate polarization of monocytes into M2 macrophages and enhance phagocytosis of apoptotic neutrophils by macrophages. The lipoxins further reduce neutrophil migration by blocking release of pro-inflammatory IL8 and TNF-α (*66*).

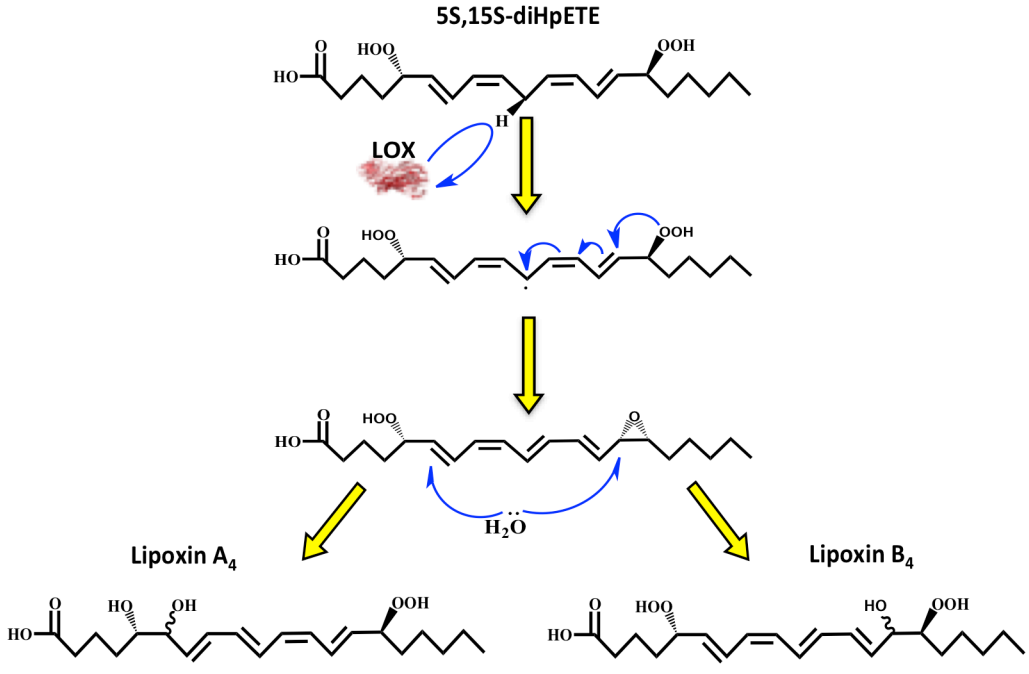

Figure 1.2. Biosynthetic mechanism for formation of lipoxins A_4 and B_4 from 5S,15S-diHpETE

1.11 Specialized Pro-Resolving Mediators

Since the discovery of the lipoxins, research into the resolution of inflammation has identified many additional molecules that play a role in this process. While the lipoxins are formed from AA, the majority of bioactive lipids with pro-resolving actions are formed from omega-3 fatty acids. These omega-3 derived signaling molecules are broadly termed specialized pro-resolving mediators (SPM's). The majority of SPM's are derived from DHA, along with many from EPA and a smaller number of molecules derived from $DPA_{\omega3}$ and $DPA_{\omega6}$ (*67, 68*). SPM's are considered a type of oxylipin, and are structurally analogous to the lipoxins in that they contain one or more hydroxyl groups incorporated into a fatty acid backbone. They are primarily biosynthesized through the action of lipoxygenases with minor contributions from the cyclooxygenases, cytochrome P450 and hydrolases.

The two main groups of SPM's are the resolvins and maresins. Along with these are smaller numbers of protectins, neuroprostanes, neuroprotectins, electrophilic oxo-derivatives and ethanolamines. These molecules have been shown to have a wide range of protective and pro-resolution effects (*69-74*). The mechanism of action of SPM's differs from that of the classic anti-inflammatory medications, in that they do not inhibit the onset of acute inflammation. Instead, they stimulate the progression of the resolution response. The switch from production of pro-inflammatory prostaglandins and leukotrienes to the lipoxins, resolvins and maresins occurs via the action of lipoxygenases. Resolution of inflammation has been shown to occur more rapidly in animal models that overexpress 15-LOX's (*75*).

The effects of SPM's are mediated by their action at cell surface receptors, the majority of which are G-protein coupled receptors (GPCR's). DHA-derived oxylipins have been shown to interact with the CB1 and CB2 cannabinoid receptors (*76*), transient receptor potential vanilloid channels (TRPV channels) (*77*) and GPR110 (*78*). LXA_4 is bound by the *N*-formyl peptide receptor 2 (FPR2) (*65*), while RvD5 binds to GPR32 (*79*).

1.12 Resolvins

The largest group of SPM's is the resolvins. They are derived from EPA, DHA, $DPA_{\omega3}$ and $DPA_{\omega6}$ and were named for their role in **resolv**ing **in**flammation. The E-series resolvins derive from EPA, while the D-series resolvins derive from DHA. There are five E-series resolvins; resolvin E1 (RvE1), 18S-resolvin E1 (18S-RvE1), resolvin E2 (RvE2), resolvin E3 (RvE3) and resolvin E4 (RvE4) (*80*). They are di- and tri-hydroxy metabolites of EPA that differ in the position and number of hydroxyl groups incorporated into their fatty acid backbone. RvE1-RvE3 all have a hydroxyl group at the 18^{th} carbon, suggesting that one step in their mechanism of formation involves COX. The locations of the remaining hydroxyl groups in these molecules suggest the involvement of lipoxygenases in their biosynthesis. RvE4 does not contain a hydroxyl at C18, instead containing hydroxyls at C5 and C15 and implying formation by two sequential lipoxygenase-catalyzed reactions.

There are six members of the D-series resolvins; resolvin D1, resolvin D2 (RvD2), resolvin D3 (RvD3), resolvin D4 (RvD4), resolvin D5 (RvD5) (**Figure 1.3)** and resolvin D6 (RvD6) which each differ in the position and number of hydroxyl groups incorporated into a DHA backbone (*80*). DHA is two carbons longer than EPA and contains one extra double bond, which allows for more combinations of oxygenation position to be formed. The D-series resolvins all incorporate a hydroxyl group at the 17th position of DHA, which is added by a 15-lipoxygenase.

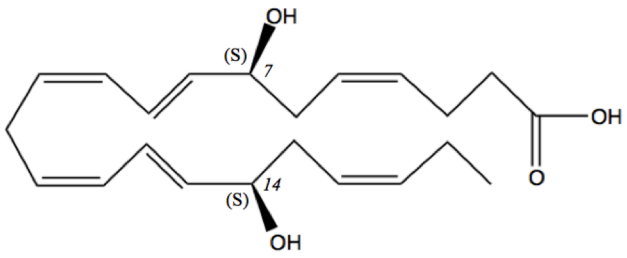

Figure 1.3. Structure of 7S,17S-diHDHA (Resolvin D5)

A third series of resolvins, termed the T-series, is composed of four di and trihydroxy metabolites of DPA$_{\omega3}$: 7S,13*R*,20S-trihydroxy-DPA$_{\omega3}$ (resolvin T1, RvT1); 7S,8S,13*R*-trihydroxy-DPA$_{\omega3}$ (resolvin T2, RvT2); 7S,12S,13*R*-trihydroxy-8*Z*,10*E*,14*E*,16*Z*,19*Z*-DPA$_{\omega3}$ (resolvin T3, RvT3) and 7S,13*R*-dihydroxy-DPA$_{\omega3}$ (resolving T4, RvT4) (*81*). These molecules share a common structure and mechanism of formation that distinguishes them from the D and E series resolvins. All of the T-series resolvins contain a hydroxyl group in the R-configuration at C13. This 13R-hydroxyl is formed when COX is exposed to aspirin or atorvastatin. Normally, the COX enzyme carries out two steps, hydroperoxidation followed by

cyclooxygenation. Aspirin and Atorvastatin covalently inhibit the second, cyclooxygenase step, causing COX2 to act solely as a hydroperoxidase (*82*). The 13R product can then further react with lipoxygenases to form the T-series resolvins. These steps are carried out through transcellular biosynthesis by mixtures of neutrophils and platelets or neutrophils and endothelium (*82*).

The resolvins promote the resolution of inflammation by opposing the effects of pro-inflammatory mediators. They reduce neutrophil extravasation, chemotaxis and generation of superoxide species(*83, 84*). RvE1 has been shown to increase bone regeneration in periodontitis and reduce thromboxane-mediated platelet aggregation (*85*). RvD5 enhances phagocytosis in neutrophils and macrophages and reduces expression of the pro-inflammatory molecules, NF-κB and TNF-α (*72*). RvD5 has at has been identified in human blood, hemorrhagic exudates and synovial fluid (*86, 87*) and is biosynthesized through two sequential lipoxygenase-mediated oxygenation events (*87, 88*). Levels of resolvins are increased in people who eat a diet supplemented with either EPA or DHA.

1.13 Maresins

The maresins are derived from oxidation of DHA by lipoxygenases. Serhan and colleagues discovered maresin 1 (MaR1) in macrophage exudates and named them **ma**crophage mediators of **res**olvin **in**flammation (*89*). There are 4 isomers of MaR1 (**Figure 1.4**), along with MaR2, MaR3 and MaR4. The isomers of MaR1 differ in the arrangement of their double bonds and the stereochemistry of their hydroxyl groups.

These differences reflect distinctive oxygenation steps contributing to formation. A similar, DHA-derived compound, Maresin2, was discovered later (*90*).

The primary effects of the maresins are on the chemotaxis and activation of macrophages and neutrophils (*91*). Maresins produced by M2 macrophages diffuse into nearby endothelial tissue lining blood vessels and attenuate the adhesion and extravasation of monocytes and neutrophils. The maresins also promote phagocytosis of apoptotic neutrophils and other dead cells by macrophages, a process referred to as efferocytosis. By limiting neutrophil migration to sites of inflammation and promoting removal of apoptotic cells, the maresins reduce the accumulation of one of the primary drivers of acute inflammation.

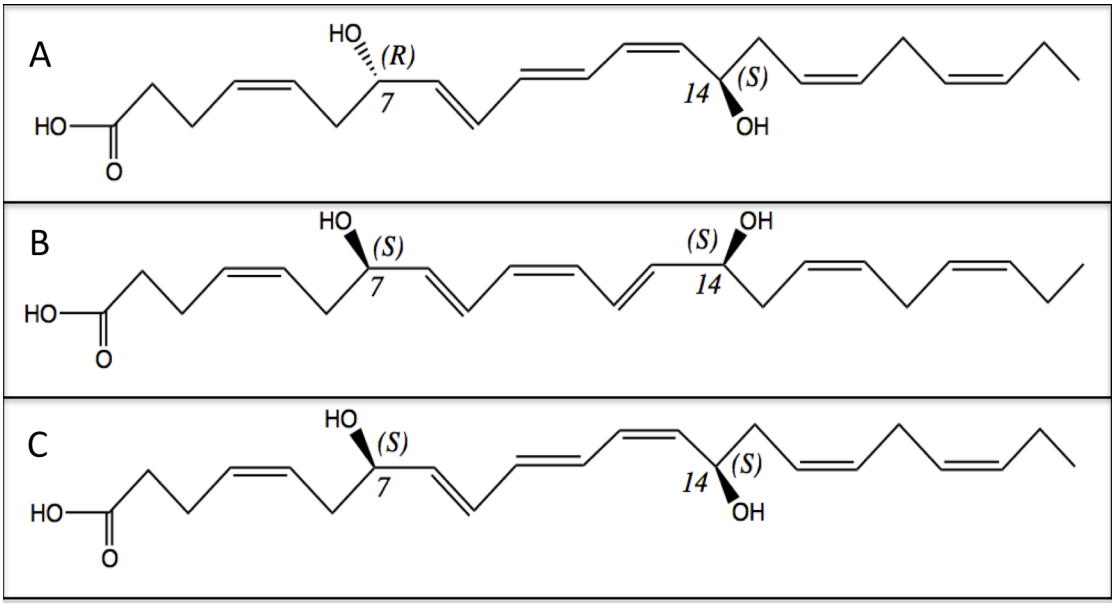

Figure 1.4. Structures of three isomers of maresin 1. **A)** 7R,14S-8Z,10E,12E-diHDHA **B)** 7S,14S-8E,10Z,12E-diHDHA **C)** 7S,14S-8Z,10E,12E-diHDHA

1.14 Lipoxygenases

Lipoxygenases are a class of enzymes that carry out the dioxygenation of poly-unsaturated fatty acids containing a 1,4-pentadiene moiety. They play an important role in synthesizing pro-inflammatory and pro-resolving mediators and in mediating the switch between inflammation and resolution. Since arachidonic acid was the first substrate discovered, Lipoxygenases are named for the carbon of AA which they insert oxygen onto. Using this nomenclature, an 8-Lipoxygenase would insert oxygen at carbon 8 of arachidonic acid while a 12-lipoxygenase would insert oxygen at C12.

1.15 Lipoxygenase Structure

Much of the structural work on Lipoxygenases is based on crystal structures of soybean 15-LOX (*92*), rabbit 15-LOX (*93*), human 15-LOX-2 (*94*) and the catalytic domain of porcine leukocyte 12-LOX (*95*). Currently there is no crystal structure of human 15-LOX-1 or human 12-LOX available. However, a general structure is shared by all mammalian lipoxygenases (**Figure 1.5**). A single polypeptide chain folds into two domains that are structurally and functionally distinct (*96*). A short inter-domain linker bridges these two domains. The smaller N-terminal domain is composed of eight anti-parallel beta sheets forming a Beta barrel (**Figure 1.5**). This region is also referred to as the PLAT domain (Polycystin-1, Lipoxygenase, Alpha-Toxin) and can be involved in membrane-association. The larger C-terminal domain is composed of 18-22 alpha helices and contains the

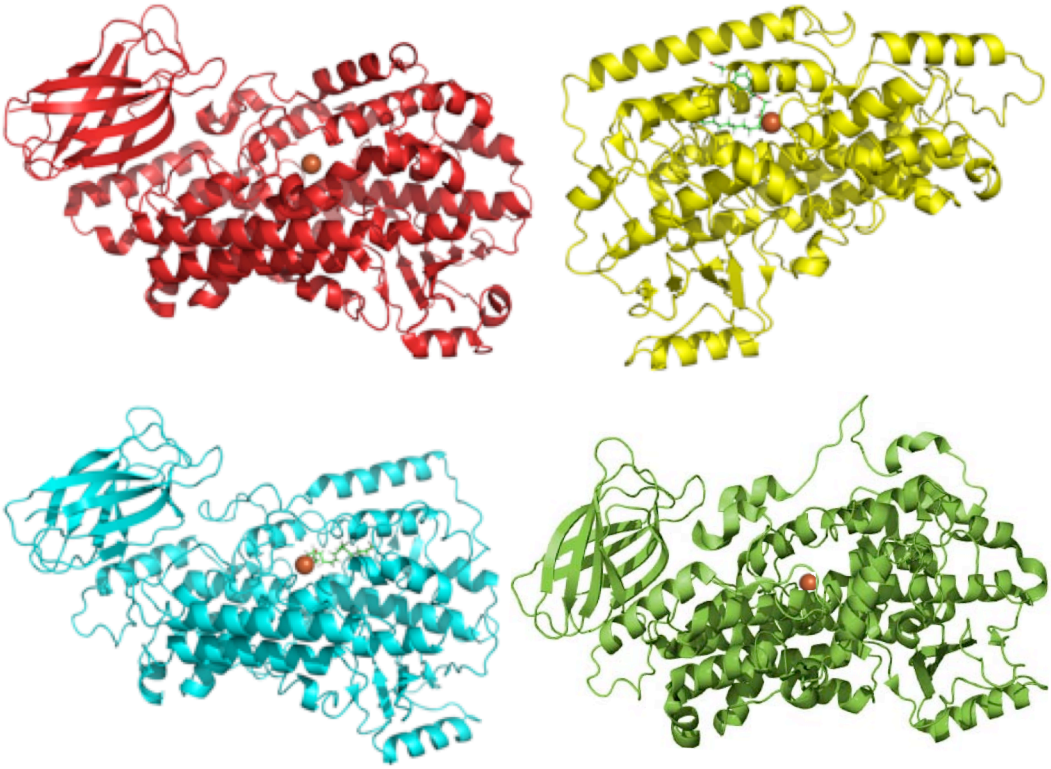

Figure 1.5. Models of h5-LOX (top left), h12-LOX (top right), h15-LOX-1 (bottom left) and h15-LOX-2 (bottom right), showing general Lipoxygenase structural elements. Beta sheet-containing PLAT. Alpha helix-containing catalytic domain and catalytic iron at center in orange.

enzymes' active site iron (*96*). There are two cavities that extend from the surface of the protein to the active site iron. The first cavity is the pathway for substrate entry and is approximately L-shaped or U-shaped (**Figure 1.6**). The second cavity is straight and narrow and functions as an oxygen channel (*92*). The substrate-binding pocket is a hydrophobic cavity with an entrance that is normally obscured by bulky amino acid side chains. Within the active site is a non-heme iron atom that is coordinated by 5 ligands; 4 histidines and the carboxylate of the C-terminal isoleucine (*97*). In some LOX's an asparagine residue can replace one of the histidines. The fifth

available coordination site of the iron is exposed to solvent within the active site and is normally occupied by a water or hydroxide. The primary iron coordination ligands form a group called the first sphere, which is supported in the correct position by a second sphere of amino acids. All lipoxygenases contain six conserved histidines, five of which are located in this region (*98*). This structural organization is in contrast to the arrangement in many other iron-containing enzymes, such as cyclooxygenase and hemoglobin, which contain an iron atom bound within a heme cofactor.

1.16 Lipoxygenase Genetics

The gene for h5-LOX is located on 10q11.2, while those encoding the remaining five human lipoxygenases are located on chromosome 17.p13. ALOX5, ALOX15a, ALOX15b and ALOX12 have 14 introns, while ALOX12R and ALOXE3 have 14. The locations of exons and introns in these genes are highly conserved (*99*). Each of the genes codes for a final product of 662-711 amino acids in length. h5-LOX can be transcribed into two alternative splice variants, both of which lack catalytic activity and may be involved in decreasing leukotriene biosynthesis by reducing turnover of the wildtype enzyme (*100*). The other LOX's contain alternative splice sites that appear to result in protein that is not catalytically active.

1.17 Lipoxygenase Homology

Lipoxygenase are ubiquitous enzymes in the domains of life. They are found in plants (*101, 102*) and much of the early work on their activity was done on soybean

15-LOX and potato 5-LOX. They have been found in lower marine organisms (*103, 104*), animals (*105, 106*) and fungi (*107*). Recently they have been identified in bacteria (*108*).

Despite sharing similarity in their positional specificity, the enzymes h15-LOX-1 and h15LOX-2 share only 35% sequence identity (*109*). Human 15-LOX-1 is more closely related to the mouse 12/15-LOX, while human 15-LOX-2 is related to the mouse 8-Lipoxygenase (*110*). Human 15-LOX-1 shares 74-81% sequence similarity with the 12/15-LOX orthologs in mice, rats and rabbits. Comparing 12/15-LOX orthologs shows that human 15-LOX-1 has the highest ratio of 15-lipoxygenating activity to 12-lipoxygenating ability, while lower primates have less and other mammals the lowest. This evolutionary relationship of reaction specificity may be related to selection for development of pro-resolving pathways (*111, 112*).

h12R-LOX shares low homology with h12S-LOX, instead having highest similarity to eLOX3, with 54% sequence homology (*113, 114*)

1.18 Lipoxygenase Substrate Acquisition and Binding

Lipoxygenases react with polyunsaturated fatty acids containing a 1,4-bisallylic pentadiene moiety (**Figure 1.1**). These substrates may include a variety of omega-3, omega-6 and omega-9 fatty acids. Although a few lipoxygenases, such as human 15-LOX1, h12R-LOX and eLOX-3 may oxygenate esterified fatty acids found in membrane phospholipids and cholesterol esters, the majority requires free fatty acids (*96*). Most cells maintain low levels of free fatty acids in their cytoplasm and

utilize various phospholipases to generate them as needed signaling. Due to this restriction, the activity of lipoxygenases are tightly coupled to the activity of PLA_2 (*96*)

Upon encountering substrate LOX's undergo a conformational change that allows substrate to enter the active site. How this process occurs is not entirely understood. Depending on the lipoxygenase, the substrate can enter the active site either methyl-end first or carboxylate-end first. Substrate orientation is thought to occur carboxylate first in h5-LOX, methyl first in both h12S-LOX and h15-LOX-2 and has been proposed to occur in both orientations in human h15-LOX-1 (**Figure 1.6**) (*115*).

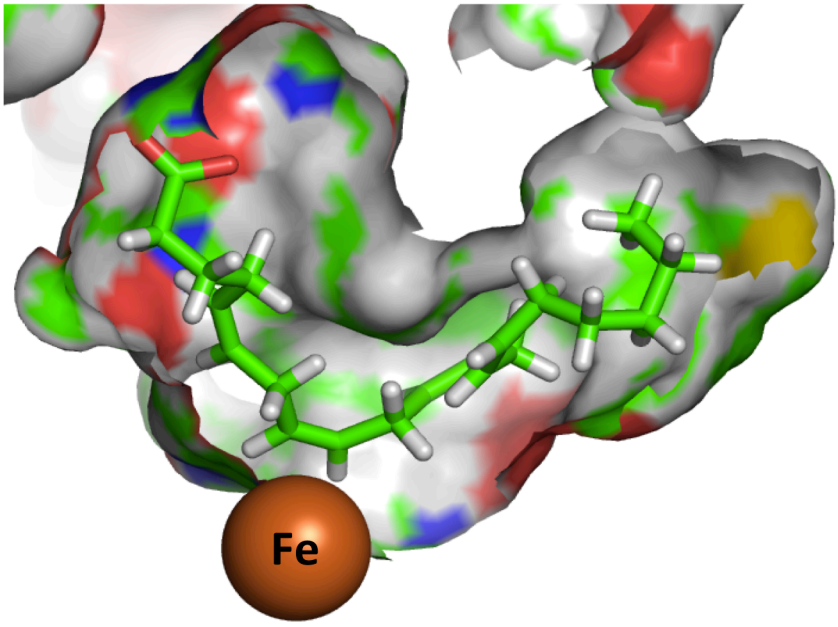

Figure 1.6. Model of arachidonic acid bound in the active site of 15-LOX-1. The methyl end of the substrate is at top right. The carboxylic acid end of the substrate is at top left, near the entrance to the active site.

1.19 Lipoxygenase Catalysis

After entering the enzymes active site, the substrate is positioned so that one of the bisallylic methylene carbons is adjacent to the iron atom (**Figure 1.6**). The iron atom can exist in two different oxidation states, the ferric Iron (III) carrying a +3 charge or the ferrous iron (II), carrying a +2 charge. In order for the enzyme's catalytic cycle to be initiated, the non-heme iron must be in the ferric state (*116*). The iron is held in place by 4 coordinating amino acid ligands. The 5th available coordination site is occupied by either a hydroxide or water depending on the oxidation state of the iron.

With the iron in its oxidized, ferric state and the substrate positioned within the distance of a standard hydrogen bond (<3.5Å), hydrogen abstraction can occur. A proton and an electron are transferred from the substrate to the hydroxide bound to the iron (III) (*117*). This reduces the iron (III) to iron (II) and changes the coordinating hydroxyl to a bound water (*118, 119*). The energy for hydrogen abstraction varies with the nearby carbon environment: a vinylic hydrogen is ~103 kcal/mol; an alkyl hydrogen is ~100 kcal/mol; an allylic hydrogen is ~85 kcal/mol; and a bisallylic ~65 kcal/mol. Despite the lower energy barrier presented by a bisallylic hydrogen, proton-coupled electron transfer requires the aid of quantum tunneling to occur (*120*). Studies on sLO have demonstrated a large kinetic isotope effect associated with the hydrogen abstraction event (*121*). Models that take this into account suggest that the reduction of the ferric iron acts as an electron sink, which makes the hydrogen tunneling step irreversible (*122*). This initial proton-coupled

electron transfer is the rate-limiting step of the lipoxygenase catalytic cycle (*123, 124*).

Once hydrogen abstraction has occurred, the substrate is left with a carbon radical (*117*). This radical becomes delocalized across the neighboring pi-electron double bond. At the same time, molecular oxygen enters through the oxygen channel and approaches the substrate from a direction antarafacial to the iron atom (*124, 125*). The unpaired radical electron attacks the oxygen, forming a covalent linkage and inducing a rearrangement in the double bond geometry from a bisallylic pentadiene to a conjugated diene (*115*). The oxygen is initially inserted as a peroxy radical, which is then reduced to a dioxygen anion and protonated to form a hydroperoxy group. Most lipoxygenases, with the exception of 12R-LOX, form hydroperoxy product with S-stereochemistry (*96, 124, 126*).

At this point, the hydroperoxy may undergo two fates. A second hydrogen may be abstracted, leading to formation of an epoxide that can act as a signaling molecule or intermediate in the synthesis of various derivatives. Conversely, the hydroperoxy may be reduced to an alcohol moiety by ubiquitous glutathione peroxidases (*96*). Cells maintain their cytoplasm as a reductive environment, so hydroperoxides and epoxides generally have a short half-life compared to their reduced counterparts.

1.20 Lipoxygenase Isozymes

There are 6 different lipoxygenase isozymes found in humans: arachidonate 5-lipoxygenase (h5-LOX, or ALOX5), platelet 12-lipoxygenase (h12-LOX), arachidonate 12R-lipoxygenase (h12R-LOX), reticulocyte 15-lipoxygenase-1 (h15-LOX-1), arachidonate 15-lipoxygenase-2 (h15-LOX-2) and epidermal-lipoxygenase-3 (eLOX-3). Since arachidonic acid was the first substrate discovered for Lipoxygenases, they are named for the carbon of AA that they insert oxygen into (**Figure 1.7**).

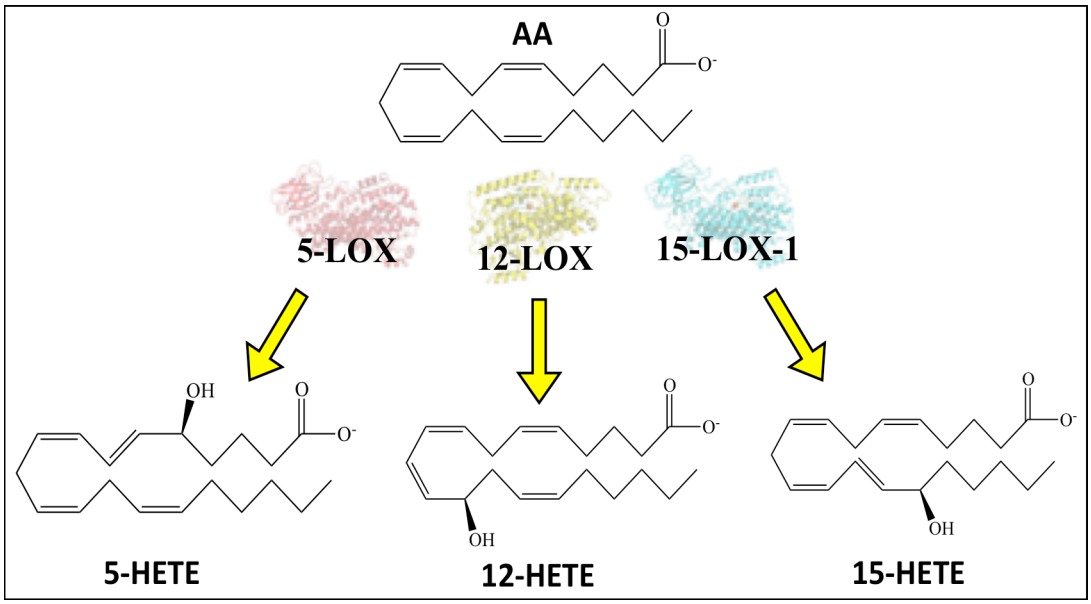

Figure 1.7. Lipoxygenases are named for their positional specificity with arachidonic acid (AA). h5-LOX catalyzes oxygenation of AA at carbon 5, to create 5S-hydroxy-eicosatetraenoic acid (5S-HETE). h12-LOX catalyzes oxygenation of AA at carbon 12, to create 12S-hydroxy-eicosatetraenoic acid (12S-HETE). h15-LOX's catalyze oxygenation of AA at carbon 15, to create 15S-hydroxy-eicosatetraenoic acid (15S-HETE).

1.21 5-Lipoxygenase

h5-LOX is a 78kD protein containing two domains formed from a single polypeptide chain 673 amino acids in length. It primarily oxygenates AA at carbon 5 to produce 5S-HpETE (**Figure 1.7),** which is a precursor to the leukotrienes, lipoxins and 5-oxo-eicosatetraenoic acid (5-oxo-ETE). h5-LOX reacts with EPA to create 5S-hydroxy-eicosapentaenoic acid (5S-HEPE), which is a precursor to the E-series resolvins, 5-oxo-EPE as well as the 5-series leukotrienes LTB_5, LTC_5, LTD_5, and LTE_5 (*127*). When reacting with DHA, which is 2 carbons longer than AA and EPA, h5-LOX primarily produces 7S-HpDHA, which serves as a precursor for the maresins and D-series resolvins (*vide infra*, chapter 1). h5-LOX also reacts with DPAω3 and DPAω6 to produce 7S-hydroxy-docosaapentaenoic acid (7S-$HDPA_{\omega3}$) and 7S-hydroxy-docosaapentaenoic acid (7S-$HDPA_{\omega6}$).

The available structural information for human 5-LOX comes from the crystal structure of a stable mutant in which a large alpha helix segment was modified to decrease the intrinsic instability of the enzyme (*128*). The N-terminal beta barrel of h5-LOX has a number of specialized regulatory roles. It has been shown to bind calcium, which is thought to mediate association with membrane phospholipids (*129*). The N-terminal PLAT domain also contains binding sites for ATP. The catalytic iron is contained in the C-terminal domain, along with a proline-rich region with an SH3-like domain that may function in protein-protein binding.

In cells, h5-LOX is normally found in the cytoplasm and nucleoplasm. Calcium influx into cells causes the enzyme to translocate to either the endoplasmic or nuclear membranes (*130*). There, it associates with 5-Lipoxygenase activating protein (FLAP), which enhances h5-LOX activity by presenting fatty acids from the membrane to the h5-LOX active site (*131*). The activity of the enzyme is also increased through binding to ATP (*132*). Recent work has shown that serine 663 of h5-LOX can be phosphorylated, which causes the enzyme to switch its positional specificity from 5-hydroperoxidation to 15-hydroperoxidation (*133*). This is proposed to occur by flipping substrate orientation from carboxy-end first to methyl-end first.

h5-LOX is primarily expressed in cells of the immune system, especially granulocytes such as neutrophils, mast cells, eosinophils and basophils (*134*). It is also found at lower levels in macrophages, monocytes and dendritic cells.

1.22 15-Lipoxygenase-1

h15-LOX-1 (ALOX15) is a 75kD protein containing two domains formed from a single polypeptide chain 662 amino acids in length. There is currently no crystal structure of h15-LOX-1, so most structural information is based on the crystal structure of rabbit reticulocyte 15-lipoxygenase (*93*). h15-LOX-1 was the first of the two 15-LOX's to be discovered and is named for its ability to oxygenate AA at carbon 15 to produce 15S-HpETE (**Figure 1.7).** This compound can be reduced in cells to 15S-HETE or further metabolized to 5S,15S-diHpETE, 15-oxo-ETE (*135*) and the lipoxins (*29*). Compared to other human lipoxygenases, h15-LOX-1 is

notable for its dual positional specificity. In addition to 15S-HpETE, it produces minor amounts of 12S-HpETE from AA. This activity is seen in a number of substrates. For instance, h15-LOX-1 produces mainly 17S-HDHA from DHA along with 14S-HDHA as a minor product. Despite being named for its positional specificity with AA, h15-LOX-1 prefers reacting with linoleic acid to produce 13-HpODE. h15-LOX-1 is also distinguished by its ability to oxygenate PUFA's esterified to phospholipids, although it is less active with these than with un-esterified substrates (*136*).

h15-LOX-1 is expressed at high levels in reticulocytes (*137*), eosinophil (*138*) and epithelial cells (*139*) and at lower levels in M2 macrophages (*140*), neutrophils, vascular endothelium and fibroblasts. Expression of h15-LOX-1 is up-regulated by Interleukin-4 (IL-4) (*141*).

1.23 15-Lipoxygenase-2

Human epithelial Lipoxygenase-2 (h15-LOX-2 or ALOX15B) is a 76 kD protein composed of 662 amino acids. The crystal structure reveals a putative membrane insertion loop and a calcium binding site that may help in activation and association with membrane phospholipids (*94*). Similar to h15-LOX-1, it is named for its ability to incorporate oxygen at the 15^{th} carbon of AA to generate 15S-HpETE. The discovery of h15-LOX-2 occurred much later than h15-LOX-1 after investigations by Brash and colleagues. In contrast to h15-LOX-1, h15-LOX-2 does not react well with linoleic acid and shows strict regio-specificity with AA, producing

100% 15S-HpETE without the minor products seen from h15-LOX-1 (*109*). It is expressed at high levels in skin and prostate and at lower levels in macrophages (*142*). Historically, it has been thought to have fewer physiological functions than h15-LOX-1. However, recent research has revealed an expanded role for it in cardiovascular disease, as it mediates the progression of macrophages into foam cells in atherosclerotic plaques (*143, 144*).

1.24 12S-Lipoxygenase

Human platelet 12-Lipoxygenase (h12-LOX, or ALOX12A), is a 75kD protein containing two domains formed from a single polypeptide chain 663 amino acids in length. Recent research suggests it exists as a homodimer (unpublished data). h12-LOX was the first human lipoxygenase discovered, when in 1974, Sammuelson and Hamberg found that platelets metabolize AA into a cyclooxygenase-independent product, 12S-HpETE (*145*). This ability to catalyze the transformation of AA into 12S-HpETE gives h12-LOX its name (**Figure 1.7)**. 12S-HpETE can be reduced to 12S-HETE or converted into the keto derivative, 12-oxo-ETE, and various di-oxygenated hepoxilins (*146*). Along with AA, DGLA can also serve as a substrate for h12-LOX, forming 12(S)-hydroperoxy-eicosatrienoic acid (12S-HETrE), which has anti-thrombotic effects in platelets (*147*). h12-LOX can also take part in maresin formation by oxygenating C14 of DHA.

h12-LOX is expressed at high levels in in platelets and leukocytes and to a lesser extent in pancreatic islets of Langerhans (*96*). Similar to h15-LOX-1, h12-LOX

expression is up-regulated by Interleukin-4 (IL-4), suggesting a shared functional role (*148*).

1.25 12R-Lipoxygenase

12R-LOX is a 771 amino acid protein named for its ability to metabolize AA to 12R-HpETE, in contrast to h12S-LOX, which metabolizes AA to 12S-HpETE. However, despite this naming, 12R-LOX reacts poorly with AA and is though to react primarily with esterified linoleic acid by adding a hydroperoxy group at carbon 9 (*149*). Linoleic acid is the most common fatty acid in the epidermis and is generally found esterified with very long chain fatty acids in a class of ceramides called omega-hydroxyacyl-sphingosine. These long waxy lipids play an important role in the development and maintenance of the skin's stratum corneum layer (*99*). Disruption of 12R-LOX is associated with congenital ichthyosiform erythroderma, a skin disorder causing thickened, scaly epidermal layers (*149*). Interestingly; these are the same symptoms of essential fatty acid deficiency, which results primarily from LA deficiency. Surprisingly, h12R-LOX shares low homology with 12S-LOX, instead having highest similarity to eLOX3, with 54% homology (*113, 114*). In addition to skin, it is also expressed in the tongue and tonsils (*150*).

1.26 Epithelial Lipoxygenase-3

Compared to other LOXs, eLOX3 has very little dioxygenase ability. Instead, it acts primarily as a hydroperoxide isomerase by converting HPETEs to epoxy and

keto derivatives. While most lipoxygenases prefer un-oxygenated fatty acids (*vide infra*), eLOX3 prefers substrates containing a hydroxyl group with R-stereochemistry (*99, 149*). eLOX3 is expressed in epidermis, where it reacts with esterified 9(*R*)-hydroperoxy linoleic acid created by 12R-LOX (*151*). The primary products of this reaction are 9*R*,10*R*-trans-epoxide,13*R*-hydroxy-octadecenoic acid, 9-keto-octadecadienoic acid, and 9*R*,10*R*-trans-epoxy-13-keto-octadecenoic acid (*99, 151*), which help form the water impermeable layer of the skin's strateum corneum. eLOX3 shares high homology with 12R-LOX and knock outs of either of these enzymes have similar, deleterious effects on skin barrier function.

1.27 Transcellular biosynthesis

Many cell types express only a single lipoxygenase isozyme. As many oxlipins incorporate oxygen at two or three different positions, formation of these compounds requires exchange of intermediates between nearby cells. This process is termed transcellular biosynthesis (*152*). While the biosynthesis of pro-inflammatory leukotrienes involves only a single lipoxygenase, formation of many of the pro-resolving maresins, resolvins and lipoxins requires two sequential lipoxygenase reactions (**Figure 1.8**). As they require two different lipoxygenases for their formation, the biosynthesis of many pro-resolving molecules is highly dependent on interactions between different cell types in an area of inflammation (*90, 153, 154*). For instance, M1 and M2 macrophages have been shown to express different lipoxygenases resulting from the process of polarization. Neutrophils can convert

17(S)-dihydroxy-4Z,7Z,10Z,13Z,15E,19Z docosahexaenoic acid (17S-HDHA) into RvD5, suggesting that h5-LOX reacts with 17-HDHA to produce RvD5 (*87*). Isolated

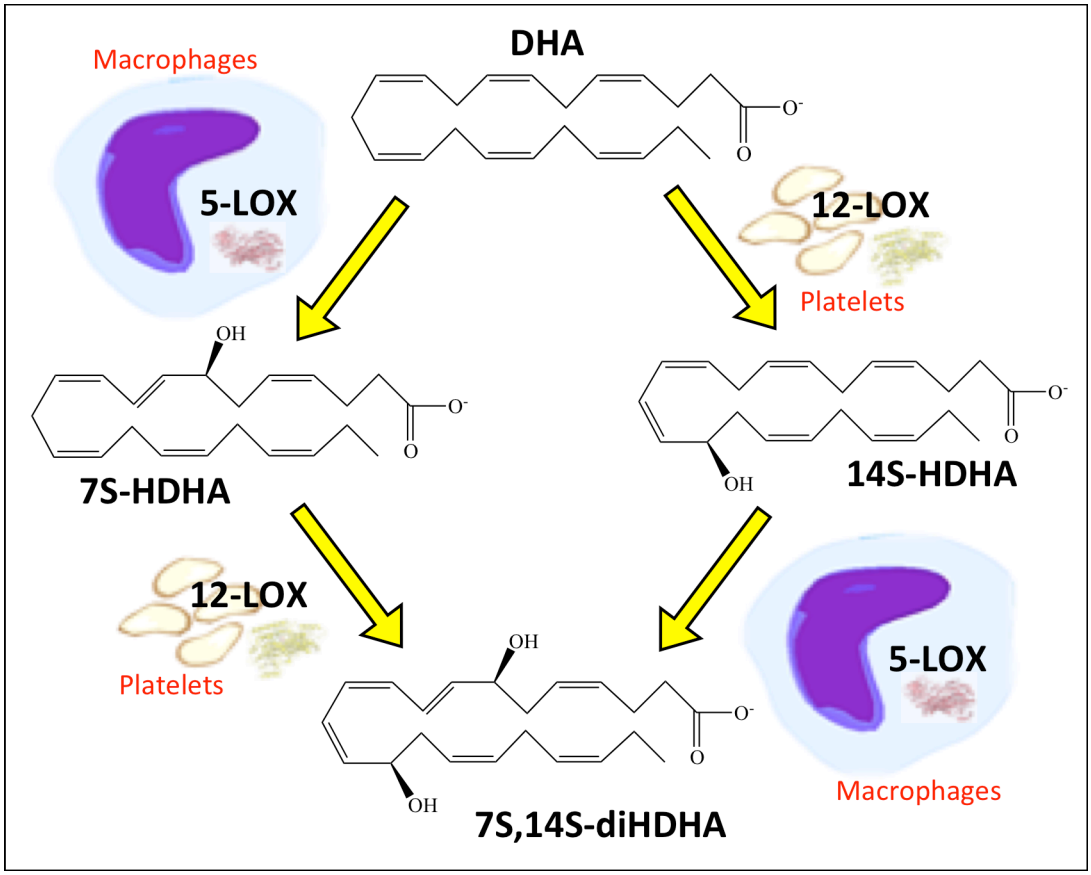

Figure 1.8. 7S,14S-8E,10Z,12E-diHDHA is proposed to be formed by transcellular biosynthesis through the combined action of 5-LOX, expressed in macrophages, and 12-LOX, expressed in platelets.

platelets lack the ability to produce RvD5. However, RvD5 is detectable in late-stage blood clots *in vivo* and found to increase over their lifetime (*155*), suggesting involvement of a second cells type in its generation.

1.28 Anti-inflammatories as treatments

The eicosanoid system is an active area of research for treatment of numerous diseases. Many anti-inflammatory drugs exert their effects through bioactive lipid signaling systems. Two well-known examples are Ibuprofen and Aspirin, which inhibit the production of prostaglandins by COX and are termed non-steroidal anti-inflammatory medications (NSAID's). These drugs have an added analgesic effect that stems from their anti-inflammatory properties. Prostaglandins potentiate pain signaling by binding transient receptor potential vanilloid (TRPV1) channels, so reducing their levels also reduced feelings of pain in an injured area (*156*). Unfortunately, long-term use of NSAIDS can lead to stomach ulcers and a risk of death from GI bleeding (*157-159*), Other undesirable side effects of NSAID's include asthma exacerbations and kidney damage.

Overproduction of leukotrienes by lipoxygenases contributes to the chronic inflammation seen in asthma, allergic rhinitis and osteoarthritis (*160*). Despite the abundance of drugs that have been developed that target COX, there are few compounds that modulate the lipoxygenase system. Only one clinically approved medication is available that directly targets a lipoxygenase, Zileuton, which inhibits h5-LOX and is prescribed for long-term maintenance therapy of chronic asthma (*161*). Other treatments for chronic asthma include Zafirlukast and Montelukast, which work by blocking the action of the cysteinyl leukotrienes at the cysteinyl leukotriene receptor, CysLT1 (*162*). However, since leukotriene production is

unaffected by these medications, leukotriene signaling at receptors other than CsyLT1 remains active.

Lipoxygenase inhibitors have been discovered at low levels in several foods and supplements; hyperforin, found in St Johns wort (*163*); curcumin found in turmeric and ginger (*164*); and caffeic acid, found in coffee, yerba mate and spearmint (*164*). Most of these compounds have poor oral bioavailability or drawbacks that make them unsuitable for drug development. Another example is baicalein, found in Thyme and several Chinese herbal medications. It has been widely used in cell studies to elucidate the biosynthetic roles of 12-LOX and 5-LOX. However, work in the Holman lab has shown that baicalein works through a non-specific redox mechanism resulting from the presence of a catechol moiety (*165*). This redox activity allows it to inhibit h15-LOX-1 and h15-LOX-2, and may complicate the results of previous *ex vivo* work.

The important role of Lipoxygenases in inflammation and its resolution makes development of potent and selective LOX inhibitors an important and under-explored area of research. In pursuit of this goal, the Holman lab has discovered several lipoxygenase inhibitors for use as research tools, with the long-term goal of developing a clinically viable LOX inhibitor. These compounds include the h12-LOX inhibitor, ML355; the h15-LOX-1 inhibitor ML351 (*166*) and ketaminazole, a dual inhibitor of h5-LOX and fungal CYP51 (*167*).

1.29 Platelet Biology

Proper coagulation is required to prevent blood loss in the event of gross tissue injury. The coagulation system is maintained in a careful homeostasis to ensure that clotting only occurs at sites of blood vessel endothelial damage. When this balance becomes disrupted, then coagulation can occur at improper locations and may lead to blood vessel damage or occlusion. Cholesterol deposits that accumulate in blood vessel walls are phagocytized by macrophages. Macrophages that have ingested large quantities of cholesterol can morph into foam cells, which secrete pro-inflammatory mediators and lead to atherosclerosis. Damaged blood vessel endothelium and disrupted hemostasis can also lead to the formation of blood clots that can become lodged in small blood vessels, occluding their flow and leading to myocardial infarction (MI) and ischemic stroke. Current treatments for these conditions come with many serious side effects, and therefore, development of alternative therapeutic modalities are desirable.

Blood coagulation occurs through two different processes; fibrin formation and platelet activation (*168*). Lipoxygenases products have been shown to modulate platelet activation and clot formation (*169*). Aggregation of platelets occurs when they encounter exposed collagen in the extracellular matric and blood vessel basement membrane. This leads to release of platelet granules, followed by morphological changes leading to von-Willibrand factor mediated adhesion to collagen and other platelets (*170*). Platelets are also be activated by ADP (*171*) and thrombin (*172*). Collagen binding also induces calcium influx and activation of PLA_2,

which cleaves arachidonic acid from membrane phospholipids, making it available to react with lipoxygenases.

Anti-thrombotic and cardio-protective effects have been shown to occur with dietary supplementation of the omega-6 fatty acid, DGLA (*173, 174*). These effects are mediated by 12S-HETrE, an oxylipin formed by reaction of 12-LOX with DGLA (*147*). Since DGLA can be incorporated into membrane phospholipids in place of AA, diets high in this fatty acid are thought to increase production of 12S-HETrE by platelets. Along with 12S-HETrE, several other lipoxygenase-derived oxylipins have been shown to modulate platelet aggregation. The role of lipoxygenases in clot formation remains an active area of research.

The current work focuses on the roles of h5-LOX, h12-LOX, 15-LOX-1 and 15-LOX-2 in the biosynthesis of lipoxins, resolvins and maresins. The biochemistry, structural foundations and biological implications of these roles in the resolution of inflammation are investigated. In particular, the positional specificity of 15-LOX-1 with oxylipins is explored along with the implications in the aforementioned biosynthetic pathways.

1.30 References

1. Perdiguero, E. G., and Geissmann, F. (2016) The development and maintenance of resident macrophages, *Nature immunology 17*, 2-8.

2. van Furth, R., and Cohn, Z. A. (1968) The origin and kinetics of mononuclear phagocytes, *The Journal of experimental medicine 128*, 415-435.

3. Kumar, H., Kawai, T., and Akira, S. (2011) Pathogen recognition by the innate immune system, *International reviews of immunology 30*, 16-34.

4. Land, W. G. (2015) The Role of Damage-Associated Molecular Patterns in Human Diseases: Part I - Promoting inflammation and immunity, *Sultan Qaboos University medical journal 15*, e9-e21.

5. Dammermann, W., Wollenberg, L., Bentzien, F., Lohse, A., and Luth, S. (2013) Toll like receptor 2 agonists lipoteichoic acid and peptidoglycan are able to enhance antigen specific IFNgamma release in whole blood during recall antigen responses, *Journal of immunological methods 396*, 107-115.

6. Mahla, R. S., Reddy, M. C., Prasad, D. V., and Kumar, H. (2013) Sweeten PAMPs: Role of Sugar Complexed PAMPs in Innate Immunity and Vaccine Biology, *Frontiers in immunology 4*, 248.

7. (2007) *Rubin's Pathology: Clinicopathologic Foundations of Medicine*, Fifth Edition ed.

8. Monk, P. N., Scola, A. M., Madala, P., and Fairlie, D. P. (2007) Function, structure and therapeutic potential of complement C5a receptors, *British journal of pharmacology 152*, 429-448.

9. Eming, S. A., Krieg, T., and Davidson, J. M. (2007) Inflammation in wound repair: molecular and cellular mechanisms, *The Journal of investigative dermatology 127*, 514-525.

10. Hahne, M., Jager, U., Isenmann, S., Hallmann, R., and Vestweber, D. (1993) Five tumor necrosis factor-inducible cell adhesion mechanisms on the surface of mouse endothelioma cells mediate the binding of leukocytes, *The Journal of cell biology 121*, 655-664.

11. Bevilacqua, M. P., Pober, J. S., Mendrick, D. L., Cotran, R. S., and Gimbrone, M. A., Jr. (1987) Identification of an inducible endothelial-leukocyte adhesion molecule, *Proceedings of the National Academy of Sciences of the United States of America 84*, 9238-9242.

12. Zou, X., Shinde Patil, V. R., Dagia, N. M., Smith, L. A., Wargo, M. J., Interliggi, K. A., Lloyd, C. M., Tees, D. F., Walcheck, B., Lawrence, M. B., and Goetz, D. J. (2005) PSGL-1 derived from human neutrophils is a high-efficiency ligand for endothelium-expressed E-selectin under flow, *American journal of physiology. Cell physiology 289*, C415-424.

13. Barreiro, O., Yanez-Mo, M., Serrador, J. M., Montoya, M. C., Vicente-Manzanares, M., Tejedor, R., Furthmayr, H., and Sanchez-Madrid, F. (2002) Dynamic interaction of VCAM-1 and ICAM-1 with moesin and ezrin in a novel endothelial docking structure for adherent leukocytes, *The Journal of cell biology 157*, 1233-1245.

14. Serhan, C., Ward, P., Gilroy, W. (2010) *Fundamentals of Inflammation*, Cambrige University Press.

15. Nathan, C. (2006) Neutrophils and immunity: challenges and opportunities, *Nature reviews. Immunology 6*, 173-182.

16. Birgens, H. S. (1985) Lactoferrin in plasma measured by an ELISA technique: evidence that plasma lactoferrin is an indicator of neutrophil turnover and bone marrow activity in acute leukaemia, *Scandinavian journal of haematology 34*, 326-331.

17. Flannagan, R. S., Jaumouille, V., and Grinstein, S. (2012) The cell biology of phagocytosis, *Annual review of pathology 7*, 61-98.

18. Segal, A. W. (2005) How neutrophils kill microbes, *Annual review of immunology 23*, 197-223.

19. Hampton, M. B., Kettle, A. J., and Winterbourn, C. C. (1998) Inside the neutrophil phagosome: oxidants, myeloperoxidase, and bacterial killing, *Blood 92*, 3007-3017.

20. Greenhalgh, D. G. (1998) The role of apoptosis in wound healing, *The international journal of biochemistry & cell biology 30*, 1019-1030.

21. Ovchinnikov, D. A. (2008) Macrophages in the embryo and beyond: much more than just giant phagocytes, *Genesis 46*, 447-462.

22. Mills, C. D. (2012) M1 and M2 Macrophages: Oracles of Health and Disease, *Critical reviews in immunology 32*, 463-488.

23. Chen, Y., and Zhang, X. (2017) Pivotal regulators of tissue homeostasis and cancer: macrophages, *Experimental hematology & oncology 6*, 23.

24. Velasco-Velazquez, M. A., Barrera, D., Gonzalez-Arenas, A., Rosales, C., and Agramonte-Hevia, J. (2003) Macrophage--Mycobacterium tuberculosis interactions: role of complement receptor 3, *Microbial pathogenesis 35*, 125-131.

25. Goto, H., and Prianti, M. (2009) Immunoactivation and immunopathogeny during active visceral leishmaniasis, *Revista do Instituto de Medicina Tropical de Sao Paulo 51*, 241-246.

26. Hesketh, M., Sahin, K. B., West, Z. E., and Murray, R. Z. (2017) Macrophage Phenotypes Regulate Scar Formation and Chronic Wound Healing, *International journal of molecular sciences 18*.

27. Moore, K. J., Sheedy, F. J., and Fisher, E. A. (2013) Macrophages in atherosclerosis: a dynamic balance, *Nature reviews. Immunology 13*, 709-721.

28. Cotran RVK, C. T. (1999) *Robbins Pathologic Basis of Disease*, Saunders, Philadelphia:.

29. Serhan, C. N., Hamberg, M., and Samuelsson, B. (1984) Trihydroxytetraenes: a novel series of compounds formed from arachidonic acid in human leukocytes, *Biochemical and biophysical research communications 118*, 943-949.

30. Rigaudy, J. K., S. P. (1979) *Nomenclature of Organic Chemistry*, Pergamon.

31. Burr, G. O. B., M.M. (1930) On the nature and role of the fatty acids essential in nutrition, *J. Biol. Chem. 86*.

32. Collins, F. D., Sinclair, A. J., Royle, J. P., Coats, D. A., Maynard, A. T., and Leonard, R. F. (1971) Plasma lipids in human linoleic acid deficiency, *Nutrition and metabolism 13*, 150-167.

33. Hastings, N., Agaba, M., Tocher, D. R., Leaver, M. J., Dick, J. R., Sargent, J. R., and Teale, A. J. (2001) A vertebrate fatty acid desaturase with Delta 5 and Delta 6 activities, *Proceedings of the National Academy of Sciences of the United States of America 98*, 14304-14309.

34. Fleming, J. A., and Kris-Etherton, P. M. (2014) The evidence for alpha-linolenic acid and cardiovascular disease benefits: Comparisons with eicosapentaenoic acid and docosahexaenoic acid, *Adv Nutr 5*, 863S-876S.

35. Los, D. A., and Murata, N. (1998) Structure and expression of fatty acid desaturases, *Biochimica et biophysica acta 1394*, 3-15.

36. Park, W. J., Kothapalli, K. S., Lawrence, P., Tyburczy, C., and Brenna, J. T. (2009) An alternate pathway to long-chain polyunsaturates: the FADS2 gene product Delta8-desaturates 20:2n-6 and 20:3n-3, *Journal of lipid research 50*, 1195-1202.

37. Nakamura, M. T., and Nara, T. Y. (2003) Essential fatty acid synthesis and its regulation in mammals, *Prostaglandins, leukotrienes, and essential fatty acids 68*, 145-150.

38. Metherel, A. H., and Bazinet, R. P. (2019) Updates to the n-3 polyunsaturated fatty acid biosynthesis pathway: DHA synthesis rates, tetracosahexaenoic acid and (minimal) retroconversion, *Progress in lipid research 76*, 101008.

39. Sanders, T. A. (2009) DHA status of vegetarians, *Prostaglandins, leukotrienes, and essential fatty acids 81*, 137-141.

40. Tocher, D. R., Leaver, M. J., and Hodgson, P. A. (1998) Recent advances in the biochemistry and molecular biology of fatty acyl desaturases, *Progress in lipid research 37*, 73-117.

41. Meller, S. M., Stilp, E., Walker, C. N., and Mena-Hurtado, C. (2013) The link between vasculogenic erectile dysfunction, coronary artery disease, and peripheral artery disease: role of metabolic factors and endovascular therapy, *The Journal of invasive cardiology 25*, 313-319.

42. Dutta-Roy, A. K., Demarco, A. C., Raha, S. K., Shay, J., Garvey, M., and Horrobin, D. F. (1990) Effects of linoleic and gamma-linolenic acids (efamol evening primrose oil) on fatty acid-binding proteins of rat liver, *Molecular and cellular biochemistry 98*, 177-182.

43. Oh, D. Y., Talukdar, S., Bae, E. J., Imamura, T., Morinaga, H., Fan, W., Li, P., Lu, W. J., Watkins, S. M., and Olefsky, J. M. (2010) GPR120 is an omega-3 fatty acid receptor mediating potent anti-inflammatory and insulin-sensitizing effects, *Cell 142*, 687-698.

44. Xu, L., and Porter, N. A. (2014) Reactivities and products of free radical oxidation of cholestadienols, *J Am Chem Soc 136*, 5443-5450.

45. Yin, H., Xu, L., and Porter, N. A. (2011) Free radical lipid peroxidation: mechanisms and analysis, *Chemical reviews 111*, 5944-5972.

46. V.BHAGAVAN (2002) *Medical Biochemistry, CHAPTER 18 - Lipids I: Fatty Acids and Eicosanoids*, 4th edition ed.

47. Dennis, E. A. (1994) Diversity of group types, regulation, and function of phospholipase A2, *The Journal of biological chemistry 269*, 13057-13060.

48. Bergstroem, S., Danielsson, H., and Samuelsson, B. (1964) The Enzymatic Formation of Prostaglandin E2 from Arachidonic Acid Prostaglandins and Related Factors 32, *Biochimica et biophysica acta 90*, 207-210.

49. Vane, J. R. (1971) Inhibition of prostaglandin synthesis as a mechanism of action for aspirin-like drugs, *Nature: New biology 231*, 232-235.

50. Goldblatt, M. W. (1935) Properties of human seminal plasma, *The Journal of physiology 84*, 208-218.

51. Smith, W. L., and Lands, W. E. (1972) Oxygenation of polyunsaturated fatty acids during prostaglandin biosynthesis by sheep vesicular gland, *Biochemistry 11*, 3276-3285.

52. Xie, W. L., Chipman, J. G., Robertson, D. L., Erikson, R. L., and Simmons, D. L. (1991) Expression of a mitogen-responsive gene encoding prostaglandin synthase is regulated by mRNA splicing, *Proceedings of the National Academy of Sciences of the United States of America 88*, 2692-2696.

53. Salmon, J. A., and Higgs, G. A. (1987) Prostaglandins and leukotrienes as inflammatory mediators, *British medical bulletin 43*, 285-296.

54. Powell, W. S., and Rokach, J. (2015) Biosynthesis, biological effects, and receptors of hydroxyeicosatetraenoic acids (HETEs) and oxoeicosatetraenoic acids (oxo-ETEs) derived from arachidonic acid, *Biochimica et biophysica acta 1851*, 340-355.

55. Samuelsson, B., Dahlen, S. E., Lindgren, J. A., Rouzer, C. A., and Serhan, C. N. (1987) Leukotrienes and lipoxins: structures, biosynthesis, and biological effects, *Science 237*, 1171-1176.

56. Rudberg, P. C., Tholander, F., Andberg, M., Thunnissen, M. M., and Haeggstrom, J. Z. (2004) Leukotriene A4 hydrolase: identification of a common carboxylate recognition site for the epoxide hydrolase and aminopeptidase substrates, *The Journal of biological chemistry 279*, 27376-27382.

57. Yokomizo, T., Izumi, T., Chang, K., Takuwa, Y., and Shimizu, T. (1997) A G-protein-coupled receptor for leukotriene B4 that mediates chemotaxis, *Nature 387*, 620-624.

58. Lammermann, T., Afonso, P. V., Angermann, B. R., Wang, J. M., Kastenmuller, W., Parent, C. A., and Germain, R. N. (2013) Neutrophil swarms require LTB4 and integrins at sites of cell death in vivo, *Nature 498*, 371-375.

59. Penrose, J. F. (1999) LTC4 synthase. Enzymology, biochemistry, and molecular characterization, *Clinical reviews in allergy & immunology 17*, 133-152.

60. Lee, C. W., Lewis, R. A., Corey, E. J., and Austen, K. F. (1983) Conversion of leukotriene D4 to leukotriene E4 by a dipeptidase released from the specific granule of human polymorphonuclear leucocytes, *Immunology 48*, 27-35.

61. Morris, H. R., Taylor, G. W., Piper, P. J., and Tippins, J. R. (1980) Structure of slow-reacting substance of anaphylaxis from guinea-pig lung, *Nature 285*, 104-106.

62. Haeggstrom, J. Z., and Funk, C. D. (2011) Lipoxygenase and leukotriene pathways: biochemistry, biology, and roles in disease, *Chemical reviews 111*, 5866-5898.

63. Dahlen, S. E., Bjork, J., Hedqvist, P., Arfors, K. E., Hammarstrom, S., Lindgren, J. A., and Samuelsson, B. (1981) Leukotrienes promote plasma leakage and leukocyte adhesion in postcapillary venules: in vivo effects with relevance to the acute inflammatory response, *Proceedings of the National Academy of Sciences of the United States of America 78*, 3887-3891.

64. Serhan, C. N. (2002) Lipoxins and aspirin-triggered 15-epi-lipoxin biosynthesis- an update and role in anti-inflammation and pro-resolution, *Prostaglandins & other lipid mediators*, 433-455.

65. Clish, C. B., Levy, B. D., Chiang, N., Tai, H. H., and Serhan, C. N. (2000) Oxidoreductases in lipoxin A4 metabolic inactivation: a novel role for 15-onoprostaglandin 13-reductase/leukotriene B4 12-hydroxydehydrogenase in inflammation, *The Journal of biological chemistry 275*, 25372-25380.

66. Basil, M. C., and Levy, B. D. (2016) Specialized pro-resolving mediators: endogenous regulators of infection and inflammation, *Nature reviews. Immunology 16*, 51-67.

67. Dangi, B., Obeng, M., Nauroth, J. M., Teymourlouei, M., Needham, M., Raman, K., and Arterburn, L. M. (2009) Biogenic synthesis, purification, and chemical characterization of anti-inflammatory resolvins derived from docosapentaenoic acid (DPAn-6), *The Journal of biological chemistry 284*, 14744-14759.

68. Serhan, C. N., Gotlinger, K., Hong, S., and Arita, M. (2004) Resolvins, docosatrienes, and neuroprotectins, novel omega-3-derived mediators, and their aspirin-triggered endogenous epimers: an overview of their protective roles in catabasis, *Prostaglandins & other lipid mediators 73*, 155-172.

69. Ariel, A., Li, P. L., Wang, W., Tang, W. X., Fredman, G., Hong, S., Gotlinger, K. H., and Serhan, C. N. (2005) The docosatriene protectin D1 is produced by TH2 skewing and promotes human T cell apoptosis via lipid raft clustering, *The Journal of biological chemistry 280*, 43079-43086.

70. Ariel, A., and Serhan, C. N. (2007) Resolvins and protectins in the termination program of acute inflammation, *Trends Immunol 28*, 176-183.

71. Badr, K. F., DeBoer, D. K., Schwartzberg, M., and Serhan, C. N. (1989) Lipoxin A4 antagonizes cellular and in vivo actions of leukotriene D4 in rat glomerular mesangial cells: evidence for competition at a common receptor, *Proceedings of the National Academy of Sciences of the United States of America 86*, 3438-3442.

72. Chiang, N., Fredman, G., Backhed, F., Oh, S. F., Vickery, T., Schmidt, B. A., and Serhan, C. N. (2012) Infection regulates pro-resolving mediators that lower antibiotic requirements, *Nature 484*, 524-528.

73. Dona, M., Fredman, G., Schwab, J. M., Chiang, N., Arita, M., Goodarzi, A., Cheng, G., von Andrian, U. H., and Serhan, C. N. (2008) Resolvin E1, an EPA-derived mediator in whole blood, selectively counterregulates leukocytes and platelets, *Blood 112*, 848-855.

74. Elajami, T. K., Colas, R. A., Dalli, J., Chiang, N., Serhan, C. N., and Welty, F. K. (2016) Specialized proresolving lipid mediators in patients with coronary artery disease and their potential for clot remodeling, *FASEB journal : official publication of the Federation of American Societies for Experimental Biology 30*, 2792-2801.

75. Serhan, C. N., Jain, A., Marleau, S., Clish, C., Kantarci, A., Behbehani, B., Colgan, S. P., Stahl, G. L., Merched, A., Petasis, N. A., Chan, L., and Van Dyke, T. E. (2003) Reduced inflammation and tissue damage in transgenic rabbits overexpressing 15-lipoxygenase and endogenous anti-inflammatory lipid mediators, *J Immunol 171*, 6856-6865.

76. Pan, J. P., Zhang, H. Q., Wei, W., Guo, Y. F., Na, X., Cao, X. H., and Liu, L. J. (2011) Some subtypes of endocannabinoid/endovanilloid receptors mediate docosahexaenoic acid-induced enhanced spatial memory in rats, *Brain research 1412*, 18-27.

77. Park, C. K., Lu, N., Xu, Z. Z., Liu, T., Serhan, C. N., and Ji, R. R. (2011) Resolving TRPV1- and TNF-alpha-mediated spinal cord synaptic plasticity and inflammatory pain with neuroprotectin D1, *J Neurosci 31*, 15072-15085.

78. Lee, J. W., Huang, B. X., Kwon, H., Rashid, M. A., Kharebava, G., Desai, A., Patnaik, S., Marugan, J., and Kim, H. Y. (2016) Orphan GPR110 (ADGRF1) targeted by N-docosahexaenoylethanolamine in development of neurons and cognitive function, *Nature communications 7*, 13123.

79. Krishnamoorthy, S., Recchiuti, A., Chiang, N., Yacoubian, S., Lee, C. H., Yang, R., Petasis, N. A., and Serhan, C. N. (2010) Resolvin D1 binds human phagocytes with evidence for proresolving receptors, *Proceedings of the National Academy of Sciences of the United States of America 107*, 1660-1665.

80. Qu, Q., Xuan, W., and Fan, G. H. (2015) Roles of resolvins in the resolution of acute inflammation, *Cell biology international 39*, 3-22.

81. Dalli, J., Colas, R. A., and Serhan, C. N. (2013) Novel n-3 immunoresolvents: structures and actions, *Scientific reports 3*, 1940.

82. Dalli, J., Chiang, N., and Serhan, C. N. (2015) Elucidation of novel 13-series resolvins that increase with atorvastatin and clear infections, *Nature medicine 21*, 1071-1075.

83. Serhan, C. N., and Petasis, N. A. (2011) Resolvins and protectins in inflammation resolution, *Chem Rev 111*, 5922-5943.

84. Ohira, T., Arita, M., Omori, K., Recchiuti, A., Van Dyke, T. E., and Serhan, C. N. (2010) Resolvin E1 receptor activation signals phosphorylation and phagocytosis, *J Biol Chem 285*, 3451-3461.

85. Fredman, G., Oh, S. F., Ayilavarapu, S., Hasturk, H., Serhan, C. N., and Van Dyke, T. E. (2011) Impaired phagocytosis in localized aggressive periodontitis: rescue by Resolvin E1, *PloS one 6*, e24422.

86. Giera, M., Ioan-Facsinay, A., Toes, R., Gao, F., Dalli, J., Deelder, A. M., Serhan, C. N., and Mayboroda, O. A. (2012) Lipid and lipid mediator profiling of human synovial fluid in rheumatoid arthritis patients by means of LC-MS/MS, *Biochimica et biophysica acta 1821*, 1415-1424.

87. Hong, S., Gronert, K., Devchand, P. R., Moussignac, R. L., and Serhan, C. N. (2003) Novel docosatrienes and 17S-resolvins generated from docosahexaenoic acid in murine brain, human blood, and glial cells. Autacoids in anti-inflammation, *The Journal of biological chemistry 278*, 14677-14687.

88. Serhan, C. N., Gotlinger, K., Hong, S., Lu, Y., Siegelman, J., Baer, T., Yang, R., Colgan, S. P., and Petasis, N. A. (2006) Anti-inflammatory actions of neuroprotectin D1/protectin D1 and its natural stereoisomers: assignments of dihydroxy-containing docosatrienes, *J Immunol 176*, 1848-1859.

89. Serhan, C. N., Yang, R., Martinod, K., Kasuga, K., Pillai, P. S., Porter, T. F., Oh, S. F., and Spite, M. (2009) Maresins: novel macrophage mediators with potent antiinflammatory and proresolving actions, *The Journal of experimental medicine 206*, 15-23.

90. Deng, B., Wang, C. W., Arnardottir, H. H., Li, Y., Cheng, C. Y., Dalli, J., and Serhan, C. N. (2014) Maresin biosynthesis and identification of maresin 2, a new anti-inflammatory and pro-resolving mediator from human macrophages, *PloS one 9*, e102362.

91. Serhan, C. N., Dalli, J., Karamnov, S., Choi, A., Park, C. K., Xu, Z. Z., Ji, R. R., Zhu, M., and Petasis, N. A. (2012) Macrophage proresolving mediator maresin 1 stimulates tissue regeneration and controls pain, *FASEB journal : official publication of the Federation of American Societies for Experimental Biology 26*, 1755-1765.

92. Minor, W., Steczko, J., Stec, B., Otwinowski, Z., Bolin, J. T., Walter, R., and Axelrod, B. (1996) Crystal structure of soybean lipoxygenase L-1 at 1.4 A resolution, *Biochemistry 35*, 10687-10701.

93. Gillmor, S. A., Villasenor, A., Fletterick, R., Sigal, E., and Browner, M. F. (1997) The structure of mammalian 15-lipoxygenase reveals similarity to the lipases and the determinants of substrate specificity, *Nature structural biology 4*, 1003-1009.

94. Kobe, M. J., Neau, D. B., Mitchell, C. E., Bartlett, S. G., and Newcomer, M. E. (2014) The structure of human 15-lipoxygenase-2 with a substrate mimic, *The Journal of biological chemistry 289*, 8562-8569.

95. Xu, S., Mueser, T. C., Marnett, L. J., and Funk, M. O., Jr. (2012) Crystal structure of 12-lipoxygenase catalytic-domain-inhibitor complex identifies a substrate-binding channel for catalysis, *Structure 20*, 1490-1497.

96. Kuhn, H., Banthiya, S., and van Leyen, K. (2015) Mammalian lipoxygenases and their biological relevance, *Biochimica et biophysica acta 1851*, 308-330.

97. Boyington, J. C., Gaffney, B. J., and Amzel, L. M. (1993) The three-dimensional structure of an arachidonic acid 15-lipoxygenase, *Science 260*, 1482-1486.

98. Steczko, J., Donoho, G. P., Clemens, J. C., Dixon, J. E., and Axelrod, B. (1992) Conserved histidine residues in soybean lipoxygenase: functional consequences of their replacement, *Biochemistry 31*, 4053-4057.

99. Krieg, P., and Furstenberger, G. (2014) The role of lipoxygenases in epidermis, *Biochimica et biophysica acta 1841*, 390-400.

100. Boudreau, L. H., Bertin, J., Robichaud, P. P., Laflamme, M., Ouellette, R. J., Flamand, N., and Surette, M. E. (2011) Novel 5-lipoxygenase isoforms affect the biosynthesis of 5-lipoxygenase products, *FASEB journal : official publication of the Federation of American Societies for Experimental Biology 25*, 1097-1105.

101. Grechkin, A. (1998) Recent developments in biochemistry of the plant lipoxygenase pathway, *Progress in lipid research 37*, 317-352.

102. Mack, A. J., Peterman, T. K., and Siedow, J. N. (1987) Lipoxygenase isozymes in higher plants: biochemical properties and physiological role, *Isozymes 13*, 127-154.

103. Hawkins, D. J., and Brash, A. R. (1987) Eggs of the sea urchin, Strongylocentrotus purpuratus, contain a prominent (11R) and (12R) lipoxygenase activity, *The Journal of biological chemistry 262*, 7629-7634.

104. Hada, T., Swift, L. L., and Brash, A. R. (1997) Discovery of 5R-lipoxygenase activity in oocytes of the surf clam, Spisula solidissima, *Biochimica et biophysica acta 1346*, 109-119.

105. Brash, A. R. (1999) Lipoxygenases: occurrence, functions, catalysis, and acquisition of substrate, *The Journal of biological chemistry 274*, 23679-23682.

106. Kuhn, H., and Thiele, B. J. (1999) The diversity of the lipoxygenase family. Many sequence data but little information on biological significance, *FEBS letters 449*, 7-11.

107. Su, C., and Oliw, E. H. (1998) Manganese lipoxygenase. Purification and characterization, *The Journal of biological chemistry 273*, 13072-13079.

108. Porta, H., and Rocha-Sosa, M. (2001) Lipoxygenase in bacteria: a horizontal transfer event?, *Microbiology 147*, 3199-3200.

109. Brash, A. R., Boeglin, W. E., and Chang, M. S. (1997) Discovery of a second 15S-lipoxygenase in humans, *Proceedings of the National Academy of Sciences of the United States of America 94*, 6148-6152.

110. Jisaka, M., Kim, R. B., Boeglin, W. E., Nanney, L. B., and Brash, A. R. (1997) Molecular cloning and functional expression of a phorbol ester-inducible 8S-lipoxygenase from mouse skin, *The Journal of biological chemistry 272*, 24410-24416.

111. Adel, S., Karst, F., Gonzalez-Lafont, A., Pekarova, M., Saura, P., Masgrau, L., Lluch, J. M., Stehling, S., Horn, T., Kuhn, H., and Heydeck, D. (2016) Evolutionary alteration of ALOX15 specificity optimizes the biosynthesis of antiinflammatory and proresolving lipoxins, *Proceedings of the National Academy of Sciences of the United States of America 113*, E8006.

112. Horn, T., Adel, S., Schumann, R., Sur, S., Kakularam, K. R., Polamarasetty, A., Redanna, P., Kuhn, H., and Heydeck, D. (2015) Evolutionary aspects of lipoxygenases and genetic diversity of human leukotriene signaling, *Progress in lipid research 57*, 13-39.

113. Klein, A., Pappas, S. C., Gordon, P., Wong, A., Kellen, J., Kolin, A., Robinson, J. B., and Malkin, A. (1988) The effect of nonviral liver damage on the T-lymphocyte helper/suppressor ratio, *Clinical immunology and immunopathology 46*, 214-220.

114. Bylund, J., Kunz, T., Valmsen, K., and Oliw, E. H. (1998) Cytochromes P450 with bisallylic hydroxylation activity on arachidonic and linoleic acids studied with human recombinant enzymes and with human and rat liver microsomes, *The Journal of pharmacology and experimental therapeutics 284*, 51-60.

115. Kuhn, H. (2000) Structural basis for the positional specificity of lipoxygenases, *Postaglandins & other Lipid Mediators 62*, 255–270.

116. Schilstra, M. J., Veldink, G. A., and Vliegenthart, J. F. (1994) The dioxygenation rate in lipoxygenase catalysis is determined by the amount of iron (III) lipoxygenase in solution, *Biochemistry 33*, 3974-3979.

117. McGinley, C. M., and van der Donk, W. A. (2003) Enzymatic hydrogen atom abstraction from polyunsaturated fatty acids, *Chem Commun (Camb)*, 2843-2846.

118. Petersson, L. S., S; Martinus, C; Feiters, J; Vliegenthart, F.G. (1987) Magnetic susceptibility studies on yellow and anaerobically substrate-treated yellow soybean lipoxygenase-1, *Biochimica et Biophysica Acta (BBA) - Protein Structure and Molecular Enzymology 913*, 228-237.

119. Lehnert, N., and Solomon, E. I. (2003) Density-functional investigation on the mechanism of H-atom abstraction by lipoxygenase, *Journal of biological inorganic chemistry : JBIC : a publication of the Society of Biological Inorganic Chemistry 8*, 294-305.

120. Nagel, Z. D., and Klinman, J. P. (2006) Tunneling and dynamics in enzymatic hydride transfer, *Chemical reviews 106*, 3095-3118.

121. Michael H. Glickman, J. S. W. a. J. P. K. Extremely Large Isotope Effects in the Soybean Lipoxygenase-Linoleic Acid Reaction, *Journal of the American Chemical Society 116*, 793-794.

122. Nimrod Moiseyev, J. R., Michael H. Glickman. (1997) Reduction of Ferric Iron Could Drive Hydrogen Tunneling in Lipoxygenase Catalysis, *J. Am. Chem. Soc. 119*, 3853-3860.

123. Thorlakur Jonsson, M. H. G., and Shujun Sun, a. J. P. K. (1996) Experimental evidence for extensive tunneling of hydrogen in the lipoxygenase reaction: implications for enzyme catalysis, *Journal of the American Chemical Society 118*, 10319-10320.

124. Egmond, M. R., Veldink, G. A., Vliegenthart, J. F., and Boldingh, J. (1973) C-11 H-abstraction from linoleic acid, the rate-limiting step in lipoxygenase catalysis, *Biochemical and biophysical research communications 54*, 1178-1184.

125. Maas, R. L., and Brash, A. R. (1983) Evidence for a lipoxygenase mechanism in the biosynthesis of epoxide and dihydroxy leukotrienes from 15(S)-hydroperoxyicosatetraenoic acid by human platelets and porcine leukocytes, *Proceedings of the National Academy of Sciences of the United States of America 80*, 2884-2888.

126. Mashima, R., and Okuyama, T. (2015) The role of lipoxygenases in pathophysiology; new insights and future perspectives, *Redox biology 6*, 297-310.

127. Terano, T., Salmon, J. A., and Moncada, S. (1984) Biosynthesis and biological activity of leukotriene B5, *Prostaglandins 27*, 217-232.

128. Gilbert, N. C., Bartlett, S. G., Waight, M. T., Neau, D. B., Boeglin, W. E., Brash, A. R., and Newcomer, M. E. (2011) The structure of human 5-lipoxygenase, *Science 331*, 217-219.

129. Hammarberg, T., Reddy, K. V., Persson, B., and Radmark, O. (2002) Calcium binding to 5-lipoxygenase, *Advances in experimental medicine and biology 507*, 117-121.

130. Peters-Golden, M., and Brock, T. G. (2001) Intracellular compartmentalization of leukotriene synthesis: unexpected nuclear secrets, *FEBS letters 487*, 323-326.

131. Peters-Golden, M., and Brock, T. G. (2003) 5-lipoxygenase and FLAP, *Prostaglandins, leukotrienes, and essential fatty acids 69*, 99-109.

132. Smyrniotis, C. J., Barbour, S. R., Xia, Z., Hixon, M. S., and Holman, T. R. (2014) ATP allosterically activates the human 5-lipoxygenase molecular mechanism of arachidonic acid and 5(S)-hydroperoxy-6(E),8(Z),11(Z),14(Z)-eicosatetraenoic acid, *Biochemistry 53*, 4407-4419.

133. Gilbert, N. C., Rui, Z., Neau, D. B., Waight, M. T., Bartlett, S. G., Boeglin, W. E., Brash, A. R., and Newcomer, M. E. (2012) Conversion of human 5-lipoxygenase to a 15-lipoxygenase by a point mutation to mimic phosphorylation at Serine-663, *FASEB journal : official publication of the Federation of American Societies for Experimental Biology 26*, 3222-3229.

134. Jakschik, B. A., Harper, T., and Murphy, R. C. (1982) The 5-lipoxygenase and leukotriene forming enzymes, *Methods in enzymology 86*, 30-37.

135. Bui, P., Imaizumi, S., Beedanagari, S. R., Reddy, S. T., and Hankinson, O. (2011) Human CYP2S1 metabolizes cyclooxygenase- and lipoxygenase-derived eicosanoids, *Drug metabolism and disposition: the biological fate of chemicals 39*, 180-190.

136. Ivanov, I., Kuhn, H., and Heydeck, D. (2015) Structural and functional biology of arachidonic acid 15-lipoxygenase-1 (ALOX15), *Gene 573*, 1-32.

137. Schewe, T., Wiesner, R., and Rapoport, S. M. (1981) Lipoxygenase from rabbit reticulocytes, *Methods in enzymology 71 Pt C*, 430-441.

138. Sigal, E., Grunberger, D., Cashman, J. R., Craik, C. S., Caughey, G. H., and Nadel, J. A. (1988) Arachidonate 15-lipoxygenase from human eosinophil-enriched leukocytes: partial purification and properties, *Biochemical and biophysical research communications 150*, 376-383.

139. Sigal, E., Dicharry, S., Highland, E., and Finkbeiner, W. E. (1992) Cloning of human airway 15-lipoxygenase: identity to the reticulocyte enzyme and expression in epithelium, *The American journal of physiology 262*, L392-398.

140. Werner, M., Jordan, P. M., Romp, E., Czapka, A., Rao, Z., Kretzer, C., Koeberle, A., Garscha, U., Pace, S., Claesson, H. E., Serhan, C. N., Werz, O., and Gerstmeier, J. (2019) Targeting biosynthetic networks of the proinflammatory and proresolving lipid metabolome, *FASEB journal : official publication of the Federation of American Societies for Experimental Biology 33*, 6140-6153.

141. Conrad, D. J., Kuhn, H., Mulkins, M., Highland, E., and Sigal, E. (1992) Specific inflammatory cytokines regulate the expression of human monocyte 15-lipoxygenase, *Proceedings of the National Academy of Sciences of the United States of America 89*, 217-221.

142. Hulten, L. M., Olson, F. J., Aberg, H., Carlsson, J., Karlstrom, L., Boren, J., Fagerberg, B., and Wiklund, O. (2010) 15-Lipoxygenase-2 is expressed in macrophages in human carotid plaques and regulated by hypoxia-inducible factor-1alpha, *Eur J Clin Invest 40*, 11-17.

143. Gertow, K., Nobili, E., Folkersen, L., Newman, J. W., Pedersen, T. L., Ekstrand, J., Swedenborg, J., Kuhn, H., Wheelock, C. E., Hansson, G. K., Hedin, U., Haeggstrom, J. Z., and Gabrielsen, A. (2011) 12- and 15-lipoxygenases in human carotid atherosclerotic lesions: associations with cerebrovascular symptoms, *Atherosclerosis 215*, 411-416.

144. Wuest, S. J., Crucet, M., Gemperle, C., Loretz, C., and Hersberger, M. (2012) Expression and regulation of 12/15-lipoxygenases in human primary macrophages, *Atherosclerosis 225*, 121-127.

145. Hamberg, M., and Samuelsson, B. (1974) Prostaglandin endoperoxides. Novel transformations of arachidonic acid in human platelets, *Proceedings of the National Academy of Sciences of the United States of America 71*, 3400-3404.

146. Pace-Asciak, C. R. (2015) Pathophysiology of the hepoxilins, *Biochimica et biophysica acta 1851*, 383-396.

147. Yeung, J., and Holinstat, M. (2017) Who is the real 12-HETrE?, *Prostaglandins & other lipid mediators 132*, 25-30.

148. Heydeck, D., Thomas, L., Schnurr, K., Trebus, F., Thierfelder, W. E., Ihle, J. N., and Kuhn, H. (1998) Interleukin-4 and -13 induce upregulation of the murine macrophage 12/15-lipoxygenase activity: evidence for the involvement of transcription factor STAT6, *Blood 92*, 2503-2510.

149. Munoz-Garcia, A., Thomas, C. P., Keeney, D. S., Zheng, Y., and Brash, A. R. (2014) The importance of the lipoxygenase-hepoxilin pathway in the mammalian epidermal barrier, *Biochimica et biophysica acta 1841*, 401-408.

150. Schneider, C., and Brash, A. R. (2002) Lipoxygenase-catalyzed formation of R-configuration hydroperoxides, *Prostaglandins & other lipid mediators 68-69*, 291-301.

151. Zheng, Y., Yin, H., Boeglin, W. E., Elias, P. M., Crumrine, D., Beier, D. R., and Brash, A. R. (2011) Lipoxygenases mediate the effect of essential fatty acid in skin barrier formation: a proposed role in releasing omega-hydroxyceramide for construction of the corneocyte lipid envelope, *The Journal of biological chemistry 286*, 24046-24056.

152. Capra, V., Rovati, G. E., Mangano, P., Buccellati, C., Murphy, R. C., and Sala, A. (2015) Transcellular biosynthesis of eicosanoid lipid mediators, *Biochimica et biophysica acta 1851*, 377-382.

153. Serhan, C. N., and Sheppard, K. A. (1990) Lipoxin formation during human neutrophil-platelet interactions. Evidence for the transformation of leukotriene A4 by platelet 12-lipoxygenase in vitro, *Journal of Clinical Investigation 85*, 772-780.

154. Sala, A., Testa, T., and Folco, G. (1996) Leukotriene A4, and not leukotriene B4, is the main 5-lipoxygenase metabolite released by bovine leukocytes, *FEBS Lett 388*, 94-98.

155. Norris, P. C., and Serhan, C. N. (2018) Metabololipidomic profiling of functional immunoresolvent clusters and eicosanoids in mammalian tissues, *Biochem Biophys Res Commun 504*, 553-561.

156. Moriyama, T., Higashi, T., Togashi, K., Iida, T., Segi, E., Sugimoto, Y., Tominaga, T., Narumiya, S., and Tominaga, M. (2005) Sensitization of TRPV1 by EP1 and IP reveals peripheral nociceptive mechanism of prostaglandins, *Molecular pain 1*, 3.

157. AL Blower, A. B., CG Fenn et al. (1997) Emergency admissions for upper gastrointestinal disease and their relation to NSAID use, *Aliment Pharmacol Ther*, 283-291.

158. KIM Antonov, D. I. (1998 gastropathy in medical practice. Annals of Internal Medicine 1997 127: 429-38.) Prescription and nonprescription analgesic use in Sweden, *Annals of Pharmacotherapy 32*, 485-494.

159. R Tamblyn, L. B., WD Dauphinee et al. . (1997) Unnecessary prescribing of NSAIDs and the management of NSAID-related gastropathy in medical practice, *Annals of Internal Medicine 127*, 429-438.

160. Laufer, S. (2003) Role of eicosanoids in structural degradation in osteoarthritis, *Current opinion in rheumatology 15*, 623-627.

161. Fanning, L. B., and Boyce, J. A. (2013) Lipid mediators and allergic diseases, *Annals of allergy, asthma & immunology : official publication of the American College of Allergy, Asthma, & Immunology 111*, 155-162.

162. Scott, J. P., and Peters-Golden, M. (2013) Antileukotriene agents for the treatment of lung disease, *American journal of respiratory and critical care medicine 188*, 538-544.

163. Albert, D., Zundorf, I., Dingermann, T., Muller, W. E., Steinhilber, D., and Werz, O. (2002) Hyperforin is a dual inhibitor of cyclooxygenase-1 and 5-lipoxygenase, *Biochemical pharmacology 64*, 1767-1775.

164. Bishayee, K., and Khuda-Bukhsh, A. R. (2013) 5-lipoxygenase antagonist therapy: a new approach towards targeted cancer chemotherapy, *Acta biochimica et biophysica Sinica 45*, 709-719.

165. Deschamps, J. D., Kenyon, V. A., and Holman, T. R. (2006) Baicalein is a potent in vitro inhibitor against both reticulocyte 15-human and platelet 12-human lipoxygenases, *Bioorganic & medicinal chemistry 14*, 4295-4301.

166. Rai, G., Kenyon, V., Jadhav, A., Schultz, L., Armstrong, M., Jameson, J. B., Hoobler, E., Leister, W., Simeonov, A., Holman, T. R., and Maloney, D. J. (2010) Discovery of potent and selective inhibitors of human reticulocyte 15-lipoxygenase-1, *J Med Chem 53*, 7392-7404.

167. Hoobler, E. K., Rai, G., Warrilow, A. G., Perry, S. C., Smyrniotis, C. J., Jadhav, A., Simeonov, A., Parker, J. E., Kelly, D. E., Kelly, S. L., and Holman, T. R. (2011) Discovery of a novel dual fungal cyp51/human 5-lipoxygenase inhibitor: Implications for anti-fungal therapy, *Antimicrobial Agents and Chemotherapy*, Submitted.

168. Furie, B., and Furie, B. C. (2005) Thrombus formation in vivo, *The Journal of clinical investigation 115*, 3355-3362.

169. Ikei, K. N., Yeung, J., Apopa, P. L., Ceja, J., Vesci, J., Holman, T. R., and Holinstat, M. (2012) Investigations of human platelet-type 12-lipoxygenase: role of lipoxygenase products in platelet activation, *Journal of lipid research 53*, 2546-2559.

170. Dubois, C., Panicot-Dubois, L., Merrill-Skoloff, G., Furie, B., and Furie, B. C. (2006) Glycoprotein VI-dependent and -independent pathways of thrombus formation in vivo, *Blood 107*, 3902-3906.

171. Murugappa, S., and Kunapuli, S. P. (2006) The role of ADP receptors in platelet function, *Frontiers in bioscience : a journal and virtual library 11*, 1977-1986.

172. Coughlin, S. R. (2000) Thrombin signalling and protease-activated receptors, *Nature 407*, 258-264.

173. Farrow, J. W., and Willis, A. L. (1975) Proceedings: Thrombolytic and anti-thrombotic properties of dihomo-gamma-linolenate in vitro, *British journal of pharmacology 55*, 316P-317P.

174. Kernoff, P. B., Willis, A. L., Stone, K. J., Davies, J. A., and McNicol, G. P. (1977) Antithrombotic potential of dihomo-gamma-linolenic acid in man, *British medical journal 2*, 1441-1444.

Chapter 2

ALTERED POSITIONAL SPECIFICITY OF 15-LIPOXYGENASE-1 IN THE BIOSYNTHESIS OF 7S,14S-DI-HDHA IMPLICATES 15-LIPOXYGENASE-2 IN BIOSYNTHESIS OF RESOLVIN D5

2.1 Introduction

Inflammation plays an essential role in protecting the body from tissue injury and foreign pathogens. In its acute form, it involves the up-regulation of localized inflammatory signaling molecules and cytokines that attract neutrophils to an area of injury (*1*). Over time, an area of injury begins producing specialized pro-resolving mediators (SPM's), which actively down-regulate the immune response (*2*), a process referred to as the resolution of inflammation. Mis-regulation of the transition to resolution can extend the early beneficial effects of acute inflammation into the damaging effects of chronic inflammation. This can contribute to cardiovascular disease (*3-5*), diabetes (*6, 7*) and autoimmune disorders (*8*), to name a few examples.

SPM's are oxylipins produced by the oxygenation of fatty acids by cyclooxygenases, lipoxygenases and cytochrome P450s (*9*). Humans have multiple non-heme iron lipoxygenases that catalyze the stereospecific peroxidation of polyunsaturated fatty acids containing a bisallylic carbon moiety (*10*). The focus of this work are the two 15-LOX isozymes, human reticulocyte 15-lipoxygenase-1 (h15-LOX-1 or ALOX15), primarily expressed in reticulocytes and macrophages, (*11, 12*), and human epithelial 15-lipoxygenase-2 (h15-LOX-2 or ALOX15b), expressed in macrophages, neutrophils, skin, hair roots and prostate. (*3, 13, 14*) They are named for their ability to stereo-specifically oxygenate at C15 of arachidonic acid (AA) (*10*). h15-LOX-1 converts AA into a mixture of approximately 90% 15(S)-hydroperoxy-5Z,8Z,11Z,13Z-eicosatetraenoic acid (15S-HpETE) and 10% 12(S)-hydroperoxy-5Z,8Z,10E,14Z-eicosatetraenoic acid (12S-HpETE), while h15-LOX-2 oxygenates

substrates with strict regiospecificity (*15*), producing 15-HpETE from AA. h15-LOX-1 is implicated in many diseases, such as inflammation, stroke, colorectal cancer, and atherosclerosis (*11*). h15-LOX-2, however, has only recently been identified as playing a role in atherosclerosis and inflammation (*4, 16*).

Many SPM's are synthesized at sites of inflammation and function in a paracrine or autocrine fashion. maresin 1 (7(R),14(S)-dihydroxy-4Z,8E,10E,12Z,16Z,19Z docosahexaenoic acid, MaR1) is a SPM made from docosahexanoic acid (DHA)(*17*), and plays a role in the resolution of inflammation by reducing neutrophil chemotaxis and platelet aggregation and increasing phagocytosis in leukocytes(*18*). In conjunction with the detection of MaR1 in cell extracts, Serhan and co-workers discovered three analogues of MaR1, 7-epi-MaR1 (7S,14S-dihydroxy-4Z,8E,10E,12Z,16Z,19Z docosahexaenoic acid), 7(R),14(S)-dihydroxy-4Z,8E,10E,12E,16Z,19Z docosahexaenoic acid (i.e. *EEE*-MaR1), and 7(S),14(S)-dihydroxy 4Z,8E,10Z,12E,16Z,19Z docosahexaenoic acid (7S,14S-diHDHA, **Figure 2.1**) (*17*). These three analogues were characterized as having biological macrophage activity, but not as great as that of MaR1. In particular, 7S,14S-diHDHA appeared to be biosynthesized in a di-oxygenation fashion without an epoxide intermediate, distinct from the other analogues. Its structure suggests that it is synthesized through two sequential LOX oxygenation reactions at C7 and C14, without the requirement of a hydrolase to open the epoxide intermediate (*19-21*). Given these oxygenation sites, as well as the enzymatic preferences of specific LOX isozymes, it is reasonable to assume that the biosynthesis of 7S,14S-diHDHA

involves h5-LOX oxidizing DHA at C7, with h12-LOX oxidizing at C14, but it is unclear which oxidation occurs first (Scheme 1, Pathway 2).

The other SPM which is of importance with regard to this work is resolvin D5 (RvD5 or 7(S),17(S)-dihydroxy 4Z,8E,10Z,13Z,15E,19Z docosahexaenoic acid (7S,17S-diHDHA), **Figure 2.1**). RvD5 is a D-series resolvin made from DHA (*22*), and has at has been identified in human blood, hemorrhagic exudates and synovial fluid (*23, 24*). RvD5 enhances phagocytosis in neutrophils and macrophages and reduces expression of the pro-inflammatory molecules, NF-κB and TNF-α (*25*). Like 7S,14S-diHDHA, the production of RvD5 appears to require two oxygenation events and is proposed to occur through the sequential reaction of two lipoxygenases (*24, 26*). Since many cell types contain only a single lipoxygenase, oxylipins with multiple oxygenation sites are often created by the interaction of multiple cell types in an area of inflammation through a process called transcellular biosynthesis (*27-29*). RvD5 has been isolated from neutrophils (*30*) and is produced late in the process of blood coagulation, increasing over the lifetime of a clot (*31*). PMN's have been shown to convert 17(S)-dihydroxy 4Z,7Z,10Z,13Z,15E,19Z docosahexaenoic acid (17S-HDHA) into 4(S),17(S)-dihydroxy 5E,7Z,10Z,13Z,15E,19Z docosahexaenoic acid (4S,17S-HDHA) and RvD5,(*24*), suggesting that h5-LOX reacts with 17-HDHA to produce RvD5.

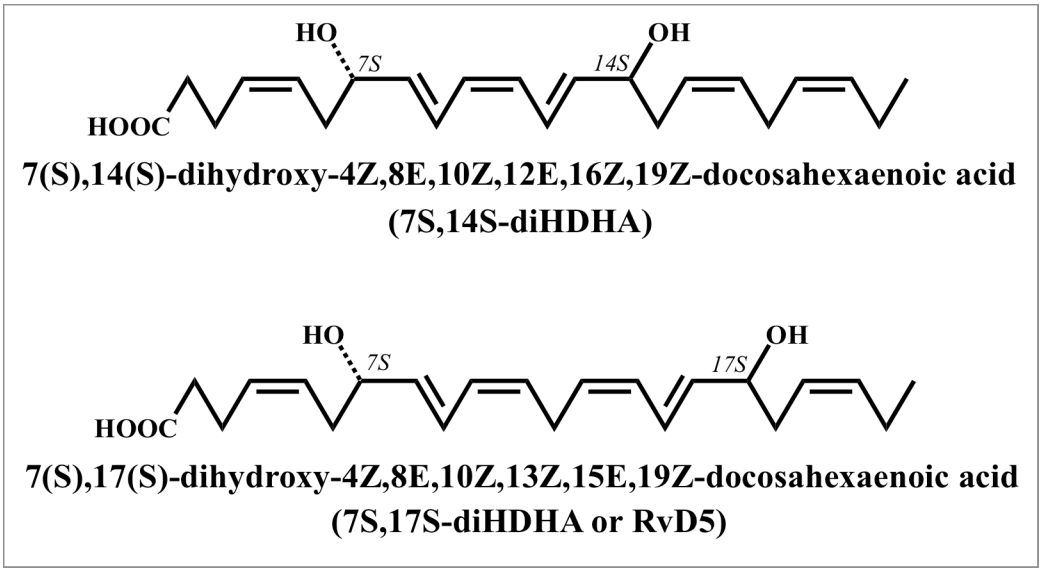

Figure 2.1. Structures of 7(S),14(S)-dihydroxy-4Z,8E,10Z,12E,16Z,19Z-docosahexaenoic acid (7S,14S-diHDHA), and 7(S),17(S)-dihydroxy-4Z,8E,10Z,13Z,15E,19Z-docosahexaenoic acid (7S,17S-diHDHA or RvD5). Note that the molecules are drawn with an artificial straight chain shape in order to highlight their similarities and differences more clearly.

As stated above, LOX isozymes play a key role in the biosynthesis of SPMs, however, the biosynthetic molecular mechanism for specific SPMs is poorly defined. For 7S,14S-diHDHA, the current understanding of its biosynthetic pathway is based on the substrate specificity of h5-LOX and h12-LOX with AA, and experimental evidence that the LOX inhibitor, baicalein reduces the production of MaR1 and 14(S)-dihydroxy 4Z,7Z,10Z,12E,16Z,19Z docosahexaenoic acid (14S-HDHA)(*32*). However, baicalein is not a selective inhibitor (*33*) and it is well recognized that LOXs can produce different products depending on the fatty acids or oxylipin used (*34*). For example, h5-LOX produces primarily 5(S)-hydroperoxy-6E,8Z,11Z,14Z-eicosatetraenoic acid (5S-HpETE) from AA, but it produces multiple products when DHA is the substrate (*35*), presumably due to the length and unsaturation differences

which affect substrate positioning for hydrogen atom abstraction. LOX's also vary widely in their ability to tolerate oxygenated substrates, as reflected in their kinetic parameters (*19*). In addition, the specific hydrogen atom abstracted can be affected by the nature of the substrate (*34*). h5-LOX abstracts a hydrogen atom from C7 of AA to produce 5S-HpETE, but it can subsequently abstract from C10 from 5S-HpETE to produce the 5,6-epoxide (*36*). This variability in product distribution is also seen with h15-LOX-1, where approximately 10% of the product made from AA is 12S-HpETE, the non-canonical product. Kuhn and coworkers proposed that this lack of specificity is linked to human evolution and specifically the human inflammatory response, with only higher primates having this LOX function (*37*). This ability of h15-LOX-1 to abstract hydrogen atoms from either C15 or C12 raises the possibility that h15-LOX-1 could also generate 7S,14S-diHDHA (*37*), as shown in Scheme 1, Pathway 3.

For RvD5, the generally accepted biosynthetic pathway is through transcellular biosynthesis, but a specific biosynthetic sequence has not been clearly identified. One proposed pathway is that h5-LOX, expressed in macrophages (*38, 39*) and PMN's(*24*), produces 7(S)-hydroxy-4Z,8E,10Z,13Z,16Z,19Z-docosahexaenoic acid (7S-HDHA) from DHA, and then h15-LOX-1 reacts with 7S-HDHA to produce RvD5 by oxidation at C17. This is a reasonable assumption since h15-LOX-1 oxygenates C17 of DHA efficiently; however, h15-LOX-2 is expressed at higher levels than h15-LOX-1 in both neutrophils and macrophages (*4, 13, 40*), so it is possible that h15-LOX-2, and not h15-LOX-1, may be involved in the formation of RvD5 from 7S-HDHA (Scheme 1). It should be noted that LOXs produce the

hydroperoxy product, but the reducing environment of the cell quickly reduces them to the hydroxy products (*41*), such as 7S,14S-diHDHA and 7S,17S-diHDHA (RvD5).

Given the biological importance of SPMs, such as 7S,14S-diHDHA and 7S,17S-diHDHA (RvD5), and the multiple possible biosynthetic pathways for their production, we investigated two critical aspects of the biosynthetic routes to producing these two SPMs: the ease of which LOXs can perform the proposed reactions *in vitro* (i.e. kinetics), and the specificity of LOXs when the substrate is an oxylipin, as opposed to the un-oxidized fatty acid. We probed these effects in the production of both 7S,14S-diHDHA and 7S,17S-diHDHA (RvD5) and determined that not only are the rates greatly affected by the nature of the oxylipin substrate, but also the product profile is altered with oxygenation of the fatty acid, raising the possibility that non-canonical LOXs may be involved in SPM production.

2.2 Experimental Procedures

2.2.1 Expression and Purification of h15-LOX-1, h15-LOX-2, h12-LOX, and h5-LOX.

Overexpression and purification of wild-type h15-LOX-1 (Uniprot entry P16050), h12-LOX (Uniprot entry P18054), h5-LOX (Uniprot entry P09917) and h15-LOX-2 (Uniprot entry O15296) were performed as previously described(*73-75*). The purity of h15-LOX-1 and h12-LOX were assessed by SDS gel to be greater than 85%, and metal content was assessed on a Finnigan inductively-coupled plasma-mass spectrometer (ICP-MS), via comparison with iron standard solution. Cobalt-EDTA

was used as an internal standard. The wt h5-LOX used in the kinetics of this work was not purified due to a dramatic loss in activity. Therefore, the amount of h5-LOX contained in the ammonium-sulfate pellet was assessed by comparing values obtained by a Bradford assay and quantitative western blotting using purified stable-h5-LOX mutant as a positive control. Western blots were performed using rabbit anti-5-lipoxygenase polyclonal (Cayman chemicals) primary antibody diluted 1:500 and goat anti-rabbit-HRP (Abcam) secondary antibody diluted 1:5000. The stable-h5-LOX mutant was expressed in Rosetta 2 cells (Novagen) transformed with the pET14b-Stable-5-LOX plasmid (a gift from Marcia Newcomer of Louisiana State University) and grown in Terrific Broth containing 34 μg mL^{-1} chloramphenicol and 100 μg mL^{-1} ampicillin at 37 °C for 3.5 h and then placed at 20 °C for an additional 26 h. Cells were pelleted and re-suspended in 50 mM Tris (pH 8.0), 500 mM NaCl, 20 mM imidazole with 1 μM Pepstatin, 100 μM PMSF, and DNaseI (2 Kunitz/g) (Sigma). The cells were lysed in a French pressure cell and centrifuged at 40,000xg for 20min. Lysate was applied to a Talon nickel-IDA Sepharose column and eluted with 50 mM Tris pH 8.0, 500 mM NaCl, 200 mM imidazole. The final product was stored at −80 °C with 10% glycerol.

2.2.2 Production and isolation of oxylipins.

7(S)-hydroperoxy-4Z,8E,10Z,13Z,16Z,19Z-docosahexaenoic acid (7S-HpDHA) was synthesized by reaction of DHA (25-50 μM) with h5-LOX. The reaction was carried out for 2 hours in 800 mL of 25mM HEPES, pH 7.5 containing

50 mM NaCl, 100 μM EDTA and 200 μM ATP. The reaction was quenched with 0.5% glacial acetic acid, extracted 3 times with 1/3 volume dichloromethane and evaporated to dryness under N2. The Products were purified isocratically via high performance liquid chromatography (HPLC) on a Higgins Haisil Semi-preparative (5 μm, 250 mm x 10 mm) C18 column with 45:55 of 99.9% acetonitrile, 0.1% acetic acid and 99.9% water, 0.1% acetic acid. 7(S)-hydroxy-4Z,8E,10Z,13Z,16Z,19Z-docosahexaenoic acid (7S-HDHA) was synthesized as performed for 7S-HpDHA with trimethylphosphite added as a reductant prior to HPLC. 7S,14S-diHDHA was synthesized by reaction of 20 μM 7S-HDHA with h15-LOX-1 in 300 mL of 25mM HEPES, pH 7.5 and purified as described above. 14(S)-hydroperoxy 4Z,7Z,10Z,12E,16Z,19Z-docosahexaenoic acid (14S-HpDHA) was synthesized by reaction of DHA (25-50 μM) with h12-LOX. The reaction was carried out for 30 minutes in 1000 mL of 25 mM HEPES, pH 8.0 The reaction was quenched with 0.5% glacial acetic acid, extracted 3 times with 1/3 volume dichloromethane and evaporated to dryness under N2. The Products were purified isocratically via HPLC on a Phenomenex Luna semi-preparative (5μm, 250mm x 10mm) silica column with 99:1 of 99.9% hexane, 0.1% trifluoroacetic acid and 99.9% isopropanol, 0.1% trifluoroacetic acid. 14(S)-hydroxy 4Z,7Z,10Z,12E,16Z,19Z-docosahexaenoic acid (14S-HDHA) was synthesized as performed for 14S-HpDHA with trimethylphosphite added as a reductant prior to HPLC. 17(S)-hydroperoxy 4Z,7Z,10Z,13Z,15E,19Z-docosahexaenoic acid (17S-HpDHA) was synthesized by reaction of DHA (25-50 μM) with soybean 15-LOX. The reaction was carried out for 1 hour in 800 mL of 100

mM Borate, pH 9.0. 17S-HDHA was synthesized by reducing 17S-HpDHA with trimethylphosphite, prior to HPLC. 7(S),17(S)-dihydroxy docosahexaenoic acid (7S,17S-diHDHA or RvD5) was synthesized by reacting 7S-HDHA (20 μM) with h15-LOX-2 in 300 mL of 25 mM HEPES, pH 7.5, with subsequent reduction/purification, as described above. The isolated products were assessed to be greater than 95% pure by LC-MS/MS.

2.2.3 Steady State Kinetics of h15-LOX-1 and h12-LOX with DHA, 7S-HDHA and 7S-HpDHA.

h15-LOX-1 reactions were performed, at ambient temperature, in a 1 cm^2 quartz cuvette containing 2 mL of 25 mM HEPES, pH 7.5 with substrate (DHA, 7S-HDHA or 7S-HpDHA). DHA concentrations were varied from 0.25-10 μM, 7S-HDHA concentrations were varied from 0.3-15 μM and 7S-HpDHA concentrations were varied from 0.3-20 μM. Concentration of DHA was determined by measuring the amount of 17S-HpDHA produced from complete reaction with soybean lipoxygenase-1 (sLO-1). Concentrations of 7S-HDHA and 7S-HpDHA were determined by measuring the absorbance at 234 nm. Reactions were initiated by the addition ~200 nM h15-LOX-1 and were monitored on a Perkin-Elmer Lambda 45 UV/VIS spectrophotometer. Product formation was determined by the increase in absorbance at 234 nm for 7S-HpDHA (ε_{234nm} = 25,000 M^{-1} cm^{-1}) and 270 nm for 7S,14S-diHDHA (ε_{270nm} = 40,000 M^{-1} cm^{-1})(*32, 76, 77*). 7S,17S-diHDHA has an absorbance max of 245 nm, however, due to overlap with the substrate peak at 234

nm formation of this product was measured at 254 nm using an extinction coefficient of 21,900 M^{-1} cm^{-1} to adjust for the decreased rate of absorbance change at this peak shoulder (*19*). KaleidaGraph (Synergy) was used to fit initial rates (at less than 20% turnover), as well as the second order derivatives (k_{cat}/K_M) to the Michaelis-Menten equation for the calculation of kinetic parameters. h12-LOX reactions were performed similarly as for h15-LOX-1 except that buffers were 25 mM HEPES, pH 8 and reactions were initiated by the addition ~50 nM h12-LOX.

2.2.4 Steady State Kinetics of h5-LOX with DHA, 14S-HDHA and 14S-HpDHA.

All h5-LOX kinetic reactions were carried out in 25mM HEPES, pH 7.5 containing 50mM NaCl, 100 μM EDTA and 200 mM ATP. Steady state kinetic values of h5-LOX with DHA were determined as for h15-LOX-1. V_{max} of h5-LOX with 14S-HDHA and 14S-HpDHA were performed in 2 mL quartz cuvettes containing 2 mL of buffer and 10 μM substrate. Reactions were initiated by the addition ~200 nM ammonium sulfate-precipitated h5-LOX and were monitored on a Perkin-Elmer Lambda 45 UV/VIS spectrophotometer. Product formation was determined by the increase in absorbance at 270 nm for 7S,14S-diHDHA (ε_{270nm} = 40,000 M^{-1} cm^{-1}) and 254 nm for 7S,17S-diHDHA (ε_{254nm} = 21,900 M^{-1} cm^{-1}). (*19, 32, 41, 76, 77*), Reactions were quenched at 0, 5, 10, 20, 30 and 60 minutes, extracted and analyzed via LCMS as described for product profiling experiments. MS2 integrated peak areas were normalized to a 13-HODE internal standard and fitted to determine V_{max}. The catalytic activity relative to protein weight for h5-LOX was

calculated by comparing V_{max} to protein concentration which was determined by quantitative western, described above. For comparison of biosynthetic flux with h5-LOX, K_{cat} values for each enzyme and substrate were converted to V_{max} at 10 μM using the Michaelis-Menten equation and then multiplied by the percentage of total product represented by each reaction product.

2.2.5 Steady State Kinetics of h15-LOX-2 with DHA, 7S-HDHA & 7S-HpDHA.

h15-LOX-2 reactions were performed, at room temperature, in a 1 cm^2 quartz cuvette containing 2 mL of 25 mM HEPES, pH 7.5 with substrate (DHA, 7S-HDHA and 7S-HpDHA.) DHA concentrations were varied from 0.2-15 μM, 7S-HDHA concentrations were varied from 0.6-30 μM, 7S-HpDHA concentrations were varied from 0.6-25 μM. The concentration of DHA was determined by measuring the amount of 17S-HpDHA produced from complete reaction with soybean lipoxygenase-1 (sLO-1). Concentrations of 7S-HDHA and 7S-HpDHA were determined by measuring absorbance at 234 nm. Reactions were initiated by the addition h15-LOX-2 (~220 nM final concentration) and were monitored on a Perkin-Elmer Lambda 45 UV/VIS spectrophotometer. Product formation was determined by the change in absorbance at 234 nm for 7S-HDHA (ε_{234nm} = 25,000 M^{-1} cm^{-1}), 270 nm for 7S,14S-diHDHA (ε_{270nm} = 40,000 M^{-1} cm^{-1}), and 254 nm for 7S,17S-diHDHA (ε_{254nm} = 21,900 M^{-1} cm^{-1}) (*19, 32, 76, 77*),. KaleidaGraph (Synergy) was used to fit initial rates (at less than 20% turnover), as well as the second order derivatives (k_{cat}/K_M) to the Michaelis-Menten equation for the calculation of kinetic parameters.

2.2.6 Product Analysis of LOX reactions.

Reactions were carried out in 2 mL of 25 mM HEPES, pH 7.5 with stirring at ambient temperature. Reactions with DHA and AA contained 10 μM substrate and ~200 nM h15-LOX-1 and h15-LOX-2. Those with 7S-HDHA, 7S-HpDHA, 14S-HDHA and 14S-HpDHA contained 20 μM substrate and ~600 nM h15-LOX-1. Those with 7S-HDHA, 7S-HpDHA, 17S-HDHA and 17S-HDHA contained 4 mL of buffer, 10 μM substrate and ~450 nM of h15-LOX-2. Reactions were monitored via UV-vis spectrophotometer and quenched at 50% turnover with 0.5% glacial acetic acid. Each quenched reaction was extracted with 6 mL of DCM and reduced with trimethylphosphite. The samples were then evaporated under a stream of N_2 to dryness and reconstituted in 50 μL of methanol containing 3 μM 13-HODE as an internal standard. Control reactions without enzymes were also conducted and used for background subtraction, ensuring oxylipin degradation products were removed from analysis. Reactions were analyzed via LC-MS/MS. The chromatography system was coupled to a Thermo-Electron LTQ LC-MS/MS for mass analysis. All analyses were performed in negative ionization mode at the normal resolution setting. MS2 was performed in a targeted manner with a mass list containing the following m/z ratios ± 0.5: 343.4 (HDHA's), 359.4 (diHDHA's), and 375.4 (triHDHA's). Products were identified by matching retention times, UV spectra, and fragmentation patterns to known standards, or in the cases were MS standards were not available, structures were deduced from comparison with known and theoretical fragments.

2.2.7 Chiral Chromatography.

7S,14S-diHDHA and 7S,17S-diHDHA were synthesized by 15-LOX-1 and 15-LOX-2, respectively and isolated via HPLC as described above. 7S,14S-diHDHA produced by 5-LOX was synthesized in 15 mL of buffer containing 10 μM 14S-HDHA and ~6 μM of ammonium-sulfate precipitated h5-LOX. Purified 7S,14S-diHDHA and 7S,17S-diHDHA were analyzed via LC-MS/MS using a Chirapak AD-RH 2.1 x 150 mm 5 μM chiral column coupled to a Thermo electron LTQ. Retention times and fragmentations were compared to RvD5, Mar1 and 7-epi-Mar standards purchased from Cayman Chemicals (Ann Arbor, MI) Analysis was carried out using a gradient from 40:60 A:B to 70:30 A:B, over 25 min. Mobile phase solvent A consisted of 99.9% acetonitrile, 0.1% formic acid and solvent B consisted of 99.9% water, 0.1% formic acid. MS/MS conditions were the same as described above.

2.2.8 Oxylipin titration into human platelets.

The University of Michigan Institutional Review Board approved all research involving human volunteers. Washed platelets were isolated from human whole blood via serial centrifugation and adjusted to 3.0 x 10^8 platelets/mL in Tyrode's buffer (10 mM HEPES, 12 mM $NaHCO_3$, 127 mM NaCl, 5 mM KCl, 0.5 mM NaH_2PO_4, 1 mM $MgCl_2$, and 5 mM glucose), as previously published. Platelets (250 μL at 3.0 x10^8 platelets/mL) were dispensed into glass cuvettes and incubated with the indicated oxylipin in half-log increments (0-10 μM) for 10 minutes at 37°C. Oxylipin-treated platelets were stimulated with 0.25 μg/mL of collagen (Chrono-log), under stirring

conditions (1100 rpm) at 37°C, in a Chrono-log Model 700D lumi-aggregometer and platelet aggregation was recorded for six minutes.

In order to determine if 7S-HDHA was enzymatically converted to another chemical *ex vivo*, one mL of platelets (1.0 x10^9 platelets/mL) was incubated with either 10 μM 7S-HDHA, 10 μM 5-HETE (positive control) or vehicle (DMSO) for 10 minutes at 37° C and then pelleted by centrifugation at 1000g for 2 minute. Supernatant was transferred to a fresh tube and snap frozen. Oxylipins were extracted and analyzed via UPLC-MS/MS, as described previously,[9] The m/z transitions for 7S-HDHA, 7S,14S-diHDHA, 7S,17S-diHDHA were 343.5→141, 359.5→141, 359.5→199, respectively.

2.2.9 Molecular Modeling.

A structure of h15-LOX-1 (ALOX15) is not available in the Protein Data Bank (PDB). Therefore, we constructed a homology model of h15-LOX-1 from its sequence (Uniprot ID: P16050) using the substrate mimetic inhibitor bound, high-resolution structure of porcine 12-LOX (PDB ID: 3rde). The h15-LOX-1 sequence is 86% identical to the porcine 12-LOX sequence, with both being considered ALOX15 genes. The homology model was constructed using Prime software (version 5.4, Schrodinger Inc). During the modeling step we retained the co-crystallized inhibitor, metal ion (Fe^{3+}), and a hydroxide ion that coordinated the metal ion from the homolog structure. The model was subsequently energy minimized using Protein Preparation Wizard module of Maestro (version 11.8, Schrodinger Inc). During this

step, hydrogen atoms were added to the protein, co-crystallized ligand and the hydroxide ion. Hydrogen atoms of the titratable residues were adjusted and side chains of Tyr, Thr, Ser, Asn and Gln were optimized so they could make better hydrogen bonding interactions. The structure was finally minimized such that the heavy atoms do not move beyond 0.3Å from their starting positions. Structures of DHA and 7S-HDHA were modeled using Edit/Build panel of Maestro and energy minimized using LigPrep software (Schrodinger Suite 2018-4, Schrodinger Inc). Both DHA and 7S-HDHA were docked to the h15-LOX-1 model using the docking software Glide (version 8.1, Schrodinger Inc) with the extra-precision (XP) docking score. We used the co-crystallized ligand coordinates to define the binding pocket. During the ligand-docking step, the protein was initially kept rigid, but despite extensive ligand conformation sampling, no low-energy docking pose was identified for the ligands. Therefore, we used InducedFit docking (Schrodinger Inc), in which both protein and ligand are treated flexibly. Specifically, during the initial docking step, side chains of Phe352, Ile413, Ile417, Met418, Cys559, and Leu588 were deleted to accommodate DHA and 7S-HDHA, because they appeared to block key portions of the active site. After generating the initial docking pose, side chain rotamers of these residues plus Arg402 and Gln595 (which have the potential to form hydrogen bonds with the ligand) were optimized. These docking and side chain optimization steps were iterated until a converged low energy docking pose was obtained.

For h15-LOX-2, structure-based docking calculations were performed using the available crystal structure of human ALOX15b (PDB id: 4nre). From the crystal structure, we retained the protein, Fe^{3+} ion, co-crystallized inhibitor, polyoxyethylene detergent (C8E), present in the active site and a hydroxide ion that co-ordinates the metal ion, all other atoms were deleted. Prior to docking, the structure was subjected to the protein-preparation step using Maestro's Protein-Preparation Wizard (Maestro version 11.8, Schrodinger Inc). Although the co-crystallized inhibitor bound in a U-shaped binding mode, it did not have a carboxylate group, and it had only 21 atoms in the main chain as opposed to 22 atoms present in DHA or 7S-HDHA. Therefore, we performed flexible-receptor flexible-ligand docking using InducedFit docking software (Schrodinger Inc). During induced-fit docking only the following active site residues were treated flexibly: Phe365, Val426, Val427, Arg329 and Asp602.

2.3 Results

2.3.1 Biosynthesis of 7S,14S-diHDHA

As discussed in the introduction, there are three proposed routes by which 7S,14S-diHDHA can be synthesized by LOXs (**Scheme 2.1**, Pathways 1-3). These three pathways were therefore investigated *in vitro* to determine possible *in vivo* biosynthetic routes. It should be emphasized that since these are di-oxygenation pathways, the di-hydroperoxide is formed in each of the pathways, however the biologically isolated molecule, 7S,14S-diHDHA, is the reduced form due to cellular glutathione peroxidases.

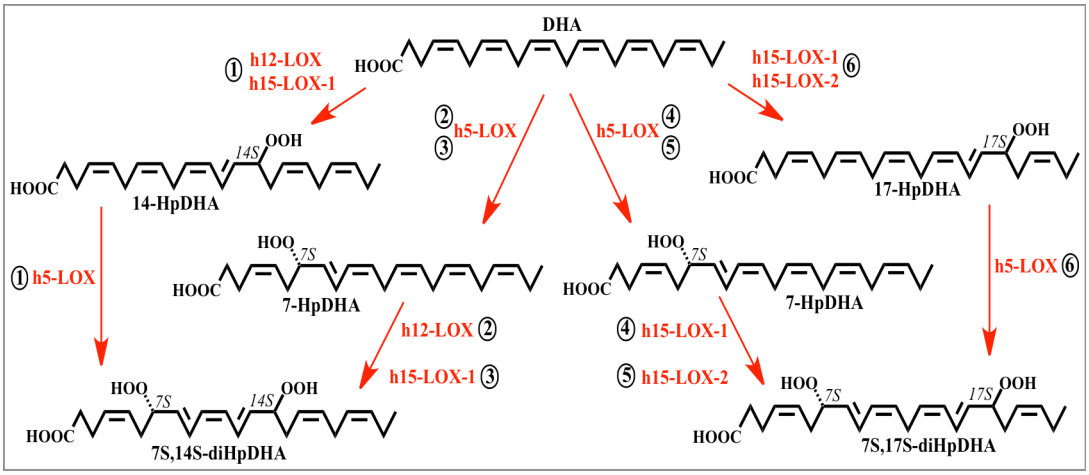

Scheme 2.1. The synthesis of 7S,14S-diHDHA from DHA may occur through one of three possible pathways: reaction of DHA with h5-LOX followed by h12-LOX (2), or reaction of DHA with h5-LOX followed h15-LOX-1 (3) or reaction of DHA with h12-LOX or h15LOX-1 followed by h5-LOX (1). The synthesis of RvD5 from DHA may also occur through three possible pathways: reaction of DHA with h5-LOX followed by h15-LOX-1 (4), or reaction of DHA with h5-LOX followed h15-LOX2 (5) or reaction of DHA with h12-LOX, h15-LOX-1 or h15LOX-2 followed by h5-LOX (6).

Pathway 1: DHA with h12-LOX to 14S-HpDHA, then h5-LOX to 7S,14S-diHpDHA.

The first possible route for biosynthesis of 7S,14S-diHDHA involves oxygenation of DHA by h12-LOX to form 14S-HpDHA (Scheme 1, Pathway 1). In order to study the ability of h12-LOX to form 14S-HpDHA, steady state kinetics and product profiles were measured. The k_{cat} for h12-LOX with DHA was measured to be 14 sec^{-1}, while the k_{cat}/K_M was found to be 13 $sec^{-1}\mu M^{-1}$ (**Table 2.1**), demonstrating that DHA is a comparable substrate to AA for h12-LOX *in vitro* (*42, 43*). The product

profile indicates that the majority of oxylipin is oxygenated at C14 (greater than 90%), with minor amounts oxygenated at C11, as previously reported (*44, 45*).

After DHA reacts with h12-LOX to form 14S-HpDHA, it may subsequently react with h5-LOX to form 7S,14S-diHpDHA (Scheme 1, Pathway 1), the oxidized form of 7S,14S-diHDHA. In order to study the ability of h5-LOX to react with 14S-HDHA and 14S-HpDHA, steady-state kinetic values and product profiles were assessed but no activity was observed by UV-vis spectroscopy (i.e. no change in absorbance at 254, 270 or 302 nm being detected). Using the more sensitive LC-MS/MS method, the V_{max} values for 14S-HDHA and 14S-HpDHA were determined to be 0.00038 and 0.0015 ($mol/sec^{-1}mol^{-1}$) at 10 mM substrate, respectively (**Table 2.2**). If we calculate the V_{max} at 10 mM of DHA (*vide supra*), the V_{max} values of 14S-HDHA and 14S-HpDHA are 368-fold and 93-fold slower than that of DHA, indicating that 14-oxylipins are poor substrates of h5-LOX. Even with this lowered kinetic rate, the major product in both reactions was the 7S,14S-oxylipin, along with trace amounts of 8,14-oxylipin and tri-oxygenated products.

Enzyme	Substrate	K_M (μM)	k_{cat} (sec^{-1})	k_{cat}/K_M ($sec^{-1}\mu M^{-1}$)
h12-LOX	DHA	1.1 ± 0.2	14 ± 1	13 ± 2
	7S-HDHA	1.8 ± 0.5	3.3 ± 0.2	1.8 ± 0.5
	7S-HpDHA	2.7 ± 1.0	0.68 ± 0.12	0.25 ± 0.10
h15-LOX-1	DHA	1.4 ± 0.3	0.95 ± 0.10	0.68 ± 0.17
	7S-HDHA	6.1 ± 0.5	3.1 ± 0.1	0.51 ± 0.09
	7S-HpDHA	6.9 ± 0.8	0.57 ±0.08	0.08 ± 0.02

Table 2.1. Steady-state kinetic values of h12-LOX and h15-LOX-1 with DHA, 7S-HDHA and 7S-HpDHA.

enzyme	substrate	V_{max} mol/sec^{-1}mol^{-1}	biosynthetic flux*
h5-LOX	DHA	0.14	0.14
	14S-HDHA	0.00038	0.00038
	14S-HpDHA	0.0015	0.0015
h12-LOX	DHA	12	6
	7S-HDHA	2.8	2.2
	7S-HpDHA	0.53	0.42
h15-LOX-1	DHA	0.84	0.56
	7S-HDHA	1.9	1.7
	7S-HpDHA	0.3	0.19

Table 2.2. V_{max} values of h5-LOX, h12-LOX and h15-LOX-1 with DHA, 14S-HDHA, 14S-HpDHA, 7S-HDHA and 7S-HpDHA, determined at 10 μM substrate concentration. The V_{max} for h5-LOX was approximated by determining the amount of h5-LOX in the ammonium sulfate pellet by Western analysis relative to a known standard. *Biosynthetic flux is calculated by multiplying each V_{max} by the percentage of total product from that reaction that serves as substrate for the next step towards synthesis of 7S,14S-diHDHA.

Pathway 2: DHA and h5-LOX to 7S-HpDHA, then h12-LOX to 7S,14S-diHpDHA (oxidized form of 7S,14S-diHDHA).

The second possible route for biosynthesis of 7S,14S-diHDHA begins with oxygenation of DHA by h5-LOX to form 7S-HpDHA (Scheme 1, Pathways 2 and 3). The ability of h5-LOX to form products from DHA was assessed through kinetic measurements and product profiles. The V_{max} for DHA at 10 mM was determined to be 0.14 mol/sec^{-1}mol^{-1} (**Table 2.2**), similar to the reported value of 0.14 mol/sec^{-1}mol^{-1} for AA (converted from k_{cat} and K_M at 10 mM AA in reference (*34*). Interestingly, the reaction of h5-LOX with DHA was found to produce 9 different products, with

7S-HpDHA being the major product at 45%, and 8 minor products comprising the remaining 55% (**Table 2.3**). The 4-product was not observed, consistent with results obtained from h5-LOX in neutrophils (*35, 46*) and monocytes (*47*). It is important to note that the increased non-specificity of h5-LOX with DHA relative to AA is a common observation for other LOX isozymes as well (*vide infra*). This appears to be a function of the structural difference between DHA and AA, with the increased length and unsaturation of DHA contributing to a substrate binding mode that inhibits the product selectivity seen with AA as the substrate.

Substrate	7-HpDHA	11-HpDHA	14-HpDHA	16-HpDHA	17-HpDHA	20-HpDHA
DHA	45%	6%	22%	6%	16%	5%

Table 2.3. Distribution of products created by reaction of h5-LOX with DHA. 7S-HpDHA is the major product, at 44% of the total and 8 minor products comprise the remaining 56%. Along with these products, trace amounts of 8-HDHA, 10-HDHA and 13-HDHA were occasionally seen. The percent error for these values does not exceed 10%.

7S-HpDHA produced by h5-LOX from DHA contains bisallylic carbons that may react further with h12-LOX to produce the dioxygenated oxylipin, 7S,14S-diHDHA (Scheme 1, Pathway 2). To test this possibility, steady-state kinetic values were determined for the reaction of h12-LOX with 7S-HDHA and 7S-HpDHA. The k_{cat} for 7S-HDHA and 7S-HpDHA were found to be 3.3 sec^{-1} and 0.68 sec^{-1}, respectively and the k_{cat}/K_M's for 7S-HDHA and 7S-HpDHA were found to be 1.8 $sec^{-1}\mu M^{-1}$ and 0.25 $sec^{-1}\mu M^{-1}$, respectively (**Table 2.1**), which are markedly greater than the kinetic parameters of h5-LOX with the 14-oxylipins. The products of h12-

LOX reacting with 7S-HDHA were exclusively dioxygenated oxylipins, with 79% of 7S,14S-diHDHA and 21% of 7S,17S-diHDHA being generated. The production of 7S,17S-diHDHA is a remarkable result since h12-LOX is known to produce mostly 14S-HpDHA and only a minor amount of 11-HpDHA from DHA. The formation of 11-HpDHA indicates that DHA inserts deeper into the cavity for hydrogen atom abstraction at C10. However, with 7S-HDHA as the substrate, the minor product is 7S,17S-diHDHA, not 7S,11S-diHDHA, suggesting that 7S-HDHA does not enter as deep into the active site, allowing for abstraction at C15 and the generation of 7S,17S-diHDHA. The reaction of 7S-HpDHA with h12-LOX produced comparable products as that from 7S-HDHA, indicating that no dehydration occurred to form the epoxide or its derivatives (**Table 2.4**).

Substrate	13-product	14-product	17-product
7S-HDHA	-	79%	21%
7S-HpDHA	3%	79%	18%

Table 2.4. Distribution of products produced by h12-LOX from 7S-HDHA as determined by LCMS/MS. The major product of the reaction of h12-LOX with 7S-HDHA is the 7S,14S-Product. The percent error for these values does not exceed 10%.

Pathway 3: DHA and h5-LOX to 7S-HpDHA, then h15-LOX-1 to 7S,14S-diHpDHA (oxidized form of 7S,14S-diHDHA).

The third pathway involves the non-canonical reaction of h15-LOX-1 with 7S-HpDHA to produce 7S,14S-diHpDHA, which is subsequently reduced to 7S,14S-diHDHA (Scheme 1, Pathway 3). h15-LOX-1 was reacted with DHA, 7S-HDHA and

7S-HpDHA, with 7S-HDHA demonstrating a comparable rate to that of DHA, but 7S-HpDHA showing a slower rate, with k_{cat}/K_M values of 0.68, 0.51 and 0.08 $sec^{-1}\mu M^{-1}$ for DHA, 7S-HDHA and 7S-HpDHA, respectively (**Table 2.1**). Even more surprisingly, the k_{cat} value for 7S-HDHA was over 3-fold greater than that for DHA These results indicate that DHA is still the more efficient substrate at low concentration (i.e. the fastest rate of substrate capture, k_{cat}/K_M) (*48*), but 7S-HDHA is an alternative substrate to DHA at high concentration, having the fastest rate of product release (k_{cat}) (*48*).

To determine the oxylipins generated by h15-LOX-1 from 7S-HDHA and 7S-HpDHA, the reaction products were isolated and analyzed via LC-MS/MS Figure. Surprisingly, when h15-LOX-1 was reacted with 7S-HDHA, 90% of the products were 7S,14S-diHpDHA (i.e. the oxidized form of 7S,14S-diHDHA), with only 10% of 7S,17S-diHpDHA being produced. When 7S-HpDHA was used as the substrate, the products were comparable, with 65% 7S,14S-diHpDHA (i.e. the oxidized form of 7S,14S-diHDHA) and 35% 7S,17S-diHpDHA. This specificity is the opposite of that seen with AA as the substrate for h15-LOX-1, where 90% of the 15-HpETE is made and only 10% of the 12-HpETE. To confirm the product structures, UV-vis absorbance maxima, C18-reverse phase retention times and MS/MS fragmentations were matched to known patterns for 7S,14S-diHDHA (**Figure 2.2**), indicating that h15-LOX-1 has a different positional specificity in its reaction with 7S-HDHA than it does with DHA. For comparison, h15-LOX-1 was reacted with DHA to generate 65% of the canonical 17S-HpDHA product, with a variety of minor products (22% 14S-

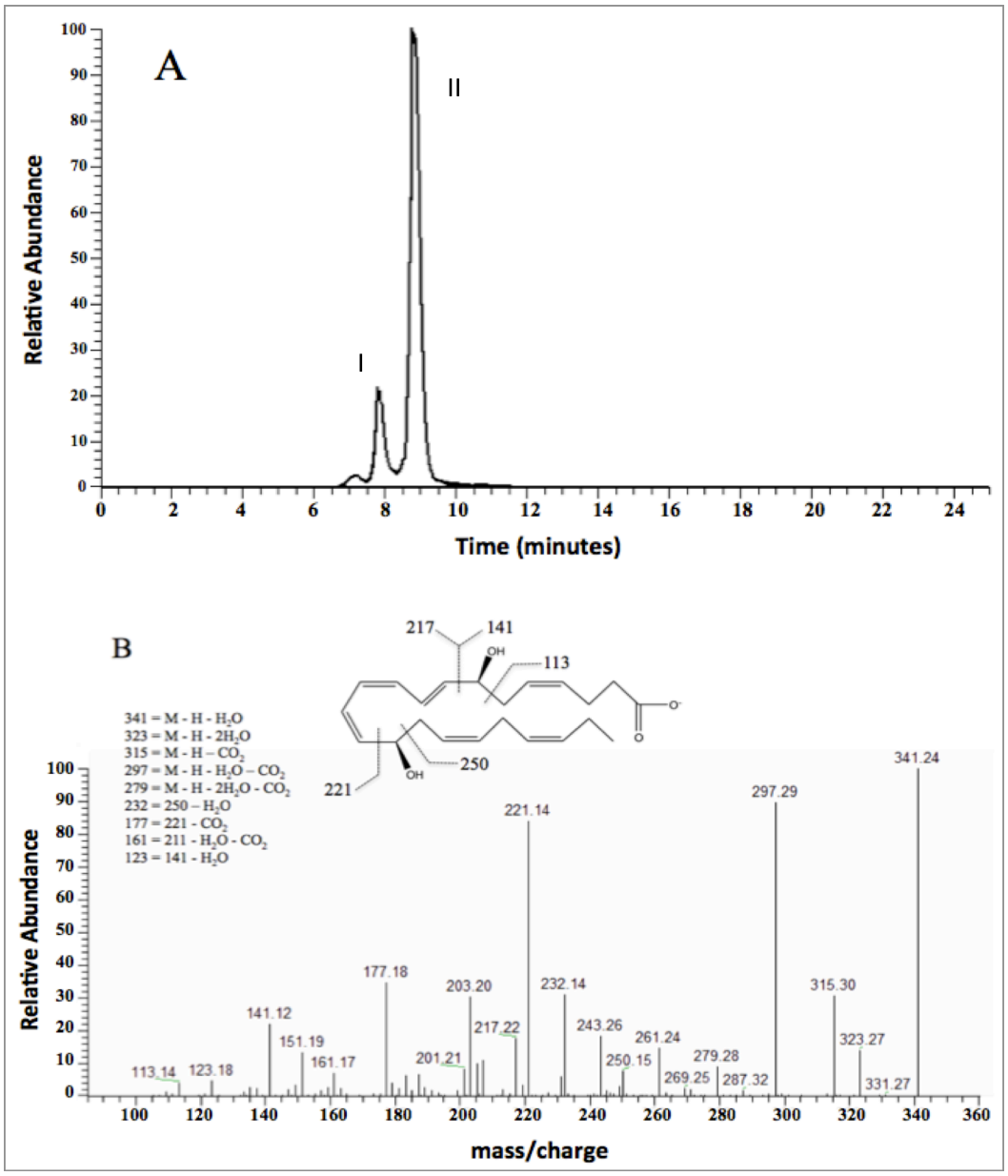

Figure 2.2. h15-LOX-1 primarily synthesizes 7S,12S-diDHA from 7S-HDHA. (A) Selected ion chromatogram at m/z of 335.2. Smaller peak at 7.8 min is 7S,17S-diHDHA. Larger peak at 9.0 min is 7S,14S-diHDHA. (B) MS/MS spectra of 7S,14S-diHDHA prepared from reaction of h15-LOX-1 with 7S-HDHA. Samples were reduced to form the di-alcohol products.

HpDHA, 7% 11-HpDHA and 6% 20-HpDHA)(**Table 2.5**). The presence of 22% 14S-HpDHA is consistent with oxidation at the omega-9 position (10% 12-HpETE from AA), however, the observation of the 10-HpDHA and 20-HpDHA minor products is unusual and indicates that the added length and unsaturation of DHA leads to multiple productive catalytic poses of DHA in h15-LOX-1, similar to that seen with h5-LOX. These data support both Pathway 2 and 3 (**Scheme 2.1**) as the most likely in vitro biosynthetic routes for 7S,14S-diHDHA production.

Substrate	11-product	14-product	17-product	20-product
DHA	7%	22%	65%	6%
7S-HDHA	0	90%	10%	0
7S-HpDHA	0	65%	35%	0

Table 2.5.. Distribution of products produced by h15-LOX-1 from DHA, 7S-HDHA and 7S-HpDHA, as determined by LCMS/MS. h15-LOX-1 shows altered positional specificity when reacting with 7S-HDHA and 7S-HpDHA. Note, the abbreviation, "11-product" etc., is used to simplify the complexity of the table labels. The percent error for these values does not exceed 10%.

2.3.2 Reaction of 7S-HDHA and 7S-HpDHA with h15-LOX-2 in biosynthesis of 7S,17S-diHDHA.

As observed above, h15-LOX-1 only produces a small amount of 7S,17S-diHDHA when reacting with 7S-HDHA. This result raises the possibility that h15-LOX-2 could be the primary LOX isozyme responsible for the generation of 7S,17S-diHDHA (RvD5). In order to study this reaction further, h15-LOX-2 was reacted with

DHA, 7S-HDHA and 7S-HpDHA and all three were determined to have comparable rates (**Table 2.6**). The k_{cat} for DHA was 1.5 sec^{-1}, the k_{cat} for 7S-HDHA was 4-fold higher at 5.8 sec^{-1}, while the k_{cat} for 7S-HpDHA was 3.4 sec^{-1}. Due to the lower K_M for DHA, the k_{cat}/K_M for DHA was 25-fold greater than that of 7S-HDHA (k_{cat}/K_M = 0.14 $sec^{-1}\mu M^{-1}$) and 42-fold greater than 7S-HpDHA (k_{cat}/K_M = 0.08 $sec^{-1}\mu M^{-1}$). These values indicate that DHA has the fastest rate of substrate capture (k_{cat}/K_M), but 7S-HDHA has the fastest rate of product release (k_{cat}) (*48*). For comparison, the kinetic parameters for AA are 5.6 sec^{-1} for k_{cat} and 0.23 $sec^{-1}\mu M^{-1}$ for k_{cat}/K_M (*42*), indicating that at low substrate concentration, 7S-HDHA is a comparable substrate to that of AA, but DHA is preferred. These data support Pathway 5 (Scheme 1) as the most likely *in vitro* biosynthetic route for RvD5 production. It should be noted that no products were observed from the reaction of h15-LOX-2 with either 17S-HDHA or 17S-HpDHA using UV-vis spectroscopy or LC-MS/MS, indicating that 7S,17S-diHDHA is not biosynthesized through the reverse orientation of the substrate. In addition, h15-LOX-2 was not observed to produce the 16,17-epoxide product from 17S-HpDHA, reinforcing its selective reactivity.

substrate	**k_{cat} (sec^{-1})**	**k_{cat}/K_M ($sec^{-1}\mu M^{-1}$)**	**K_M (μM)**
AA	0.64 ± 0.02	0.16 ± 0.02	4.0 ± 0.02
DHA	1.5 ± 0.08	3.4 ± 0.5	0.43 ± 0.06
7S-HDHA	5.8 ± 0.4	0.15 ± 0.02	40 ± 4
7S-HpDHA	3.4 ± 0.4	0.08 ± 0.01	41 ± 7

Table 2.6. Steady-state kinetic values for h15-LOX-2 with DHA, 7S-HDHA and 7S-HpDHA. Values for AA were published previously.

To determine the oxylipins produced by h15-LOX-2 from DHA, 7S-HDHA and 7S-HpDHA, the reaction products were isolated and analyzed via LC-MS/MS. The reaction of h15-LOX-2 with DHA produced 95% 17S-HDHA, 3% 14S-HDHA and 2% 20-HDHA, similar to its high level of specificity with AA as the substrate (i.e. greater than 95% 15-HpETE). The reaction with 7S-HDHA with produced 100% 7S,17S-diHDHA, while reaction with 7S-HpDHA produced 98% 7S,17S-diHDHA and 2% 7S,20-HDHA (**Table 2.7**). The 7S,17S-diHDHA produced by h15-LOX-2 from 7S-HDHA was compared with standards and found to have identical UV-vis maxima, LC-MS/MS retention time and fragmentation as 7S,17S-diHDHA (RvD5).

substrate	14-product	17-product	20-product
DHA	3%	95%	2%
7S-HDHA	0%	100%	0%
7S-HpDHA	0%	98%	2%
17S-HDHA	no rxn	no rxn	no rxn
17S-HpDHA	no rxn	no rxn	no rxn

Table 2.7. Products made from reaction of h15-LOX-2 with DHA-derived oxylipins. DHA, 7S-HDHA, 7S-HpDHA, 17S-HDHA and 17S-HpDHA were reacted with h15-LOX-2, extracted and analyzed via LC-MS/MS. No reaction (no rxn) was detectable after the incubation of h15-LOX-2 with either 17S-HDHA or 17S-HpDHA. The percent error for these values does not exceed 10%.

2.3.3 Formation of 7S,17S-diHDHA by h5-LOX from 17S-HDHA and 17S-HpDHA.

17S-HDHA was reacted with h5-LOX to investigate the rate of 7S,17S-diHDHA synthesis, relative to the production of 7S,17S-diHDHA from h15-LOX-2 and 7S-HDHA. Despite achieving complete turnover of DHA with h5-LOX in ~1

minute, an identical amount of h5-LOX did not produce an observable reaction with 17S-HDHA or 17S-HpDHA when monitoring at 254 and 270 nm, using UV-vis spectroscopy. However, analyzing the reaction at multiple time points using LC-MS/MS allowed for the estimation of the Vmax value. Compared to the reaction of h5-LOX with AA and DHA, the reaction rates with 17S-HDHA and 17S-HpDHA were over 100-fold slower (**Table 2.8**). The products of the reaction of h5-LOX with both 17S-HDHA and 17S-HpDHA were approximately 90% 7S,17S-diHDHA, along with minor amounts of 16,17-diHDHA and 10,17-diHDHA. For comparison, similar reactions were performed with h15-LOX-2 and the 7S-oxylipins and the V_{max} rates were significantly greater than observed with h5-LOX (**Table 2.8**), indicating that Pathway 6, **Scheme 2.1** is not efficient *in vitro*. As with h15-LOX-2, it is possible that 7S,17S-diHDHA could also be biosynthesized through a reverse binding orientation to h5-LOX, however, no reaction was observable between h5-LOX and 7S-HDHA or 7S-HpDHA, using UV-vis spectroscopy. When analyzed by LC-MS/MS, 7S,17S-diHDHA was observed, but the reaction rates of h5-LOX with 7S-HDHA and 7S-HpDHA were over 1000-fold slower than with AA and DHA and were considered inconsequential (i.e. no reaction).

enzyme	substrate	V_{max} Mol/Sec^{-1}Mol^{-1}	biosynthetic flux*
h5-LOX	DHA	0.14	0.062
	17S-HDHA	0.0012	0.0012
	17S-HpDHA	0.0014	0.0014
h15-LOX-2	DHA	1.4	1.4
	7S-HDHA	1.2	1.2
	7S-HpDHA	0.67	0.65
h15-LOX-1	DHA	0.84	0.56
	7S-HDHA	1.9	0.19
	7S-HpDHA	0.3	0.11

Table 2.8. V_{max} values of reaction steps in the biosynthesis of RvD5 were calculated at 10 μM substrate concentration for comparison. *Biosynthetic flux is calculated by multiplying each $V_{max.}$ by the percentage of total product from that reaction that serves as substrate for the next step in the synthesis of 7S,17S-diHDHA. The percent error for these values does not exceed 10%.

2.3.4 Chiral chromatography characterization of 7S,14S-diHDHA and 7S,17S-diHDHA (RvD5).

We predicted that the oxygen on C14 of 7S,14S-diHDHA is in the S-configuration because h15-LOX-1 typically performs stereospecific oxygenation generating the S-configured product when the substrate enters the active site methyl-end first. To determine the relative stereochemistry of the 7S,14S-diHDHA produced by reacting 7S-HDHA with h15-LOX-1, the products of this reaction were isolated, reduced and compared to standards via reverse phase chiral chromatography. 7-epi-MaR1, MaR1 and the 7S,14S-diHDHA produced by h15-LOX-1 from 7S-HDHA eluted at distinct times when analyzed via chiral HPLC (**Figure 2.3**). 7-epi-MaR1

eluted with a RT of 11.60 min, MaR1 with a RT of 8.45 min and the enzymatically-synthesized 7S,14S-diHDHA eluted with a RT of 4.65 min. All three compounds shared identical fragmentations when analyzed via LC/MS/MS. Since h5-LOX also typically generates product in the S-configuration from substrates that enter the active site methyl-end first, the reaction of h5-LOX with 14S-HDHA is predicted to produce 7S,14S-diHDHA. A comparison of this product with that generated by h15-LOX-1 from 7S-HDHA revealed identical fragmentations, reverse-phase retention times and chiral retention times, indicating that both oxylipins are 7S,14S-diHDHA, just produced in a different order of LOX biosynthetic steps. While it is conceivable that both h15-LOX-1 and h5-LOX change their product profile and generate the R-configuration oxylipin, this appears unlikely based on the chiral column results. It should be noted that we have attempted to determine the absolute stereochemistry of 7S,14S-diHpDHA by generating the double Mosher derivative, but unfortunately NMR peak overlap prohibits the assignment of the molecules' stereochemistry.

To determine the relative stereochemistry of the 7,17-oxylipin produced by h15-LOX-2 and 7S-HDHA, the molecule was compared to a RvD5 standard using reverse-phase, chiral HPLC coupled to MS/MS. The retention time and fragmentation of the 7,17-oxylipin produced by h15-LOX-2 and 7S-HDHA was identical to that of the RvD5 standard (**Table 2.9**), confirming its identity as 7S,17S-diHDHA (RvD5).

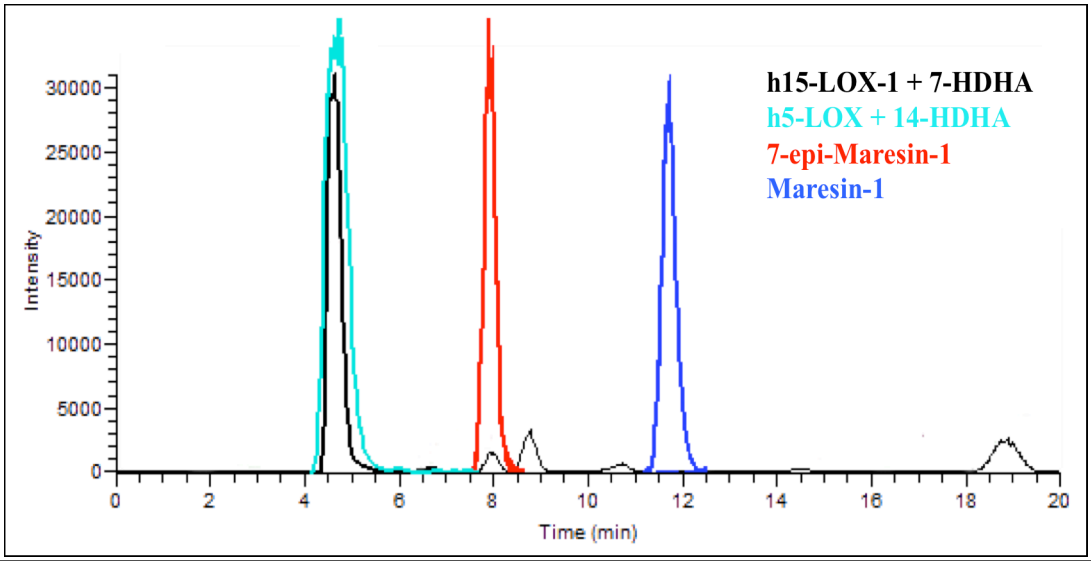

compound	full name	RT
7S,14SdiHDHA (h15-LOX-1 +7S-HDHA)	7(S),14(S)-dihydroxy-4Z,8E,10Z,12E,16Z,19Z docosahexaenoic acid*	4.65 min
7S,14SdiHDHA (h5-LOX +14S-HDHA)	7(S),14(S)-dihydroxy-4Z,8E,10Z,12E,16Z,19Z docosahexaenoic acid*	4.80 min
7-epi-MaR1	7(S),14(S)-dihydroxy-4Z,8E,10E,12Z,16Z,19Z docosahexaenoic acid	8.45 min
MaR1	7(R),14(S)-dihydroxy-4Z,8E,10E,12Z,16Z,19Z docosahexaenoic acid	11.60 min

Figure 2.3. Chiral chromatogram of maresin isomers. 7S,14S-diHDHA formed both by h15-LOX-1 from 7S-HDHA and by h5-LOX from 14-HDHA were analyzed via Chiral LCMS along with MaR1 and 7-epi-MaR1. Retention times are shown in minutes. *The proposed stereochemistry for the product resulting from the reaction of h15-LOX-1 and 7S-HDHA is 7(S),14(S)-dihydroperoxy 4Z,8E,10Z,12E,16Z,19Z docosahexaenoic acid (7S,14S-diHDHA, as reduced form), based on the analytical results and the product specificity of h15-LOX-1 and h5LOX.

compound	full name	RT
RvD5 (Standard)	7(S),17(S)-dihydroxy 4Z,8E,10Z,13Z,15E,19Z docosahexaenoic acid	15.89 min
RvD5 (h15-LOX-2 + 7-HDHA)	7(R),17(S)-dihydroxy 4Z,8E,10Z,12Z,15E,19Z docosahexaenoic acid	15.89 min

Table 2.9. Chiral chromatography of RvD5. 7S,17S-diHDHA formed by h15-LOX-2 from 7S-HDHA was compared to a RvD5 standard using Chiral LCMS. Based on the analytical results and the product specificity of h15-LOX-2, the proposed stereochemistry for the product resulting from the reaction with 7S-HDHA is 7(S),17(S)-dihydroxy 4Z,8E,10E,12Z,16Z,19Z docosahexaenoic acid

2.3.5 Molecular Modeling of DHA and 7S-HDHA bound to h15-LOX-1.

The shift in product profile seen with h15-LOX-1 for DHA and 7S-HDHA suggests that 7S-HDHA has a different binding mode than DHA, and therefore molecular modeling was employed to assess this possibility. **Figure 2.4** shows the InducedFit docking poses of DHA and 7S-HDHA with h15-LOX-1, with corresponding extra-precision docking scores of -9.5 and -10.8 respectively. In the docking model, the carboxylate groups of both DHA and 7S-HDHA form hydrogen bonds with the side chain of Arg402 and the hydrophobic tails of both substrates are buried deep in the hydrophobic pocket created by residues Phe352, Ile417 and Ile592. However, a key difference is that the C7 hydroxyl group of 7S-HDHA forms a hydrogen bond with the backbone carbonyl oxygen of Ile399. This difference in binding between DHA and 7S-HDHA is manifested in their distances between the iron-hydroxide oxygen atom and the hydrogen on the reactive carbons, C12 and C15. The modeling data indicate that for 7S-HDHA, the C12 hydrogen is markedly closer

to the iron-hydroxide moiety than C15 hydrogen (**Table 2.10**). Considering that C12 hydrogen atom abstraction leads to 7S,14S-diHDHA, while C15 hydrogen atom abstraction leads to 7S,17S-diHDHA, these docking results are consistent with the enzymatic results. For DHA, the distance for the C15 hydrogen is slightly shorter than that of C12, consistent with the experimental results, but the distance difference is not as distinct as that for 7S-HDHA, possibly due to the more homogeneous hydrophobic nature of DHA compared to 7S-HDHA. Interestingly, there is no difference between the pro-S and pro-R hydrogens indicating the limitation of the docking model.

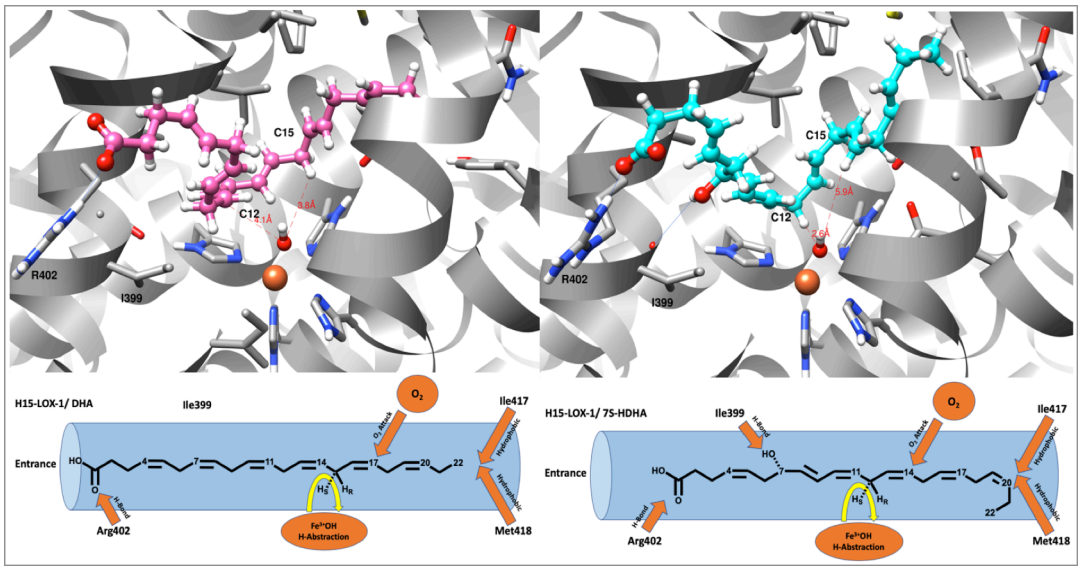

Figure 2.4. InducedFit docking poses of (a) DHA and (b) 7S-HDHA against the active site of h15-LOX1. DHA and 7S-HDHA atoms, hydroxide ion and metal ion are shown in ball-and-stick representation. Protein residues are shown in stick representations. Carbon atoms of DHA, 7S-HDHA and protein are shown in pink, cyan and gray, respectively; nitrogen, oxygen and hydrogen atoms are shown respectively in blue, red and white. Fe^{3+} is shown in orange. Hydroxide oxygen to C12-hydrogen and C15- hydrogen distances of DHA and 7S-HDHA are also shown. Below each docking structure, a cartoon representation is presented for positional emphasis.

Substrate	Hydroxide oxygen to pro-S C12-hydrogen Distance (Å)	Hydroxide oxygen to pro-S C15-hydrogen Distance (Å)
DHA	4.1	3.8
7S-HDHA	2.6	5.9

Table 2.10. Distances between hydroxide-ion oxygen atom and the pro-S hydrogens of the reactive carbons, C12 and C15, of DHA and 7S-HDHA against h15-LOX-1.

2.3.6 Molecular modeling of DHA and 7S-HDHA bound to h15-LOX-2.

For h15-LOX-2, we chose the extra-precision (XP) scoring function for Glide docking within the InducedFit docking module, which allowed for extensive sampling of the substrate conformations during docking. The XP docking score of the low-energy docking pose of DHA and 7S-HDHA against h15-LOX-2 are -7.09 and -9.31 respectively and their docking poses are shown in **Figure 2.5.** Both substrates bind into the active site tail first, utilizing a U-shaped binding mode. The carboxylate groups of both DHA and 7S-HDHA make a salt-bridge interaction with the R429 residue on the helix α12. In contrast, h15-LOX-1 utilizes R402 (helix α11) to hydrogen bond with the carboxylate group of the substrate, possibly leading to their different product specificities. The hydrophobic tails of both substrates are buried deeply in the hydrophobic pocket created by residues F365, L420, I421, V427, F438, and L607. The hydroxyl group of 7S-HDHA makes a hydrogen bond to the backbone carbonyl oxygen of L419. The distance between reactive pro-S hydrogen of C15 and the oxygen atom of the hydroxide ion is 4.1Å and 2.7Å for DHA and 7S-HDHA, respectively (**Table 2.11**). These distances are shorter than the pro-S hydrogen of C12 and the oxygen atom of the hydroxide ion for DHA and 7S-HDHA (7.2 Å and 4.0 Å, respectively (**Table 2.11**). These two binding modes are consistent

with the enzymatic reaction involving abstraction of the pro-S hydrogen from C15 for both DHA and 7S-HDHA, to produce the 17-product exclusively (**Table 2.11**) (*49-53*) and not the 14-product from C12 hydrogen abstraction.

Substrate	Hydroxide oxygen to pro-S C12-hydrogen Distance (Å)	Hydroxide oxygen to pro-S C15- hydrogen Distance (Å)
DHA	7.2	4.1
7S-HDHA	4.0	2.7

Table 2.11. Distances between hydroxide-ion oxygen atom and the pro-S and pro-R hydrogens of the reactive carbons, C12 and C15, of DHA and 7S-HDHA with h15-LOX-2.

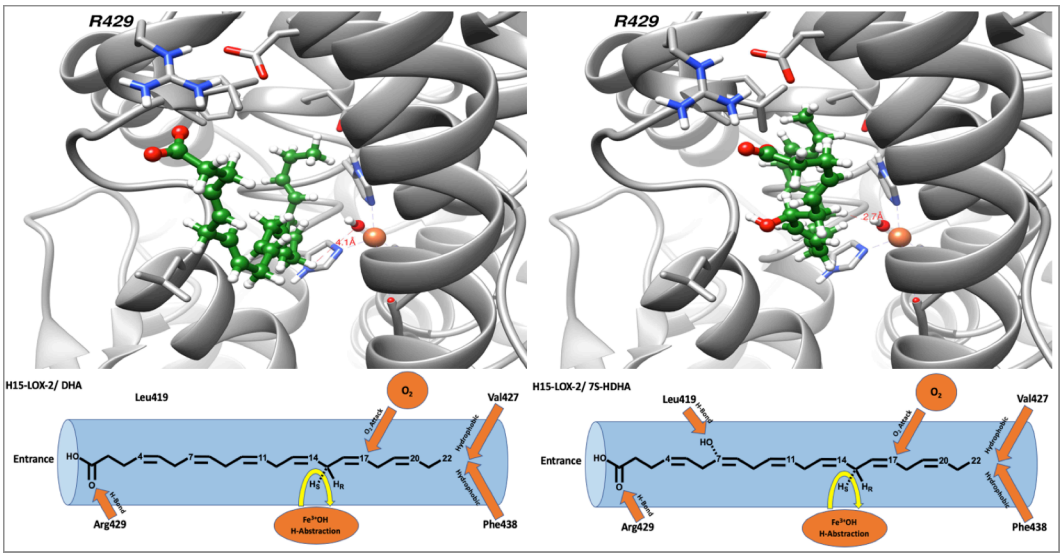

Figure 2.5. InducedFit docking poses of (a) DHA and (b) 7S-HDHA against the h15-LOX-2 active site. DHA and 7S-HDHA atoms, hydroxide ion and metal ion are shown in ball-and-stick representation and protein residues are shown in stick representation. Carbon atoms of DHA and 7S-HDHA are shown in green color and protein are shown in gray color; nitrogen, oxygen and hydrogen atoms are shown respectively in blue, red and white colors. Fe^{3+} ion is shown in orange. The distance between reactive pro-S hydrogen atom of C15 and the oxygen atom of the hydroxide ion is 4.1Å and 2.7Å for DHA and 7S-HDHA respectively. Below each docking structure, a cartoon representation is presented for positional emphasis.

2.3.7 Effect of 7S,14S-diHDHA and RvD5 on Platelets

Previous studies have shown that DHA and the h12-LOX-derived oxylipins of DHA have antiplatelet effects (*54*). Therefore, to determine the effect of RvD5, 7S,14S-diHDHA and related maresin isomers on platelet activation, washed platelets were treated with oxylipins in half-log increments and then stimulated with collagen (0.25 μg/mL) in an aggregometer. 7S,14S-diHDHA fully inhibited platelet aggregation at 10 μM, while reducing aggregation by 65% at 3 μM. (**Figure 2.6**). Platelets treated with 3 and 10 μM of RvD5 had an approximate reduction in aggregation of 65% and 90%, respectively, while MaR1 and 7-epi-MaR1 were the least potent, reducing aggregation by approximately 70% at 10 μM. 12S-HETrE, a h12-LOX-derived oxylipin of DGLA with known antiplatelet activity (*55-57*), displayed slightly greater potency than 7S,14S-diHDHA and 7S,17S-diHDHA (RvD5), reducing collagen-mediated platelet aggregation by 68% at 1 μM. Together this data demonstrates that 12-HETrE was more potent than both 7S,17S-diHDHA (RvD5) and 7S,14S-diHDHA for inhibiting collagen-induced platelet aggregation, but that at 10 μM, all three molecules inhibited aggregation completely. It should be noted that these conditions (0.25 μg/mL collagen as activator) are more sensitive to inhibition than our previously published conditions (20 μM PAR1-AP as agonist) (*58*) and therefore demonstrate a greater effect on aggregation at lower concentrations of 12S-HETrE.

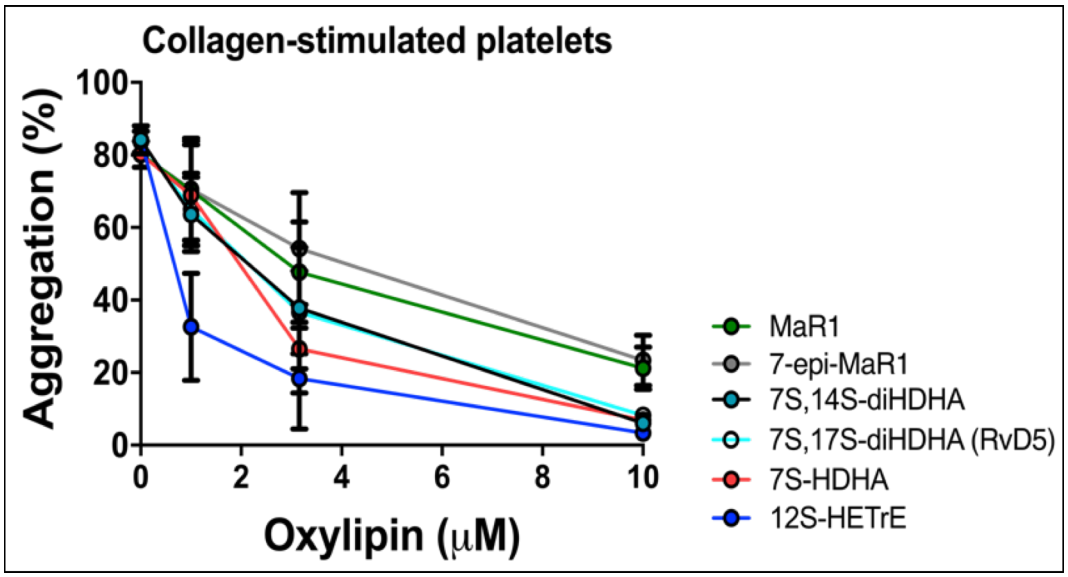

Figure 2.6. The effect of MaR1, 7-epi-MaR1, 7S,14S-diHDHA, 7S,17S-diHDHA (RvD5), 7S-HDHA, 12S-HETrE, Mar1 and 7-epi-Mar1 on aggregation of activated platelets. Washed human platelets were treated with vehicle (DMSO) or MaR1, 7-epi-MaR1, 7S,14S-diHDHA, 7S,17S-diHDHA, 7S-diHDHA, or 12S-HETrE in half-log increments ranging from 1-10 μM for ten minutes and then stimulated with collagen (0.25 μg/mL) in an aggregometer. Note, the data for 7S,14S-diHDHA and 7S,17S-diHDHA are nearly identical and thus overlap significantly. Data represent the mean ± S.E.M of 5 independent experiments. Statistical analysis was performed using one-way ANOVA with Dunnett's test comparing the aggregation of platelets treated with each concentration of oxylipin to the aggregation of vehicle-treated platelets. **P<0.01, ***P<0.001

2.3.7 Platelet Lipidomics with 7S-HDHA

The reduction in aggregation seen in platelets incubated with 7S-HDHA could be caused by either the 7S-HDHA itself or by a biosynthetic product produced by platelets during incubation. To investigate the latter possibility, platelets were incubated with 7S-HDHA and analyzed for the presence of 7S-HDHA metabolites using LC-MS/MS. Although large amounts of unreacted 7S-HDHA were detectable

in the samples, no levels of any di-HDHA's or tri-HDHA's were detectable. As a control, platelets incubated with 5S-HETE were also analyzed for the presence of 5S-HETE metabolites. Although large levels of 12-HETE were detectable from endogenous AA, no appreciable levels of 5S-HETE metabolites were detectable down to 2 ng/mL. This is an unexpected result since h12-LOX is capable of reacting with 7S-HDHA *in vitro* to produce 7S,14S-diHDHA. The fact that no 7S,14S-diHDHA is produced indicates both that 7S-HDHA is most likely the bioactive species and that 7S-HDHA does not react appreciably with h12-LOX in the cellular milieu of the platelet.

2.4 Discussion

2.4.1 Biosynthesis of 7S,14S-diHDHA

7S,14S-diHDHA is an analogue of MaR1 (*17*) and is proposed to have a distinct biosynthetic pathway from MaR1. Its structure suggests three possible routes for its biosynthesis. Pathway 1 involves oxidation of DHA at C14 by h12-LOX, followed by oxidation at C7 by h5-LOX. However, the *in vitro* data of this work suggests this is a very unfavorable biosynthetic route. Although DHA is a good substrate for h12-LOX, forming 14S-HpDHA at a rate similar to 12S-HpETE formation from AA (*43*), the second step in this pathway is kinetically unfavorable. Compared with DHA, the V_{max} of h5-LOX with 14S-HDHA is ~368 fold slower (**Table 2.2**).

For Pathway 2 in **Scheme 2.1**, DHA is oxidized at C7 by h5-LOX followed by

oxidation at C14 by h12-LOX. In comparison to Pathway 1, Pathway 2 is a kinetically favorable *in vitro* biosynthetic route. The first step, formation of 7S-HpDHA from DHA by h5-LOX, occurs rapidly with a V_{max} comparable to that of AA kinetics. The second step is also favorable, as the reaction of h12-LOX with 7S-HDHA has k_{cat} and k_{cat}/K_M values that are within 10-fold the rate of DHA. The slowest step in this pathway is over 350 times faster than the reaction of h5-LOX with 14S-HDHA.

Interestingly, Pathway 2 also presents a possible novel pathway to biosynthesizing 7S,17S-diHDHA (RvD5). The production of 7S,17S-diHpDHA is 21% of that of 7S,14S-diHpDHA, which is a significant percentage given the potency of RvD5 (*25*). The result also indicates a product promiscuity rarely seen for h12-LOX. h12-LOX produces over 95% 12S-HpETE from AA, so to produce 25% 7S,17S-diHpDHA is noteworthy. Another interesting aspect of this result is the mechanism of 7S,17S-diHpDHA formation. For 7S,17S-diHpDHA to form, h12-LOX must abstract from C15 of 7S-HpDHA, which indicates that the methyl tail of 7S-HpDHA is not positioned as deep in the active site pocket as that for 7S,14S-diHpDHA formation. These data suggest that the alcohol on C7 of 7S-HpDHA could interact with the active site and prevent the full penetration of the methyl tail into the bottom of the active site pocket.

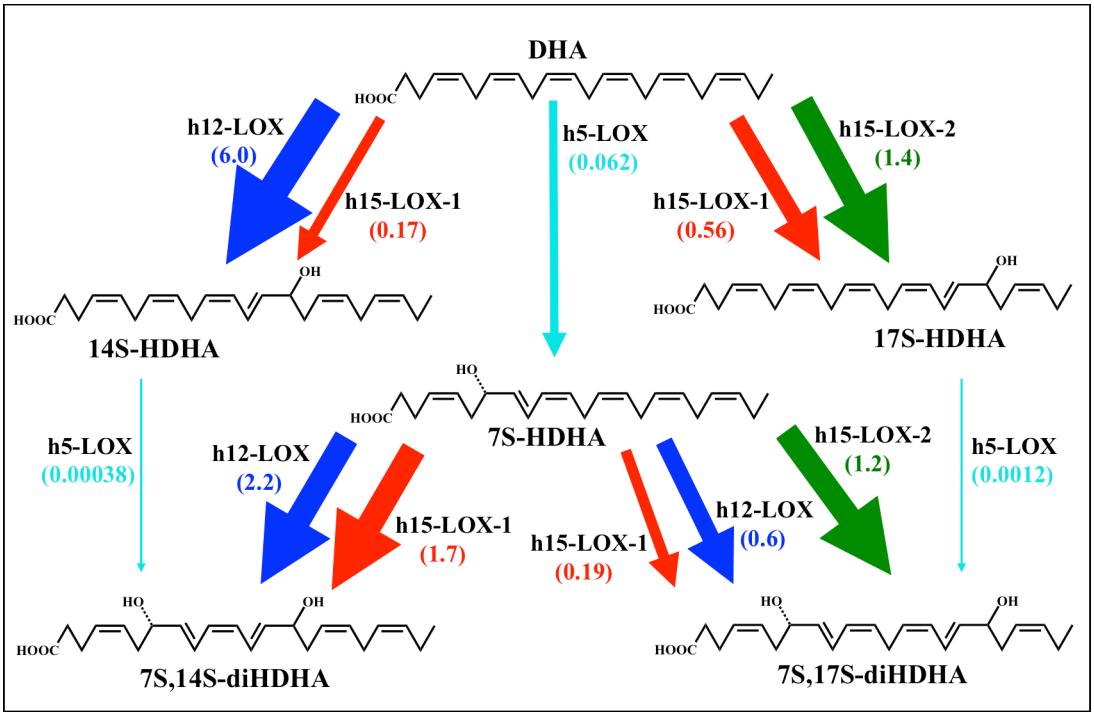

Scheme 2.2. Comparison of pathways for the biosynthesis of RvD5.and 7S,14S-diHDHA. The total biosynthetic flux for the reactions of h5-LOX, h12-LOX and h15-LOX-1 with DHA, 14S-HpDHA and 7S-HpDHA are compared by multiplying V_{max} values (mol/sec^{-1}mol^{-1}) at 10 mM substrate by the percent product for each reaction. In all pathways, turnover by h5-LOX is the rate-limiting step and we have assumed that the hydroperoxides are reduced to the alcohols.

The final biosynthetic route examined, Pathway 3, is the oxidation of DHA at C7 by h5-LOX, followed by oxidation at C14 by h15-LOX-1, and is a non-canonical pathway. h15-LOX-1 reacts with DHA and produces a majority of 17S-HpDHA (65%), with a smaller amount of 14S-HpDHA (22%). As shown with AA (*59*), product specificity is dictated by the methyl end of the fatty acid, with the majority of oxygenation occurring on the w-6 carbon (C15 for AA and C17 for DHA), with a minority occurring on the w-9 carbon (C12 for AA and C14 for DHA). Therefore, it

is reasonable to expect a similar distribution of products with 7S-HDHA as the substrate, however, this is not the case. Pathway 3 produces over 9–fold more of 7S,14S-diHDHA than 7S,17S-diHDHA. In addition, this unusual product pathway is kinetically favorable *in vitro*. Both the first step, formation of 7S-HpDHA from DHA by h5-LOX, and the second, reaction of 7S-HDHA with h15-LOX-1 occur relatively rapidly. The k_{cat} for h15-LOX-1 and 7S-HDHA is 3.2-fold faster than that of DHA and the k_{cat}/K_M for DHA and 7S-HDHA are nearly identical. These results indicate that, although the hydroxyl group on C7 has a large effect on the positional specificity of the enzyme, it has little effect on catalysis, leading to a favorable overall kinetic condition. In summary, if we consider both the rate and the percent product formation, then we obtain the biosynthetic flux (**Scheme 2.2**), which indicates that the most efficient pathway for making 7S,14S-diHDHA is thru h5-LOX and then h12-LOX or h15-LOX-1, since the reaction of h5-LOX with 14-HpDHA is a rate-limiting step in the biosynthesis of 7S,14S-diHpDHA.

The finding that h15-LOX-1 primarily oxygenates C17 on DHA, but C14 on 7S-HDHA is surprising, but changes in the positional specificity of LOXs have been demonstrated before (*19*). In order to obtain a better understanding of this binding event, DHA and 7S-HDHA were docked to a model of h15-LOX-1. In the case of DHA, both C12 and C15 are at a reasonable distance for hydrogen abstraction (*60*), whereas in case of 7S-HDHA, C12 is closer to the metal ion than C15, supporting the experimental results (**Table 2.10**). The model explains this result by having the hydroxyl group at C7 in 7S-HDHA forming a hydrogen bond with the backbone

carbonyl of I399, which subsequently positions C12 closer to the metal ion. Without a similar restraint, the flexibility of DHA positions both C12 and C15 close to the metal ion, helping to explain the greater number of products made by h15-LOX-1 from DHA compared with AA. This model suggests that 7S- HDHA is positioned further inside the active site than DHA, overcoming steric interactions to position C12 for hydrogen atom abstraction (**Figure 2.4**). What is remarkable is that this is the opposite from what appears to occur with 7S-HDHA in h12-LOX. In h12-LOX, the C7 alcohol holds the substrate back from the bottom of the pocket to abstract a hydrogen atom closer to the methyl tail generating the 7S,17S-diHDHA, while in h15-LOX-1, the C7 alcohol positions the substrate deeper into the active site generating 7S,14S-diHDHA. We are currently investigating the active sites of both h12-LOX and h15-LOX-1 with mutagenesis to better understand the binding requirements and differences between h12-LOX and h15-LOX-1 in more detail.

2.4.2 Biosynthesis of 7S,17S-diHDHA (RvD5*)*

The discovery of Pathway 3 as a relevant route to the biosynthesis of 7S,14S-diHDHA raises questions with respect to the biosynthetic route to making 7S,17S-diDHA (RvD5). Previously, RvD5 was proposed to be biosynthesized from DHA in two steps; initial oxygenation of C7 by h5-LOX, followed by oxygenation of C17 by h15-LOX-1 (*24, 26*). This hypothesis was based on the prevalence of h15-LOX-1 in the inflammasome and the preference of h15-LOX-1 to oxygenate DHA at C17. However, our work shows that h15-LOX-1 shifts its positional specificity when

reacting with 7S-HDHA *in vitro*, mainly creating 7S,14S-diHDHA and very little of 7S,17S-diHDHA. This marked change in substrate specificity indicates that another LOX, such as h15-LOX-2, could be responsible for the biosynthesis of RvD5.

h15-LOX-2 reacts favorably with DHA, manifesting a k_{cat} of 1.5 sec^{-1}, which is comparable to values published for AA, EPA, DGLA, GLA (*61*), indicating h15-LOX-2 maintains similar rates of product release (k_{cat}) across a wide range of fatty acid substrates (*48*). The k_{cat}/K_M of DHA with h15-LOX-2 is over 20-fold greater than that for AA and 10-fold greater than that of other fatty acids, making DHA one of the most reactive polyunsaturated fatty acids with h15-LOX-2. Since the reaction of h15-LOX-2 with DHA produces 95% 17S-HDHA, and the fact that h15-LOX-1 specific inhibitors do not block production of 17S-HDHA in neutrophils and eosinophils (*40*), it is possible that the likely source of 7S,17S-diHDHA is h15-LOX-2. In fact, 7S-HDHA and 7S-HpDHA are viable substrates of h15-LOX-2, with greater k_{cat} values than DHA, but lower k_{cat}/K_M values, making them less reactive substrates than DHA at low concentration with h15-LOX-2. Previous work comparing the reaction of AA and 5S-HpETE with h15-LOX-2 demonstrated a similar trend, with 5S-HpETE having a greater k_{cat} but a smaller k_{cat}/K_M than AA (*15*). Considering that hydrogen atom abstraction is generally the first irreversible rate-determining step for k_{cat} and k_{cat}/K_M for fatty acid substrates, these results suggest that the rate of oxylipin binding is markedly slower relative to fatty acid binding for h15-LOX-2 (*15*).

With respect to the biosynthetic pathway of RvD5, the fact that RvD5 contains two hydroxyls on C7 and C17 suggests two likely routes for the biosynthesis

of RvD5 from DHA (Pathways 4, 5 and 6, **Scheme 2.1**). The first route could be the oxygenation at C7 by h5-LOX followed by oxygenation of C17 by a 15-LOX isozyme (Pathway 4 or 5, **Scheme 2.1**), either h15LOX-1 or h15-LOX-2. The second route is the reverse, with oxygenation of C17 by a 15-LOX isozyme, followed by oxygenation of C7 by h5-LOX (Pathway 6, **Scheme 2.1**). In the current study, we find that h5-LOX reacts well with DHA, however, it reacts significantly slower with 7S-HDHA and 17S-HDHA. For a direct comparison, the V_{max} at 10 μM substrate was determined to be 0.14 mol/sec^{-1}mol^{-1} for h5-LOX with DHA (**Table 2.8**), which is over 100 times greater than the rate observed with 17S-HDHA (V_{max} = 0.0012 mol/sec^{-1}mol^{-1} at 10 μM). This is consistent with the low reactivity of h5-LOX and 14S-HDHA, indicating that h5-LOX does not react well with oxygenated derivatives of DHA and brings into question Pathway 6 as a viable *in viv*o biosynthetic route. Pathway 4 also appears unfavorable since the current work indicates that h15-LOX-1 reacts with 7S-HDHA to produce 90% 7S,14S-diHDHA (*vide supra*). It therefore appears that h15-LOX-1 may not contribute much to the *in vitro* biosynthesis of RvD5. h15-LOX-2, however, reacts well with 7S-HDHA (V_{max} = 1.2 mol/sec^{-1}mol^{-1} at 10 μM) (**Table 2.8),** indicating that the rate of oxygenation at C7 by h5-LOX followed by oxygenation of C17 by h15-LOX-2 is a markedly faster pathway than the rate of oxygenation of C17 by h15-LOX-2 followed by oxygenation of C7 by h5-LOX. Therefore, if we calculate the biosynthetic flux (i.e. the rates time the percent product formation (**Scheme 2.2**)), it is apparent that the preferred pathway of RvD5 production *in vitro* is thru h5-LOX and then h15-LOX-2.

Previously, it was shown that h15-LOX-2 oxygenated 5S-HpETE, but not 12S-HpETE or 15S-HpETE (*15*). Together with the current work, this suggests that the h15-LOX-2 active site tolerates substrates that are oxygenated close to the carboxylate end but not those substrates oxygenated closer to the methyl end. This is consistent with the substrate-binding model, where the methyl-end of the substrate binds at the bottom of the active site (*59, 62, 63*), allowing for the abstraction of a hydrogen atom from C15 and the subsequent oxidation at C17. In order to understand this binding event in more detail, DHA and 7S-HDHA were modeled into the active site of h15-LOX-2. Both substrates bind in a tail first, U-shaped binding mode with their carboxylate groups forming a salt-bridge with R429 on the helix α12. Their hydrophobic tails are buried deep in a hydrophobic pocket created by residues F365, L420, I421, V427, F438 and L607 (**Figure 2.5**), and the reactive pro-S hydrogen of C15 of 7S-HDHA is 2.7Å from the active site hydroxide-ferric moiety. This binding mode is consistent with the abstraction of the pro-S hydrogen atom from C15 to produce 7S,17S-diHpDHA. Parenthetically, the pro-S hydrogen is also abstracted in formation of 12-HETE, 5-HETE, and 15-HETE by h12-LOX, h5LOX and h15-LOX-1 respectively (*49-53*).

2.4.3 Biological Consequences

If we consider that the *in vitro* biosynthetic pathways outlined above for 7S,14S-diHDHA and 7S,17S-diHDHA could be viable in *in vivo* systems and the fact that both molecules are biologically active, then a few cellular consequences should

be discussed. First, the ability of h15-LOX-1 to produce 7S,14S-diHDHA from 7S-HDHA opens up the possibility for involvement of new cells types not previously considered in 7S,14S-diHDHA formation. For example, cellular interactions within blood clots are proposed to lead to the synthesis of SPM through the process of transcellular biosynthesis (*27, 28*), therefore, cell types that contain h5-LOX and h15-LOX-1 may participate in the transcellular biosynthesis of 7S,14S-diHDHA. For example, h15-LOX-1 is expressed at high levels in macrophages, but it is not found in blood vessel endothelium or in platelets (*64-66*), while h5-LOX is expressed at high levels in neutrophils (*67-69*). As macrophages and neutrophils are often co-localized at sites of inflammation and thrombosis, these two cell types may be involved in the transcellular biosynthesis of 7S,14S-diHDHA. In addition, macrophages can express both h5-LOX and h15-LOX-1, so in the simplest terms, macrophages may be able to synthesize 7S,14S-diHDHA without participation of other cell types for transcellular biosynthesis.

Second, if h15-LOX-2 is the primary enzyme involved in the *in vivo* RvD5 biosynthesis, then the role of h15-LOX-2 in human disease could be larger than expected. It is known that h15-LOX-2 converts the h5-LOX-derived pro-inflammatory oxylipins, 5S-HETE and 5,6-diHETE, into pro-resolving molecules, such as lipoxins, *in vitro* (*70*). With the knowledge that h15-LOX-2 also efficiently produces RvD5 from 7S-HDHA, it could be that h15-LOX-2 is important in mediating the switch between inflammation and resolution. For example, neutrophils express both h5-LOX and h15-LOX-2, so it is conceivable that neutrophils produce

RvD5 independently, without the need for a transcellular synthesis mechanism. However, it should be noted that RvD5 production was observed by exposing isolated neutrophils to 17S-HpDHA (*40*), suggesting h5-LOX can produce RvD5 in neutrophils. This result is in contrast to our *in vitro* results and suggests that there may be a factor in the neutrophils, similar to the role of 5-lipoxygenase activating protein (FLAP), which could increase the h5-LOX activity with 17S-HDHA (*71*).

With respect to blood coagulation, this work shows that RvD5 has micromolar potency in inhibiting platelet activation, indicating that h15-LOX-2 may also play a role in hemostasis. RvD5 levels are reduced in blood treated with anticoagulants *in vitro* (*72*) and RvD5 formation does not occur during initial platelet activation, however, it is produced in later stages of clot progression (*72*). Given our result that RvD5 reduces platelet activation, the production of RvD5 could be a signal to diminish the clot size. Given that platelets do not produce h15-LOX-2 and thus cannot make RvD5, these results suggest that RvD5 is formed by h15-LOX-2 in macrophages and/or neutrophils, which migrate into the area of late-stage clots and increase their RvD5 production by increasing the h15-LOX-2 expression, and not that of h15-LOX-1 (*4*). We are currently investigating the role of h15-LOX-2 in more detail with our specific/potent h15-LOX-2 inhibitors (*73*) with the hope of understanding the correct biosynthesis pathway of RvD5 and hence its role in coagulation and atherosclerotic disorders.

2.5 Conclusion

7S,14S-diHDHA is synthesized *in vitro* by the sequential reactions of h5-LOX and h12-LOX with DHA. However, we have also discovered a novel alternative biosynthetic pathway for the production of 7S,14S-diHDHA, which involves h15-LOX-1. The alcohol on 7S-HDHA changes the binding position of the oxylipin in the active site, thus altering the product specificity. This non-canonical result has far-reaching ramifications. It first indicates a possible alternative biosynthetic pathway for 7S,14S-diHDHA, but more importantly, the result indicates that our knowledge of LOX reactivities with fatty acids, may not extend to oxylipins, and therefore further study is needed to determine the exact biosynthetic pathways for oxylipins, such as lipoxins, protectins and maresins. In addition, this result suggests that the biosynthesis of 7S,17S-diHDHA (RvD5) is achieved with h15-LOX-2 and thus its role in human disease may be more important than previously suspected. These results are especially relevant since we have discovered that both 7S,14S-diHDHA and 7S,17S-diHDHA (RvD5) are micromolar, anti-aggregation effector molecules that could possibly be synthesized directly from macrophages or neutrophils, respectively, without the need for a transcellular mechanism of biosynthesis, suggesting that both 7S,14S-diHDHA and 7S,17S-diHDHA (RvD5) may be more intimately involved in stopping the aggregation process in clot resolution than previously suspected. Thus, targeting the kinetics of platelet aggregation or clot resolution at sites of inflammation by inhibiting the biosynthesis of either 7S,14S-diHDHA and 7S,17S-diHDHA (RvD5) may represent a new therapeutic target for future development.

2.6 Authorship Contributions

Steven C. Perry, Benjamin E. Tourdot, Chakrapani Kalyanaraman, William S. Conrad, Oluwayomi Akinkugbe, John Cody Freedman, Michael Holinstat, Matthew P. Jacobson, and Theodore R. Holman

SP, BT, and CK designed the experiments. SP, BT, CK and OA, SC carried out experiments. SP, BT, CK analyzed data, SP wrote the manuscript, edited by TH, MH, MJ

2.7 References

1. Tabas, I., and Glass, C. K. (2013) Anti-inflammatory therapy in chronic disease: challenges and opportunities, *Science 339*, 166-172.

2. Serhan, C., and Petasis, N. (2011) Resolvins and Protectins in Inflammation Resolution, *Chemical Reviews ASAP*.

3. Hulten, L. M., Olson, F. J., Aberg, H., Carlsson, J., Karlstrom, L., Boren, J., Fagerberg, B., and Wiklund, O. (2010) 15-Lipoxygenase-2 is expressed in macrophages in human carotid plaques and regulated by hypoxia-inducible factor-1alpha, *Eur J Clin Invest 40*, 11-17.

4. Gertow, K., Nobili, E., Folkersen, L., Newman, J. W., Pedersen, T. L., Ekstrand, J., Swedenborg, J., Kuhn, H., Wheelock, C. E., Hansson, G. K., Hedin, U., Haeggstrom, J. Z., and Gabrielsen, A. (2011) 12- and 15-lipoxygenases in human carotid atherosclerotic lesions: associations with cerebrovascular symptoms, *Atherosclerosis 215*, 411-416.

5. Danielsson, K. N., Rydberg, E. K., Ingelsten, M., Akyurek, L. M., Jirholt, P., Ullstrom, C., Forsberg, G. B., Boren, J., Wiklund, O., and Hulten, L. M. (2008) 15-Lipoxygenase-2 expression in human macrophages induces chemokine secretion and T cell migration, *Atherosclerosis 199*, 34-40.

6. Weaver, J. R., Holman, T. R., Imai, Y., Jadhav, A., Kenyon, V., Maloney, D. J., Nadler, J. L., Rai, G., Simeonov, A., and Taylor-Fishwick, D. A. (2012) Integration of pro-inflammatory cytokines, 12-lipoxygenase and NOX-1 in pancreatic islet beta cell dysfunction, *Mol Cell Endocrinol 358*, 88-95.

7. Cole, B. K., Lieb, D. C., Dobrian, A. D., and Nadler, J. L. (2013) 12- and 15-lipoxygenases in adipose tissue inflammation, *Prostaglandins & other lipid mediators 104-105*, 84-92.

8. Mangino, M. J., Brounts, L., Harms, B., and Heise, C. (2006) Lipoxin biosynthesis in inflammatory bowel disease, *Prostaglandins & other lipid mediators 79*, 84-92.

9. Serhan, C. N., Chiang, N., and Van Dyke, T. E. (2008) Resolving inflammation: dual anti-inflammatory and pro-resolution lipid mediators, *Nat Rev Immunol 8*, 349-361.

10. Ivanov, I., Heydeck, D., Hofheinz, K., Roffeis, J., O'Donnell, V. B., Kuhn, H., and Walther, M. (2010) Molecular enzymology of lipoxygenases, *Archives of biochemistry and biophysics 503*, 161-174.

11. Colakoglu, M., Tuncer, S., and Banerjee, S. (2018) Emerging cellular functions of the lipid metabolizing enzyme 15-Lipoxygenase-1, *Cell proliferation 51*, e12472.

12. Ford-Hutchinson, A. W. (1991) Arachidonate 15-lipoxygenase; characteristics and potential biological significance, *Eicosanoids 4*, 65-74.

13. Brash, A. R., Boeglin, W. E., and Chang, M. S. (1997) Discovery of a second 15S-lipoxygenase in humans, *Proceedings of the National Academy of Sciences of the United States of America 94*, 6148-6152.

14. Jisaka, M., Kim, R. B., Boeglin, W. E., Nanney, L. B., and Brash, A. R. (1997) Molecular cloning and functional expression of a phorbol ester-inducible 8S-lipoxygenase from mouse skin, *J Biol Chem 272*, 24410-24416.

15. Green, A. R., Barbour, S., Horn, T., Carlos, J., Raskatov, J. A., and Holman, T. R. (2016) Strict Regiospecificity of Human Epithelial 15-Lipoxygenase-2 Delineates Its Transcellular Synthesis Potential, *Biochemistry 55*, 2832-2840.

16. Magnusson, L. U., Lundqvist, A., Karlsson, M. N., Skaʹleʹn, K., Levin, M., Wiklund, O., Boreʹn, J., and Hulteʹn, L. M. (2012) Arachidonate 15-Lipoxygenase Type B Knockdown Leads to Reduced Lipid Accumulation and Inflammation in Atherosclerosis.pdf, *PloS one 7*.

17. Serhan, C. N., Yang, R., Martinod, K., Kasuga, K., Pillai, P. S., Porter, T. F., Oh, S. F., and Spite, M. (2009) Maresins: novel macrophage mediators with potent antiinflammatory and proresolving actions, *J Exp Med 206*, 15-23.

18. Gu, Z., Lamont, G. J., Lamont, R. J., Uriarte, S. M., Wang, H., and Scott, D. A. (2016) Resolvin D1, resolvin D2 and maresin 1 activate the GSK3beta anti-inflammatory axis in TLR4-engaged human monocytes, *Innate immunity 22*, 186-195.

19. Green, A. R., Freedman, C., Tena, J., Tourdot, B. E., Liu, B., Holinstat, M., and Holman, T. R. (2018) 5 S,15 S-Dihydroperoxyeicosatetraenoic Acid (5,15-diHpETE) as a Lipoxin Intermediate: Reactivity and Kinetics with Human Leukocyte 5-Lipoxygenase, Platelet 12-Lipoxygenase, and Reticulocyte 15-Lipoxygenase-1, *Biochemistry*.

20. Edenius, C., Haeggstrom, J., and Lindgren, J. A. (1988) Transcellular conversion of endogenous arachidonic acid to lipoxins in mixed human platelet-granulocyte suspensions, *Biochem Biophys Res Commun 157*, 801-807.

21. Sheppard, K. A., Greenberg, S. M., Funk, C. D., Romano, M., and Serhan, C. N. (1992) Lipoxin generation by human megakaryocyte-induced 12-lipoxygenase, *Biochimica et biophysica acta 1133*, 223-234.

22. Dalli, J., Colas, R. A., and Serhan, C. N. (2013) Novel n-3 immunoresolvents: structures and actions, *Sci Rep 3*, 1940.

23. Giera, M., Ioan-Facsinay, A., Toes, R., Gao, F., Dalli, J., Deelder, A. M., Serhan, C. N., and Mayboroda, O. A. (2012) Lipid and lipid mediator profiling of human synovial fluid in rheumatoid arthritis patients by means of LC-MS/MS, *Biochimica et biophysica acta 1821*, 1415-1424.

24. Hong, S., Gronert, K., Devchand, P. R., Moussignac, R. L., and Serhan, C. N. (2003) Novel docosatrienes and 17S-resolvins generated from docosahexaenoic acid in murine brain, human blood, and glial cells. Autacoids in anti-inflammation, *The Journal of biological chemistry 278*, 14677-14687.

25. Chiang, N., Fredman, G., Backhed, F., Oh, S. F., Vickery, T., Schmidt, B. A., and Serhan, C. N. (2012) Infection regulates pro-resolving mediators that lower antibiotic requirements, *Nature 484*, 524-528.

26. Serhan, C. N., Gotlinger, K., Hong, S., Lu, Y., Siegelman, J., Baer, T., Yang, R., Colgan, S. P., and Petasis, N. A. (2006) Anti-inflammatory actions of neuroprotectin D1/protectin D1 and its natural stereoisomers: assignments of dihydroxy-containing docosatrienes, *J Immunol 176*, 1848-1859.

27. Serhan, C. N., and Sheppard, K. A. (1990) Lipoxin formation during human neutrophil-platelet interactions. Evidence for the transformation of leukotriene A4 by platelet 12-lipoxygenase in vitro, *Journal of Clinical Investigation 85*, 772-780.

28. Deng, B., Wang, C. W., Arnardottir, H. H., Li, Y., Cheng, C. Y., Dalli, J., and Serhan, C. N. (2014) Maresin biosynthesis and identification of maresin 2, a new anti-inflammatory and pro-resolving mediator from human macrophages, *PloS one 9*, e102362.

29. Sala, A., Testa, T., and Folco, G. (1996) Leukotriene A4, and not leukotriene B4, is the main 5-lipoxygenase metabolite released by bovine leukocytes, *FEBS Lett 388*, 94-98.

30. Barden, A. E., Shinde, S., Burke, V., Puddey, I. B., Beilin, L. J., Irish, A. B., Watts, G. F., and Mori, T. A. (2018) The effect of n-3 fatty acids and coenzyme Q10 supplementation on neutrophil leukotrienes, mediators of inflammation resolution and myeloperoxidase in chronic kidney disease, *Prostaglandins & other lipid mediators 136*, 1-8.

31. Norris, P. C., and Serhan, C. N. (2018) Metabololipidomic profiling of functional immunoresolvent clusters and eicosanoids in mammalian tissues, *Biochem Biophys Res Commun 504*, 553-561.

32. Serhan, C. N., Dalli, J., Karamnov, S., Choi, A., Park, C. K., Xu, Z. Z., Ji, R. R., Zhu, M., and Petasis, N. A. (2012) Macrophage proresolving mediator maresin 1 stimulates tissue regeneration and controls pain, *FASEB journal : official publication of the Federation of American Societies for Experimental Biology 26*, 1755-1765.

33. Deschamps, J. D., Kenyon, V. A., and Holman, T. R. (2006) Baicalein is a potent in vitro inhibitor against both reticulocyte 15-human and platelet 12-human lipoxygenases, *Bioorg Med Chem 14*, 4295-4301.

34. Kutzner, L., Goloshchapova, K., Heydeck, D., Stehling, S., Kuhn, H., and Schebb, N. H. (2017) Mammalian ALOX15 orthologs exhibit pronounced dual positional specificity with docosahexaenoic acid, *Biochimica et biophysica acta. Molecular and cell biology of lipids 1862*, 666-675.

35. Lee, T. H., Mencia-Huerta, J. M., Shih, C., Corey, E. J., Lewis, R. A., and Austen, K. F. (1984) Effects of exogenous arachidonic, eicosapentaenoic, and docosahexaenoic acids on the generation of 5-lipoxygenase pathway products by ionophore-activated human neutrophils, *The Journal of clinical investigation 74*, 1922-1933.

36. Smyrniotis, C. J., Barbour, S. R., Xia, Z., Hixon, M. S., and Holman, T. R. (2014) ATP Allosterically Activates the Human 5-Lipoxygenase Molecular Mechanism of Arachidonic Acid and 5(S)-Hydroperoxy-6(E),8(Z),11(Z),14(Z)-eicosatetraenoic Acid, *Biochemistry*.

37. Adel, S., Karst, F., Gonzalez-Lafont, A., Pekarova, M., Saura, P., Masgrau, L., Lluch, J. M., Stehling, S., Horn, T., Kuhn, H., and Heydeck, D. (2016) Evolutionary alteration of ALOX15 specificity optimizes the biosynthesis of antiinflammatory and proresolving lipoxins, *Proceedings of the National Academy of Sciences of the United States of America 113*, E8006.

38. Abrial, C., Grassin-Delyle, S., Salvator, H., Brollo, M., Naline, E., and Devillier, P. (2015) 15-Lipoxygenases regulate the production of chemokines in human lung macrophages, *British journal of pharmacology 172*, 4319-4330.

39. Snodgrass, R. G., Zezina, E., Namgaladze, D., Gupta, S., Angioni, C., Geisslinger, G., Lutjohann, D., and Brune, B. (2018) A Novel Function for 15-Lipoxygenases in Cholesterol Homeostasis and CCL17 Production in Human Macrophages, *Frontiers in immunology 9*, 1906.

40. Archambault, A. S., Turcotte, C., Martin, C., Provost, V., Larose, M. C., Laprise, C., Chakir, J., Bissonnette, E., Laviolette, M., Bosse, Y., and Flamand, N. (2018) Comparison of eight 15-lipoxygenase (LO) inhibitors on the biosynthesis of 15-LO metabolites by human neutrophils and eosinophils, *PloS one 13*, e0202424.

41. Maas, R. L., Turk, J., Oates, J. A., and Brash, A. R. (1982) Formation of a novel dihydroxy acid from arachidonic acid by lipoxygenase-catalyzed double oxygenation in rat mononuclear cells and human leukocytes, *The Journal of biological chemistry 257*, 7056-7067.

42. Wecksler, A. T., Jacquot, C., van der Donk, W. A., and Holman, T. R. (2009) Mechanistic Investigations of Human Reticulocyte 15- and Platelet 12-Lipoxygenases with Arachidonic Acid, *Biochemistry 48*, 6259-6267.

43. Segraves, E. N., and Holman, T. R. (2003) Kinetic investigations of the rate-limiting step in human 12- and 15-lipoxygenase, *Biochemistry 42*, 5236-5243.

44. Aveldano, M. I., and Sprecher, H. (1983) Synthesis of hydroxy fatty acids from 4, 7, 10, 13, 16, 19-[1-14C] docosahexaenoic acid by human platelets, *The Journal of biological chemistry 258*, 9339-9343.

45. Guichardant, M., and Lagarde, M. (1985) Studies on platelet lipoxygenase specificity towards icosapolyenoic and docosapolyenoic acids, *Biochimica et biophysica acta 836*, 210-214.

46. Cipollina, C., Salvatore, S. R., Muldoon, M. F., Freeman, B. A., and Schopfer, F. J. (2014) Generation and dietary modulation of anti-inflammatory electrophilic omega-3 fatty acid derivatives, *PloS one 9*, e94836.

47. Koltsida, O., Karamnov, S., Pyrillou, K., Vickery, T., Chairakaki, A. D., Tamvakopoulos, C., Sideras, P., Serhan, C. N., and Andreakos, E. (2013) Toll-like receptor 7 stimulates production of specialized pro-resolving lipid mediators and promotes resolution of airway inflammation, *EMBO molecular medicine 5*, 762-775.

48. Northrop, D. B. (1998) On the meaning of Km and V/K in enzyme kinetics, *J. Chem. Ed. 75*, 1153-1157.

49. Suardiaz, R., Jambrina, P. G., Masgrau, L., Gonzalez-Lafont, A., Rosta, E., and Lluch, J. M. (2016) Understanding the Mechanism of the Hydrogen Abstraction from Arachidonic Acid Catalyzed by the Human Enzyme 15-Lipoxygenase-2. A Quantum Mechanics/Molecular Mechanics Free Energy Simulation, *Journal of chemical theory and computation 12*, 2079-2090.

50. Maas, R. L., Ingram, C. D., Taber, D. F., Oates, J. A., and Brash, A. R. (1982) Stereospecific removal of the DR hydrogen atom at the 10-carbon of arachidonic acid in the biosynthesis of leukotriene A4 by human leukocytes, *The Journal of biological chemistry 257*, 13515-13519.

51. Brash, A. R. (1999) Lipoxygenases: occurrence, functions, catalysis, and acquisition of substrate, *The Journal of biological chemistry 274*, 23679-23682.

52. Newcomer, M. E., and Brash, A. R. (2015) The structural basis for specificity in lipoxygenase catalysis, *Protein science : a publication of the Protein Society 24*, 298-309.

53. Hamberg, M., and Samuelsson, B. (1967) On the specificity of the oxygenation of unsaturated fatty acids catalyzed by soybean lipoxidase, *The Journal of biological chemistry 242*, 5329-5335.

54. Yeung, J., Hawley, M., and Holinstat, M. (2017) The expansive role of oxylipins on platelet biology, *J Mol Med (Berl) 95*, 575-588.

55. Tourdot, B. E., Adili, R., Isingizwe, Z. R., Ebrahem, M., Freedman, J. C., Holman, T. R., and Holinstat, M. (2017) 12-HETrE inhibits platelet reactivity and thrombosis in part through the prostacyclin receptor, *Blood advances 1*, 1124-1131.

56. Ikei, K. N., Yeung, J., Apopa, P. L., Ceja, J., Vesci, J., Holman, T. R., and Holinstat, M. (2012) Investigations of human platelet-type 12-lipoxygenase: role of lipoxygenase products in platelet activation, *Journal of lipid research 53*, 2546-2559.

57. Yeung, J., Tourdot, B. E., Adili, R., Green, A. R., Freedman, C. J., Fernandez-Perez, P., Yu, J., Holman, T. R., and Holinstat, M. (2016) 12(S)-HETrE, a 12-Lipoxygenase Oxylipin of Dihomo-gamma-Linolenic Acid, Inhibits Thrombosis via Galphas Signaling in Platelets, *Arteriosclerosis, thrombosis, and vascular biology 36*, 2068-2077.

58. Ikei, K. N., Yeung, J., Apopa, P. L., Ceja, J., Vesci, J., Holman, T. R., and Holinstat, M. (2012) Investigations of human platelet-type 12-lipoxygenase: role of lipoxygenase products in platelet activation, *J Lipid Res*.

59. Gan, Q.-F., Browner, M. F., Sloane, D. L., and Sigal, E. (1996) Defining the arachidonic acid binding site of human 15-lipoxygenase, *J. Biol. Chem. 271*, 25412 - 25418.

60. Horitani, M., Offenbacher, A. R., Carr, C. A., Yu, T., Hoeke, V., Cutsail, G. E., 3rd, Hammes-Schiffer, S., Klinman, J. P., and Hoffman, B. M. (2017) (13)C ENDOR Spectroscopy of Lipoxygenase-Substrate Complexes Reveals the Structural Basis for C-H Activation by Tunneling, *J Am Chem Soc 139*, 1984-1997.

61. Joshi, N., Hoobler, E. K., Perry, S., Diaz, G., Fox, B., and Holman, T. R. (2013) Kinetic and structural investigations into the allosteric and pH effect on the substrate specificity of human epithelial 15-lipoxygenase-2, *Biochemistry 52*, 8026-8035.

62. Sloane, D. L., Leung, r., Craik, C. S., and Sigal, E. (1991) A Primary determinant for Lipoxygenase positional specificity, *Nature 354*, 149-152.

63. Kuhn, H. (2000) Structural basis for the positional specificity oflipoxygenases, *Postaglandins & other Lipid Mediators 62*, 255–270.

64. Yla-Herttuala, S., Rosenfeld, M. E., Parthasarathy, S., Glass, C. K., Sigal, E., Witztum, J. L., and Steinberg, D. (1990) Colocalization of 15-lipoxygenase mRNA and protein with epitopes of oxidized low density lipoprotein in macrophage-rich areas of atherosclerotic lesions, *Proceedings of the National Academy of Sciences of the United States of America 87*, 6959-6963.

65. Kuhn, H., Belkner, J., Zaiss, S., Fahrenklemper, T., and Wohlfeil, S. (1994) Involvement of 15-Lipoxygenase in Early Stages of Atherogenesis, *Journal of Experimental Medicine 179*, 1903-1911.

66. Folcik, V. A., Nivar-Aristy, R. A., Krajewski, L. P., and Cathcart, M. K. (1995) Lipoxygenase contributes to the oxidation of lipids in human atherosclerotic plaques, *The Journal of clinical investigation 96*, 504-510.

67. Woods, J. W., Evans, J. F., Ethier, D., Scott, S., Vickers, P. J., Hearn, L., Heibein, J. A., Charleson, S., and Singer, II. (1993) 5-lipoxygenase and 5-lipoxygenase-activating protein are localized in the nuclear envelope of activated human leukocytes, *The Journal of experimental medicine 178*, 1935-1946.

68. Rouzer, C. A., Matsumoto, T., and Samuelsson, B. (1986) Single protein from human leukocytes possesses 5-lipoxygenase and leukotriene A4 synthase activities, *Proceedings of the National Academy of Sciences of the United States of America 83*, 857-861.

69. Ueda, N., Kaneko, S., Yoshimoto, T., and Yamamoto, S. (1986) Purification of arachidonate 5-lipoxygenase from porcine leukocytes and its reactivity with hydroperoxyeicosatetraenoic acids, *J Biol Chem 261*, 7982-7988.

70. Ringholz, F. C., Buchanan, P. J., Clarke, D. T., Millar, R. G., McDermott, M., Linnane, B., Harvey, B. J., McNally, P., and Urbach, V. (2014) Reduced 15-lipoxygenase 2 and lipoxin A4/leukotriene B4 ratio in children with cystic fibrosis, *The European respiratory journal 44*, 394-404.

71. Peters-Golden, M., and Brock, T. G. (2003) 5-lipoxygenase and FLAP, *Prostaglandins, leukotrienes, and essential fatty acids 69*, 99-109.

72. Norris, P. C., Libreros, S., Chiang, N., and Serhan, C. N. (2017) A cluster of immunoresolvents links coagulation to innate host defense in human blood, *Sci Signal 10*.

73. Jameson, J. B., Kantz, A., Schultz, L., Kalyanaraman, C., Jacobson, M. P., Maloney, D. J., Jadhav, A., Simeonov, A., and Holman, T. R. (2014) A High Throughput Screen Identifies Potent and Selective Inhibitors to Human Epithelial 15-Lipoxygenase-2, *PloS one 9*.

74. Amagata, T., Whitman, S., Johnson, T. A., Stessman, C. C., Loo, C. P., Lobkovsky, E., Clardy, J., Crews, P., and Holman, T. R. (2003) Exploring sponge-derived terpenoids for their potency and selectivity against 12-human, 15-human, and 15-soybean lipoxygenases, *J Nat Prod 66*, 230-235.

75. Robinson, S. J., Hoobler, E. K., Riener, M., Loveridge, S. T., Tenney, K., Valeriote, F. A., Holman, T. R., and Crews, P. (2009) Using enzyme assays to evaluate the structure and bioactivity of sponge-derived meroterpenes, *J Nat Prod 72*, 1857-1863.

76. Johnathan Fitzgerald, R. C., Masakazu Shinohara, Jesmond Dalli, Charles Serhan. (2014) Lipid Mediator Metabololipidomics LC-MS--MS Spectra Book 2014.

77. Butovich, I. A. (2006) A one-step method of 10,17-dihydro(pero)xydocosahexa-4Z,7Z,11E,13Z,15E,19Z-enoic acid synthesis by soybean lipoxygenase, *Journal of lipid research 47*, 854-863.

Chapter 3

A ROLE FOR HUMAN 15-LIPOXYGNENASE-2 IN THE BIOSYNTHESIS OF THE LIPOXIN INTERMEDIATE, 5S,15S-DI-HPETE, IS INDICATED BY THE ALTERED POSITIONAL SPECIFICITY OF HUMAN 15-LIPOXYGENASE-1

3.1 Introduction

The process of inflammation plays an important role in tissue homeostasis and is tightly regulated through the balance of pro-inflammatory and pro-resolving signals. In the initial stage of inflammation, damaged tissues produce pro-inflammatory signaling molecules, such as the leukotrienes, that recruit neutrophils and macrophages to sites of injury (*1*). During the resolution stage of inflammation cells generate specialized pro-resolving mediators (SPM's), such as the lipoxins (*2*), which limit inflammation by antagonizing leukotriene-mediated pro-inflammatory processes (*3-5*) and enhancing phagocytosis of apoptotic neutrophils by macrophages (*6*). Without proper resolution, chronic inflammation can contribute to a variety of diseases, such as diabetend cancer (*7-9*).

Lipoxins and leukotrienes are oxylipins produced by lipoxygenase-catalyzed oxygenation of arachidonic acid (AA) (*10*). Lipoxygenases are non-heme iron enzymes that catalyze the stereospecific hydroperoxidation of AA, and other poly-unsaturated fatty acids (PUFAs) (*11*). There is one 12-LOX isozyme and two human 15-LOX isozymes. Human platelet 12-ipoxygenase (h12-LOX or ALOX12) is expressed in platelets and pancreatic islets of Langerhans (*12*), human reticulocyte 15-lipoxygenase-1 (h15-LOX-1 or ALOX15) is expressed in reticulocytes and macrophages (*13, 14*), and human epithelial 15-lipoxygenase-2 (h15-LOX-2 or ALOX15b) is expressed in macrophages, neutrophils, epithelium and prostate tissue (*15-17*). When reacting with AA, h12-LOX produces only 12(S)-hydroperoxy-5Z,8Z,10E,14Z-eicosatetraenoic acid (12S-HpETE), h15-LOX-1 produces mostly

15(S)-hydroperoxy-5Z,8Z,11Z,13E-eicosatetraenoic acid (15S-HpETE), along with a minor amount of 12S-HpETE, while h15-LOX-2 produces only 15S-HpETE (*18*). These LOX isozymes are also postulated to oxygenate 5S-HpETE to produce 5(S),12(S)-6E,8Z,10E,14Z-dihydroxyeicosatetraenoic acid (5S,12S-diHpETE) and 5(S),15(S)-dihydroperoxy-6E,8Z,11Z,13E-eicosatetraenoic acid (5S,15S-diHpETE), which is the focus of the current work.

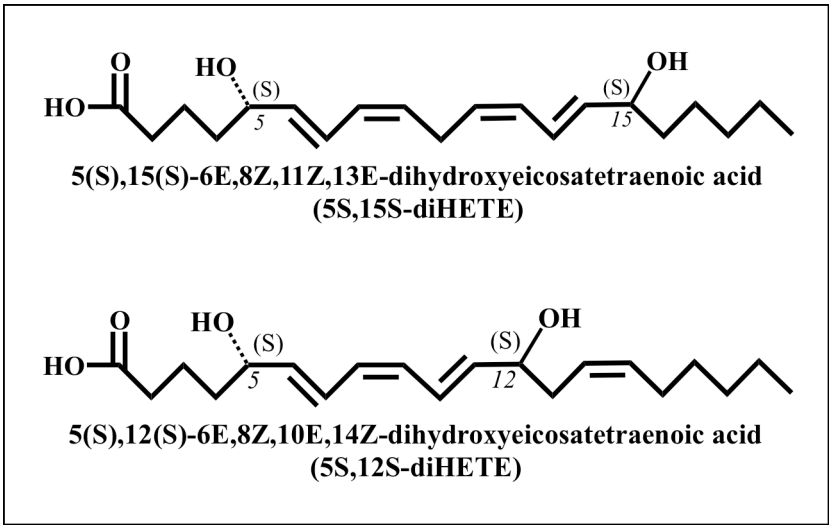

Figure 3.1. Structures of 5S,12S-diHETE and 5S,15S-diHETE.

5S,15S-diHpETE (**Figure 3.1**) is proposed to be an intermediate in the biosynthesis of lipoxins (**Figure 1.3**) (*19-22*) and 5-oxo-15S-HETE, an eosinophil chemoattractant (*23*). 5S,15S-diHpETE is found in macrophages and PMN's (*20, 24*) and is elevated in PMN's isolated from patients with asthma (*29*) and rheumatoid arthritis (*25*). 5S,15S-diHpETE and its reduced form, 5S,15S-diHETE, have chemotactic activity towards eosinophils (*26*), potentiate neutrophil degranulation (*27*) and inhibit platelet aggregation (*28*). 5S,15S-diHpETE is proposed to be formed

by two lipoxygenase-catalyzed di-oxygenation reactions and can be produced from either 5S-HETE or 15S-HpETE, as the starting reagent (*20, 29-32*). It was postulated that h5-LOX and h15-LOX carried out this biosynthesis, however, the order of the reaction and the relative efficiency of these two pathways has not been examined *in vitro*.

5S,12S-diHETE (**Figure 3.1**) is an isomer of Leukotriene B_4 (LTB_4) and appears to be biosynthesized in a similar manner as 5S,15S-diHETE, through sequential LOX oxygenations, followed by reduction. It is produced by both platelets and neutrophils (*32-34*) and manifests at elevated levels in patients with psoriasis (*35*). 5S,12S-diHETE can be produced in cells at higher amounts than LTB_4 (*36*), but has lower chemotactic activity towards PMN's compared to LTB_4 (*37-39*). Based on cell studies, 5S,12S-diHETE is proposed to be formed through two sequential lipoxygenase-catalyzed di-oxygenations (*40-42*) by either h5-LOX from 12S-HETE or by h12-LOX from 5S-HETE (*40, 41, 43*). However, the relative efficiency of these two pathways is unknown and there has been no investigation into a possible role of h15-LOX-1 in the formation of 5S,12S-diHETE.

In general, it is postulated that AA binds into the active site of both h12-LOX (*44*) and h15-LOX-1 (*45*), methyl-end first, with amino acid positions 417 and 418 defining the bottom of the pocket (*46*). If these two residues are enlarged in volume by mutagenesis, the percentage of 15-HpETE production increases for h12-LOX, due to the AA positioning shallower into the active site (*44, 47*). If these two residues are reduced in volume by mutagenesis, the percentage of 12-HpETE production increases

for h15-LOX-1, due to the AA positioning deeper into the active site (*48*). However, recent work has demonstrated that h15-LOX-1 has altered positional specificity when reacting with the oxygenated derivative of docosahexaenoic acid (DHA), 7-hydroxy docosahexaenoic acid (7-HDHA) (chapter 2). When reacting with DHA, h15-LOX-1 abstracts a hydrogen atom from the w-8 carbon, and oxygenates C17, however when reacting with 7-HDHA, h15-LOX-1 oxygenates primarily on C14. A docking model proposes that the backbone carbonyl of Ile399 hydrogen-bonds with the alcohol on C7, thus positioning 7-HDHA deeper into the active site, leading to the 14-product, 7S,14S-HDHA.

This shift in product profile raises questions as to the role of h15-LOX-1 in the biosynthesis of 5S,12S-diHETE and 5S,15S-diHETE. If the C5 alcohol of 5S-HpETE also hydrogen bonds to the backbone carbonyl of Ile399, then the presumed biosynthetic pathways of 5S,12S-diHETE and 5S,15S-diHETE could be redefined. In addition, the contribution of h15-LOX-2 to the formation of lipoxin intermediates has been largely overlooked, as it reacts poorly with AA compared to h15-LOX-1 and was initially thought to have limited tissue expression (*15*). More recent studies indicate that h15-LOX-2 does not show altered positional specificity when reacting with 7-HDHA, producing >98% of 7S,17S-diHDHA (chapter 2) and is expressed in primary macrophages at levels higher than both h15-LOX-1 and h12-LOX (*17, 49*), suggesting a greater role for h15-LOX-2 in the biosynthesis of Resolvin D5 (RvD5 or 7S,17S-diHETE).

In the current work, we investigate whether the positional specificity of h15-LOX-1 and h15-LOX-2 with 7S-HDHA extends to the analogous AA-derived oxylipin, 5S-HETE, and determine the relative roles of h5-LOX, h12-LOX, h15-LOX-1 and h15-LOX-2 in the *in vitro* biosynthesis of 5S,15S-diHETE, 5S,12S-diHETE and their unreduced counterparts.

3.2 Experimental Procedures

3.2.1 Expression and Purification of h15-LOX-1, h15-LOX-2, h12-LOX, and h5-LOX.

Overexpression and purification of wild-type h15-LOX-1 (Uniprot entry P16050), h12-LOX (Uniprot entry P18054), h5-LOX (Uniprot entry P09917) and h15-LOX-2 (Uniprot entry O15296) were performed as previously described (*50-52*). The purity of h15-LOX-1 and h12-LOX were assessed by SDS gel to be greater than 85%, and metal content was assessed on a Finnigan inductively-coupled plasma-mass spectrometer (ICP-MS), via comparison with iron standard solution. Cobalt-EDTA was used as an internal standard. The wt h5-LOX used in the kinetics of this work was not purified due to a dramatic loss in activity. Therefore, the amount of h5-LOX contained in the ammonium-sulfate pellet was assessed by comparing values obtained by a Bradford assay and quantitative western blotting using purified stable-h5-LOX mutant as a positive control. Western blots were performed using rabbit anti-5-lipoxygenase polyclonal (Cayman chemicals) primary antibody diluted 1:500 and goat anti-rabbit-HRP (Abcam) secondary antibody diluted 1:5000. The stable-h5-

LOX mutant was expressed in Rosetta 2 cells (Novagen) transformed with the pET14b-Stable-5-LOX plasmid (a gift from Marcia Newcomer of Louisiana State University) and grown in Terrific Broth containing 34 μg ml^{-1} chloramphenicol and 100 μg ml^{-1} ampicillin at 37 °C for 3.5 h and then placed at 20 °C for an additional 26 h. Cells were pelleted and resuspended in 50 mM Tris (pH 8.0), 500 mM NaCl, 20 mM imidazole with 1 μM Pepstatin, 100 μM PMSF, and DNaseI (2 Kunitz/g) (Sigma). The cells were lysed in a French pressure cell and centrifuged at 40,000xg for 20min. Lysate was applied to a Talon nickel-IDA Sepharose column and eluted with 50 mM Tris pH 8.0, 500 mM NaCl, 200 mM imidazole. The final product was stored at −80 °C with 10% glycerol. The k_{cat} and k_{cat}/K_M values determined for our ammonium-sulfate precipitated h5-LOX are similar to values seen from the purified stable h5-LOX mutant (*53*) when accounting for addition of ATP to buffers in the current work, which induces a 5-fold increase in h5-LOX activity (*54*). Due to the difficulty determining the iron content of crude ammonium sulfate-precipitated extracted enzyme, the metalation of h5-LOX was assumed to be 100%.

3.2.2 Production and isolation of Oxylipins

5(S)-hydroperoxyeicosatetraenoic acid (5S-HpETE) was synthesized by reaction of AA (40 μM) with ~200mg of ammonium-sulfate precipitated h5-LOX. The reaction was carried out for 1 hour in 1000 ml of 25mM HEPES, pH 7.5 containing 50mM NaCl, 100 μM EDTA and 200 μM ATP. The reaction was quenched with 0.5% glacial acetic acid, extracted 3 times with 1/3 volume dichloromethane and

evaporated to dryness under N2. The Products purified isocratically via high performance liquid chromatography (HPLC) on a Higgins Haisil Semi-preparative (5μm, 250mm x 10mm) C18 column with 50:50 of 99.9% acetonitrile, 0.1% acetic acid and 99.9% water, 0.1% acetic acid. The isolated products were assessed to be greater than 95% pure by LC-MS/MS. 5(S)-hydroxyeicosatetraenoic acid (5S-HETE) was synthesized as performed for 5S-HpETE with trimethylphosphite added as a reductant prior to HPLC. 12S-HpETE was synthesized by reaction of AA (25-50 μM) with h12-LOX. The reaction was carried out for 30 min in 500 ml of 25mM HEPES, pH 8.0. 15(S)-hydroperoxyeicosatetraenoic acid (15S-HpETE) was synthesized by reaction of AA (25-50 μM) with soybean 15-LOX. The reaction was carried out for 30 min in 500 ml of 50mM Borate, pH 9.0. 15(S)-hydroxyeicosatetraenoic acid (15S-HETE) and 12(S)-hydroxyeicosatetraenoic acid (12S-HETE) were synthesized as performed for 15S-HpETE and 12S-HpETE with trimethylphosphite added as a reductant prior to HPLC. The Products were extracted and purified isocratically via HPLC as described above for 5S-HpETE.

3.2.3 Steady State Kinetics of h5LOX, h12-LOX, h15-LOX-1 and h15-LOX-2.

Steady-state kinetic reactions were performed, at ambient temperature, in a 1 cm^2 quartz cuvette and were monitored on a Perkin-Elmer Lambda 45 UV/VIS spectrophotometer. Reactions contained 2 mL of either 25 mM HEPES, pH 7.5 (h15-LOX-1 and h15-LOX-2), 25 mM HEPES, pH 8.0 (h12-LOX) or 25 mM HEPES, pH 7.5, 50 mM NaCl, 100 mM EDTA and 200 mM ATP. (h5-LOX). Substrate

concentrations were varied from 0.25 μM to 10 μM for AA or 0.5 μM to 40 μM for 5S-HETE and 5S-HpETE. Reactions were initiated by the addition of either; h5-LOX (~300-900 nM final concentration), h12-LOX (~300-900 nM final concentration), h15-LOX-1 (~200-600 nM final concentration), or h15-LOX-2 (~300-700 nM final concentration) and were monitored on a Perkin-Elmer Lambda 45 UV/VIS spectrophotometer. Product formation was determined by the increase in absorbance at 234 nm for 5S-HETE (ε_{234nm} = 27,000 M^{-1} cm^{-1}), 270 nm for 5S,12S-diHETE (ε_{234nm} = 40,000 M^{-1} cm^{-1}), and 254 nm for 5S,15S-diHETE (ε_{234nm} = 21,500 M^{-1} cm^{-1}) (*20*). 5S,15S-diHDHA has an absorbance max of 245 nm, however, due to overlap with the substrate peak at 234 nm formation of this product was measured at 254 nm using an extinction coefficient of 21,900 M^{-1} cm^{-1} to adjust for the decreased rate of absorbance change at this peak shoulder (*28*). KaleidaGraph (Synergy) was used to fit initial rates (at less than 20% turnover), as well as the second order derivatives (k_{cat}/K_M) to the Michaelis-Menten equation for the calculation of kinetic parameters.

3.2.4 Product Analysis of LOX reactions with AA, 5S-HETE and 5S-HpETE

Reactions were carried out with stirring at ambient temperature in the buffers indicated above. Reactions with AA contained 10 μM substrate and a final concentration of either; h5-LOX (~300 nM), h12-LOX (~300 nM), h15-LOX-1 (~200 nM), or h15-LOX-2 (~350 nM). Those with 5S-HETE and 5S-HpETE contained 10 μM substrate and a final concentration of either h12-LOX (950 nM), h15-LOX-1 (550 nM) or h15-LOX-2 (700 nM). Reactions with 15S-HETE and 15S-HpETE,

12S-HETE and 12S-HpETE contained 20 μM substrate and (1100 nM) h5-LOX. Reactions were monitored via UV-vis spectrophotometer and quenched at 50% turnover with 0.5% glacial acetic acid. Each quenched reaction was extracted with 6 mL of DCM and reduced with trimethylphosphite. The samples were then evaporated under a stream of N_2 to dryness and reconstituted in 50 μL of 90% acetonitrile/10% water containing 0.1% formic acid and 3 μM 13-HODE as an internal standard. Control reactions without enzymes were also conducted and used for background subtraction, ensuring oxylipin degradation products were removed from analysis. Reactions were analyzed via LC-MS/MS. The chromatography system was coupled to a Thermo-Electron LTQ LC-MS/MS for mass analysis. All analyses were performed in negative ionization mode at the normal resolution setting. MS2 was performed in a targeted manner with a mass list containing the following m/z ratios ± 0.5: 319.4 (HETE's), 335.4 (diHETE's), and 351.4 (triHETE's). Products were identified by matching retention times, UV spectra, and fragmentation patterns to known standards, or in the cases were MS standards were not available, structures were deduced from comparison with known and theoretical fragments.

3.2.5 Chiral Chromatography

5S,12S-diHETE and 5S,15S-diHETE were synthesized and isolated via HPLC as described above. Purified 5S,12S-diHETE and 5S,15S-diHETE were analyzed via LC-MS/MS using a Chirapak AD-RH 2.1x150 mm 5μM chiral column coupled to a Thermo electron LTQ. Retention times and fragmentations were compared to 5S,12S-

diHETE, 5S,15S-diHETE, LTB_4 and 6-trans12-epi-LTB_4 standards purchased from Cayman Chemicals (Ann Arbor, MI) Analysis was carried out using a gradient from 40:60 A:B to 70:30 A:B, over 25 min. Mobile phase solvent A consisted of 99.9% acetonitrile, 0.1% formic acid and solvent B consisted of 99.9% water, 0.1% formic acid. MS/MS conditions were the same as described above.

3.2.6 5S-HETE titration into human platelets.

The University of Michigan Institutional Review Board approved all research involving human volunteers. Washed platelets were isolated from human whole blood via serial centrifugation and adjusted to 3.0 x 10^8 platelets/mL in Tyrode's buffer (10 mM HEPES, 12 mM $NaHCO_3$, 127 mM NaCl, 5 mM KCl, 0.5 mM NaH_2PO_4, 1 mM $MgCl_2$, and 5 mM glucose), as previously published. Platelets (250 µL at 3.0 x10^8 platelets/mL) were dispensed into glass cuvettes and incubated with the indicated 5S-HETE at 1 µM, 10 µM and 15 µM) for 10 minutes at 37°C. Oxylipin-treated platelets were stimulated with 0.25 µg/mL of collagen (Chrono-log), under stirring conditions (1100 rpm) at 37°C, in a Chrono-log Model 700D lumi-aggregometer and platelet aggregation was recorded for six minutes.

In order to determine if 5S-HETE was enzymatically converted to another chemical *ex vivo*, one mL of platelets (1.0 x10^9 platelets/mL) was incubated with 10 µM 5-HETE or vehicle (DMSO) for 10 minutes at 37° C and then pelleted by centrifugation at 1000g for 2 minute. Supernatant was transferred to a fresh tube and snap frozen. Oxylipins were extracted and analyzed via UPLC-MS/MS, as described

previously,[9] The m/z transitions for 5S-HETE, 5S,12S-diHETE, 5S,15S-diHETE were 319.4→205.4, 335.4→195.4, 351.4→235.4, respectively.

3.3 Results

3.3.1 Biosynthesis of 5S,15S-diHpETE

The two pathways by which 5S,15S-diHpETE might be synthesized depend on the order of the LOX isozyme reaction (**Scheme 3.1**). These two pathways were therefore investigated in order to compare the relative ability of h5-LOX, h15-LOX-1 and h15-LOX-2 to form the pathway intermediates *in vitro*.

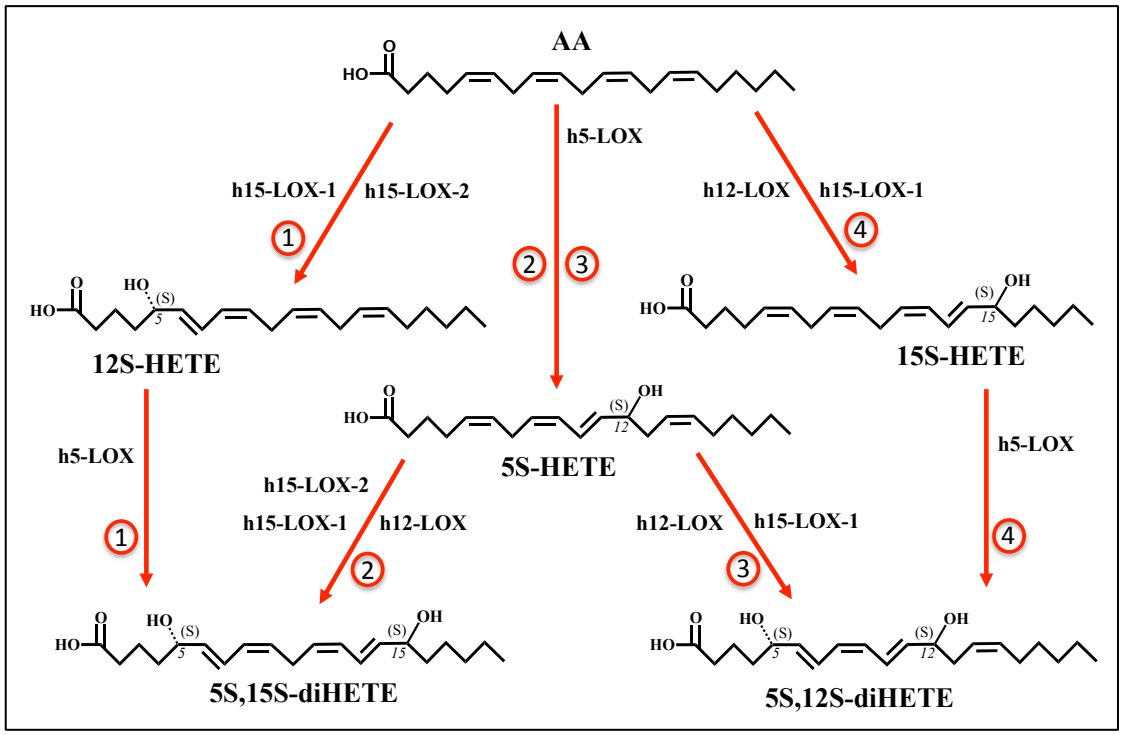

Scheme 3.1. Possible biosynthetic pathways of 5S,12S-diHETE and 5S,15S-diHETE. It should be noted that LOX's initially produce hydroperoxides that are subsequently reduced by glutathione peroxidases. Reduced products have been listed for simplicity.

Pathway 1: AA and h15-LOX-1 or h15-LOX-2 to 15S-HpETE, then h5-LOX to 5S,15S-diHpETE (Scheme 1, #1).

The first possible route that may contribute to formation of 5S,15S-diHpETE involves oxidation of AA by h15-LOX-1 or h15-LOX-2 to form 15S-HpETE. In order to study this reaction, steady-state kinetics and product profile were measured. h15-LOX-1 was found to have a k_{cat} with AA of 10 sec^{-1}, while the k_{cat}/K_M was 2.1 $sec^{-1}\mu M^{-1}$. The major product of the reaction was 15S-HpETE (84%), with 12S-HpETE comprising the remaining 16%, as previously observed (*47*). The k_{cat} for AA with h15-LOX-2 was measured to be 0.96 sec^{-1}, while the k_{cat}/K_M was found to be 0.19 $sec^{-1}\mu M^{-1}$ (**Table 3.1**). The reaction of h15-LOX-2 with AA produced 100% 15S-HpETE. Multiplying k_{cat}/K_M by product percentages allows calculation of the biosynthetic flux. Comparing these flux data indicate that h15-LOX-1 (2.1 $sec^{-1}\mu M^{-1}$ *0.84 = 1.8) is 10-fold more efficient than h15-LOX-2 (0.19 $sec^{-1}\mu M^{-1}$ *1 = 0.19) in producing 15S-HpETE (**Table 3.4**).

The 15S-HpETE formed by h15-LOX-1 or h15-LOX-2 can then react with h5-LOX to form 5S,15S-diHpETE. The ability of h5-LOX to carry out this reaction was performed but no reaction was observable at either 234, 270 or 302 nm using UV-vis spectroscopy. However, by analyzing multiple time points with LC-MS/MS, a small amount of product was observed from both 15S-HETE and 15S-HpETE, consisting entirely of 5S,15S-diHETE. Although K_{cat} and K_M values could not be obtained for thesereactions due to their slow rates, the V_{max} values for 15S-HETE and 15S-HpETE were determined to be 0.0013 and 0.020 ($mol/sec^{-1}mol^{-1}$), respectively.

Compared with the rate of h5-LOX and AA at 10 mM, these values for 15S-HETE and 15S-HpETE catalysis with h15-LOX-1 are 129-fold and 88-fold slower, respectively.

enzyme	substrate	k_{cat} (sec^{-1})	k_{cat}/K_M ($sec^{-1}\mu M^{-1}$)	K_M (μM)
h5-LOX	AA	1.2* ± 0.35	0.35* ± 0.04	3.3 ± 0.92
h12-LOX	AA	9.7 ± 0.4	5.8 ± 1.0	1.7 ± 0.3
	5S-HETE	0.088 ± 0.006	0.051 ± 0.013	1.7 ± 0.4
	5S-HpETE	0.15 ± 0.01	0.15 ± 0.02	1.0 ± 0.2
h15-LOX-1	AA	10 ± 1	2.1 ± 0.3	5.0 ± 0.3
	5S-HETE	1.1 ± 0.4	0.23 ± 0.03	4.9 ± 0.6
	5S-HpETE	1.8 ± 0.2	0.23 ± 0.04	7.8 ± 1.7
h15-LOX-2	AA	0.96 ± 0.09	0.19 ± 0.02	5.0 ± 0.2
	5S-HETE	2.1 ±0.2	0.072 ± 0.008	29 ± 2
	5S-HpETE	2.0 ± 0.2	0.035 ± 0.004	57 ± 3

Table 3.1. Steady-state kinetic values of h5-LOX, h12-LOX, h15-LOX-1 and h15-LOX-2 with substrates that serve as intermediates in the biosynthesis of 5S,12S-diHETE and 5S,15S-diHETE. *Iron content for ammonium sulfate-precipitated h5-LOX is assumed to be 100%.

enzyme	substrate	V_{max} $Mol/sec^{-1}Mol^{-1}$
5LOX	AA	0.17
5LOX	15-HETE	0.0013
5LOX	15-HpETE	0.0020
5LOX	12-HETE	0.00057
5LOX	12-HpETE	0.0029

Table 3.2. V_{max} values ($Mol/sec^{-1}Mol^{-1}$) of h5-LOX with 12S-HETE, 12S-HpETE, 15S-HETE and 15S-HpETE.

enzyme	Substrate	C5-product	C12-product	C15-product
h5-LOX	AA	98%*	-	-
	12S-HETE	100%	-	-
	12S-HpETE	100%	-	-
	15S-HETE	100%	-	-
	15S-HpETE	100%	-	-
h12-LOX	AA	-	100%	-
	5S-HETE	-	87%	13%
	5S-HpETE	-	90%	10%
h15-LOX-1	AA	-	84%	16%
	5S-HETE	-	14%	86%
	5S-HpETE	-	60%	30%
h15-LOX-2	AA	-	-	100%
	5S-HETE	-	-	100%
	5S-HpETE	-	-	100%

Table 3.3. Distribution of products created by reaction of h5-LOX, h12-LOX, h15-LOX-1 and h15-LOX-2 with substrates that serve as intermediates in the biosynthesis of 5S,12S-diHETE and 5S,15S-diHETE. The product label (i.e. C5) refers to the carbon that is oxygenated on the substrate. *In addition to 5-HpETE, h5-LOX produced trace oxylipins from AA that were likely epoxide degradation products. Error for all products does not exceed 7%.

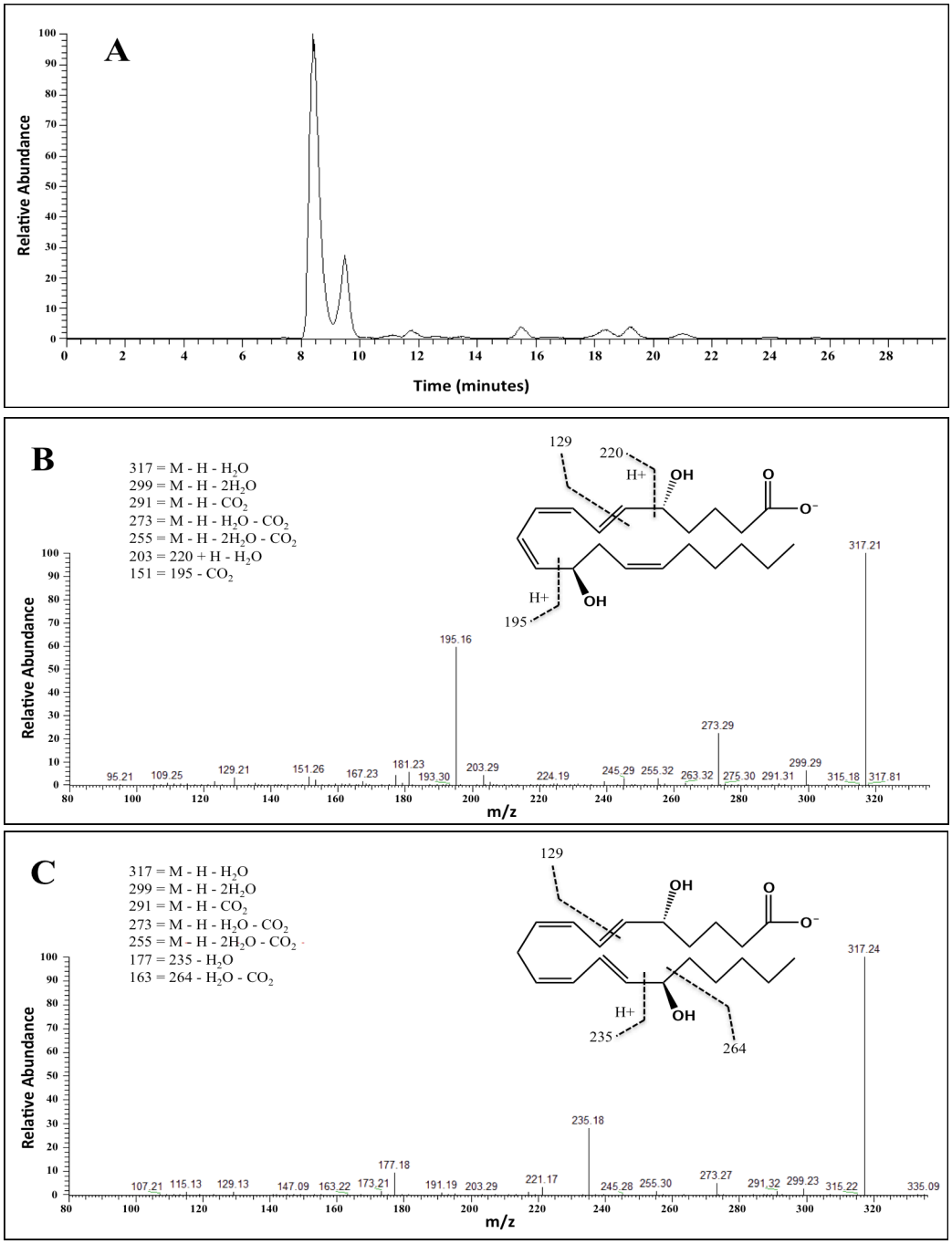

Figure 3.2. h15-LOX-1 primarily synthesizes 5S,12S-diHETE from 5S-HETE. (A) Selected ion chromatogram at m/z of 335. Larger peak at 8.5 min is 5S,12S-diHETE. Smaller peak at 9.5 min is 5S,15S-diHETE. (B) MS/MS spectra of 5S,15S-diHETE prepared from reaction of h15-LOX-1 with 5S-HETE. (C) MS/MS spectra of 5S,15S-diHETE prepared from reaction of h15-LOX-1 with 5S-HETE. Samples were reduced to form the di-alcohol products.

Pathway 2: AA and h5-LOX to 5S-HpETE, then h15-LOX-1, h15-LOX-2 or h12-LOX to 5S,15S-diHpETE (Scheme 1, #2)

The second route of formation of 5S,15S-diHpETE begins with the oxidation of AA by h5-LOX to form 5S-HpETE. The kinetics and product profile of this reaction determined a K_{cat} of 1.2 sec^{-1}, a K_{cat}/K_M of 0.35 $sec^{-1}\mu M^{-1}$ and produced 98% 5S-HpETE, with trace amounts of other oxylipins. 5S-HpETE generated by h5-LOX can further react with a h15-LOX isozyme to form 5S,15S-diHpETE. The k_{cat} of 5S-HETE with h15-LOX-1 was 1.1 sec^{-1} and the k_{cat}/K_M was 0.23 sec^{-1} μM^{-1} (**Table 3.1**), however, the majority of the product produced was 5S,12S-diHETE (85% of the total), with 5S,15S-diHETE comprising the remaining 14% (**Table 3.3**). This unusual result was previously observed, with h15-LOX-1 converting 7-HDHA to the non-canonical ω-9 product, 7S,14S-diHDHA (*vide supra*, chapter 2). This altered product specificity of h15-LOX-1 indicates that it is inefficient in producing 5S,15S-diHETE from 5S-HETE. In contrast, h15-LOX-2 was found to have a k_{cat} of 2.1 sec^{-1}, a k_{cat}/K_M of 0.072 sec^{-1} μM^{-1} with 5S-HETE (**Table 3.1**) and it produced only the canonicalproduct, 5S,15S-diHETE, with no altered positional specificity. These flux data indicate that h15-LOX-1 (0.23 $sec^{-1}\mu M^{-1}$ *0.14 = 0.032) is 2-fold less efficient than h15-LOX-2 (0.072 $sec^{-1}\mu M^{-1}$ *1 = 0.072) in producing 5S,15S-HpETE (**Table 3.4**).

enzyme	substrate	k_{cat}/K_M ($sec^{-1}\mu M^{-1}$)	5S,12S-diHETE flux*	5S,15S-diHETE flux*
h5-LOX	AA	0.35	0.35	0.35
h12-LOX	AA	5.8	5.8	-
	5S-HETE	0.051	0.044	0.0066
	5S-HpETE	0.15	0.14	0.015
h15-LOX-1	AA	2.1	0.33	1.8
	5S-HETE	0.23	0.20	0.032
	5S-HpETE	0.23	0.14	0.092
h15-LOX-2	AA	0.19	-	0.19
	5S-HETE	0.072	-	0.072
	5S-HpETE	0.035	-	0.035

Table 3.4. Biosynthetic flux of reactions leading to the production of 5S,12S-diHETE and 5S,15S-diHETE. Biosynthetic flux is calculated by multiplying each k_{cat}/K_M value ($sec^{-1}\mu M^{-1}$) by the percentage of total product from each reaction that serves as intermediate in the synthesis of either 5S,12S-diHETE or 5S,15S-diHETE.

3.3.2 Biosynthesis of 5S,12S-diHETE

In addition to identification of 5S,15S-diHETE in biological samples, 5S,12S-diHETE has also been observed, indicating a possible biological activity (*32-34*). Therefore, each of the two possible biosynthetic routes of 5S,12S-diHETE (**Scheme 3.1)** was investigated in order to compare their relative efficiency *in vitro*.

Pathway 1: AA and h12-LOX or h15-LOX-1 to 12S-HpETE, then h5-LOX to 5S,12S-diHpETE (Scheme 1, #4)

The first possible route for generating 5S,12S-diHETE begins when h12-LOX oxidizing AA to form 12S-HpETE. The k_{cat} for AA with h12-LOX was measured to

be 9.7 sec^{-1}, while the k_{cat}/K_M was found to be 5.8 sec^{-1} μM^{-1} (**Table 3.1**). The reaction produced 100% 12S-HpETE (**Table 3.3**), consistent with previously published values (*55*). Along with h12-LOX, h15-LOX-1 also contributes to the formation of 12S-HpETE, producing 14% 12S-HpETE and 86% 15S-HpETE, with a k_{cat} of 10 sec^{-1} and a k_{cat}/K_M of 2.1 $sec^{-1}\mu M^{-1}$ (**Table 3.1),** similar to previously work (*47, 56, 57*). Multiplying their k_{cat}/K_M values by their product percentages results in a biosynthetic flux to be 5.8 for h12-LOX and 0.35 for h15-LOX-1, indicating that h12-LOX is a 16-fold more efficient in producing 12S-HpETE than h15-LOX-1 (**Table 3.4**).

Once 12S-HpETE is produced by h12-LOX or h15-LOX-1, it may react further with h5-LOX to form 5S,12S-diHpETE. The ability of h5-LOX to carry out this reaction was investigated, however, no reaction was observable at either 234, 270 or 302 nm, using UV-vis spectroscopy. The more sensitive LC-MS/MS method detected small amounts of only 5S,12S-diHETE from 12S-HETE and 12s-HpETE with V_{max} values of 0.00086 and 0.0044 ($mol/sec^{-1}mol^{-1}$), respectively (**Table 3.2**). Compared with AA, the values for 12S-HETE and 12S-HpETE reactivity are 300-fold and 59-fold slower, respectively.

Pathway 2: AA and h5-LOX to 5S-HpETE, then h12-LOX, h15-LOX-1 to 5S,12S-diHpETE (Scheme 1, #3)

As reported above, h5-LOX and AA was found to have a k_{cat} of 1.2 sec^{-1} and a k_{cat}/K_M of 0.30 $sec^{-1}\mu M^{-1}$, with the major product of the reaction being 5S-HpETE, which can subsequently react with h12-LOX. Investigating the kinetic and product

profile of h12-LOX reacting with 5S-HETE revealed that 87% of the product made was 5S,12S-diHETE, while 13% was 5S,15S-diHETE. The k_{cat} with 5S-HETE was 0.088 sec^{-1} and the k_{cat}/K_M was 0.051 $sec^{-1}\mu M^{-1}$, which are 14-fold and 6-fold slower than that of AA, respectively. This dramatic decrease in catalytic activity of h12-LOX with 5S-HETE indicates that h15-LOX-1 is a more efficient biocatalyst in synthesizing of 5S,12S-diHETE, as described above. In comparing the biosynthetic flux of these two enzymes, h12-LOX was found to have a flux 5-fold less than that of h15-LOX-1, (0.051 sec^{-1} μM^{-1} * 0.87 = 0.044) and (0.23 sec^{-1} μM^{-1} * 0.85 = 0.20 sec^{-1} μM^{-1}), respectively, demonstrating a novel biosynthetic pathway for producing 5S,12S-diHETE (**Table 3.4**).

3.3.3 Chiral chromatography

When reacting with poly-unsaturated fatty acids (PUFA's), h5-LOX, h12-LOX, h15-LOX-1 and h15-LOX-2 produce an S-configured hydroperoxide with an E,Z-conjugated double bond (*58, 59*). For the doubly oxygenated products of the current work, 5S,12S-diHETE and 5S,15S-diHETE, it was assumed similar region- and stereo-selectivity would also occur. This assumption was confirmed when 5S,12S-diHETE and 5S,15S-diHETE were analyzed via LCMS using a reverse-phase chiral-C18 column, demonstrating identical retention times and fragmentations with known standards (**Table 3.5**). As controls, an LTB_4 standard eluted at 5.6 minutes, while a 6-trans-12-epi-LTB_4 standard eluted at 9.6 minutes, demonstrating adequate separation of these isomers.

Compound	Source	Retention time
5S,15S-diHETE	standard	27.5 min
	h5-LOX + 15S-HETE	27.2 min
	h12-LOX + 5S-HETE	27.9 min
	h15-LOX-1 + 5S-HETE	27.9 min
	h15-LOX-2 + 5S-HETE	27.8 min
5S,12S-diHETE	standard	4.2 min
	h5-LOX + 12S-HETE	4.2 min
	h12-LOX + 5S-HETE	4.3 min
	h15-LOX-1 + 5S-HETE	4.2 min
LTB_4	standard	5.6 min
6-trans-12-epi-LTB_4	standard	9.6 min

Table 3.5. 5,15-diHETE and 5,12-diHETE produced through different LOX pathways were compared to 5S,15S-diHETE, 5S,12S-diHETE, LTB_4 and 6-trans-12-epi-LTB_4 standards using LCMS with a reverse-phase chiral column.

3.3.4 Platelet reactivity toward 5S-HETE

The presence of 5S,12S-diHETE *in vivo* has been assumed to result from the activity of h5-LOX and h12-LOX, however, our current work (*vide supra*) indicates that 5S-HETE is a poor substrate for h12-LOX *in vitro*. To assess the ability of h12-LOX to react with 5S-HETE *in vivo*, thrombin activated platelets were incubated with 5S-HETE and found to not produce 5S,12S-diHETE. This result is consistent with the *in vitro* data, however the fact that no 5S,12S-diHETE was observed is remarkable since the *in vitro* data would suggest trace amounts could be formed. In addition, 5S,12S-diHETE was previously observed when 5S-HETE was added to platelets, but the conditions were different. It is possible that the recently discovered allosteric site

in h12-LOX may play a role *in vivo*. We are currently investigating this further in order to understand the *in vivo* activity of h12-LOX in platelets.

5S,12S-diHETE was then titrated with activated platelets and found to have low potency, 50 ± 20 % aggregation at 10 mM (**Figure 3.3**). This is in contrast to 5S,15S-diHETE and 12S-HETrE, which demonstrated 5 ± 2 and 0 ± 2 % aggregation at 10 mM, respectively. Despite the low potency of 5S,12S-diHETE against platelets aggregation, the fact that it is observed at such high levels in biological samples suggests that 5S,12S-diHETE may be a precursor to some downstream molecule or have an unidentified role in another biological process.

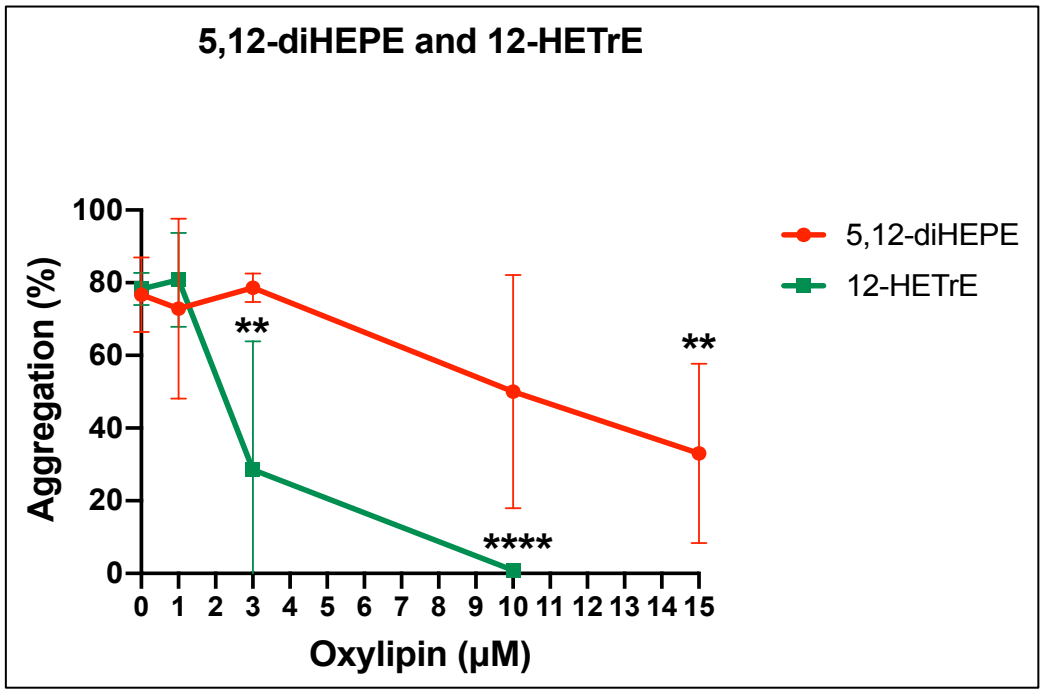

Figure 3.3. Platelets were pre-incubated with 1, 3, 10 or 15 µM 5,12-diHETE and tested for aggregation in response to collagen. 12-HETrE, a known inhibitor of platelet aggregation was used as a positive control.

3.4 Discussion

3.4.1 Biosynthesis of 5S,15S-diHETE

There are two pathways for synthesizing 5S,15S-diHpETE. **Pathway 1** involves formation of 15S-HpETE by either h15-LOX-1 or h15-LOX-2, followed by reaction with h5-LOX to form 5S,15S-diHpETE. Formation of 15S-HpETE occurs rapidly through oxidation of AA by h15-LOX-1, with k_{cat} and k_{cat}/K_M values 15-fold and 12-fold greater than that of h15-LOX-2, respectively. However, once formed, 15S-HETE is a comparatively poor substrate for h5-LOX, reacting with a V_{max} almost 130-fold less than that seen with AA. This is consistent with previous work which indicated that h5-LOX reacts poorly with oxygenated fatty acids (*28*) (*vide supra,* chapter 2). The slow reaction of h5-LOX with 15S-HETE makes this the rate-limiting step and a relatively poor mechanistic pathway for producing 5S,15S-diHpETE *in vitro*.

In **Pathway 2**, 5S-HETE is first formed through oxygenation of AA by h5-LOX and is subsequently oxidized by an h15-LOX isozyme to form 5S,15S-diHpETE. h5-LOX reacts rapidly with AA to generate a 100% yield of 5S-HpETE. This is in contrast to the reaction of h5-LOX and DHA, which produces multiple mono-oxylipins, including 7S-HpDHA, 14S-HpDHA and 17S-HpDHA (*vide supra*, chapter 2). The implication is that the added length and unsaturation of DHA decreases the product selectivity of h5-LOX. After 5S-HpETE is formed, the second step in **Pathway 2** is the formation of 5S,15S-diHETE, which has been assumed to be performed by h15-LOX-1. This is a reasonable assumption, given that h15-LOX-1

primarily oxygenates C15 of AA, and is markedly faster at reacting with fatty acids than h15-LOX-2 (*57*). However, the role of h15-LOX-1 in this pathway may be less significant, given that h15-LOX-1 shows an altered positional specificity with 7S-HDHA, primarily oxygenating the ω-9 carbon, C14, instead of the expected w-6 carbon, C17. This altered positional specificity is confirmed in the current work, where h15-LOX-1 is shown to primarily oxygenate at the ω-9 carbon, C12, when reacting with 5S-HETE. This is a significant result as it demonstrates that the altered positional specificity seen with 7S-HDHA, also occurs with 5S-HETE and indicates this is a new canonical reaction for h15-LOX-1. A model was previously developed for 7S-HDHA binding to h15-LOX-1, where the C7 alcohol hydrogen bonded with the backbone carbonyl of I399, thus pushing the methyl end of 7S-HDHA further into the active site, allowing for the generation of 7S,14S-diHDHA. A similar docking procedure was performed with 5S-HETE and a similar binding mode observed.

With h15-LOX-1 primarily generating 5S,12S-diHpETE from 5S-HETE, this indicates that h15-LOX-2 may have a larger role in making 5S,15S-diHpETE than previously thought (**Scheme 2**). The current work confirms this hypothesis, with h15-LOX-2 demonstrating a biosynthetic flux for 5S,15S-diHpETE that is 2-fold greater than that of h15-LOX-1, despite the fact that h15-LOX-1 has 10-fold higher activity with AA than h15-LOX-2 (**Scheme 3.2**). Therefore, the most kinetically favorable route in producing 5S,15S-diHETE is the formation of 5S-HETE by h5-LOX, followed by oxygenation at carbon 15 by h15-LOX-2 or h15-LOX-1 (**Scheme 3.2**). This unrecognized role of h15-LOX-2 in the synthesis of 5S,15S-diHETE is mirrored

by previous work showing that h15-LOX-2 is more efficient than h15-LOX-1 in forming RvD5, due to the altered positional specificity of h15-LOX-1 with 7S-HDHA (chapter 2).

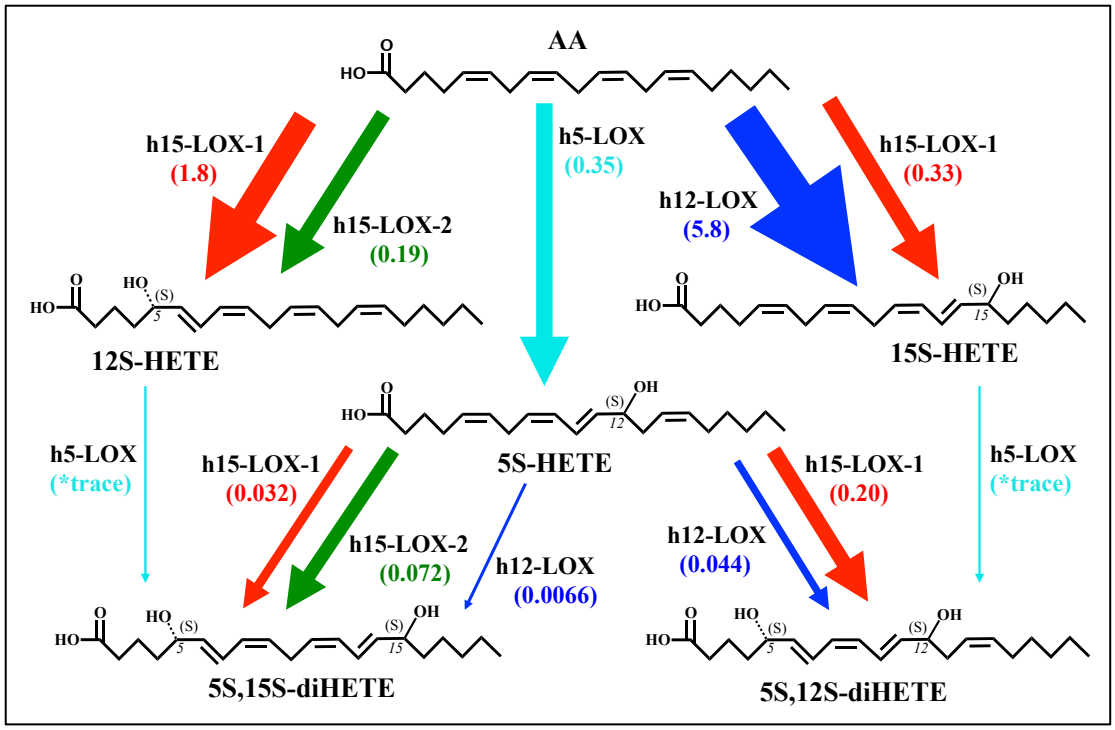

Scheme 3.2. 5S,12S-diHETE and 5S,15S-diHETE biosynthesis pathways compared. The total flux for the reactions of h5-LOX, h12-LOX and h15-LOX-1 and h15-LOX-2 with AA, 12S-HETE, 15S-HETE and 5S-HETE are compared by multiplying k_{cat}/K_M values ($sec^{-1}mM^{-1}$) by the percentage of total product from each reaction that serves as intermediate in the synthesis of 5S,12S-diHETE or 5S,15S-diHETE. *Flux values are not reported for h5-LOX due to its low reactivity and its inability to manifest a k_{cat}/K_M value. It should be noted that LOX's initially produce hydroperoxides that are subsequently reduced by glutathione and other cellular peroxidases. Only reduced products are shown for simplicity.

3.4.2 Biosynthesis of 5S,12S-diHETE

As discussed previously, 5S,12S-diHETE has been observed in lipidomic analysis and is thus potentially a significant biomolecule with respect to

inflammation. There are two main pathways for producing 5S,12S-diHETE, with the first, **Pathway 1,** involving the formation of 12S-HpETE by either h12-LOX or h15-LOX-1, followed by reaction with h5-LOX to form 5S,12S-diHpETE. Although 12S-HpETE is formed rapidly by h12-LOX, the second step in this pathway, reaction of h5-LOX with 12S-HpETE, occurs relatively slowly. Similar to that seen with other mono-oxylipins, the reaction with h5-LOX and 12S-HETE occurs at a rate almost 300-fold lower than its rate with AA, making it the rate-limiting step of this pathway.

However, **Pathway 2**, involving formation of 5S,12S-diHETE from 5S-HETE, is not as rate restricted. The reaction of h5-LOX with AA occurs rapidly producing 5S-HETE (*vide supra*). The second step with h12-LOX produces the expected 5S,12S-diHETE product, however, 5S-HETE is a relatively poor substrate for h12-LOX, with a k_{cat} and k_{cat}/K_M over 100-fold less than the reaction with AA. In contrast, 5S-HETE is a relatively better substrate for h15-LOX-1, with a k_{cat}/K_M value being ~4-fold greater than that of h12-LOX, despite the fact that h12-LOX is more efficient reacting with AA than h15-LOX-1. The comparatively high kinetic values of h15-LOX-1 with 5S-HETE, combined with its altered product profile make its biosynthetic flux almost 5-fold greater at producing 5S,12S-diHETE than h12-LOX. This result is consistent with previous *in vitro* results, where h15-LOX-1 is 20-fold more efficient than h12-LOX at producing lipoxins from 5,15-diHpETE (*19, 60*) and indicates a negative bias against oxylipin substrates for h12-LOX relative to h15-LOX-1. In addition, these results suggest that h15-LOX-1 could be a source of the

5S,12S-diHETE detected in biological samples, where 5S-HETE is the available substrate.

It should be noted that h12-LOX shows a small shift in product specificity while reacting with 5S-HETE, producing 13% 5S,15S-diHpETE instead of the expected 100% 5S,12S-diHpETE. A similar shift was previously observed when h12-LOX reacted with 7-HDHA to produce 7S,17S-diHpDHA (chapter 2). These results indicate that both h12-LOX and h15-LOX-1 have altered product profiles when reacting with oxylipins, and this needs to be taken into account when considering biosynthetic pathways for specific oxylipins.

3.4.3 Biological Consequences

5S,15S-diHETE is an oxylipin that is produced in high abundance in many inflammatory conditions, including asthma (*29*) and rheumatoid arthritis (*25*). It is speculated that while the reduced form is observed, the original molecule, 5S,15S-diHpETE is the intermediate that allows for the production of both LXA_4 and LXB_4. This is because the hydroperoxide is required for the critical dehydration step by a LOX isozyme to generate the epoxide intermediate, which is then hydrolyzed to the corresponding lipoxin (*19, 61*). Previously, it was shown that h15-LOX-1 converted 5S,15S-diHpETE to LXB_4 *in vitro*, while h15-LOX-2 was unable to do so *(61),* implicating that h15-LOX-2 is not involved in the biosynthesis of LXB_4. However, increases in h15-LOX-2 concentrations were observed to coincide with increases in lipoxin levels in airway epithelial cells (*62*). This data, combined with our *in vitro*

data, may indicate that both 15-LOX isozymes are involved in LXB_4 biosynthesis *in vivo*, with h15-LOX-2 generating 5S,15S-diHpETE from 5S-HETE, and h15-LOX-1 performing the final step to produce LXB_4. This is a remarkable hypothesis because the presumption has been that h15-LOX-1 and not h15-LOX-2 is the isozyme producing 5S,15S-diHETE, due to its greater enzymatic activity in producing 15-HpETE from AA. In the current *in vitro* work, h15-LOX-1 is not efficient in producing 5S,15S-diHETE from 5S-HETE, but rather it synthesizes 5S,12S-diHETE. h15-LOX-2 however does react well with 5S-HETE, producing only 5S,15S-diHETE and suggests that the role of h15-LOX-2 in producing 5S,15S-diHETE *in vivo* may be larger than previously suspected. Previous *in vivo* work supports this hypothesis, where up-regulation of h15-LOX-2 in dendritic cells is linked to increased 5S,15S-diHETE production (*63*) and keratinocytes expressed/produced h15-LOX-2 and 5S,15S-diHETE when incubated with 5S-HETE (*15-17*).

If h15-LOX-2 does have a greater role in lipoxin biosynthesis *in vivo*, then this may affect the predicted involvement of specific cells (*20, 29-32*). For example, h15-LOX-2 is expressed at high levels in macrophages (*17, 49*) and since macrophages also express h5-LOX and h15-LOX-1 (*13, 64*), they could contain all the enzymes necessary to produce lipoxins on their own. This hypothesis is supported by the fact that expression of h5-LOX is elevated in pro-inflammatory M1 macrophages (*65*), while h15-LOX-1 expression is upregulated in the pro-resolving M2 subtype (*63, 65, 66*). Therefore, lipoxin production may occur with changes in macrophage LOX expression, without the need for a transcellular mechanism of

synthesis. Nevertheless, the proposed *in vitro* biosynthetic routes (*vide supra*) should be considered with caution when extrapolating to *in vivo* systems. Although h5-LOX is a poor biocatalyst with oxylipins *in vitro* (*vide supra*), its activity can be altered by the presence of FLAP (*67*), calcium (*20*) and hydroperoxides in the cell (*68-70*). In addition, 15-LOX isozymes are know to have altered catalysis with allosteric effector molecules, which could be present *in vivo* (*57, 71*). Therefore, we are currently utilizing specific LOX inhibitors in primary cells to determine which LOX isozyme play a role in specific oxylipin biosynthetic pathways.

In conclusion, the altered positional specificity of h15-LOX-1 extends beyond 7-HDHA to 5S-HETE. Therefore, biosynthesis of di-oxylipins such as 5S,15S-diHETE and 5S,12S-diHETE can occur by routes that may not be obvious when extrapolating from LOX activity with AA. In particular, h15-LOX-2 possibly makes an larger contribution to the biosynthesis of oxylipins, which was previously attributed solely to h15-LOX-1 and therefore, interpretation of *in vivo* data should be carefully evaluated with the current work in mind.

3.5 Authorship Contributions

Steven C. Perry, Thomas Horn, Adriana Yamaguchi', Oluwayomi Akinkugbe, William S. Conrad, Michael Holinstat, Theodore R. Holman

S Perry designed experiments, acquired, analyzed and interpreted data, and wrote the manuscript. A Yamaguchi, T Horn, O Akinkugbe and WS Conrad acquired data and analyzed data, T.R. Holman and Michael Holinstat designed experiments and revised the manuscript.

3.6 References

1. Tabas, I., and Glass, C. K. (2013) Anti-inflammatory therapy in chronic disease: challenges and opportunities, *Science 339*, 166-172.

2. Serhan, C. N., Hamberg, M., and Samuelsson, B. (1984) Trihydroxytetraenes: a novel series of compounds formed from arachidonic acid in human leukocytes, *Biochemical and biophysical research communications 118*, 943-949.

3. Badr, K. F., DeBoer, D. K., Schwartzberg, M., and Serhan, C. N. (1989) Lipoxin A4 antagonizes cellular and in vivo actions of leukotriene D4 in rat glomerular mesangial cells: evidence for competition at a common receptor, *Proceedings of the National Academy of Sciences of the United States of America 86*, 3438-3442.

4. Hedqvist, P., Raud, J., Palmertz, U., Haeggstrom, J., Nicolaou, K. C., and Dahlen, S. E. (1989) Lipoxin A4 inhibits leukotriene B4-induced inflammation in the hamster cheek pouch, *Acta physiologica Scandinavica 137*, 571-572.

5. Mangino, M. J., Brounts, L., Harms, B., and Heise, C. (2006) Lipoxin biosynthesis in inflammatory bowel disease, *Prostaglandins & other lipid mediators 79*, 84-92.

6. Serhan, C. N. (2010) Novel lipid mediators and resolution mechanisms in acute inflammation: to resolve or not?, *The American journal of pathology 177*, 1576-1591.

7. Nathan, C., and Ding, A. (2010) Nonresolving inflammation, *Cell 140*, 871-882.

8. Weaver, J. R., Holman, T. R., Imai, Y., Jadhav, A., Kenyon, V., Maloney, D. J., Nadler, J. L., Rai, G., Simeonov, A., and Taylor-Fishwick, D. A. (2012) Integration of pro-inflammatory cytokines, 12-lipoxygenase and NOX-1 in pancreatic islet beta cell dysfunction, *Mol Cell Endocrinol 358*, 88-95.

9. Cole, B. K., Lieb, D. C., Dobrian, A. D., and Nadler, J. L. (2013) 12- and 15-lipoxygenases in adipose tissue inflammation, *Prostaglandins & other lipid mediators 104-105*, 84-92.

10. Serhan, C. N., Chiang, N., and Van Dyke, T. E. (2008) Resolving inflammation: dual anti-inflammatory and pro-resolution lipid mediators, *Nat Rev Immunol 8*, 349-361.

11. Ivanov, I., Heydeck, D., Hofheinz, K., Roffeis, J., O'Donnell, V. B., Kuhn, H., and Walther, M. (2010) Molecular enzymology of lipoxygenases, *Archives of biochemistry and biophysics 503*, 161-174.

12. Kuhn, H., Banthiya, S., and van Leyen, K. (2015) Mammalian lipoxygenases and their biological relevance, *Biochimica et biophysica acta 1851*, 308-330.

13. Colakoglu, M., Tuncer, S., and Banerjee, S. (2018) Emerging cellular functions of the lipid metabolizing enzyme 15-Lipoxygenase-1, *Cell proliferation 51*, e12472.

14. Ford-Hutchinson, A. W. (1991) Arachidonate 15-lipoxygenase; characteristics and potential biological significance, *Eicosanoids 4*, 65-74.

15. Brash, A. R., Boeglin, W. E., and Chang, M. S. (1997) Discovery of a second 15S-lipoxygenase in humans, *Proceedings of the National Academy of Sciences of the United States of America 94*, 6148-6152.

16. Jisaka, M., Kim, R. B., Boeglin, W. E., Nanney, L. B., and Brash, A. R. (1997) Molecular cloning and functional expression of a phorbol ester-inducible 8S-lipoxygenase from mouse skin, *J Biol Chem 272*, 24410-24416.

17. Hulten, L. M., Olson, F. J., Aberg, H., Carlsson, J., Karlstrom, L., Boren, J., Fagerberg, B., and Wiklund, O. (2010) 15-Lipoxygenase-2 is expressed in macrophages in human carotid plaques and regulated by hypoxia-inducible factor-1alpha, *Eur J Clin Invest 40*, 11-17.

18. Green, A. R., Barbour, S., Horn, T., Carlos, J., Raskatov, J. A., and Holman, T. R. (2016) Strict Regiospecificity of Human Epithelial 15-Lipoxygenase-2 Delineates Its Transcellular Synthesis Potential, *Biochemistry 55*, 2832-2840.

19. Green, A. R., Freedman, C., Tena, J., Tourdot, B. E., Liu, B., Holinstat, M., and Holman, T. R. (2018) 5 S,15 S-Dihydroperoxyeicosatetraenoic Acid (5,15-diHpETE) as a Lipoxin Intermediate: Reactivity and Kinetics with Human Leukocyte 5-Lipoxygenase, Platelet 12-Lipoxygenase, and Reticulocyte 15-Lipoxygenase-1, *Biochemistry 57*, 6726-6734.

20. Maas, R. L., Turk, J., Oates, J. A., and Brash, A. R. (1982) Formation of a novel dihydroxy acid from arachidonic acid by lipoxygenase-catalyzed double oxygenation in rat mononuclear cells and human leukocytes, *The Journal of biological chemistry 257*, 7056-7067.

21. Kuhn, H., Wiesner, R., Alder, L., Fitzsimmons, B. J., Rokach, J., and Brash, A. R. (1987) Formation of lipoxin B by the pure reticulocyte lipoxygenase via sequential oxygenation of the substrate, *Eur J Biochem 169*, 593-601.

22. Ueda, N., Yokoyama, C., Yamamoto, S., Fitzsimmons, B. J., Rokach, J., Oates, J. A., and Brash, A. R. (1987) Lipoxin synthesis by arachidonate 12-lipoxygenase purified from porcine leukocytes, *Biochem Biophys Res Commun 149*, 1063-1069.

23. Schwenk, U., Morita, E., Engel, R., and Schroder, J. M. (1992) Identification of 5-oxo-15-hydroxy-6,8,11,13-eicosatetraenoic acid as a novel and potent human eosinophil chemotactic eicosanoid, *The Journal of biological chemistry 267*, 12482-12488.

24. Dalli, J., and Serhan, C. N. (2012) Specific lipid mediator signatures of human phagocytes: microparticles stimulate macrophage efferocytosis and pro-resolving mediators, *Blood 120*, e60-72.

25. Thomas, E., Leroux, J. L., Blotman, F., and Chavis, C. (1995) Conversion of endogenous arachidonic acid to 5,15-diHETE and lipoxins by polymorphonuclear cells from patients with rheumatoid arthritis, *Inflammation research : official journal of the European Histamine Research Society ... [et al.] 44*, 121-124.

26. Morita, E., Schroder, J. M., and Christophers, E. (1990) Identification of a novel and highly potent eosinophil chemotactic lipid in human eosinophils treated with arachidonic acid, *J Immunol 144*, 1893-1900.

27. O'Flaherty, J. T., and Thomas, M. J. (1985) Effect of 15-lipoxygenase-derived arachidonate metabolites on human neutrophil degranulation, *Prostaglandins, leukotrienes, and medicine 17*, 199-212.

28. Green, A. R., Freedman, C., Tena, J., Tourdot, B. E., Liu, B., Holinstat, M., and Holman, T. R. (2018) 5 S,15 S-Dihydroperoxyeicosatetraenoic Acid (5,15-diHpETE) as a Lipoxin Intermediate: Reactivity and Kinetics with Human Leukocyte 5-Lipoxygenase, Platelet 12-Lipoxygenase, and Reticulocyte 15-Lipoxygenase-1, *Biochemistry*.

29. Green, F. A. (1990) Transformations of 5-HETE by activated keratinocyte 15-lipoxygenase and the activation mechanism, *Lipids 25*, 618-623.

30. McDonald, P. P., McColl, S. R., Naccache, P. H., and Borgeat, P. (1992) Activation of the human neutrophil 5-lipoxygenase by leukotriene B4, *British journal of pharmacology 107*, 226-232.

31. Chavis, C., Vachier, I., Chanez, P., Bousquet, J., and Godard, P. (1996) 5(S),15(S)-dihydroxyeicosatetraenoic acid and lipoxin generation in human polymorphonuclear cells: dual specificity of 5-lipoxygenase towards endogenous and exogenous precursors, *The Journal of experimental medicine 183*, 1633-1643.

32. Serhan, C. N. (1989) On the relationship between leukotriene and lipoxin production by human neutrophils: evidence for differential metabolism of 15-HETE and 5-HETE, *Biochimica et biophysica acta 1004*, 158-168.

33. Yoshimoto, T., Miyamoto, Y., Ochi, K., and Yamamoto, S. (1982) Arachidonate 12-lipoxygenase of porcine leukocyte with activity for 5-hydroxyeicosatetraenoic acid, *Biochimica et biophysica acta 713*, 638-646.

34. Marcus, A. J., Safier, L. B., Ullman, H. L., Broekman, M. J., Islam, N., Oglesby, T. D., Gorman, R. R., and Ward, J. W. (1985) Inhibition of platelet function in thrombosis, *Circulation 72*, 698-701.

35. Sorokin, A. V., Norris, P. C., English, J. T., Dey, A. K., Chaturvedi, A., Baumer, Y., Silverman, J., Playford, M. P., Serhan, C. N., and Mehta, N. N. (2018) Identification of proresolving and inflammatory lipid mediators in human psoriasis, *Journal of clinical lipidology 12*, 1047-1060.

36. Borgeat, P., Picard, S., Vallerand, P., and Sirois, P. (1981) Transformation of arachidonic acid in leukocytes. Isolation and structural analysis of a novel dihydroxy derivative, *Prostaglandins and medicine 6*, 557-570.

37. Larfars, G., Lantoine, F., Devynck, M. A., Palmblad, J., and Gyllenhammar, H. (1999) Activation of nitric oxide release and oxidative metabolism by leukotrienes B4, C4, and D4 in human polymorphonuclear leukocytes, *Blood 93*, 1399-1405.

38. Valles, J., Santos, M. T., Marcus, A. J., Safier, L. B., Broekman, M. J., Islam, N., Ullman, H. L., and Aznar, J. (1993) Downregulation of human platelet reactivity by neutrophils. Participation of lipoxygenase derivatives and adhesive proteins, *The Journal of clinical investigation 92*, 1357-1365.

39. Sirois, P., Roy, S., Beraldin, G., Vallerand, P., and Borgeat, P. (1982) Comparative activity of natural mono-, di- and tri-hydroxy derivatives of arachidonic acid on guinea-pig lungs: myotropic effect and stimulation of cyclooxygenase activity, *Prostaglandins 24*, 405-418.

40. Borgeat, P., Fruteau de Laclos, B., Picard, S., Drapeau, J., Vallerand, P., and Corey, E. J. (1982) Studies on the mechanism of formation of the 5S, 12S-dihydroxy-6,8,10,14(E,Z,E,Z)-icosatetraenoic acid in leukocytes, *Prostaglandins 23*, 713-724.

41. Serhan, C. N., Broekman, M. J., Korchak, H. M., Marcus, A. J., and Weissmann, G. (1982) Endogenous phospholipid metabolism in stimulated neutrophils differential activation by FMLP and PMA, *Biochemical and biophysical research communications 107*, 951-958.

42. Borgeat, P., Nadeau, M., Salari, H., Poubelle, P., and Fruteau de Laclos, B. (1985) Leukotrienes: biosynthesis, metabolism, and analysis, *Advances in lipid research 21*, 47-77.

43. Maas, R. L., Ingram, C. D., Taber, D. F., Oates, J. A., and Brash, A. R. (1982) Stereospecific removal of the DR hydrogen atom at the 10-carbon of arachidonic acid in the biosynthesis of leukotriene A4 by human leukocytes, *The Journal of biological chemistry 257*, 13515-13519.

44. Suzuki, H., Kishimoto, K., Yoshimoto, T., Yamamoto, S., Kanai, F., Ebina, Y., Miyatake, A., and Tanabe, T. (1994) Site-directed mutagenesis studies on the iron-binding domain and the determinant for the substrate oxygenation site of porcine leukocyte arachidonate 12-lipoxygenase, *Biochimica et biophysica acta 1210*, 308-316.

45. Gan, Q.-F., Browner, M. F., Sloane, D. L., and Sigal, E. (1996) Defining the Arachidonic Acid Binding Site of Human 15-Lipoxygenase: MOLECULAR MODELING AND MUTAGENESIS, *The Journal of biological chemistry 271*, 25412-25418.

46. Sloane, D. L., Leung, R., Barnett, J., Craik, C. S., and Sigal, E. (1995) Conversion of human 15-lipoxygenase to an efficient 12-lipoxygenase: the side-chain geometry of amino acids 417 and 418 determine positional specificity, *Protein engineering 8*, 275-282.

47. Vogel, R., Jansen, C., Roffeis, J., Reddanna, P., Forsell, P., Claesson, H. E., Kuhn, H., and Walther, M. (2010) Applicability of the triad concept for the positional specificity of mammalian lipoxygenases, *J Biol Chem 285*, 5369-5376.

48. Sloane, D. L., Leung, r., Craik, C. S., and Sigal, E. (1991) A Primary determinant for Lipoxygenase positional specificity, *Nature 354*, 149-152.

49. Wuest, S. J., Crucet, M., Gemperle, C., Loretz, C., and Hersberger, M. (2012) Expression and regulation of 12/15-lipoxygenases in human primary macrophages, *Atherosclerosis 225*, 121-127.

50. Amagata, T., Whitman, S., Johnson, T. A., Stessman, C. C., Loo, C. P., Lobkovsky, E., Clardy, J., Crews, P., and Holman, T. R. (2003) Exploring sponge-derived terpenoids for their potency and selectivity against 12-human, 15-human, and 15-soybean lipoxygenases, *J Nat Prod 66*, 230-235.

51. Robinson, S. J., Hoobler, E. K., Riener, M., Loveridge, S. T., Tenney, K., Valeriote, F. A., Holman, T. R., and Crews, P. (2009) Using enzyme assays to evaluate the structure and bioactivity of sponge-derived meroterpenes, *J Nat Prod 72*, 1857-1863.

52. Jameson, J. B., Kantz, A., Schultz, L., Kalyanaraman, C., Jacobson, M. P., Maloney, D. J., Jadhav, A., Simeonov, A., and Holman, T. R. (2014) A High Throughput Screen Identifies Potent and Selective Inhibitors to Human Epithelial 15-Lipoxygenase-2, *PloS one 9*.

53. Gilbert, N. C., Bartlett, S. G., Waight, M. T., Neau, D. B., Boeglin, W. E., Brash, A. R., and Newcomer, M. E. (2011) The structure of human 5-lipoxygenase, *Science 331*, 217-219.

54. Smyrniotis, C. J., Barbour, S. R., Xia, Z., Hixon, M. S., and Holman, T. R. (2014) ATP Allosterically Activates the Human 5-Lipoxygenase Molecular Mechanism of Arachidonic Acid and 5(S)-Hydroperoxy-6(E),8(Z),11(Z),14(Z)-eicosatetraenoic Acid, *Biochemistry*.

55. Ikei, K. N., Yeung, J., Apopa, P. L., Ceja, J., Vesci, J., Holman, T. R., and Holinstat, M. (2012) Investigations of human platelet-type 12-lipoxygenase: role of lipoxygenase products in platelet activation, *J Lipid Res*.

56. Armstrong, M., van Hoorebeke, C., Horn, T., Deschamps, J., Freedman, J. C., Kalyanaraman, C., Jacobson, M. P., and Holman, T. (2016) Human 15-LOX-1 active site mutations alter inhibitor binding and decrease potency, *Bioorg Med Chem 24*, 5380-5387.

57. Wecksler, A. T., Kenyon, V., Deschamps, J. D., and Holman, T. R. (2008) Substrate specificity changes for human reticulocyte and epithelial 15-lipoxygenases reveal allosteric product regulation, *Biochemistry 47*, 7364-7375.

58. Borgeat, P., Hamberg, M., and Samuelsson, B. (1976) Transformation of arachidonic acid and homo-gamma-linolenic acid by rabbit polymorphonuclear leukocytes. Monohydroxy acids from novel lipoxygenases, *The Journal of biological chemistry 251*, 7816-7820.

59. Hamberg, M., and Samuelsson, B. (1974) Prostaglandin endoperoxides. Novel transformations of arachidonic acid in human platelets, *Proceedings of the National Academy of Sciences of the United States of America 71*, 3400-3404.

60. Sheppard, K. A., Greenberg, S. M., Funk, C. D., Romano, M., and Serhan, C. N. (1992) Lipoxin generation by human megakaryocyte-induced 12-lipoxygenase, *Biochimica et biophysica acta 1133*, 223-234.

61. Green, A. R., Barbour, S., Horn, T., Carlos, J., Raskatov, J. A., and Holman, T. R. (2019) Strict Regio-specificity of Human Epithelial 15- Lipoxygenase-2 Delineates its Transcellular Synthesis Potential, *Biochemistry*.

62. Ringholz, F. C., Buchanan, P. J., Clarke, D. T., Millar, R. G., McDermott, M., Linnane, B., Harvey, B. J., McNally, P., and Urbach, V. (2014) Reduced 15-lipoxygenase 2 and lipoxin A4/leukotriene B4 ratio in children with cystic fibrosis, *The European respiratory journal 44*, 394-404.

63. Spanbroek, R., Hildner, M., Kohler, A., Muller, A., Zintl, F., Kuhn, H., Radmark, O., Samuelsson, B., and Habenicht, A. J. (2001) IL-4 determines eicosanoid formation in dendritic cells by down-regulation of 5-lipoxygenase and up-regulation of 15-lipoxygenase 1 expression, *Proceedings of the National Academy of Sciences of the United States of America 98*, 5152-5157.

64. Abrial, C., Grassin-Delyle, S., Salvator, H., Brollo, M., Naline, E., and Devillier, P. (2015) 15-Lipoxygenases regulate the production of chemokines in human lung macrophages, *British journal of pharmacology 172*, 4319-4330.

65. Werner, M., Jordan, P. M., Romp, E., Czapka, A., Rao, Z., Kretzer, C., Koeberle, A., Garscha, U., Pace, S., Claesson, H. E., Serhan, C. N., Werz, O., and Gerstmeier, J. (2019) Targeting biosynthetic networks of the proinflammatory and proresolving lipid metabolome, *FASEB journal : official publication of the Federation of American Societies for Experimental Biology 33*, 6140-6153.

66. Profita, M., Sala, A., Siena, L., Henson, P. M., Murphy, R. C., Paterno, A., Bonanno, A., Riccobono, L., Mirabella, A., Bonsignore, G., and Vignola, A. M. (2002) Leukotriene B4 production in human mononuclear phagocytes is modulated by interleukin-4-induced 15-lipoxygenase, *The Journal of pharmacology and experimental therapeutics 300*, 868-875.

67. Peters-Golden, M., and Brock, T. G. (2003) 5-lipoxygenase and FLAP, *Prostaglandins, leukotrienes, and essential fatty acids 69*, 99-109.

68. Hatzelmann, A., Schatz, M., and Ullrich, V. (1989) Involvement of glutathione peroxidase activity in the stimulation of 5-lipoxygenase activity by glutathione-depleting agents in human polymorphonuclear leukocytes, *European journal of biochemistry 180*, 527-533.

69. Weitzel, F., and Wendel, A. (1993) Selenoenzymes regulate the activity of leukocyte 5-lipoxygenase via the peroxide tone, *The Journal of biological chemistry 268*, 6288-6292.

70. Petrich, K., Ludwig, P., Kuhn, H., and Schewe, T. (1996) The suppression of 5-lipoxygenation of arachidonic acid in human polymorphonuclear leucocytes by the 15-lipoxygenase product (15S)-hydroxy-(5Z,8Z,11Z,13E)-eicosatetraenoic acid: structure-activity relationship and mechanism of action, *The Biochemical journal 314 (Pt 3)*, 911-916.

71. Wecksler, A. T., Kenyon, V., Garcia, N. K., Deschamps, J. D., van der Donk, W. A., and Holman, T. R. (2009) Kinetic and structural investigations of the allosteric site in human epithelial 15-lipoxygenase-2, *Biochemistry 48*, 8721-8730.

Chapter 4

STRUCTURAL BASIS FOR ALTERED POSITIONAL SPECIFICITY OF 15-LIPOXYGENASE-1 WITH 5S-HETE AND 7S-HDHA

4.1 Introduction

Lipoxygenases (LOXs) are non-heme iron-containing dioxygenases that catalyze the hydroperoxidation of polyunsaturated acids containing 1-4-pentadiene moiety (*1, 2*). LOX's play an important role in regulating the process of inflammation. They are capable of reacting with a variety of dietary fatty acids to form products broadly classified as oxylipins. Specialized-pro-resolving mediators (SPM's) are a type of oxylipin that regulate the switch from a pro-inflammatory to a pro-resolving state (*3, 4*). LOX's can produce both pro–inflammatory mediators such as the leukotrienes, as well as anti-inflammatory SPM's, such as the lipoxins, resolvins and maresins.

The stereo and region-specificity of LOX's determines which oxylipin mediators a cell may produce, either on their own or in concert with other LOX isozymes expressed in neighboring cells through the process of transcellular biosynthesis. h15-LOX-1 is one of two 15-LOX's found in humans (*5*). No crystal structure of h15-LOX-1 is available, so most studies to date have attempted to understand the stereo- and regio-specificity of the enzyme by comparison to the structures of rabbit 15-LOX and h12-LOX (*6*). h15-LOX-1 shares 81% homology with r15-LOX, 86% homology to h12-LOX, but only 38% homology with h15-LOX-2. It primarily catalyzes abstraction of a hydrogen from C13 of arachidonic acid (AA) followed by insertion of dioxygen onto C15. The resulting molecule is protonated to produce 15S-hydroperoxyeicosatetraenoic acid (15S-HpETE), which can be reduced by glutathione peroxidases to 15S-hydroperoxyeicosatetraenoic acid (15S-HETE) (*7*).

The location of hydrogen abstraction depends on the depth of insertion of the methyl end of the substrate and which bisallylic carbon is located proximal to the enzymes' active site iron. Typically, h15-LOX-1 abstracts the hydrogen atom from the ω-8 carbon, with oxygenation at the ω-6 carbon, however, a small percentage of the ω-9 product is also made. Recently, we have determined that placing a hydroxyl group on C5 of AA or C7 of DHA changes the product profile of h15-LOX-1 with these substrates. With AA, the enzyme produces 85% 15-product (w-6) and 15% 12-product (w-9). However, h15-LOX-1 shows a shift in product profile with 5S-HETE as the substrate, producing a 15:85 ratio of the w-6 and w-9 products. This indicates that the location of hydrogen abstraction is shifted from C13 with AA to C10 with 5S-HETE. A similar shift in product profile emerges when h15-LOX-1 reacts with DHA and its oxygenated derivative, 7S-HDHA. In this case, h15-LOX-1 reacts with DHA to produce 67% of the 17-product and 20% of the 14-product, but reacts with 7S-HDHA to produce 10% of the 17-Product and 90% of the 14-product (a ratio of 10:90 ratio of the w-6 and w-9 products) (*vide infra*, chapter 1).

Altered product specificity has important implications for the biosynthesis of specialized pro-resolving mediators (SPM's). The proposed biosynthetic routes of SPM's such as 7S,14S-diHDHA, 5S,15S-diHETE and resolvin D5 (RvD5) are based on the positional specificity of h15-LOX-1 with AA and DHA. However, the altered positional specificity of h15-LOX-1 suggests that h15-LOX-2 may be the primary source of RvD5 and 5S,15S-diHETE, while h15-LOX-1 instead produces 7S,14S-diHDHA and 5S,12S-diHDHA. Therefore, the *in vivo* biosynthetic routes of these

molecules should be carefully evaluated with the altered positional specificity of h15-LOX-1 in mind.

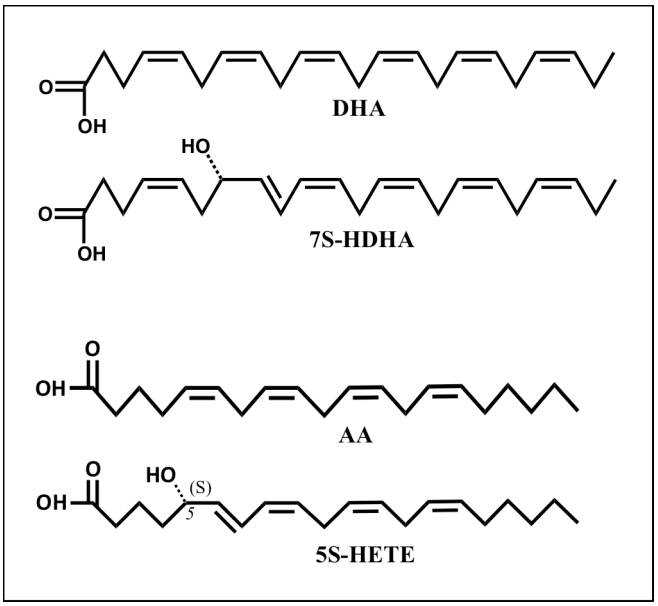

Figure 4.1. Structures of DHA, 7S-HDHA, AA and 5S-HETE

The altered positional specificity of h15-LOX-1 is unusual, as it does not occur in other LOX's. h15-LOX-2, for example, shows strict regiospecificity, producing 100% the ω-6 product, regardless if the substrate is a fatty acid (AA or DHA) or an oxylipin, such as 5S-HETE or 7S-HDHA (*8*) (*vide infra*, chapter 1). Similarly, h12-LOX produces 100% 12-product from AA and greater than 90% 12-product from 5S-HETE. This suggests that distinct structural feature of h15-LOX-1 lead to it's altered positional specificity.

The structural basis for the stereo and regiospecificity of h15-LOX-1 with AA has been investigated using site-directed mutagenesis of the active site. Three regions

of the active site have been shown to be important for determining the positional specificity of h15-LOX-1 **(Figure 4.2)** (*9*). Early work established that the aromatic ring of F414 forms a pi-pi stacking interaction with the substrate's Δ11 double bond and that R403 interacts with the terminal carboxylate (*10*). Sloane and coworkers demonstrated that I417 and I418 help define the bottom of the active site cavity and that mutating these residues to smaller amino acids allowed the substrate to slide deeper into the active site, causing the enzyme to produce more 12-product (*6*). Kuhn and coworkers expanded this work by showing that F352 further defines the active site and aids in maintaining C15 oxygenation over C12 oxygenation (*11, 12*). These studies lead to the triad hypothesis, in which the specificity of the active site is defined by amino acids in 3 areas: I417 and I418 at the bottom of the active site, R402 at the active site entrance, and F414 and F352 in the middle of the active site (*13*). These three areas are positioned in a boot-shaped cavity lined by hydrophobic residues into which the substrate enters methyl-end first. This model is supported by structural studies of h12-LOX, in which analogous mutations of conserved amino acids produced similar effects to those seen in h15-LOX-1(*14*).

h15-LOX-1 primarily catalyzes the abstraction of a pro-S hydrogen from carbon 13 of AA and carbon 15 of DHA. In order to demonstrate altered positional specificity with 5S-HETE and 7S-HDHA, h15-LOX-1 must primarily abstract from C10 of AA and C12 of DHA. This implies deeper insertion of the substrate into the active site cavity (**Figure 4.2**). Molecular modeling has suggested that the alcohol of 5S-HETE and 7S-HDHA forms a hydrogen bond with E398 that may position them

deeper in the active site compared with AA and DHA. The contribution of additional active site amino acids to substrate binding indicates that the existing model of positional specificity in h15-LOX-1 may need updating. The present study investigates whether the triad hypothesis adequately explains the structural basis for the altered positional specificity of h15-LOX-1 with 5S-HETE and 7S-HDHA.

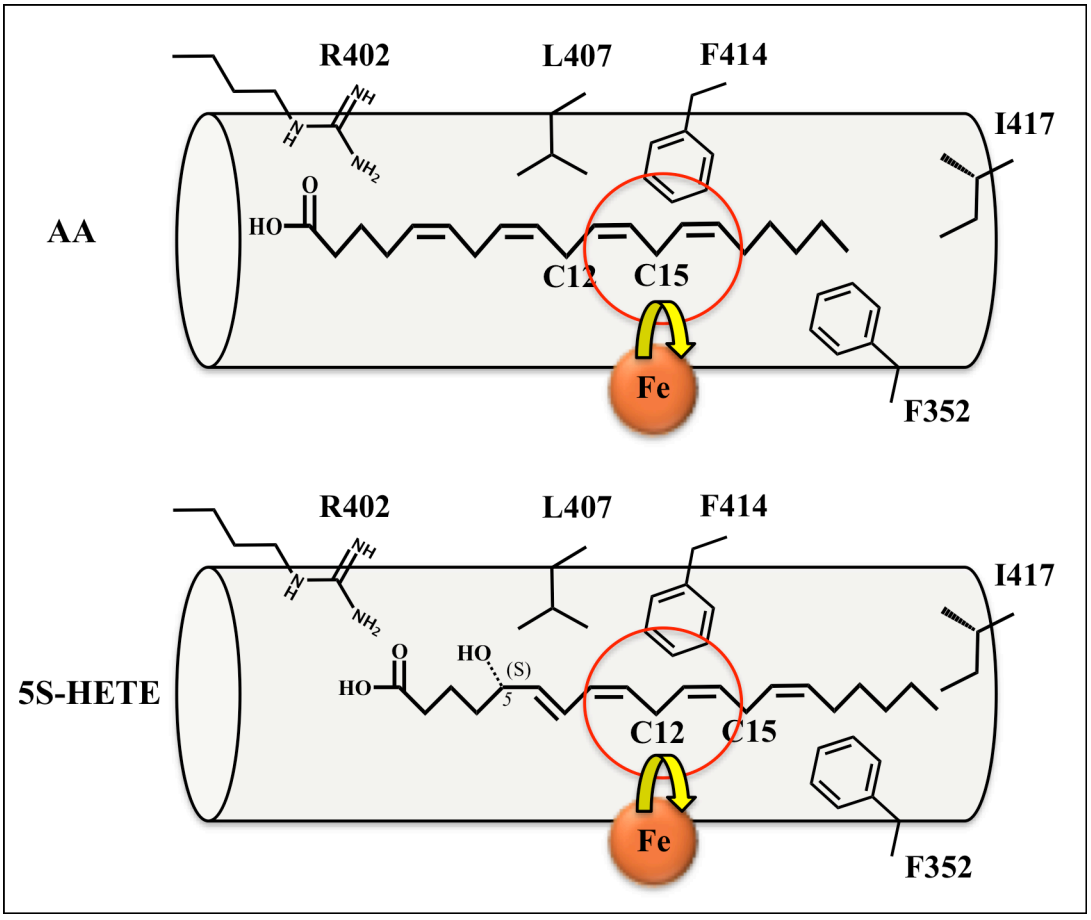

Figure 4.2. Model of the active site of h15-LOX-1, showing 5 amino acid residues hypothesized to influence positional specificity with AA. The top figure depicts positioning of AA, while the bottom depicts positioning of 5S-HETE. h15-LOX primarily abstracts a hydrogen from C15 of AA and C12 of 5S-HETE. In order for this to occur, the two substrates must be positioned differently in the active site relative to the catalytic iron.

4.2 Experimental Procedures

4.2.1 Expression and Purification of h15-LOX-1.

Overexpression and purification of his-tagged wild-type and mutant h15-LOX-1 was performed using cation exchange and nickel-affinity chromatography as previously described (*15, 16*). The purity of h15-LOX-1 and h12-LOX were assessed by SDS gel to be greater than 85%, and metal content was assessed on a Finnigan inductively-coupled plasma-mass spectrometer (ICP-MS), via comparison with iron standard solution. Cobalt-EDTA was used as an internal standard.

4.2.2 Site-directed Mutagenesis.

Amino acid numbering for h15-LOX-1 refers to the sequence with UniProt accession number P16050 without the 6XHis-tag and with the N-terminal methionine assigned as amino acid number one. The following mutations were introduced into h15-LOX-1: R402L, L407A, F414L, F414W, I417A, I417M, F352L, F352W, Q595L, E398L. Primers were designed using the Agilent Technologies (CA, USA) online primer-design tool found at: (***http://www.genomics.agilent.com/primerDesignProgram.jsp***) Mutations were introduced with a QuikChange®II site-directed mutagenesis kit from Agilent Technologies using the included protocol. The mutations were confirmed by sequencing the LOX insert in the pFastBac1 shuttle vector (Eurofins Genomics, KY, USA).

4.2.3 Expression, purification and quantification of h5-LOX.

Overexpression and purification of wild-type h5-LOX was performed by ammonium-sulfate precipitation as previously described (*15, 16*). The amount of 5-LOX protein contained in the ammonium-sulfate precipitate was assessed by comparing values obtained by bradford assay and quantitative western blotting with purified h5-LOX-octa-his mutant. Western blots were performed using rabbit anti-5-lipoxygenase polyclonal (Cayman chemicals) primary antibody diluted 1:500 and goat anti-rabbit-HRP (Abcam) secondary antibody diluted 1:5000. h5-LOX-octa-his plasmid was a gift from Marcia Newcomber of Louisiana State University. The protein was expressed as described previously and purified by nickel-affinity column. Elution was carried out using 50mM bis-tris, pH 6.5 containing 200mM Imidazole and 500mM NaCl. The purity of h5-LOX-octa-his was assessed by SDS gel to be greater than 80%.

4.2.4 Production and isolation of Oxylipins

7(S)-Hydroperoxy 4Z,8E,10Z,13Z,16Z,19Z-docosahexaenoic acid (7S-HpDHA) was synthesized by reaction of DHA (25-50 μM) with h5-LOX. The reaction was carried out for 2 hours in 800 ml of 25mM HEPES, pH 7.5 containing 50mM NaCl, 100 μM EDTA and 200 μM ATP. The reaction was quenched with 0.5% glacial acetic acid, extracted 3 times with 1/3 volume dichloromethane and evaporated to dryness under N2. The Products purified isocratically via high performance liquid chromatography (HPLC) on a Higgins Haisil Semi-preparative

(5μm, 250mm x 10mm) C18 column with 45:55 of 99.9% acetonitrile, 0.1% acetic acid and 99.9% water, 0.1% acetic acid. 7(S)-Hydroxy 4Z,8E,10Z,13Z,16Z,19Z-docosahexaenoic acid (7S-HDHA) was synthesized as performed for 7S-HpDHA with trimethylphosphite added as a reductant prior to HPLC. The isolated products were assessed to be greater than 95% pure by LC-MS/MS. The Products purified isocratically via high performance liquid chromatography (HPLC) on a Phenomenex Luna semi-preparative (5μm, 250mm x 10mm) silica column with 99:1 of 99.9% Hexane, 0.1% trifluoroacetic acid and 99.9% Isopropanol, 0.1% trifluoroacetic acid. The isolated products were assessed to be greater than 95% pure by LC-MS/MS. 5S-HpETE was synthesized by reaction of AA (25-50 μM) with h5-LOX. The reaction was carried out for 1 hour in 1000 ml of 25mM HEPES, pH 7.5 containing 50mM NaCl, 100 μM EDTA and 200 μM ATP. The reaction was quenched with 0.5% glacial acetic acid, extracted 3 times with 1/3 volume dichloromethane and evaporated to dryness under N2. The Products purified isocratically via high performance liquid chromatography (HPLC) on a Higgins Haisil Semi-preparative (5μm, 250mm x 10mm) C18 column with 45:55 of 99.9% acetonitrile, 0.1% acetic acid and 99.9% water, 0.1% acetic acid.

4.2.5 Steady State Kinetics of h15-LOX-1

h15-LOX-1 reactions were performed, at ambient temperature, in a 1 cm^2 quartz cuvette containing 2 mL of 25 mM HEPES, pH 7.5 with substrate (AA, DHA, 5S-HETE, 5S-HpETE 7S-HDHA or 7S-HpDHA.) Substrate concentrations were

varied from 0.25 μM to 10 μM for AA or 0.5 μM to 40 μM for 5S-HETE and 5S-HpETE. DHA concentrations were varied from 0.25-10 μM, 7S-HDHA concentrations were varied from 0.3-15 μM, 7S-HpDHA concentrations were varied from 0.3-20 μM. Concentration of DHA was determined by measuring the amount of 15S-HpDHA produced from complete reaction with soybean lipoxygenase-1 (sLO-1). Concentrations of 7S-HDHA and 7S-HpDHA were determined by measuring the absorbance at 234 nm. Reactions were initiated by the addition of h15-LOX-1 (~200-600 nM final concentration), and were monitored on a Perkin-Elmer Lambda 45 UV/VIS spectrophotometer. Product formation was determined by the increase in absorbance at 234 nm for 5S-HETE (ε_{234nm} = 27,000 M^{-1} cm^{-1}), 270 nm for 5S,12S-diHETE (ε_{234nm} = 40,000 M^{-1} cm^{-1}), 254 nm for 5S,15S-diHETE (ε_{234nm} = 21,500 M^{-1} cm^{-1})(*17*), 234 nm for 7S-HpDHA (ε_{234nm} = 25,000 M^{-1} cm^{-1}) and 270 nm for 7S,14S-diHDHA (ε_{270nm} = 40,000 M^{-1} cm^{-1}) (*18-20*). 5S,15S-diHDHA and 7S,17S-diHDHA have an absorbance max of 245 nm, however, due to overlap with the substrate peak at 234 nm formation of this product was measured at 254 nm using an extinction coefficient of 21,900 M^{-1} cm^{-1} to adjust for the decreased rate of absorbance change at this peak shoulder (*21*). KaleidaGraph (Synergy) was used to fit initial rates (at less than 20% turnover), as well as the second order derivatives (k_{cat}/K_M) to the Michaelis-Menten equation for the calculation of kinetic parameters.

4.2.6 Product Analysis of LOX reactions with DHA, 7S-HDHA, 7S-HpDHA

Reactions were carried out in 2 ml of 25 mM HEPES, pH 7.5 with stirring at ambient temperature. Reactions with DHA and AA contained 10 μM substrate and ~200 nM h15-LOX-1. Those with 5S-HETE, 5S-HpETE 7S-HDHA and 7S-HpDHA contained 20 μM substrate ~550 nM h15-LOX-1. Reactions were monitored via UV-vis spectrophotometer and quenched at 50% turnover with 0.5% glacial acetic acid. Each quenched reaction was extracted with 6 mL of DCM and reduced with trimethylphosphite. The samples were then evaporated under a stream of N_2 to dryness and reconstituted in 50 μL of methanol containing 3 μM 13-HODE as an internal standard. Control reactions without enzymes were also conducted and used for background subtraction, ensuring oxylipin degradation products were removed from analysis. Reactions were analyzed via LC-MS/MS. The chromatography system was coupled to a Thermo-Electron LTQ LC-MS/MS for mass analysis. All analyses were performed in negative ionization mode at the normal resolution setting. MS2 was performed in a targeted manner with a mass list containing the following m/z ratios ± 0.5: 343.4 (HDHA's), 359.4 (diHDHA's), and 375.4 (triHDHA's). Products were identified by matching retention times, UV spectra, and fragmentation patterns to known standards, or in the cases were MS standards were not available, structures were deduced from comparison with known and theoretical fragments.

4.3 Results and discussion

The triad hypothesis has been proposed for the binding of AA in the active site of h15-LOX-1. In order to determine if 5S-HETE binds in a similar fashion to AA, we created a set of mutants to investigate the binding constraints of AA and 5S-HETE and assayed their kinetic and product profiles.

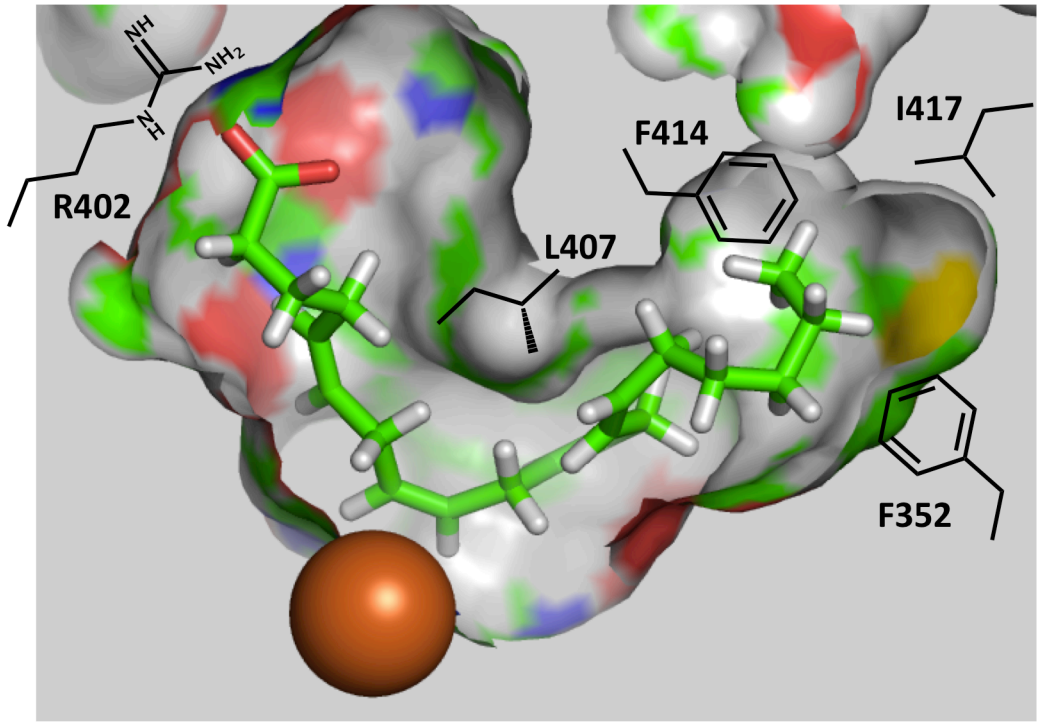

Figure 4.3. Model of the active site of h15-LOX-1 showing L-shaped binding cavity, position of catalytic iron in orange and AA in green at middle. Amino acids shown to play a role in positional specificity of AA are highlighted: R402, L407, F414, I417, F352.

4.3.1 Binding to substrate carboxylate: R402

Positively charged amino acids can play a role in binding the carboxylate of fatty acids (*22*). R402L, located near the entrance to the active site cavity, is

conserved in both h12-LOX and h15-LOX-1 and is proposed to interact with the carboxylic acid moiety of AA (*10*). This interaction is thought to stabilize the substrate fatty acid in the active site with the methyl end orientated towards the bottom of the active site pocket. In order to test whether this model can be applied to 5S-HETE, R402 was replaced with leucine in h15-LOX-1. However, little change was observed in the steady-state Michaelis-Menten kinetics of 5S-HETE compared with the wildtype enzyme (**Table 4.1**). The product profile showed that the percentage of 5S-HETE oxygenated by R402L at C12 increased slightly, from 86% to 92%, indicating R402L does not significantly impact 5S-HETE positioning relative to AA positioning. It should be noted that in the current work, the product profile of our R402L mutant was similar to previously published work (*23*), the kinetic parameters of R402L with AA where not. The mutant, R402L, demonstrated a k_{cat} which is of comparable magnitude to that of AA, and a k_{cat}/K_M of 0.73 sec-1μM-1 with AA, which is only 3-fold lower than that seen with wildtype enzyme (**Table 4.1**). This demonstrates a reduced rate of substrate capture for R402L, however is it is less than the change reported by Gan, et al (*10*). This smaller change is consistent with recent studies on h12-LOX, which demonstrated negligible kinetic effects with the R402L mutant (*14*) and suggested that other nearby positively charged amino acids may contribute to binding the substrate carboxylate.

There are a number of differences between the current study and previous work on R402L that may contribute to the smaller observed role of R402. Prior kinetic work used an extinction coefficient for AA of 23,000, which is 15% lower

than the currently accepted value. Previous methods utilized 13-HpODE for iron activation, as well as detergent and higher concentrations of fatty acid substrate, which are less physiologically relevant. The kinetic values determined in previous studies were reported in specific activity, which is not comparable to K_{cat} in situations where an enzyme experiences substrate inhibition. h15-LOX-1 shows substrate-inhibition above 10 μM, which can result in an inaccurate V_{max} value. Substrate inhibition can be affected by detergent use. Recent work has suggested that positive amino acids near the active site entrance are involved in modulating substrate inhibition (*24, 25*). It is possible that the effects of R402 mutants in different studies are caused by changes in substrate inhibition and not solely due to substrate positioning relative to the catalytic iron.

	AA			5S-HETE			AA		5S-HETE	
	K_M	k_{cat}	k_{cat}/K_M	K_M	k_{cat}	k_{cat}/K_M	% C15	% C12	% C15	% C12
wildtype	5.1	10	2.1	4.9	1.1	0.22	86	14	14	86
R402L	9.8	7.2	0.73	6.6	3.6	0.55	73	27	8	92

Table 4.1. The role of carboxylate-binding residue R402L was investigated with steady state kinetics and product profiling of wildtype and mutant h15-LOX-1 with AA and 5S-HETE. K_M is in units of μM, k_{cat} is in units of sec^{-1}, k_{cat}/K_M is in units of $sec^{-1}\mu M^{-1}$.

4.3.2 Narrow midpoint of active site cavity: L407

L546 is thought to define the corner of the L-shaped turn in the active site cavity of soybean 15-LOX, based on docking of AA into the crystal structure of soybean 15-LOX (*10, 26*). Sequence alignment shows that this leucine is conserved in

the majority of lipoxygenases and is homologous to L407 in humans (*10*). Substituting a smaller amino acid at this location in h12-LOX produced a loss in activity and a shift to greater oxygenation at C15, by widening the active site across from the catalytic iron (*14*). In order to test whether L407 influences altered positioning of 5S-HETE within the active site, this amino acid was replaced with a smaller residue, L407A. Steady-state Michaelis-Menten kinetics demonstrated that the k_{cat} and k_{cat}/K_M of 5S-HETE with L407A showed only a small change compared to wildtype (**Table 4.2**). When reacting with 5S-HETE, L407A produces 9% of the 15-product, decreased from the 14% seen with wildtype. These results indicate that L407 is not important for the catalysis of 5S-HETE by h15-LOX-1.

Kinetic data with AA showed that k_{cat} and k_{cat}/K_M were decreased by 4.5-fold compared to wildtype, indicating L407A has some effect on AA catalysis (**Table 4.2**). The percentage of oxygenation occurring on C15 decreased by 20%; from 84% in wildtype, to 67% in L407A. This suggests that this amino acid contributes to the positioning of AA in the active site. The increased space created in the active site when L407 is mutated to Alanine may allow AA to take on more conformations that position C10 closer to the iron than C13. It may also position C10 and C13 farther from the iron, slowing catalytic rates for both. L407A produces a greater effect on positional specificity in h15-LOX-1 than it does in h12-LOX, but a smaller effect on catalysis (*14*). The larger decrease in K_{cat} L407A demonstrates with AA compared to 5S-HETE, supports the idea that there is an additional interaction that helps position 5S-HETE near the active site iron.

	AA			5S-HETE			AA		5S-HETE	
	K_M	k_{cat}	k_{cat}/K_M	K_M	k_{cat}	k_{cat}/K_M	% C15	% C12	% C15	% C12
wildtype	5.1	10	2.1	4.9	1.1	0.22	86	14	14	86
L407A	4.9	2.2	0.45	7.9	0.7	0.088	67	33	9	91

Table 4.2. The role of active site constriction residue L407 was investigated with steady state kinetics and product profiling of wildtype and mutant h15-LOX-1 with AA and 5S-HETE. K_M is in units of μM, k_{cat} is in units of $sec^{-1}\mu M^{-1}$, k_{cat}/K_M is in units of $sec^{-1}\mu M^{-1}$.

4.3.3 Π-stacking interactions with substrate double bonds – F414

It has previously been determined that the Δ11 double bond of AA is positioned in the active site of h15-LOX-1 to form π–π stacking interactions with F414 (*10*). This interaction is also observed in h12-LOX with F414, and thus is considered a common structural feature in LOX biochemistry (*14*). To test whether F414 of h15-LOX-1 would also interact with 5S-HETE, the catalysis and product profile was investigated. The k_{cat} for F414I with AA decreased over 10-fold compared to wildtype (**Table 4.3**), similar to the effect seen in previous studies and the k_{cat}/K_M decreased by approximately 10-fold. Analysis of the products generated from the reaction with AA shows a marginal decrease in 15-product from 86% to 82%.

Replacing the aromatic side chain of F414 with an isoleucine decreased h15-LOX-1 catalytic activity with 5S-HETE by approximately 15-fold compared to wildtype but did not noticeably affect the product ratio. This indicates that this residue effects catalysis for both AA and 5S-HETE in a similar fashion.

Mutation of this residue to tryptophan restored the wildtype activity of the

enzyme for both AA and 5S-HETE. Both k_{cat} and k_{cat}/K_M were nearly unchanged from their wildtype values. This mutation caused more oxygenation to occur at C15 for both AA and 5S-HETE.

	AA			5S-HETE			AA		5S-HETE	
	K_M	k_{cat}	k_{cat}/K_M	K_M	k_{cat}	k_{cat}/K_M	% C15	% C12	% C15	% C12
wildtype	5.1	10	2.1	4.9	1.1	0.22	86	14	14	86
F414I	6.6	0.94	0.14	4.7	0.073	0.013	82	18	12	88
F414W	6.8	12	1.8	4.2	0.95	0.23	95	5	32	68

Table 4.3. The role of π–π stacking interactions was investigated with steady state kinetics and product profiling of wildtype and mutant h15-LOX-1 with AA and 5S-HETE. K_M is in units of μM, k_{cat} is in units of $sec^{-1}\mu M^{-1}$, k_{cat}/K_M is in units of $sec^{-1}\mu M^{-1}$.

4.3.4 Depth of the of active site cavity - I417 and F352

Previous work indicated that F353 contributes to positional specificity in soybean 15-LOX (*27*). This hypothesis was extended to the equivalent residue in h15-LOX-1 with work on chimeric mutants, which showed a similar role for the F352, (*11*). The location of F352 suggests it partially determines the depth of the active site cavity in h15-LOX-1. I417 has also been implicated in binding the methyl end of the substrate because of its position at the bottom of the active site in h12-LOX (*28*) and h15-LOX-1(*29*). Decreasing the residue size of either F352 or I417 in h15-LOX-1 increases the cavity size and thus increases oxygenation at C12 due to AA positioning deeper in the active site (*6*).

To determine if the active site depth influences the reactivity of 5S-HETE and

AA, kinetics and product profiling were investigated for both smaller and bulkier amino acids at positions 352 and 417 (**Figure 4.1**). In the current work, the product profile showed a large shift from oxygenation at C15 to C12 with both F352L and I417A, consistent with the literature.

For 5S-HETE, similar effects were seen. Compared to wildtype, the k_{cat} for I417A with 5S-HETE was decreased by half, from 1.1 to 0.5 sec^{-1}, while the product profile showed more oxygenation at C12, shifting from 86% in wildtype to 97% in the mutant (**Table 4.4**). Replacing F352 with a smaller leucine residue produced similar effects to that seen with I417A. The k_{cat} for 5S-HETE was decreased by 20%, while the change in k_{cat}/K_M was negligible. When reacting with 5S-HETE, F352L produced 95% of the 12-product, and increase in 11%. The shifts to greater oxygenation of 5S-HETE at C12 seen with both F352L and I417A are consistent with the substrate positioning deeper in the active site pocket.

	AA			**5S-HETE**			**AA**		**5S-HETE**	
	K_M	k_{cat}	k_{cat}/K_M	K_M	k_{cat}	k_{cat}/K_M	**% C15**	**% C12**	**% C15**	**% C12**
wildtype	5.1	10	2.1	4.9	1.1	0.22	86	14	14	86
I417A	3.9	5.1	1.3	3.7	0.5	0.14	22	71	3	97
F352L	4.3	8.4	1.9	4.4	0.91	0.21	16	81	5	95
I417M	1.9	8.0	4.2	3.5	3.8	1.1	87	13	16	85
F352W	3.5	11	3.1	20	1.3	0.065	96	4	69	31

Table 4.4. The role of active site depth was investigated with steady state kinetics and product profiling of wildtype and mutant h15-LOX-1 with AA and 5S-HETE. K_M is in units of μM, k_{cat} is in units of $sec^{-1}\mu M^{-1}$, k_{cat}/K_M is in units of $sec^{-1}\mu M^{-1}$.

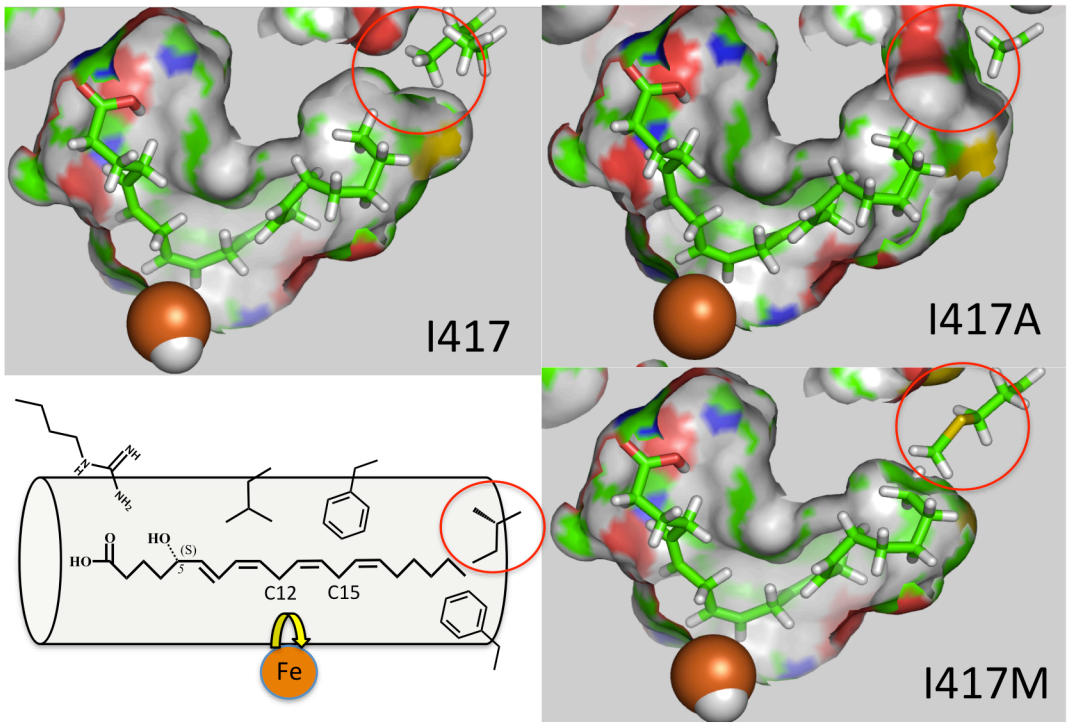

Figure 4.4. Model of the active site of h15-LOX-1 showing position of I417 and the effects various mutations on the size of the active site. I417A creates more space at the bottom of the active site, while I417M creates less space.

With smaller residues at 417 and 352 allowing the substrate to bind deeper into the active site, we hypothesize that larger residues near the bottom of the active site will have the opposite effect by restricting substrate binding and thereby shifting positional specificity from C12 to C15. Two mutants, I417M and F352W, were generated to test this hypothesis. I417M had little effect on positional specificity and kinetics with AA or 5S-HETE, likely due to its relatively small increase in size. F352W did not noticeably affect kinetics with AA, but it did produce a slight increase in oxygenation at C15, from 86% in wildtype to 96% in F352W. However, F352W

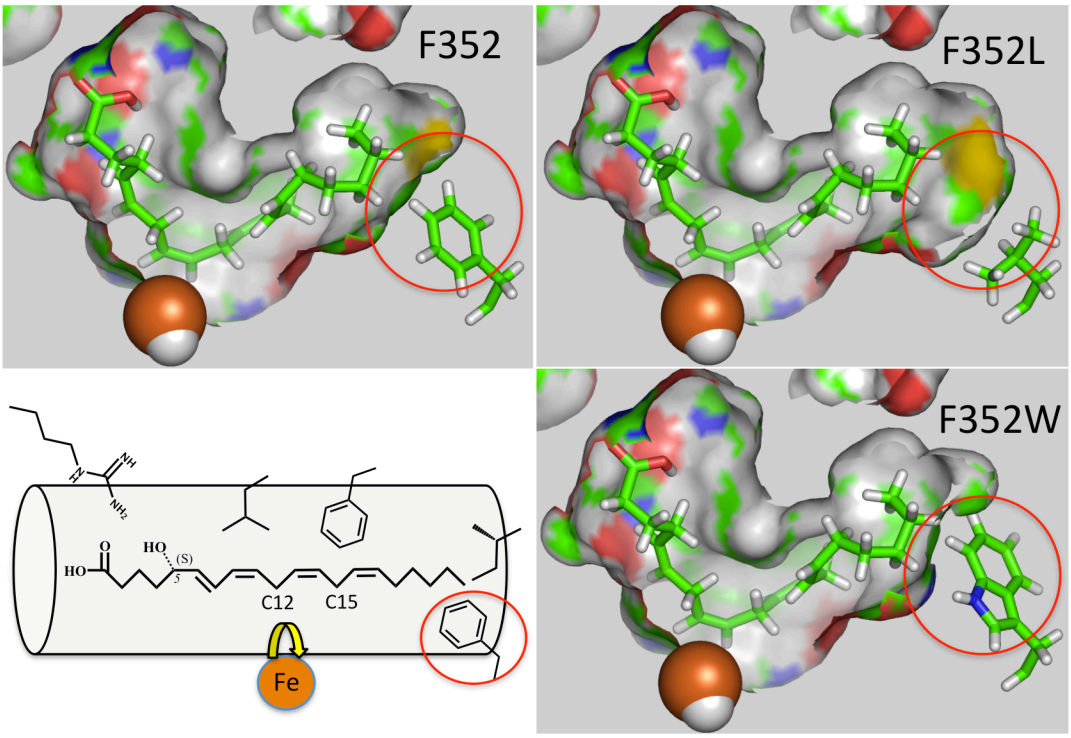

Figure 4.5. Model of the active site of h15-LOX-1 showing position of F352 and the effects various mutations on the size of the active site. F352L creates more space at the bottom of the active site, while F352W creates less space.

did have a large effect on 5S-HETE oxygenation, almost entirely reversing the altered positional specificity seen with 5S-HETE. While the wildtype enzyme produced only 14% 5S,15S-diHETE product, F352W produced 70% of the 5S,15S-diHETE product. The increased oxygenation at C15 of 5S-HETE suggests the larger tryptophan residue projects into the bottom of the active site cavity and hinders the methyl end of 5S-HETE from positioning as deep into the active site as it does in wildtype. In addition, F352W produced a 3-fold reduction in k_{cat}/K_M, from 0.22 to 0.065 $sec^{-1}\mu M^{-1}$, indicating that F352 also contributes to positioning 5S-HETE for catalysis. In total, F352 and I417 help define the shape and volume at the bottom of the active site. F352

has a particularly large effect on positioning 5S-HETE in the active site. A leucine in this position leads to 3% of oxygenation occurring at C15, while a Tryptophan causes 69% of the oxygenation to occur at C15.

4.3.5 Depth of active site with DHA and 7S-HDHA

Similar to 5S-HETE, h15-LOX-1 shows altered positional specificity with 7S-HDHA producing the non-canonical product, 7S,14S-diHDHA, instead of the canonical 7S,17S-diHDHA. Therefore, the altered positional specificity seen with 5S-HETE and the smaller active site should also occur with 7S-HDHA. To investigate this hypothesis, the positional specificity of h15-LOX-1 with 7S-HDHA was assayed with I417A, I417M, F352L and F352W. When reacting with I417A, DHA showed the expected shift to less oxygenation at C17 and greater oxygenation at C14, as the substrate was able to position deeper in the active site relative to the iron (**Table 4.5**. Reaction of DHA with I417M demonstrated a small shift to increased oxygenation at C17, resulting from the slightly bulkier methionine residue. The reaction between F352L and DHA showed the expected decrease in oxygenation at C17, however instead of an increase at C14, a large increase in oxygenation at C20 occurred. This may indicate a large change in substrate orientation occurred, either due to folding of the substrate methyl end positioning less deep in the active site. When reacting with DHA, F352W produced 79% of the 17-product, compared to 65% with wildtype, demonstrating that the bulkier amino acid substitution produces the largest shift in product profile, similar to the results with AA.

The product profile with 7S-HDHA shows that the smaller amino acids of F352L and I417A both increase the amount of oxygenation occurring on C17, from 90% in wildtype to 97% with I417A and 100% with F352L. Substituting larger amino acids in these positions had the expected, opposite effect. The reaction with I417M decreased oxygenation at C17 from 90% in wildtype to 63 % in the mutant. This is a much larger shift than seen with 5S-HETE, which may indicate that the larger size of 7S-HDHA compared with 5S-HETE, makes it more sensitive to the small change in active site depth brought about by I417M. The reaction of F352W decreased oxygenation at C17 to only 6%, nearly completely reversing the altered positional specificity seen with 7S-HDHA and the wildtype enzyme. These data indicate that the shift in positional specificity is related to the size of the amino acids at the bottom of the active site, consistent with the results obtained from 5S-HETE.

	DHA				**7S-HDHA**			
	% C11	**% C14**	**% C17**	**% C20**	**% C11**	**% C14**	**% C17**	**% C20**
wildtype	6	22	65	6	7	90	10	-
I417A	2	40	55	2	3	97	-	-
I417M	-	24	73	2	-	63	37	-
F352L	-	23	47	29	-	100	-	-
F352W	-	10	79	7	-	6	94	-

Table 4.5. The role of active site depth was investigated with steady state kinetics and product profiling of wildtype and mutant h15-LOX-1 with DHA and 7S-HDHA. K_M is in units of μM, k_{cat} is in units of $sec^{-1}\mu M^{-1}$, k_{cat}/K_M is in units of $sec^{-1}\mu M^{-1}$.

4.4 Conclusions

The triad hypothesis, developed to explain the positional specificity of 12/15-LOX's with AA, only partially explains the altered positional specificity of h15-LOX-1 with 5S-HETE and 7S-HDHA. R402L did not have a large affect 5S-HETE catalysis or positioning, indicating that this interaction with the substrate carboxylate is not important for 5S-HETE positioning. F414 plays a role in 5S-HETE catalysis and positioning, however since a change in positional specificity was observed with F414W, the effect observed with 5S-HETE may be due to steric interaction instead of the hypothesized π–π stacking. Further evidence of the importance of steric interaction at the bottom of the active site cavity comes from mutagenesis of F352 and I417, which played the largest roles in 5S-HETE positioning. Decreasing the size of the amino acids in these locations shifted oxygenation to C15, while increasing the size of the residues in this location reversed the altered positional specificity of h15-LOX-1 with 5S-HETE. Mutants at these locations demonstrated a similar effect with 7S-HDHA. Together, these data indicate that of the three regions proposed to control positional specificity of h15-LOX-1 with AA, active site cavity depth is the primary determinant of positional specificity with 5S-HETE.

4.5 Authorship Contributions

Steven C. Perry, James Sorrentino, Leslie Bautista, Oluwayomi Akinkugbe, William S. Conrad, Theodore R. Holman

S Perry designed experiments, acquired, analyzed and interpreted data, and wrote the manuscript. J Sorrentino, LBautista, O Akinkugbe and WS Conrad acquired data and analyzed data, T.R. Holman designed experiments and revised the manuscript.

4.6 References

1. Brash, A. R. (1999) Lipoxygenases: Occurrence, Functions, Catalysis and Acquisition of Substrate, *J. Biol. Chem. 274*, 23679-23682.

2. Kuhn, H., Saam, J., Eibach, S., Holzhutter, H. G., Ivanov, I., and Walther, M. (2005) Structural biology of mammalian lipoxygenases: enzymatic consequences of targeted alterations of the protein structure, *Biochemical and biophysical research communications 338*, 93-101.

3. Serhan, C. N. (2007) Resolution phase of inflammation: novel endogenous anti-inflammatory and proresolving lipid mediators and pathways, *Annu Rev Immunol 25*, 101-137.

4. Serhan, C. N. (2010) Novel lipid mediators and resolution mechanisms in acute inflammation: to resolve or not?, *The American journal of pathology 177*, 1576-1591.

5. Brash, A. R., Boeglin, W. E., and Chang, M. S. (1997) Discovery of a second 15S-lipoxygenase in humans, *Proceedings of the National Academy of Sciences of the United States of America 94*, 6148-6152.

6. Sloane, D. L., Leung, r., Craik, C. S., and Sigal, E. (1991) A Primary determinant for Lipoxygenase positional specificity, *Nature 354*, 149-152.

7. Kuhn, H., Banthiya, S., and van Leyen, K. (2015) Mammalian lipoxygenases and their biological relevance, *Biochimica et biophysica acta 1851*, 308-330.

8. Green, A. R., Barbour, S., Horn, T., Carlos, J., Raskatov, J. A., and Holman, T. R. (2016) Strict Regiospecificity of Human Epithelial 15-Lipoxygenase-2 Delineates Its Transcellular Synthesis Potential, *Biochemistry 55*, 2832-2840.

9. Ivanov, I., Kuhn, H., and Heydeck, D. (2015) Structural and functional biology of arachidonic acid 15-lipoxygenase-1 (ALOX15), *Gene 573*, 1-32.

10. Gan, Q.-F., Browner, M. F., Sloane, D. L., and Sigal, E. (1996) Defining the Arachidonic Acid Binding Site of Human 15-Lipoxygenase: MOLECULAR MODELING AND MUTAGENESIS, *The Journal of biological chemistry 271*, 25412-25418.

11. Borngraber, S., Kuban, R.-J., Anton, M., and Kuhn, H. (1996) Phenylalanine 353 is a Primary Determinant for the Positional Specificity of Mammalian 15-Lipoxygenases, *Journal of molecular biology 264*, 1145–1153.

12. Borngraber, S., Browner, M., Gillmor, S., Gerth, C., Anton, M., Fletterick, R., and Kuhn, H. (1999) Shape and specificity in mammalian 15-lipoxygenase active site. The functional interplay of sequence determinants for the reaction specificity, *The Journal of biological chemistry 274*, 37345-37350.

13. Vogel, R., Jansen, C., Roffeis, J., Reddanna, P., Forsell, P., Claesson, H. E., Kuhn, H., and Walther, M. (2010) Applicability of the triad concept for the positional specificity of mammalian lipoxygenases, *The Journal of biological chemistry 285*, 5369-5376.

14. Aleem, A. M., Tsai, W. C., Tena, J., Alvarez, G., Deschamps, J., Kalyanaraman, C., Jacobson, M. P., and Holman, T. (2019) Probing the Electrostatic and Steric Requirements for Substrate Binding in Human Platelet-Type 12-Lipoxygenase, *Biochemistry 58*, 848-857.

15. Amagata, T., Whitman, S., Johnson, T. A., Stessman, C. C., Loo, C. P., Lobkovsky, E., Clardy, J., Crews, P., and Holman, T. R. (2003) Exploring sponge-derived terpenoids for their potency and selectivity against 12-human, 15-human, and 15-soybean lipoxygenases, *J Nat Prod 66*, 230-235.

16. Robinson, S. J., Hoobler, E. K., Riener, M., Loveridge, S. T., Tenney, K., Valeriote, F. A., Holman, T. R., and Crews, P. (2009) Using enzyme assays to evaluate the structure and bioactivity of sponge-derived meroterpenes, *J Nat Prod 72*, 1857-1863.

17. Maas, R. L., Turk, J., Oates, J. A., and Brash, A. R. (1982) Formation of a novel dihydroxy acid from arachidonic acid by lipoxygenase-catalyzed double oxygenation in rat mononuclear cells and human leukocytes, *The Journal of biological chemistry 257*, 7056-7067.

18. Serhan, C. N., Dalli, J., Karamnov, S., Choi, A., Park, C. K., Xu, Z. Z., Ji, R. R., Zhu, M., and Petasis, N. A. (2012) Macrophage proresolving mediator maresin 1 stimulates tissue regeneration and controls pain, *FASEB journal : official publication of the Federation of American Societies for Experimental Biology 26*, 1755-1765.

19. Johnathan Fitzgerald, R. C., Masakazu Shinohara, Jesmond Dalli, Charles Serhan. (2014) Lipid Mediator Metabololipidomics LC-MS-MS Spectra Book 2014.

20. Butovich, I. A. (2006) A one-step method of 10,17-dihydro(pero)xydocosahexa-4Z,7Z,11E,13Z,15E,19Z-enoic acid synthesis by soybean lipoxygenase, *Journal of lipid research 47*, 854-863.

21. Green, A. R., Freedman, C., Tena, J., Tourdot, B. E., Liu, B., Holinstat, M., and Holman, T. R. (2018) 5 S,15 S-Dihydroperoxyeicosatetraenoic Acid (5,15-diHpETE) as a Lipoxin Intermediate: Reactivity and Kinetics with Human Leukocyte 5-Lipoxygenase, Platelet 12-Lipoxygenase, and Reticulocyte 15-Lipoxygenase-1, *Biochemistry*.

22. Banaszak, L., Winter, N., Xu, Z., Bernlohr, D. A., Cowan, S., and Jones, T. A. (1994) Lipid-binding proteins: a family of fatty acid and retinoid transport proteins, *Advances in protein chemistry 45*, 89-151.

23. Gan, Q.-F., Browner, M. F., Sloane, D. L., and Sigal, E. (1996) Defining the arachidonic acid binding site of human 15-lipoxygenase, *J. Biol. Chem. 271*, 25412 - 25418.

24. Poldemaa, K., Lipp, M., Jarving, I., Samel, N., and Eek, P. (2019) Gly188Arg substitution eliminates substrate inhibition in arachidonate 11R-lipoxygenase, *Biochemical and biophysical research communications 519*, 81-85.

25. Neau, D. B., Bender, G., Boeglin, W. E., Bartlett, S. G., Brash, A. R., and Newcomer, M. E. (2014) Crystal structure of a lipoxygenase in complex with substrate: the arachidonic acid-binding site of 8R-lipoxygenase, *The Journal of biological chemistry 289*, 31905-31913.

26. Minor, W., Steczko, J., Stec, B., Otwinowski, Z., Bolin, J. T., Walter, R., and Axelrod, B. (1996) Crystal structure of soybean lipoxygenase L-1 at 1.4 A resolution, *Biochemistry 35*, 10687-10701.

27. Prigge, S. T., Boyington, J. C., Gaffney, B. J., and Amzel, L. M. (1996) Structure conservation in lipoxygenases: structural analysis of soybean lipoxygenase-1 and modeling of human lipoxygenases, *Proteins 24*, 275-291.

28. Chen, X.-s., and Funk, C. D. (1993) Structure-function properties of human platelet 12-lipoxygenase- chimeric enzyme and in vitro mutagenesis studies, *The FASEB Journal 7*, 694-701.

29. Sloane, D. L., Leung, R., Barnett, J., Craik, C. S., and Sigal, E. (1995) Conversion of human 15-lipoxygenase to an efficient 12-lipoxygenase: the side-chain geometry of amino acids 417 and 418 determine positional specificity, *Protein engineering 8*, 275-282.

Chapter 5

15(S)-HYDROXYEICOSATRIENOIC ACID INHIBITS PLATELET ACTIVATION IN PART THROUGH PPARB

5.1 Introduction

Dihomo-γ-linolenic acid (DGLA; 20:3n−6), an omega-6 polyunsaturated fatty acid, has been reported to decrease human and murine platelet reactivity *in vitro* and limit thrombus formation in murine models (1). Within platelets, DGLA is metabolized by platelet-type 12-(S)-lipoxygenase (12-LOX) and cyclooxygenase (COX) into their respective biologically active oxidized lipids (oxylipins), which are critical for the antiplatelet effects of DGLA (1). The antiplatelet effects of the COX-derived prostaglandins of DGLA such as PGE_1 have been well-studied (2,3); however, until recently, the mechanism underlying the antiplatelet effects of the monohydroxylated oxylipins of DGLA remained unclear. The predominant platelet-derived monohydroxylated oxylipins of DGLA, 12-(S)-hydroxyeicosatrienoic acid (12-HETrE) and 15-(S)-hydroxyeicosatrienoic acid (15-HETrE), are produced by 12-LOX and COX, respectively, and differ in the position of their hydroxyl group (4,5). 12-HETrE was recently shown to inhibit platelet activation at least in part through the $G\alpha_s$-coupled prostacyclin receptor (6). While 15-HETrE has been shown to inhibit platelet activation, the mechanism by which this inhibition is achieved is not known (4).

Antiplatelet oxylipins can decrease platelet responsiveness by inhibiting proaggregatory oxylipin formation by COX or 12-LOX, increasing cAMP levels via Gαs-coupled receptors, or binding intracellular nuclear receptors, such as *peroxisome proliferator-activated receptors* (PPARs) (7,8). The ability of monohydroxylated oxylipins to interact with their effectors and hence mediate platelet reactivity depends

on the position of the hydroxyl group, double bond configuration, and the length of carbon backbone (7,8). 15-(S)-hydroxyeicosatetraenoic acid (15-HETE), an antiplatelet oxylipin of arachidonic acid (AA; 20:4n−6), has one more double bond than 15-HETrE. 15-HETE possesses antiplatelet functions attributed to the inhibition of proaggregatory oxylipins, but has also been shown to interact with PPARs in other cell types (9-12). It is unclear whether 15-HETrE inhibits platelet function via a 1) Gαs-coupled receptor similar to 12-HETrE, 2) inhibition of proaggregatory oxylipins similar to 15-HETE, or 3) a yet-to-be-determined signaling pathway.

The current study sought to determine the mechanism by which 15-HETrE regulates platelet reactivity. While previous studies demonstrated that 15-HETrE inhibits thromboxane receptor-mediated platelet aggregation (4), this is the first study to demonstrate that 15-HETrE inhibits platelet aggregation through multiple agonists by impinging on intracellular signaling. 15-HETrE was found to act as a weak 12-LOX inhibitor and limit platelet aggregation in a manner at least partially dependent on PPARβ activation. Hence, this study reinforces the diverse array of functions oxylipins play in platelet biology and establishes for the first time the differential regulatory mechanisms by which 15-HETrE controls platelet function. An understanding of these differences in signaling may allow for new targets to limit platelet activation that leads to occlusive thrombus formation, myocardial infarction, and stroke.

5.2 Experimental Methods

5.2.1 Isolation of human platelets

All research involving human subjects was approved by the University of Michigan Institutional Review Board. Prior to blood collection written informed consent was obtained from all subjects in this study. Blood was collected into vacutainers containing sodium citrate (Becton, Dickinson and Company (BD), Franklin Lakes, New Jersey) and centrifuged for 10 minutes at 200 x g to obtain platelet rich plasma. Acid citrate dextrose (2.5% sodium citrate tribasic, 1.5% citric acid, 2.0% D-glucose) and apyrase (0.02 U/ml) were added to the platelet rich plasma, which was then was centrifuged for 10 minutes at 2000 x g. The pelleted platelets were resuspended in Tyrode's buffer (10 mM HEPES, 12 mM $NaHCO_3$, 127 mM NaCl, 5 mM KCl, 0.5 mM NaH_2PO_4, 1 mM $MgCl_2$, and 5 mM glucose) and adjusted to 3.0 x 10^8 platelets/mL, unless otherwise stated.

5.2.2 Leukocyte-depletion of platelets

Washed platelets (5.0 x10^8 platelets/mL) were incubated with magnetic CD45 MicroBeads (10 μl/mL) (Miltenyi Biotec Inc.) for 30 minutes. Following incubation, platelets were treated with EDTA (2.5 mM) and filtered through a magnetic-activated cell sorting separation column that selectively captured CD45 positive cells. Platelets were pelleted from the column flow through by centrifugation following treatment with acid citrate dextrose and apyrase, as described above.

5.2.3 Quantification of platelet-derived oxylipins

Leukocyte-depleted platelets were incubated with DMSO or DGLA (10 μM) for 10 minutes at 37°C, pelleted at 1000 x g for 1 min, and the supernatant was frozen. Subsequently, 13S-hydroxy-9Z,11E-octadecadienoic-9,10,12,13-d_4 acid (D4-13HODE) (20 ng) was added to the thawed supernatant and oxylipins were extracted with 1.5 mL dichloromethane, reduced with 20 μL of trimethylphosphite, and dried under a stream of N_2. Samples were resuspended in 50 uL of MeOH containing 10 ng of D8-12HETE. Prior to chromatography, 100 μL of 0.1% formic acid in water were added to samples, and 90 μL were injected for analysis. UPLC-MS/MS was performed as previously described (6), with the addition of the following m/z transitions: 15-HETE: 319→219, 15-HETrE: 321→221, 14,15-diHETE: 335→205, 8,15-diHETE: 335→155. Quantitation was performed with a 15-HETE standard curve. Quantitation of 14,15-diHETE was based on relative ionization efficiency of a diHETE standard to 15-HETE standard (0.98 +/-0.2).

5.2.4 Production and isolation of oxylipins

The synthesis of 15-HETE was performed as previously described (47-49). Briefly, 15S-hydroperoxy-8Z,11Z,13E-eicosatrienoic acid (15-HPETrE) was synthesized by reaction of DGLA (25-50 μM) with soybean lipoxygenase-1. The hydroperoxide product, 15-HPETrE, was reduced to the alcohol, 15-HETrE, with trimethylphosphite and purified by HPLC using a C18 HAIsil 250 × 10 mm semiprep column.

5.2.5 Platelet aggregation and dense granule secretion

A Chrono-log Model 700D lumi-aggregometer was used to measure platelet aggregation and ATP release under stirring conditions (1100 rpm) at 37°C for six minutes, following the addition of collagen (Chrono-log), thrombin (Enzyme Research Laboratories), AA (Cayman Chemical Company), or ADP (Sigma-Aldrich).

5.2.6 PKC substrate phosphorylation

Platelets were incubated with metabolite prior to stimulation with collagen for 5 minutes in an aggregometer. Reactions were stopped with the addition of 5X Laemmli sample buffer, boiled, and separated on a 10% SDS-PAGE gel. Western blots were performed with antibodies to GAPDH **(**Santa Cruz Biotechnology) and PKC substrate (Cell Signaling Technology).

5.2.7 Quantification of calcium mobilization and $\alpha_{IIb}\beta_3$ activation via flow cytometry

Washed platelets (1.0 x 10^6 platelets/mL) were incubated with DMSO, 15-HETE, or 15-HETrE (10 μM) for 10 minutes at 37ºC. Platelets were then treated for 5 minutes with either Fluo-4-AM (0.5 μg; Thermo Fisher Scientific) or PAC-1 (BD), an antibody that binds the active conformation of $\alpha_{IIb}\beta_3$. Platelets, supplemented with $CaCl_2$ (1 mM), were stimulated with convulxin (2.5 ng/mL, from Dr. Kenneth J. Clemetson) and the mean fluorescence intensity of the sample was continuously

measured on an Accuri C6 flow cytometer (BD) for 5 minutes for Ca^{2+} and 10 minutes for integrin activation.

5.2.8 α-granule secretion

Human platelets treated with metabolite for 10 minutes were stimulated with collagen (5 μg/mL) for 5 minutes under stirring conditions in the presence of the tetrapeptide Arg-Gly-Asp-Ser (RGDS; 2 mM; Sigma) to prevent platelet aggregation. A PE-conjugated P-selectin antibody (BD) was added to the stimulated platelets for 10 minutes and P-selectin surface expression was quantified by flow cytometry.

5.2.9 VASP phosphorylation

Platelets were incubated with oxylipins (10 μM), forskolin (5 μM), or DMSO for 10 minutes prior to the addition of 5X Laemmli sample buffer. Samples were boiled and then separated on a 10% SDS-PAGE gel. Western blots were performed with antibodies to phosphorylated (pS157) and total VASP **(**Santa Cruz Biotech.).

5.2.10 Thromboxane B2 (TXB_2) and 12-HETE formation

Platelets pretreated with 15-HETE or 15-HETrE (10 μM), were stimulated with collagen (5 μg/mL) for 5 minutes in an aggregometer. Platelets were pelleted by centrifugation at 1000 x g for 1 min and the supernatant was transferred to a new tube. The supernatant was immediately placed on dry ice. TXB_2 and 12-HETE were quantified by UPLC-MS/MS, as described above.

5.2.11 MS analysis of 12-LOX enzymatic products

Briefly, 12-LOX (60 pmoles) was reacted with 10 μM of each oxylipin, quenched, extracted three times, reduced with trimethylphosphite, and evaporated under a stream of nitrogen gas. Reactions were analyzed via LC-MS/MS. The chromatography system was coupled to a Thermo-Electron LTQ LC-MS/MS for mass analysis. All analyses were performed in negative ionization mode at the normal resolution setting. $MS^{/MS}$ was performed in a targeted manner with a mass list containing the following m/z ratios $\pm$ 0.5: 319.5 (HETE's), 321.5 (HETrE's), 335.5 (diHETE's), 337.4 (diHETrE's), 351.5 (triHETE's), and 353.5 (triHETrE's).

5.2.12 Determination of IC50 of 15-HETE and 15-HETrE against 12-LOX

Overexpression and purification of human 12-LOX were performed as previously described (50). Purified 12-LOX was added to 10 μM AA in 2 mL of 25 mM HEPES, pH 8.0, in the presence of the control or oxylipin. IC_{50} values were obtained by determining the enzymatic rate at various 15-HETE and 15-HETrE concentrations and plotting against 15-HETE and 15-HETrE concentrations, followed by a hyperbolic saturation curve fit via KaleidaGraph (Synergy).

5.2.13 Statistical analysis

GraphPad Prism 7 software (GraphPad Software, La Jolla, CA) was used to analyze data and calculate statistical significance.

5.3 Results

5.3.1 Platelets produce more 12-HETrE than 15-HETrE

12-HETrE and 15-HETrE, antiplatelet oxylipins derived from DGLA, have both independently been shown to be produced by DGLA-treated platelets (1,13,14). The levels of 12-HETrE and 15-HETrE in the releasate of platelets treated with DGLA (10 μM) were quantified by mass spectrometry (MS) to determine their ratio of formation from a common sample. Since leukocytes are a common contaminate of isolated platelets and a potential source of 15-HETrE via 15-lipoxygenase-dependent oxidation, washed human platelets were leukocyte-depleted by magnetic-activated cell sorting (15-17). The purity of the leukocyte-depleted platelets was quantified by flow cytometry using leukocyte (CD45) and platelet (GPIbα) specific antibodies. The leukocyte-depleted platelets contained 40 ± 11.34 (mean ± SEM; n= 7) leukocytes per

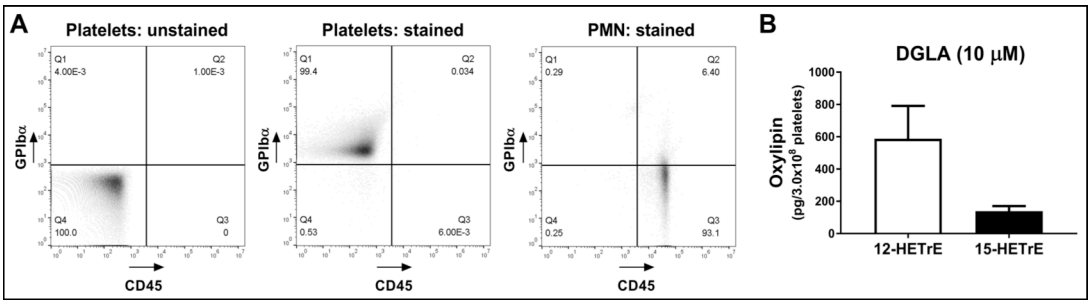

Figure 5.1: Leukocyte-depleted platelets produce 15-HETrE. A) Leukocyte-depleted platelets were stained with antibodies specific to platelets (GPIbα) and leukocytes (CD45), and analyzed by flow cytometry to quantify the number of residual polymorphonuclear leukocytes (PMNs) (CD45-positive, GPIbα-negative cells) in each sample. **B)** The levels of 12-HETrE and 15-HETrE were measured in the releasate of leukocyte-depleted platelets (n=3) treated with DGLA (10 μM). Data represents mean ± S.E.M

million platelets as detected by flow cytometry **(Figure 5.1A)**. Leukocyte-depleted platelets treated with DGLA produce approximately four times as much 12-HETrE (588 ± 352 ng/ml) as 15-HETrE (139 ± 54 ng/ml) **(Figure 5.1B).**

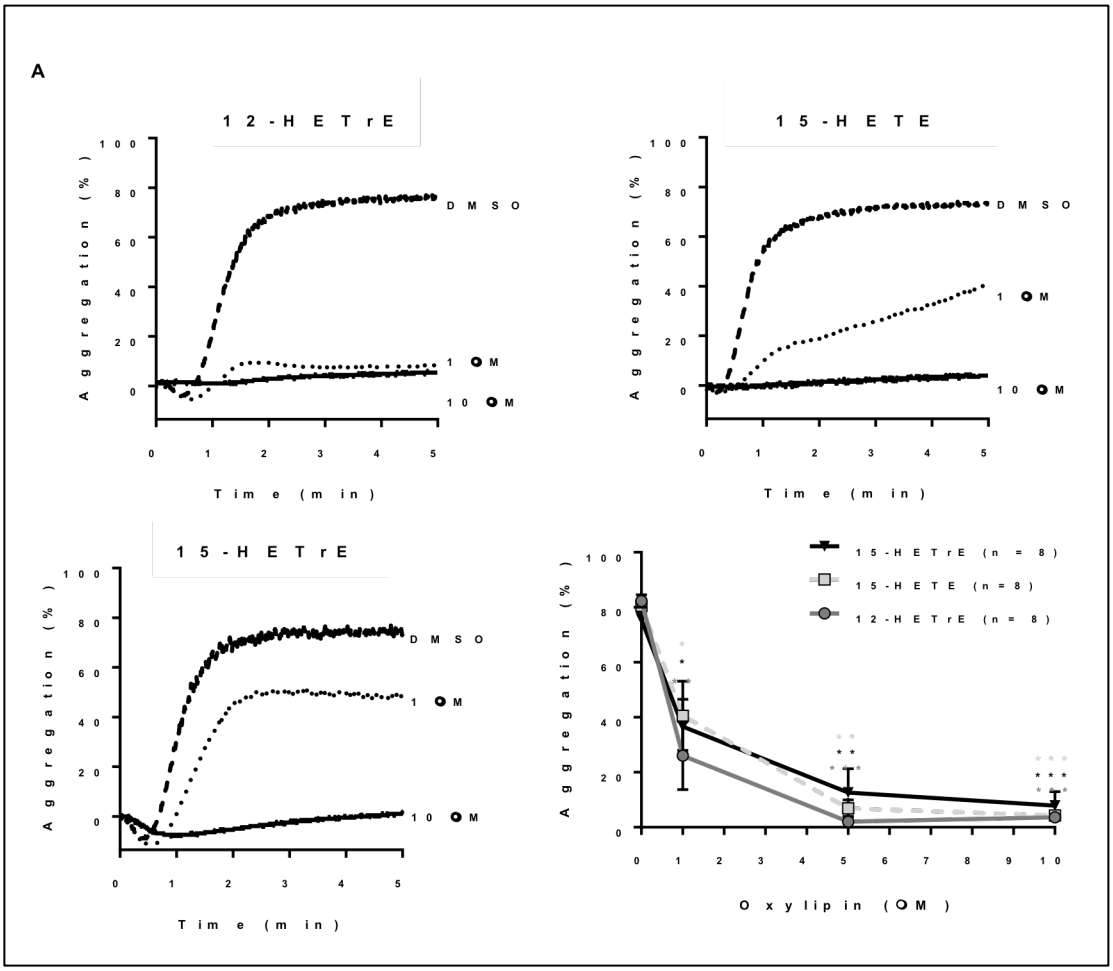

Figure 5.2A: 15-HETrE inhibits platelet aggregation independent of agonist tested. A) Human platelets (n= 6-8) were treated with increasing concentrations of 12-HETrE, 15-HETE, or 15-HETrE and then stimulated with collagen (.25 μg/mL). Data represents mean ± S.E.M. One-way ANOVA statistical analysis with Dunn's multiple comparison post-test was performed.

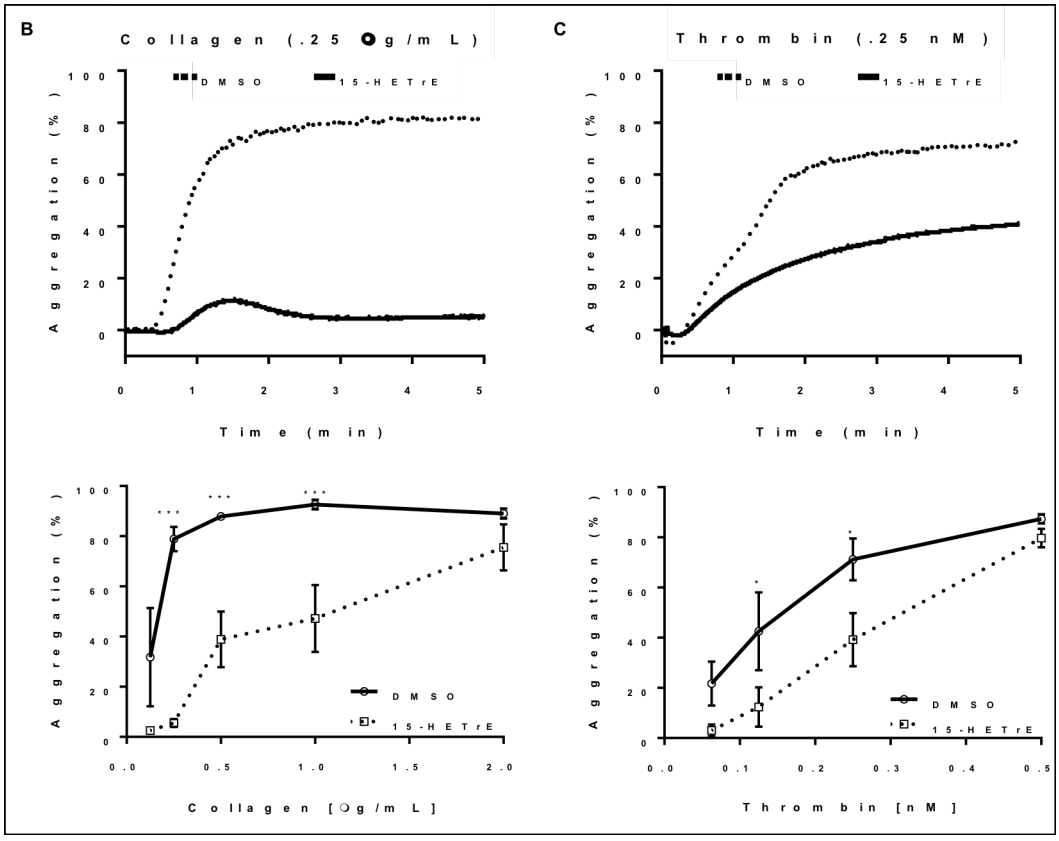

Figure 5.2B & 5.2C: 15-HETrE inhibits platelet aggregation independent of agonist tested. Human platelets (n= 4-6) were treated with 15-HETrE (10 μM) or vehicle (DMSO) for 10 minutes and then stimulated with increasing concentrations of **B)** collagen (n=4-6), **C)** thrombin (n=6**)** in an aggregometer. Data represents mean ± S.E.M. One-way ANOVA statistical analysis with Dunn's multiple comparison post-test was performed.

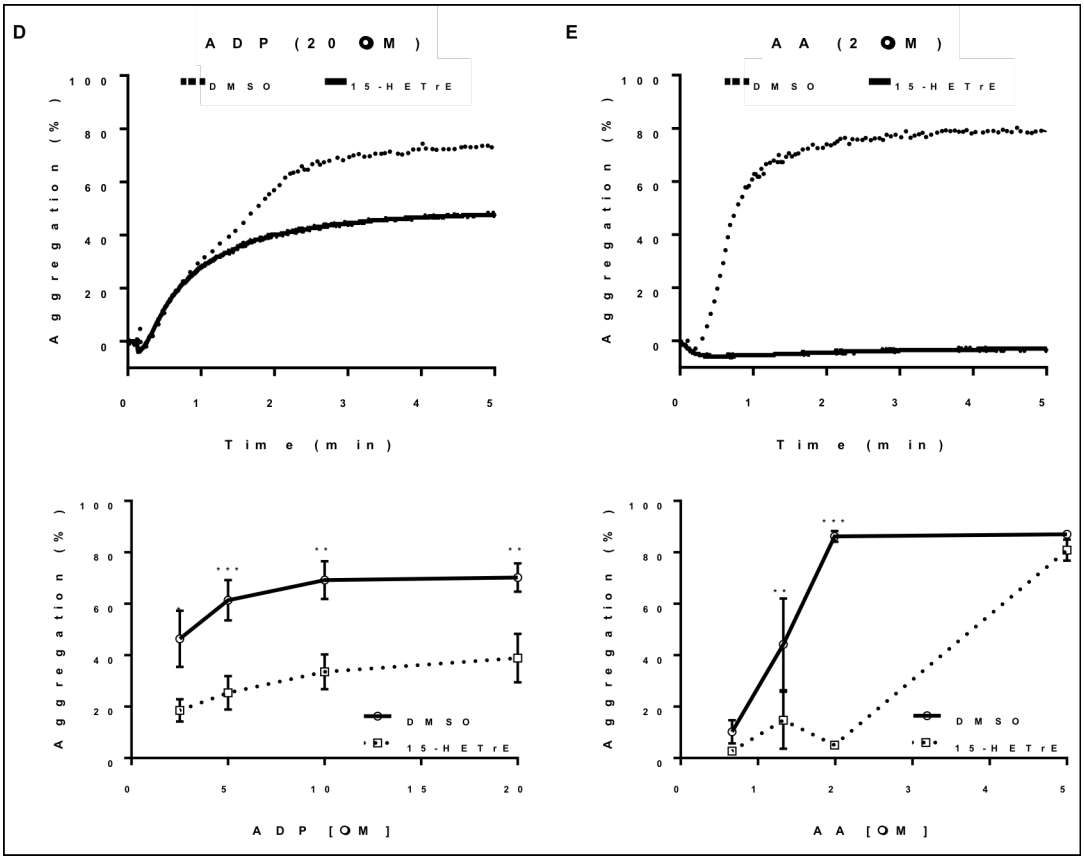

Figure 5.2D & 5.2E: 15-HETrE inhibits platelet aggregation independent of agonist tested. Human platelets (n= 4-6) were treated with 15-HETrE (10 μM) or vehicle (DMSO) for 10 minutes and then stimulated with increasing concentrations of **D)** ADP (n=6) or **E)** AA (n=6) in an aggregometer. Data represents mean ± S.E.M. One-way ANOVA statistical analysis with Dunn's multiple comparison post-test was performed.

5.3.2 15-HETrE inhibits platelet aggregation in an agonist-independent manner

While micromolar levels of 15-HETrE were previously reported to inhibit thromboxane receptor-mediated platelet aggregation,[4] it was unknown whether 15-HETrE inhibits platelet activation through other receptors such as PARs, GPVI, or $P2Y_{12}$. Platelets were treated with increasing concentrations of 15-HETrE prior to stimulation with collagen, the GPVI and $\alpha_2\beta_1$ agonist, to determine whether 15-HETrE inhibited collagen-mediated

platelet aggregation. 15-HETrE inhibited platelet aggregation in response to collagen (.25 μg/mL) with maximal inhibition of aggregation achieved at 10 μM of 15-HETrE (**Figure 5.2A**). Collagen-stimulated platelets were also incubated with 12-HETrE or 15-HETE to determine the relative potency of 15-HETrE-dependent inhibition of aggregation compared to previously identified antiplatelet monohydroxylated oxylipins (6,11,18,19). The three monohydroxylated oxylipins (15-HETrE, 12-HETrE, or 15-HETE) inhibited collagen-mediated platelet aggregation with similar potency inhibitor (**Figure 5.2A**). To determine the potency of 15-HETrE at inhibiting platelet aggregation in response to common platelet agonists, aggregation was measured in 15-HETrE-treated platelets that were stimulated with increasing concentrations of collagen, thrombin, ADP, or AA. 15-HETrE was effective at inhibiting low concentration of all agonists tested; however, higher doses of collagen, AA, and thrombin were able to overcome the inhibitory effects of 15-HETrE (**Figure 5.2B-E**). Interestingly, aggregation induced by high doses of ADP (20 μM) remained inhibited by 15-HETrE (**Figure 5.2D**).

5.3.3 15-HETrE inhibits intracellular platelet signaling

The mechanism by which either 15-HETE or 15-HETrE inhibit platelet activation is not well understood. To assess whether 15-HETE or 15-HETrE attenuated platelet aggregation through modulation of intracellular signaling, Ca^{2+} mobilization, integrin activation, protein kinase C (PKC) activation and granule secretion were evaluated in GPVI-stimulated platelets treated with 15-HETE or 15-HETrE (20). Ca^{2+} mobilization, a key regulator of integrin $\alpha_{IIb}\beta_3$ activation, was evaluated in platelets treated with oxylipins in real-time by flow cytometry to

determine if Ca^{2+} mobilization was inhibited in the presence of 15-HETE and 15-HETrE. Collagen is a large insoluble molecule that poorly activates platelets in the static conditions required to measure Ca^{2+} mobilization and integrin activation in real-time on a flow cytometer (21). Therefore, convulxin (CVX), a snake venom toxin was used to stimulate GPVI for real-time flow cytometer experiments. Pretreatment of platelets with 15-HETE or 15-HETrE (10 μM) resulted in a decrease in Ca^{2+} mobilization following stimulation with CVX compared to control-treated platelets **(Figure 5.3A)**. Since Ca^{2+} mobilization is required for activation of the integrin $\alpha_{IIb}\beta_3$, a platelet specific receptor required for aggregation (22), 15-HETE and 15-HETrE were assessed for their ability to attenuate $\alpha_{IIb}\beta_3$ activation. 15-HETE- or 15-HETrE-treated platelets were stimulated with CVX (2.5 ng/mL) and activation was measured using flow cytometry in the presence of PAC-1, an antibody that recognizes the active conformation of $\alpha_{IIb}\beta_3$. Compared to DMSO, treatment of platelets with 15-HETE or 15-HETrE significantly inhibited $\alpha_{IIb}\beta_3$ activation in CVX-stimulated platelets (**Figure 5.3B**).

Since the activation of conventional isoforms of PKC are dependent on Ca^{2+}(23), the ability of 15-HETE and 15-HETrE to inhibit PKC in platelets was tested. At low concentrations of collagen (0.5 μg/mL), 15-HETE- and 15-HETrE-treated platelets showed a significantly reduced level of PKC substrate phosphorylation compared to control (**Figure 5.3C**). Consistent with the aggregation data, there was no difference in PKC activation between control- and oxylipin-treated platelets at higher concentrations of collagen (5 μg/mL) (**Figure 5.3C**). Agonist-

dependent granule release was also assessed as a measurement of platelet activation including both dense and α-granules, whose contents are known to potentiate platelet activation (24). To evaluate whether 15-HETE or 15-HETrE has an effect on dense granule secretion, platelets were stimulated with increasing concentrations of collagen in the presence of 15-HETE, 15-HETrE, or control. Collagen-stimulated platelets incubated with 15-HETE or 15-HETrE released less ATP, a marker of dense granule secretion, than platelets treated with DMSO (**Figure 5.3D**). To determine if 15-HETE or 15-HETrE inhibits α-granule secretion, platelets were stimulated with collagen (5 μg/mL) in the presence of 15-HETE or 15-HETrE, and surface expression of P-selectin was measured by flow cytometry (25). Platelets treated with 15-HETE or 15-HETrE had a decrease in P-selectin surface expression compared to control-treated platelets (**Figure 5.3E**).

5.3.4 15-HETE more potently inhibits 12-LOX than 15-HETrE

Previous studies have demonstrated that the antiplatelet effects of 15-HETE were due in part to its ability to selectively inhibit COX (10), 12-LOX (9,11,26), or both (18). To evaluate whether 15-HETrE inhibits platelet activation via inhibiting COX or 12-LOX, the levels of their respective AA-derived metabolite, TXB_2 and 12-HETE, were quantified in the releasate of collagen-stimulated platelets. Since Ca^{2+} mobilization is required for TXB_2 and 12-HETE formation (27), high concentration of collagen (5 μg/mL) were used that caused similar levels of Ca^{2+} mobilization and aggregation in platelets treated with either 15-HETrE or control (**Figure 5.2B**).

Platelets incubated with 15-HETE (10 μM) prior to collagen stimulation had a 97±1% decrease in 12-HETE (**Figure 4A**) generation with no effect on TXB_2 (**Figure 5.4B**) formation compared to vehicle-treated platelets. Treatment of platelets with 15-HETrE (10 μM) prior to collagen stimulation decreased 12-HETE formation by 44±11%, and also had no effect on the formation of TXB_2 compared to vehicle-treated platelets (**Figure 5.4**). Together this data indicates that while 15-HETrE can partially inhibit 12-HETE production, 15-HETE inhibits 12-HETE production more effectively.

Although treatment of platelets with 15-HETE or 15-HETrE diminished their ability to produce 12-HETE, it remains unknown if 15-HETrE could directly inhibit 12-LOX. The formation of 12-HETE was measured *in vitro* following the incubation of AA with recombinant 12-LOX in the presence of 15-HETE, 15-HETrE, or control to determine if 15-HETE or 15-HETrE directly inhibit 12-LOX. Similar to the data obtained with platelets (**Figure 5.4**), 15-HETE (IC_{50} = 46±19 μM) was a more potent inhibitor of purified 12-LOX than 15-HETrE (IC_{50} = 105±55 μM). The *in vitro* data are consistent with the ability of 15-HETE to more potently inhibit 12-HETE production in platelets than 15-HETrE.

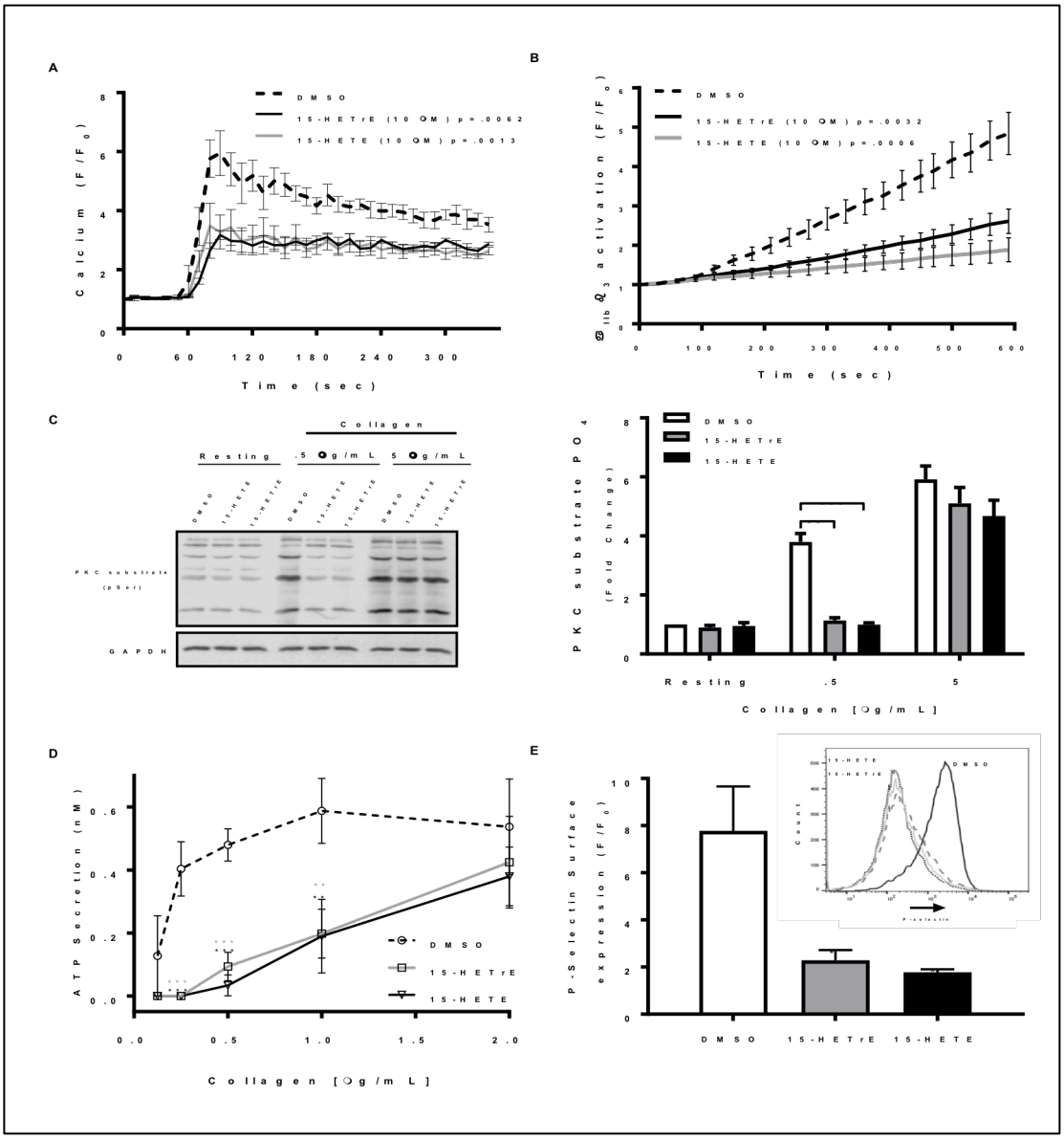

Figure 5.3: 15-HETE and 15-HETrE inhibit intracellular platelet signaling. A) Platelets (n=4) were treated with a 15-HETE or 15-HETrE (10 μM) and Fluo-4-AM, a cell-permeable, calcium-sensitive dye, then stimulated with convulxin (CVX; 2.5 ng/ml), and Ca^{2+} mobilization was analyzed by flow cytometry in real-time. **B)** Platelets (n=9) that had been treated with 15-HETE or 15-HETrE (10 μM) were stimulated with CVX (2.5 ng/ml) in the presence of FITC-conjugated PAC-1, an antibody specific to the active conformation of $\alpha_{IIb}\beta_3$, and analyzed by flow cytometry in real-time. Two-way ANOVA. **C)** Collagen-stimulated platelets (n=5) pretreated with either 15-HETE (10 μM) or 15-HETrE (10 μM) were lysed, and Western blots were performed with antibodies to the phospho-serine PKC substrate motif and GAPDH. Two-tailed paired t test. **D)** ATP secretion, a marker of dense granule secretion, was measured from platelets (n= 4-5) incubated with 15-HETE or 15-

HETrE (10 μM) in a lumi-aggregometer in the presence of increasing concentrations of collagen. Two-way ANOVA with Dunnett's multiple comparison post-test. **E)** P-selectin surface expression, a marker of α-granule secretion, was quantified in collagen-stimulated platelets (n=4) treated with 15-HETE or 15-HETrE (10 μM) by flow cytometry using a PE-conjugated P-selectin antibody. Data represents mean ± S.E.M. *P<0.05, **P<0.01, ***P<0.001

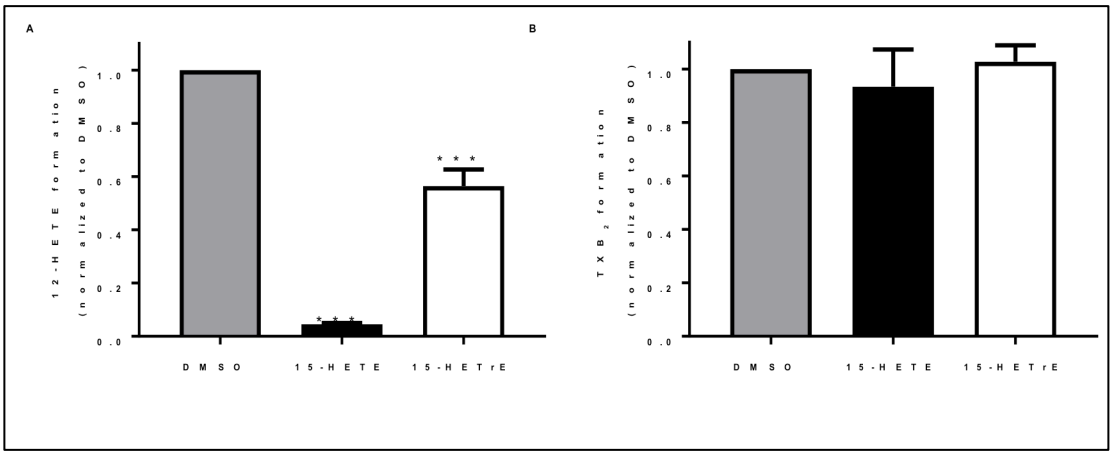

Figure 5.4: 15-HETE and 15-HETrE inhibit 12-LOX. The levels of **A)** 12-HETE and **B)** TXB_2 were quantified in the lysate of collagen-stimulated (5 ug/mL) platelets (n= 5) pretreated with 15-HETE (10 μM) or 15-HETrE (10 μM). Two-tailed paired t-test. Data represents mean ± S.E.M. ***P<0.001

5.3.5 12-LOX poorly metabolizes 15-HETE and 15-HETrE

15-HETE can be further metabolized by 12-LOX to form diHETEs such as 14,15- and 8,15-diHETE, that have been observed to inhibit platelet activation in the micromolar range (13,28,29). To determine if diHETEs or diHETrEs play a significant role in the antiplatelet effects of 15-HETE or 15-HETrE, respectively, their levels were measured following incubation with purified 12-LOX. Consistent with previous studies, 12-LOX reacted poorly with 15-HETE *in vitro*, producing only ≈1% of diHETEs before enzymatic inactivation occurred, with more 14,15-diHETE (87±7%) being produced than 8,15-diHETE (13±4%), of the total diHETE amount.

Consistent with the low diHETE yield, the K_{cat} and K_{cat}/K_M values for 12-LOX with 15-HETE or 15-HETrE ranged from 5% to 1%, relative to AA (**Table 5.1**). These rates were slightly increased with the addition of 13-HPODE, with values roughly two-fold higher relative to the untreated samples. Interestingly, the hydroperoxide substrates, 15-HPETE and 15-HPETrE, had a 4- to 10-fold increase in kinetic rates compared to 15-HETE and 15-HETrE (**Table 5.1**). These data suggest that 12-LOX diHETE products are incapable of oxidizing the inactive ferrous species to the active ferric species, which has previously been observed with other LOX isozymes (41).

Finally, the formation of diHETEs or diHETrEs was measured in platelet incubated with 15-HETE (10 μM) or 15-HETrE (10 μM). A small increase in the 14,15-diHETE product (≈1%) was observed, but no apparent 8,15-diHETE or 5,15-diHETE products were detected in the platelet sample, which is also consistent with

Substrate	K_{cat} (sec^{-1})	K_{cat}/K_M ($sec^{-1}\mu M^{-1}$)	K_M (μM)
AA	1.0 ± 0.05	1.0 ± 0.2	1.9 ± 0.4
AA*	1.0 ± 0.05	0.39 ± 0.05	4.8 ± 0.7
15-HETE	0.038 ± 0.001	0.054 ± 0.01	1.3 ± 0.3
15-HPETE	0.20 ± 0.01	0.19 ± 0.03	2.1 ± 0.3
15-HETE*	0.057 ± 0.003	0.072 ± 0.01	1.5 ± 0.3
15-HETrE	0.019 ± 0.001	0.009 ± 0.003	4.0 ± 1.2
15-HPETrE	0.22 ± 0.01	0.044 ± 0.008	9.4 ± 1.5
15-HETrE*	0.043 ± 0.001	0.014 ± 0.002	6.0 ± 0.5

Table 5.1: Relative steady-state kinetic parameters of 12-LOX. The rates are relative to AA, with the errors shown afterward. The values determined with AA and 12-LOX were comparable to previously published work (k_{cat} = 7.4 (0.4) sec^{-1}, k_{cat}/K_M = 3.9 (0.8) $sec^{-1}mM^{-1}$). An asterisk next to a substrate indicates that 13-HPODE was added to the reaction to oxidize 12-LOX to its active ferric form.

the kinetic data. Together, these data suggest minimal metabolism of the 15-HETE or 15-HETrE occurs by 12-LOX *in vitro* or in the platelet.

5.3.6 15-HETE and 15-HETrE inhibit platelet activation via unique PPARs

Independent of direct effects on oxygenases, oxylipins have additionally been proposed to reduce platelet activation through either the initiation of $G\alpha_s$-coupled receptor signaling or stimulation of PPARs (30). The inhibitory effects of the $G\alpha_s$ signaling pathway proceed through cAMP-dependent PKA activation (31). In platelets, the major substrate of PKA is VASP serine 157 (S157) (32). To determine if 15-HETE or 15-HETrE regulates platelet function in this manner, VASP phosphorylation was measured in platelets treated with oxylipins (10 μM) to assess their ability to initiate $G\alpha_s$ signaling. VASP (S157) phosphorylation did not increase in platelets incubated with 15-HETE or 15-HETrE compared to either DMSO or 12-HETE, a negative control (**Figure 5.5A**). As expected, platelets treated with either forskolin, a direct adenylyl cyclase agonist, or 12-HETrE, a 12-LOX oxylipin that signals through a $G\alpha_s$-coupled receptor (19), had enhanced VASP phosphorylation (**Figure 5.5A**). This data suggests that 15-HETE and 15-HETrE do not inhibit platelet activation via a $G\alpha_s$-coupled receptor.

Platelets express all three PPAR isoforms (α, β, and γ) and activation of any of these isoforms inhibit platelet function through a non-genomic mechanism (33,34). Since 15-HETE and 15-HETrE have been shown to activate PPARs in other cell types (35,36) we sought to determine if either 15-HETE or 15-HETrE inhibits platelet

aggregation in a PPAR-dependent manner in platelets. Platelets were incubated with the previously characterized inhibitors of PPARα (GW6471; 10 μM), PPARβ (GSK3787; 10 μM), or PPARγ (GW9662; 10 μM), prior to treatment with 15-HETE

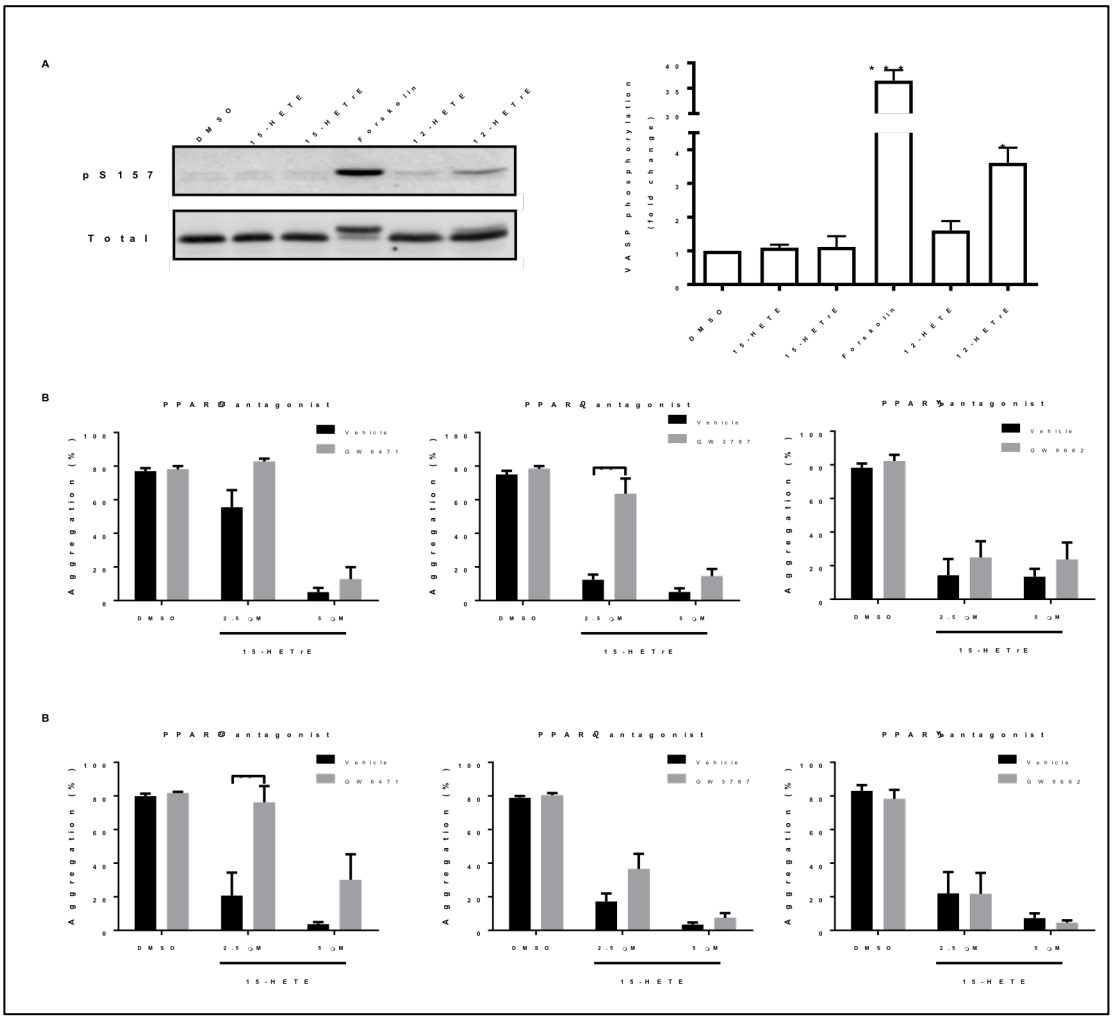

Figure 5.5: 15-HETE and 15-HETrE inhibit platelet activation via distinct mechanisms. A) The lysates of platelets (n=3-4) treated with forksolin, a direct adenylyl cyclase agonist, oxylipins (10 μM) or DMSO were separated on a 10% SDS-PAGE gel and Western blots were performed with antibodies to phospho- and total VASP. **B)** Platelets were incubated with PPARα (GW6471; 10 μM; n= 3-6), PPARβ (GW3787; 10 μM; n= 3-6), or PPARγ (GW9662; 10 μM; n= 3-6) antagonist, prior to the treatment with 15-LOX oxylipin, and then stimulated with collagen (.25-1 μg/mL). Data represents mean ± S.E.M. Two-tailed paired t test.

or 15- HETrE and subsequent collagen stimulation (33,37-39). Inhibition of PPARα, but not PPARβ or PPARγ, reversed the ability of low concentrations of 15-HETE (2.5 μM) to inhibit collagen-induced aggregation **(Figure 5.5D)**. In contrast, inhibition of PPARβ, but not PPARα or PPARγ, reversed the antiplatelet effects of low concentrations of 15-HETrE (2.5 μM) in collagen-stimulated platelets **(Figure 5.5D)**. None of the PPAR antagonists tested were able to reverse the inhibitory effects of higher concentrations of 15-HETE or 15-HETrE (5 μM), suggesting these oxylipins only partially signal through PPARs.

5.4 Discussion

DGLA can be oxidized to form antiplatelet oxylipins such as PGE_1, 12-HETrE, and 15-HETrE (4,7). The antiplatelet effects of PGE_1 and 12-HETrE have been well studied (1,3,6); however, less is known about the antiplatelet effects of 15-HETrE. The current study sought to characterize the mechanism by which 15-HETrE exerts its antiplatelet effects and determine whether these effects are achieved in a manner similar to previously characterized monohydroxylated oxylipins, such as 12-HETrE and 15-HETE (1,6,40). This study is the first to demonstrate that 15-HETrE inhibits platelet aggregation through multiple intracellular pathways including activation of PPARβ and inhibition of 12-LOX. Overall, the inhibitory actions of 15-HETrE were found to be closely related to those of 15-HETE, with the distinct difference lying in its regulation of PPARb as opposed to PPARα (9,11,26).

This was the first study to demonstrate that micromolar levels of 15-HETrE attenuated aggregation initiated by low doses of multiple agonist including collagen, thrombin, ADP, and AA (**Figure 5.2**). Interestingly, while higher concentrations of thrombin, collagen, and AA stimulation were able to overcome 15-HETrE-dependent platelet inhibition, 15-HETrE was able to inhibit ADP-mediated platelet aggregation at all concentrations of ADP tested **(Figure 5.2)**. The ability of 15-HETrE to inhibit platelet aggregation in response to multiple agonists suggests that 15-HETrE impinges on a common signaling event downstream of receptor activation in the platelet aggregation pathway. Further, assessment of platelet signaling following GPVI stimulation showed that 15-HETrE inhibited the activation of common signaling events including Ca^{2+} mobilization, and activation of $\alpha_{IIb}\beta_3$ (**Figure 5.3**). Interestingly, while some 12-LOX oxylipins such as 12-HETrE have been previously shown to inhibit platelet function through activation of the IP receptor on the surface of the platelet resulting in activation of Ga_s, formation of cAMP, and activation of PKA, neither 15-HETE nor 15-HETrE resulted in VASP-phosphorylation, a protein in the platelet phosphorylated by PKA suggesting these oxylipins inhibit platelet function in a IP receptor-independent manner (**Figure 5.5**) (1,6).

The steps required for platelet activation have been well studied and several biochemical intermediates such as calcium mobilization, PKC activation, and integrin activation are known to be required for platelet aggregation to occur. While several biochemical steps were shown in the current study to be similarly regulated by 15-HETE and 15-HETrE, the proximal regulatory steps preceding these central

biochemical regulators were identified as unique to each of the metabolites studied. 15-HETrE was found to be a specific agonist for PPARβ, while 15-HETE and 15-HETrE appear to function at least partially through the activation of PPARα and PPARβ, respectively (**Figure 5.5**). While PPAR antagonists reversed the inhibitory effects of lower concentrations of 15-HETE and 15-HETrE, PPAR inhibitors could not reverse higher concentrations of these oxylipins. It is also possible that 15-HETE and 15-HETrE function predominantly through PPARs, but that at higher concentrations they outcompete the PPAR antagonists. Mice deficient in select PPAR isoforms in the platelet would help to delineate which of these two hypotheses is viable; however, since neither of these mice are readily available, creation of transgenic animals deficient in PPARa or PPARb will be required to further identify the role of PPAR in 15-LOX oxylipin platelet activation.

A number of monohydroxylated oxylipins have antiplatelet activity; however, how the structure of these oxylipins regulates their mechanism of action remains poorly understood.[8] Recently, the independent discoveries that 19-HETE (41) and 12-HETrE (6) both inhibit platelet activation by signaling through the prostacyclin receptor warranted a further investigation into the structure–activity relationship of antiplatelet monohydroxylated oxylipins. A number of attributes have been shown to influence the functionality of monohydroxylated oxylipins including carbon length, double bond configuration, and position/stereochemistry of oxygenation. HETEs and HETrEs both have 20 carbon backbones and double bonds at the 8, 10, and 14 carbons, but HETEs contain an additional double bond at the 5th carbon. 12-HETE

and 12-HETrE have been shown to have opposite effects on platelet activity, suggesting the double bond configuration may be a major contributor to monohydroxylated oxylipin function (1). Interestingly, in contrast to the opposite effects observed with 12-HETE and 12-HETrE, the current study found that 15-HETE and 15-HETrE have similar but unique functionality. In the current study, the difference in a single double bond does not change the overall inhibitory effect on platelet function observed with 15-HETE and 15-HETrE rather shifts the isoform of PPAR that is activated.

Oxylipin regulation of platelet function through negative feedback inhibition of the oxylipins has been previously shown. In agreement with previous publications, 15-HETE and 15-HETrE were shown in the current study to partially inhibit 12-HETE formation, which helps explain the inability of PPAR inhibitors to fully reverse 15-HETE's antiplatelet effects. Interestingly, the oxylipins showed a differential ability to inhibit 12-LOX as platelets treated with 15-HETE and 15-HETrE had a 90% and 40% decrease in 12-LOX product formation, respectively **(Figure 5.4)**. However, the COX-derived product of AA, TXB_2, was not decreased in platelets treated with either 15-HETE or 15-HETrE which suggests that 15-HETE and 15-HETrE are selectively inhibiting 12-LOX and not the availability of the substrate, AA **(Figure 5.4)**. Further, 15-HETE and 15-HETrE were shown to inhibit recombinant 12-LOX *in vitro* demonstrating the ability of these oxylipins to directly inhibit 12-LOX. Finally, platelets showed a surprising oxidation of monohydroxylated oxylipins, which were further metabolized by 12-LOX into

bioactive dihydroxylated oxylipins, which have previously been shown to have antiplatelet activity (29). However, since only a small fraction (~1%) of the 15-HETE and 15-HETrE were converted into dihydroxylated oxylipins, their contribution to the antiplatelet effects of 15-HETE and 15-HETrE were thought to be negligible.

The physiological concentration of 15-HETrE in the blood of healthy individuals is in the nanomolar range (42); however, individuals who consume GLA supplementation have been shown to have micromolar levels of DGLA in circulation, which would likely increase the amount of 15-HETrE produced by platelets (43). In accordance with previous findings (4,13), 15-HETrE was detected in the releasate of leukocyte-depleted platelets treated with DGLA (**Figure 5.1B**). Further, previous studies have found that 15-HETrE is produced in a COX-dependent manner (4), which was consistent with the ability of recombinant COX to metabolize AA into 15-(S)-HETE *in vitro* (44). As COX enzymes are ubiquitously expressed, and since other vascular cells such as endothelial cells and smooth muscle have been shown to produce 15-HETE (45,46), it is expected that in addition to platelets, other cells in the vessel likely contribute to the overall levels of serum 15-HETrE in individuals taking DGLA supplementation.

The distinct antiplatelet effects of 15-HETrE compared to either 12-HETE or 15-HETE highlighted by this work demonstrate the unique responses elicited by monohydroxylated oxylipins. Hence, studying monohydroxylated oxylipin effects has helped elucidate important mechanisms that represent future therapeutic approaches to treat cardiovascular disease.

5.5 Authorship Contributions

Benjamin E. Tourdot, Steven C. Perry, Abigail R. Green,, James Sorrentino, Megan Hawley, Jennifer Yeung, Cecilia Li, J. Cody Freedman, Theodore R. Holman, and Michael Holinstat,

B. E. Tourdot acquired, analyzed and interpreted platelet based data, as well as wrote the platelet-related section of the manuscript. S.C. Perry acquired data, analyzed data and wrote the analytical chemistry section of the manuscript. A. R. Green, J. Sorrentino, M. Hawley, C. Li, J.C. Freedman acquired data and analyzed data, T.R. Holman and M. Holinstat designed experiments, interpreted data and revised the manuscript.

5.6 References

1. Yeung J, Tourdot BE, Adili R, et al. 12 (S)-HETrE, a 12-Lipoxygenase Oxylipin of Dihomo-γ-Linolenic Acid, Inhibits Thrombosis via Gαs Signaling in PlateletsHighlights. *Arteriosclerosis, thrombosis, and vascular biology.* 2016;36(10):2068-2077.

2. Lagarde M, Berciaud P, Burtin M, Dechavanne M. Refractoriness of diabetic platelets to inhibitory prostaglandins. *Prostaglandins and medicine.* 1981;7(4):341-347.

3. Kirtland SJ. Prostaglandin E1: a review. *Prostaglandins, leukotrienes and essential fatty acids.* 1988;32(3):165-174.

4. Guichardant M, Naltachayan-Durbin S, Lagarde M. Occurrence of the 15-hydroxy derivative of dihomogammalinolenic acid in human platelets and its biological effect. *Biochimica et Biophysica Acta (BBA)-Lipids and Lipid Metabolism.* 1988;962(1):149-154.

5. Ikei KN, Yeung J, Apopa PL, et al. Investigations of human platelet-type 12-lipoxygenase: role of lipoxygenase products in platelet activation. *Journal of lipid research.* Dec 2012;53(12):2546-2559.

6. Tourdot BE, Adili R, Isingizwe ZR, et al. 12-HETrE inhibits platelet reactivity and thrombosis in part through the prostacyclin receptor. *Blood Advances.* 2017;1(15):1124-1131.

7. Tourdot BE, Ahmed I, Holinstat M. The emerging role of oxylipins in thrombosis and diabetes. *Frontiers in pharmacology.* 2014;4:176.

8. Yeung J, Hawley M, Holinstat M. The expansive role of oxylipins on platelet biology. *Journal of Molecular Medicine.* 2017:1-14.

9. Vanderhoek J, Bryant R, Bailey J. 15-hydroxy-5, 8, 11, 13-eicosatetraenoic acid: A potent and selective inhibitor of platelet lipoxygenase. *Journal of Biological Chemistry.* 1980;255(13):5996-5998.

10. Setty B, Stuart MJ. 15-Hydroxy-5, 8, 11, 13-eicosatetraenoic acid inhibits human vascular cyclooxygenase. Potential role in diabetic vascular disease. *Journal of Clinical Investigation.* 1986;77(1):202.

11. Vericel E, Lagarde M. 15-Hydroperoxyeicosatetraenoic acid inhibits human platelet aggregation. *Lipids.* 1980;15(6):472-474.

12. Kozak KR, Gupta RA, Moody JS, et al. 15-Lipoxygenase Metabolism of 2-Arachidonylglycerol GENERATION OF A PEROXISOME PROLIFERATOR-ACTIVATED RECEPTOR α AGONIST. *Journal of Biological Chemistry.* 2002;277(26):23278-23286.

13. Wong PY, Westlund P, Hamberg M, Granstrom E, Chao PH, Samuelsson B. 15-Lipoxygenase in human platelets. *J Biol Chem.* Aug 5 1985;260(16):9162-9165.

14. Falardeau P, Hamberg M, Samuelsson B. Metabolism of 8, 11, 14-eicosatrienoic acid in human platelets. *Biochimica et Biophysica Acta (BBA)-Lipids and Lipid Metabolism.* 1976;441(2):193-200.

15. Paul BZ, Jin J, Kunapuli SP. Preparation of mRNA and cDNA Libraries From Platelets and Megakaryocytes. *Platelets and Megakaryocytes: Volume 2: Perspectives and Techniques.* 2004:435-453.

16. Spector AA, Gordon JA, Moore SA. Hydroxyeicosatetraenoic acids (HETES). *Progress in lipid research.* 1988;27(4):271-323.

17. Vanderhoek JY, Bailey J. Activation of a 15-lipoxygenase/leukotriene pathway in human polymorphonuclear leukocytes by the anti-inflammatory agent ibuprofen. *Journal of Biological Chemistry.* 1984;259(11):6752-6756.

18. Vedelago HR, Mahadevappa VG. Differential effects of 15-HPETE on arachidonic acid metabolism in collagen-stimulated human platelets. *Biochemical and biophysical research communications.* 1988;150(1):177-184.

19. Yeung J, Tourdot BE, Adili R, et al. 12-HETrE, a 12-Lipoxygenase Oxylipin of Dihomo-γ-Linolenic Acid, Inhibits Thrombosis via Gαs Signaling in Platelets. *Arteriosclerosis, Thrombosis, and Vascular Biology.* 2016:ATVBAHA. 116.308050.

20. Bergmeier W, Stefanini L. Platelet ITAM signaling. *Current opinion in hematology.* 2013;20(5):445-450.

21. Moers A, Wettschureck N, Gruner S, Nieswandt B, Offermanns S. Unresponsiveness of platelets lacking both Galpha(q) and Galpha(13). Implications for collagen-induced platelet activation. *The Journal of biological chemistry.* Oct 29 2004;279(44):45354-45359.

22. Shattil SJ, Kim C, Ginsberg MH. The final steps of integrin activation: the end game. *Nature reviews Molecular cell biology.* 2010;11(4):288-300.

23. Harper M, Poole A. Diverse functions of protein kinase C isoforms in platelet activation and thrombus formation. *Journal of Thrombosis and Haemostasis.* 2010;8(3):454-462.

24. Fitch-Tewfik JL, Flaumenhaft R. Platelet granule exocytosis: a comparison with chromaffin cells. *The regulated secretory pathway in neuroendocrine cells.* 2014:117.

25. Furie B, Furie BC, Flaumenhaft R. A journey with platelet P-selectin: the molecular basis of granule secretion, signalling and cell adhesion. *THROMBOSIS AND HAEMOSTASIS-STUTTGART-.* 2001;86(1):214-221.

26. MITCHELL PD, HALLAM C, HEMSLEY PE, LORD GH, WILKINSON D. Inhibition of platelet 12-lipoxygenase by hydroxy-fatty acids. *Biochemical Society Transactions.* 1984;12(5):839-841.

27. Holinstat M, Boutaud O, Apopa PL, et al. Protease-activated receptor signaling in platelets activates cytosolic phospholipase A2α differently for cyclooxygenase-1 and 12-lipoxygenase catalysis. *Arteriosclerosis, thrombosis, and vascular biology.* 2011;31(2):435-442.

28. Dadaian M, Westlund P. Albumin modifies the metabolism of hydroxyeicosatetraenoic acids via 12-lipoxygenase in human platelets. *Journal of lipid research.* 1999;40(5):940-947.

29. Bild G, Bhat S, Axelrod B, Iatridis P. Inhibition of aggregation of human platelets by 8, 15-dihydroperoxides of 5, 9, 11, 13-eicosatetraenoic and 9, 11, 13-eicosatrienoic acids. *Prostaglandins.* 1978;16(5):795-801.

30. Tourdot BE, Ahmed I, Holinstat M. The emerging role of oxylipins in thrombosis and diabetes. *Front Pharmacol.* Jan 7 2014;4:176.

31. Smolenski A. Novel roles of cAMP/cGMP-dependent signaling in platelets. *Journal of Thrombosis and Haemostasis.* 2012;10(2):167-176.

32. Butt E, Abel K, Krieger M, et al. cAMP- and cGMP-dependent protein kinase phosphorylation sites of the focal adhesion vasodilator-stimulated phosphoprotein (VASP) in vitro and in intact human platelets. *J Biol Chem.* May 20 1994;269(20):14509-14517.

33. Ali FY, Davidson SJ, Moraes LA, et al. Role of nuclear receptor signaling in platelets: antithrombotic effects of PPARβ. *The FASEB Journal.* 2006;20(2):326-328.

34. Lannan KL, Sahler J, Kim N, et al. Breaking the mold: transcription factors in the anucleate platelet and platelet-derived microparticles. *Frontiers in immunology.* 2015;6:48.

35. Naruhn S, Meissner W, Adhikary T, et al. 15-hydroxyeicosatetraenoic acid is a preferential peroxisome proliferator-activated receptor β/δ agonist. *Molecular pharmacology.* 2010;77(2):171-184.

36. Thuillier P, Brash AR, Kehrer JP, et al. Inhibition of peroxisome proliferator-activated receptor (PPAR)-mediated keratinocyte differentiation by lipoxygenase inhibitors. *Biochemical Journal.* 2002;366(3):901-910.

37. Ali FY, Armstrong PC, Dhanji A-RA, et al. Antiplatelet actions of statins and fibrates are mediated by PPARs. *Arteriosclerosis, thrombosis, and vascular biology.* 2009;29(5):706-711.

38. Du H, Hu H, Zheng H, Hao J, Yang J, Cui W. Effects of peroxisome proliferator-activated receptor γ in simvastatin antiplatelet activity: influences on cAMP and mitogen-activated protein kinases. *Thrombosis research.* 2014;134(1):111-120.

39. Moraes LA, Spyridon M, Kaiser WJ, et al. Non-genomic effects of PPARγ ligands: inhibition of GPVI-stimulated platelet activation. *Journal of Thrombosis and Haemostasis.* 2010;8(3):577-587.

40. Salari H, Braquet P, Borgeat P. Comparative effects of indomethacin, acetylenic acids, 15-HETE, nordihydroguaiaretic acid and BW755C on the metabolism of arachidonic acid in human leukocytes and platelets. *Prostaglandins, Leukotrienes and Medicine.* 1984;13(1):53-60.

41. Tunaru S, Chennupati R, Nüsing RM, Offermanns S. Arachidonic acid metabolite 19 (S)-HETE induces vasorelaxation and platelet inhibition by activating prostacyclin (IP) receptor. *PloS one.* 2016;11(9):e0163633.

42. Walenga RW, Boone S, Stuart MJ. Analysis of blood HETE levels by selected ion monitoring with ricinoleic acid as the internal standard. *Prostaglandins.* 1987;34(5):733-748.

43. Johnson MM, Swan DD, Surette ME, et al. Dietary supplementation with gamma-linolenic acid alters fatty acid content and eicosanoid production in healthy humans. *J Nutr.* Aug 1997;127(8):1435-1444.

44. Thuresson ED, Lakkides KM, Smith WL. Different catalytically competent arrangements of arachidonic acid within the cyclooxygenase active site of prostaglandin endoperoxide H synthase-1 lead to the formation of different oxygenated products. *Journal of Biological Chemistry.* 2000;275(12):8501-8507.

45. Bailey JM, Bryant R, Whiting J, Salata K. Characterization of 11-HETE and 15-HETE, together with prostacyclin, as major products of the cyclooxygenase pathway in cultured rat aorta smooth muscle cells. *Journal of lipid research.* 1983;24(11):1419-1428.

46. Buchanan M, Horsewood P, Brister S. Regulation of endothelial cell and platelet receptor-ligand binding by the 12-and 15-lipoxygenase monohydroxides, 12-, 15-HETE and 13-HODE. *Prostaglandins, leukotrienes and essential fatty acids.* 1998;58(5):339-346.

47. Wecksler AT, Kenyon V, Garcia NK, Deschamps JD, van der Donk WA, Holman TR. Kinetic and structural investigations of the allosteric site in human epithelial 15-lipoxygenase-2. *Biochemistry.* 2009;48(36):8721-8730.

48. Smyrniotis CJ, Barbour SR, Xia Z, Hixon MS, Holman TR. ATP Allosterically Activates the Human 5-Lipoxygenase Molecular Mechanism of Arachidonic Acid and 5 (S)-Hydroperoxy-6 (E), 8 (Z), 11 (Z), 14 (Z)-eicosatetraenoic Acid. *Biochemistry.* 2014;53(27):4407-4419.

49. Lewis ER, Johansen E, Holman TR. Large competitive kinetic isotope effects in human 15-lipoxygenase catalysis measured by a novel HPLC method. *Journal of the American Chemical Society.* 1999;121(6):1395-1396.

50. Ikei KN, Yeung J, Apopa PL, et al. Investigations of human platelet-type 12-lipoxygenase: role of lipoxygenase products in platelet activation. *Journal of lipid research.* 2012;53(12):2546-2559.